Whin Sill metamorphism in Teesdale

Robinson, Douglas

WHIN SILL METAMORPHISM IN TEESDALE

by: Douglas Robinson, B.Sc. (London),
Department of Geology,
Science Laboratories,
University of Durham.

Submitted for the degree of Doctor of Philosophy
at the University of Durham

November, 1971

Graduate Society

TABLE OF CONTENTS

Page

CHAPTER IV

Page

CHAPTER VI

ABSTRACT

The Whin Sill complex is briefly reviewed. Theoretical temperatures have been calculated for the metamorphic aureoles in the Teesdale, Rookhope and Ninebanks areas, for comparative purposes with the observed metamorphism.

The major and trace element geochemistry of a suite of argillaceous and arenaceous sediments has been examined using R-mode factor analysis. Only one factor is interpreted as a metamorphic feature. This factor is indicative of an increase in Na in beds towards the contact but is of minor volumetric importance accounting for less than 10% of the data variance. The remaining factors can all be interpreted as sedimentary features.

X-ray diffraction studies of argillaceous sediments have shown an increase in the crystallinity and a change in the polymorph, from a 1Md to a 2M variety, of illite, towards the contact.

Pure limestones have been recrystallized to saccharoidal marbles, which are restricted to the Upper Teesdale region. Dark-coloured limestones are not recrystallized because the carbon present in these sediments prevents grain-boundary movement (Robinson, 1971).

Calcareous sediments have been the most susceptible to the metamorphism and a varied calc-silicate mineralogy is developed up to 25 m from the Whin Sill contact. Potassic feldspar, andradite, hedenbergite, prehnite and datolite are recorded for the first time from the contact-rocks of the Whin Sill aureole.

The mineralogy developed in the calcareous sediments is

indicative of two or possibly three facies and is interpreted as non-equilibrium conditions. The difference in metamorphism between calcareous and non-calcareous sediments is attributed to higher reaction kinetics in the calcareous sediments.

Metamorphism by the Whin Sill is virtually non-existent outside the Upper Teesdale region. This is suggested to be due to a magma source in this area, giving rise to anomalous conditions as compared to a simple intrusion into cold country-rocks.

The increase of Na in certain beds within 10 m of the contact is not attributed to metasomatic introduction from the Whin Sill. Instead the Na is suggested to have been present as NaCl in hypersaline pore-waters of the sediments, at the time of the Whin Sill intrusion. It is shown that the mineralogy developed in the contact-rocks has largely been the consequence of reaction between illite and the NaCl pore-waters. Haematite has been formed by the release of Fe^{3+} from the illite structure.

Finally it is shown that the unique geology of the Upper Teesdale area, especially the development of saccharoidal marbles, has been of major importance in the sustenance of the rare arctic-alpine flora for which the area is biologically renowned (Johnson, Robinson and Hornung, 1971).

ACKNOWLEDGEMENTS

Professors G.M. Brown and M.H.P. Bott are gratefully acknowledged for the use of facilities provided by the Geology Department of the University of Durham.

Professor Brown is further thanked for his supervision and for reading the manuscript of this thesis. Dr. G.A.L. Johnson is sincerely thanked also for his supervision, constant encouragement, advice and for reading the manuscript.

Fellow research students, especially Mr. E.B. Curran, Mr. J.G. Fitton, Dr. G.H. Gale, Mr. A.J. Hall and Dr. M.J. Reeves, are thanked for help and discussion, especially in computer programming.

The academic staff are thanked for help with X-ray fluorescence (Dr. J.G. Holland) and electron microprobe techniques (Dr. C.H. Emeleus and Dr. A. Peckett).

The technical staff are thanked for their support and work during the three years of this study, especially Mr. G. Dresser for photographic work.

The Tees Valley and Cleveland Water Board is gratefully acknowledged for permission to study and sample from the Cow Green boreholes.

Mrs. G.C. Robinson is thanked for her help and encouragement over the last three years and for typing the thesis with Mrs. J. Myatt.

Mrs. C. Reynolds is thanked for translating the article by Bartholomé (1970).

Finally the Nature Conservancy is thanked for the Award (N.E.R.C. Research Assistantship), which made this work possible.

CHAPTER I

INTRODUCTION

OBJECT OF RESEARCH

The present investigation of the metamorphosed bedrock of Upper Teesdale has been a natural continuation of the pedological survey, undertaken by Dr. M. Hornung. The survey of Upper Teesdale was initiated in 1966 when N.E.R.C. made available a research grant, for the study of the bedrock, drift and soils in the vicinity of the celebrated biological sites of the area. This work has been centered in Durham under the direction of Dr. G. A. L. Johnson.

It has been known for some time that a relationship exists between the Teesdale flora, the rendzinas and bedrock marble, and it was particularly requested, therefore, that a special study be made of the saccharoidal marble, which is restricted to the area. A great volume of research has been undertaken on the Whin Sill itself, but little attention has been paid to the associated metamorphism. The aim of the present study was, therefore, to give a detailed, modern account of the metamorphism; the only previous detailed work was that of Hutchings (1898). The project was made possible when permission was kindly given by the Tees Valley and Cleveland Water Board, for access to and sampling from the cores of boreholes, drilled during the site investigation for the Cow Green reservoir. Thirty boreholes were available, which give unique sections through the contact rocks of the area.

Figure 1.1 Geological map of north-east England. After Johnson (1970a).

Figure 1.2 Geological map of the Upper Teesdale area. After Johnson *et al.* (1971).

s - well developed rotten marble and calcite sand rendzinas.

Figure 1.1

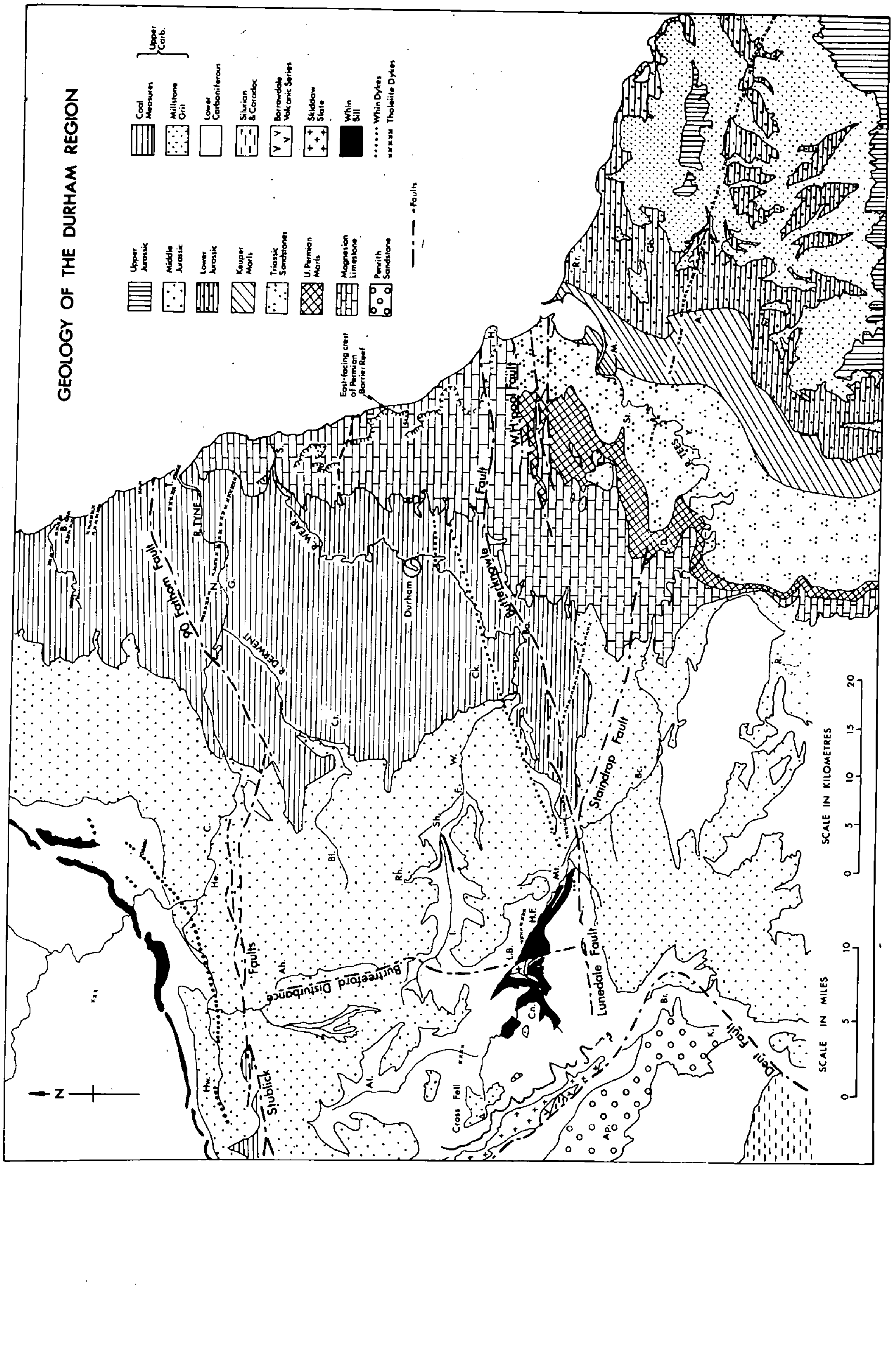
GEOLOGY OF THE DURHAM REGION
Upper Jurassic
Middle Jurassic
Lower Jurassic
Keuper Marls
Triassic Sandstones
U. Permian Marls
Magnesian Limestone
Penrith Sandstone
Faults
Coal Measures
Millstone Grit
Upper Carb.
Lower Carboniferous
Silurian & Caradoc
Borrowdale Volcanic Series
Skiddaw Slate
Whin Sill
Whin Dykes
Tholeiite Dykes
East-facing crest of Permian Barrier Reef
90 Fathom Fault
Butterknowle Fault
Staindrop Fault
Lunedale Fault
Burtreeford Disturbance
Stublick
Faults
Dent Fault
R. TYNE
R. WEAR
R. DERWENT
TEES
Durham
Cross Fell
SCALE IN KILOMETRES
SCALE IN MILES

PREVIOUS RESEARCH

The literature on the Whin Sill is voluminous, but little detailed work has been undertaken on the contact metamorphism. The only extensive work was that of Hutchings (1898), who gave detailed descriptions of the alteration produced in the contact aureole. He was also the first to note the increase in Na in some of the beds close to the contact but could not explain its patchy distribution. Since Hutchings's work various authors have mentioned the metamorphism, Smythe (1930, 1950), Dunham (1948) and Randall (1959), but no modern, detailed work has been undertaken.

GEOLOGICAL SETTING OF UPPER TEESDALE

The geological setting of the Upper Teesdale region is shown in Fig. 1.1. No discussion is given on the general geology, as excellent accounts are readily available, Dunham (1948), Bott and Johnson (1970) and Johnson (1970a). Part of the great aerial extent of the Whin Sill may be seen from Fig. 1.1. The southernmost outcrop is along the Hett dyke system, but just to the north, large outcrops of the sill are present in Upper Teesdale. The sill is also found along the full length of the western escarpment of the northern Pennines, but near Brampton it turns north-eastwards along the Roman Wall and continues across Northumberland up to the Farne Islands, where the northernmost limit of the complex is formed by the Holy Island dyke.

It is in Upper Teesdale, however, that the present study has concentrated and the geology of this region is shown in greater detail in Fig. 1.2.

Figure 1.2

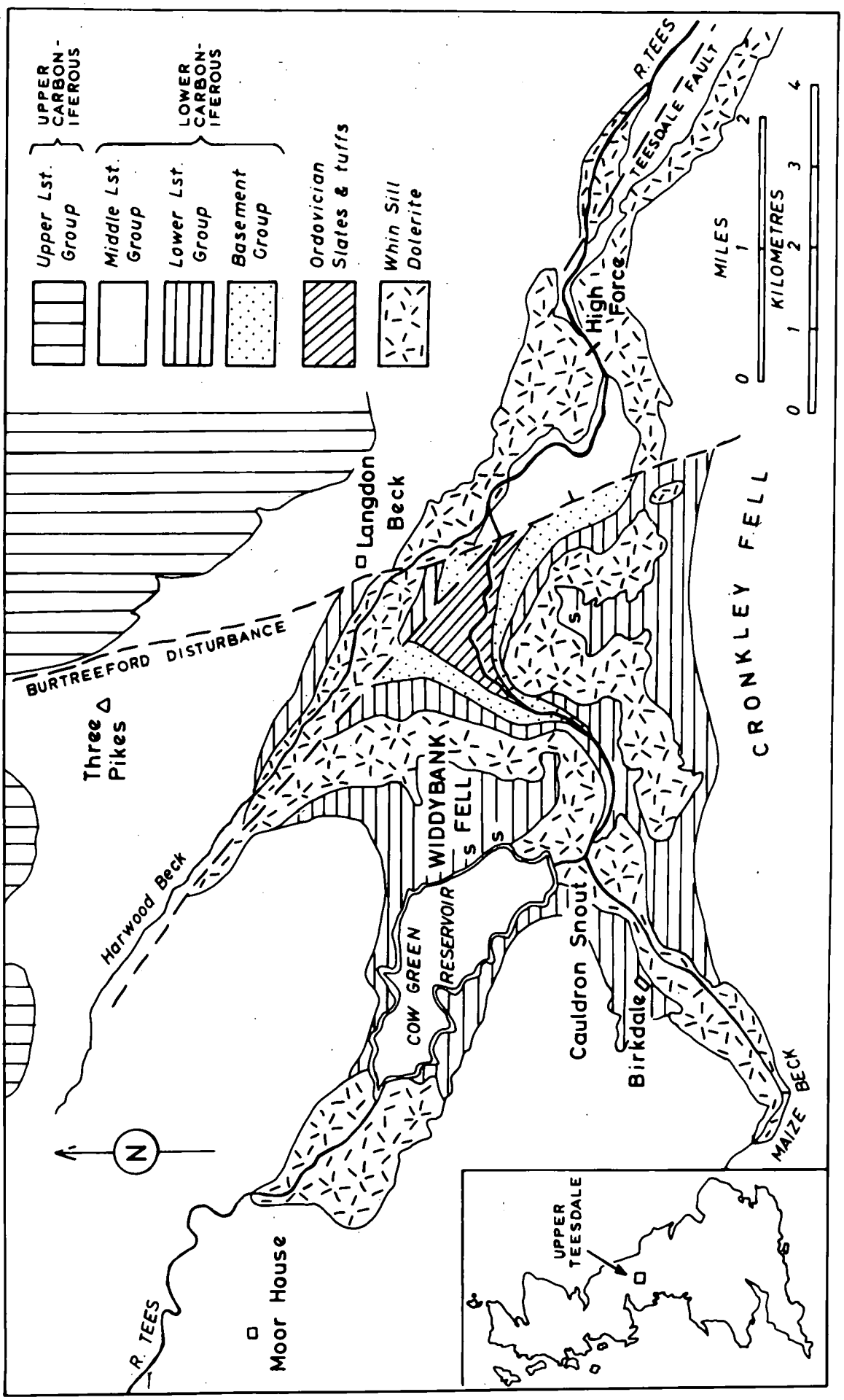
UPPER CARBON-IFEROUS
LOWER CARBON-IFEROUS
Upper Lst. Group
Middle Lst. Group
Lower Lst. Group
Basement Group
Ordovician Slates & tuffs
Whin Sill Dolerite
R. TEES
TEESDALE FAULT
High Force
MILES
KILOMETRES
Langdon Beck
BURTREEFORD DISTURBANCE
Three Pikes
Harwood Beck
WIDDYBANK FELL
COW GREEN RESERVOIR
Cauldron Snout
Birkdale
CRONKLEY FELL
MAIZE BECK
Moor House
R. TEES
N
UPPER TEESDALE

Local stratigraphy

The area of main interest extends from High Force, in the south-east, north-westwards across Widdybank Fell to Moor House, and south-west of Harwood Beck (Fig. 1.2). Lower Carboniferous sediments are found in this region, a detailed account of which is given, for the Moor House area, by Johnson and Dunham (1963). A simplified stratigraphical column, showing the succession at Cow Green mine, is given in Fig. 1.3 (after Dunham, 1948), and is used as a reference for the area. For the purpose of this study the Lower Carboniferous succession has been divided into three groups namely:- 1) Basement Group, 2) Lower Limestone Group and 3) Middle Limestone Group. A detailed discussion of the relation of these local terms to the international sub-divisions of the Carboniferous, is given in Johnson and Dunham (1963) and Johnson (1970b).

The floor of the Tees valley, near Langdon Beck, is composed of folded Skiddaw Slates and tuffs (Fig. 1.2), which are unconformably overlain by the almost horizontal Carboniferous strata. The Carboniferous commences with the Basement Group, composed of basal conglomerates overlain by sandstones and shales with thin, interbedded limestones. The Basement Group is overlain by the Lower Limestone Group, dominated by the thick (38 m), massive, light-coloured Melmerby Scar Limestone, which has occasional shale horizons. The upper part of this group and the overlying Middle Limestone Group consist of a series of rhythmic units composed of dominantly dark-coloured limestones with interbedded sandstones and shales. The Whin Sill is intruded at its lowest stratigraphical horizon at Cronkley Scar,

Figure 1.3 Simplified stratigraphical succession at Cow Green mine. After Dunham (1948).

Figure 1.3

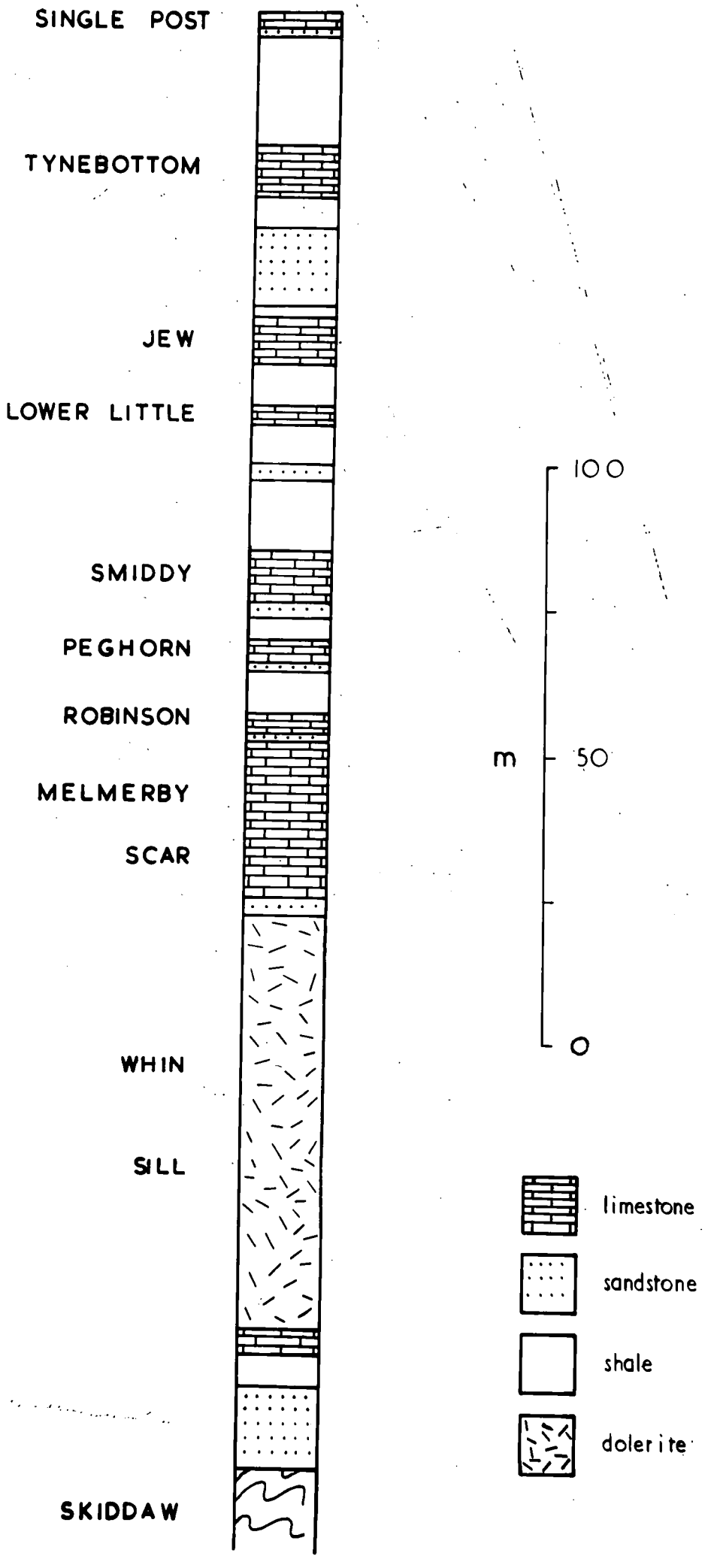
SINGLE POST
TYNEBOTTOM
JEW
LOWER LITTLE
SMIDDY
PEGHORN
ROBINSON
MELMERBY
SCAR
WHIN
SILL
SKIDDAW
100
m
50
0
limestone
sandstone
shale
dolerite

where it is found some 27 m beneath the Melmerby Scar Limestone, Dunham (1948). In the Cow Green area the sill is intruded some 27 m below the upper surface of the Melmerby Scar Limestone (Fig. 1.3). North-west from this area the sill gradually rises in the succession and at Greenhurth mine is found at the base of the Lower Little Limestone (Johnson and Dunham, 1963).

The samples studied, in this investigation, (Appendix 1.1) have mainly been collected from a series of boreholes drilled during the site investigation for the Cow Green reservoir. These boreholes were sunk in a zone extending from near Birkdale (Fig. 1.2), north-eastwards across Widdybank Fell to Harwood Beck. The location of, and the detailed stratigraphical successions, of these boreholes, are given in a supplement to Knill (1966).

The Upper Teesdale area is bisected by the NNW to SSE trending Burtreeford disturbance. This structure is an eastward facing faulted monocline with a downthrow of some 200 m to the east. This has brought the Middle Limestone Group, on the east of the structure, into juxtaposition with the Lower Limestone Group, in the west. The disturbance was active before the intrusion of the Whin Sill as it cuts across the structure from a position near the Tyne Bottom Limestone in the east, to a horizon near the base of the Melmerby Scar Limestone, in the west.

METHODS OF ANALYSIS

Electron microprobe analysis

The electron microprobe analyses have been made using a Cambridge Scientific Instruments Co., Geoscan Mark 2, with two spectrometers and a take-off angle of 75°. An accelerating

voltage of 15 K.V. was used throughout the analyses, except where volatilization of the sample might have occurred, such as in the cases of prehnite, chlorite and datolite, when 12 K.V. and a defocussed beam were used. Flow-proportional counters were used throughout and the E.H.T. of the counters was set prior to each element analysis, as was the threshold value (E). A window setting (δE) was not used, in order to minimize the effect of pulse-height drift.

The polished slices, of the samples, were carbon-coated along with the standards, which were from the departmental collection, at Durham, and consisted of minerals, elements and oxides of known, homogenous composition and purity. The particular standard used for each element and the analysing crystal are shown in Table 1.1.

Table 1.1 Standards and analysing crystals used in electron microprobe analysis

Element	Standard	Crystal
Si	Wollastonite	K.A.P.
Al	Corundum / Plagioclase (M11)	K.A.P.
Fe	Iron / Olivine (OLGB)	Li.F.
Mg	Olivine (OLGB) / Periclase	K.A.P.
Ca	Wollastonite	Quartz
Na	Jadeite	K.A.P.
K	Orthoclase (AF15)	Quartz
Ti	Rutile	Li.F.
Mn	Manganese	Li.F.

The 2θ values are those given in standard tables, and these were 'peaked' prior to each element analysis. Background readings were taken for all elements, low and high 2θ values were taken

for Si and Al. A fixed counting time of ten seconds was used exclusively, although at least two readings were taken on each point.

The raw data, on the tape print-out from the electron microprobe, were reduced using the computer programme EMPADR VII, written by Rucklidge and Gasparrini (1969). A copy of this programme was kindly sent to Durham by Professor Rucklidge and it has been adapted for use on the IBM 360/67 N.U.M.A.C. computer, at Durham, by the writer. The correction procedures used, in the programme, are those suggested by Sweatman and Long (1969), a description is not given here as the workings of the programme are described in detail by Rucklidge and Gasparrini (1969).

X-ray fluorescence analysis

Major and trace element analyses have been made, on whole rocks, using a Phillips PW 1212 automatic X-ray fluorescence (X.R.F.) spectrometer with a printed tape output. The rocks were initially crushed in a tungsten-carbide Tema disc-mill and then the resultant powders were briquetted, as described by Holland and Brindle (1966). The standards used in the X.R.F. analysis of whole rocks were a selected portion of the argillaceous standards used in the Dept. of Geology, Durham. The error due to instrumental drift was minimized, during the analyses, by taking an intensity measurement of the characteristic radiation for each element by ratio against a monitor. The sources of error inherent in X.R.F. analysis, are not discussed here, as a comprehensive review of such features, and the operating conditions used, are given by Reeves (1971). The

conditions laid out by Reeves, are identical to those used in this work, the same equipment being used over a short period of time by both Reeves and the present author.

The analyses presented in Appendix 4.1 are direct comparisons with the standards except for the elements Si, Al and Fe, for which matrix corrections were applied. These corrections were applied as it was found that the standard error of estimate of the calibration curves, for these elements, was thus significantly reduced (Reeves, 1971). Water determinations have not been made for the samples (Appendix 4.1) and for this reason all the analyses, except for those with a high carbonate content, have been normalized, after the correction outlined above. The analyses have been derived using a computer programme written by Reeves (1971).

The Whin Sill major element analyses (Appendix 2.1) were direct comparisons with the standards. In this case the close range calibration method was used and samples of the Little Whin Sill, analysed wet-chemically, (Dunham and Kaye, 1965) were used as standards.

Trace-element analysis has also been undertaken by X.R.F., using a series of standard powders, made from Pilkington glass casts, as described by Brown et al. (1970). Background scatter was used as an internal standard, peak and background readings were taken at the appropriate 2θ values. The raw data were then processed, peak to background ratios were calculated for each element and referred to the calibration curves of the standards, using a computer programme written by R.C.O. Gill of the Dept. of Geology, University of Durham.

A series of separate standards, for the limestone determinations, (Appendix 4.3) were prepared by the author, using the internal standard method by the spiking of a sample, with the element to be determined. The detection limits for the trace-elements in the limestone determinations are shown in Table 1.2, with the standard deviations for the three elements, found consistently above the detection limit.

Table 1.2 Detection limits and standard deviations of trace element determinations in limestones.

Sample 18/4 marble

Element	^{x}Mean ppm	Std. dev. ppm	$^{+}$Detection limit ppm
Zr	-	-	3
Cu	11	3.4	3
Zn	-	-	4
Ni	-	-	2
Ba	30	9.1	5
Sr	264	2.7	3
Rb	-	-	4

(+), Detection limit = $3b^{\frac{1}{2}}$ b = background counts

(x), 15 readings

Appendix 1.1 Location of samples

Borehole 17

Sample		Depth m
17/1	marble	29.6
17/2	"	32.6
17/3	"	35.7
17/4	shale	38.0
17/5	marble	38.7
17/6	"	42.0
17/7	shale	42.2
17/8	sandstone	49.0
17/9	marble	50.3
17/10	sandstone	50.4
17/10A	calc-silicate	50.4
17/11	sandstone	50.5
17/13	"	51.5
17/14	shale	51.7
17/15	marble	51.7
17/17	"	52.4
17/18	"	53.9
17/20	Whin	55.1
17/24	sandstone	21.0
17/25	"	21.2
17/26	limestone	21.4
17/28	"	22.9
17/29	shale	25.3
17/30	"	25.5
17/31	limestone	26.8
17/34	"	42.0
17/35	sandstone	45.0
17/36	"	45.7
17/37	"	46.2
17/38	"	46.3
17/39	marble	49.2
17/40	"	50.1
17/41	calc-silicate	50.5
17/43	sandstone	42.3

Borehole 18

18/2	limestone	8.8
18/3	marble	10.9
18/4	"	13.9
18/6	"	16.8
18/7	"	17.0
18/8	"	20.0
18/9	"	23.1
18/10	"	26.1
18/11	Whin	31.4
18/12	"	38.1
18/13	"	40.9
18/14	"	42.5

Borehole 18

Sample		Depth m
18/16	Whin	43.8
18/17	"	45.5
18/19	"	48.3
18/20	"	54.3
18/21	"	57.3
18/22	"	58.8

Borehole 19

19/1	shale	25.2
19/4	calc-silicate	24.1
19/5	limestone	23.8
19/8	calc-silicate	23.0
19/9	"	27.5
19/10	sandstone	21.3
19/19	calc-silicate	25.0
19/20	"	25.2

Borehole 21

21/1	Whin	21.7
21/2	marble	21.3
21/4	"	18.0
21/5	sandstone	17.5
21/6	"	16.2
21/7	"	15.4
21/8	shale	15.3
21/9	marble	15.2
21/11	"	12.7
21/12	limestone	10.6
21/13	shale	4.8
21/14	"	4.1
21/15	sandstone	2.6
21/16	"	1.7
21/17	Whin	30.3
21/18	"	33.4
21/19	shale	5.6
21/20	"	5.8
21/21	siltstone	6.4
21/22	"	7.2
21/22A	"	8.5
21/23	limestone	10.2

Borehole 22

22/1	marble	40.3
22/2	"	38.7
22/3	"	37.4
22/5	Whin	68.2
22/7	marble	61.0
22/11	"	66.4

Appendix 1.1 Location of samples

Borehole 35

Sample		Depth m
35/1	Whin	20.1
35/2	"	18.3
35/3	"	16.5
35/4	calc-silicate	15.0
35/5	marble	14.9
35/6	"	14.6
35/11	"	7.6
35/13	limestone	4.1

Borehole 39

39/3	marble	88.1
39/4	"	86.6
39/7	limestone	85.3
39/8	"	83.9
39/19	marble	72.1
39/20	limestone	70.6
39/25	"	65.2

Borehole 40

40/2	marble	84.0
40/3	"	82.3
40/5	sandstone	80.6
40/6	"	79.3
40/7	wollastonite	78.4
40/9	"	78.1
40/10	marble	75.1
40/11	sandstone	74.9
40/12	"	74.4
40/13	limestone	72.9
40/14	shale	71.6
40/15	siltstone	69.0
40/16	sandstone	65.5
40/17	"	64.2
40/18	marble	63.4
40/19	limestone	61.2
40/20	marble	61.0
40/21	limestone	59.5
40/22	"	58.3
40/23	siltstone	58.0
40/25	sandstone	55.4
40/26	"	53.5
40/27	limestone	53.2

Borehole 41

41/1	sandstone	85.1
41/3	"	84.0
41/5	marble	82.5
41/7	limestone	82.3
41/8	"	81.4
41/9	marble	80.4

Borehole 41

Sample		Depth m
41/10	sandstone	79.9
41/11	limestone	79.7
41/12	"	78.9
41/13	"	77.9
41/14	mudstone	77.3
41/15	"	75.3
41/16	"	73.8
41/17	shale	72.7
41/18	sandstone	72.3
41/19	"	70.2
41/20	marble	70.0
41/21	"	67.5
41/22	"	67.1
41/23	"	65.8
41/24	limestone	65.6
41/25	"	65.5
41/27	mudstone	64.2
41/28	"	63.1
41/31	shale	59.2
41/32	sandstone	86.8
41/35	mudstone	91.7
41/36	contact-rock	92.3

Borehole 43

43/2	contact-rock	54.5
43/4	calc-silicate	53.5
43/5	"	53.1
43/6	"	53.0
43/7	limestone	52.7
43/7A	calc-silicate	52.1
43/8	sandstone	51.3
43/9	"	49.8
43/10	calc-silicate	48.9
43/11	impure lst.	48.3
43/12	sandstone	47.0
43/13	"	46.4
43/16	shale	41.3
43/21	limestone	33.5
43/22	calc-silicate	32.7
43/23	mudstone	32.3
43/25	"	29.7
43/27	sandstone	25.4
43/28	"	24.3
43/29	"	23.8
43/30	"	23.5
43/33	"	19.2
43/35	siltstone	15.4
43/36	sandstone	10.4

Appendix 1.1 Location of samples

Borehole 44

Sample		Depth m
44/7	calc-silicate	31.7
44/8	impure lst.	30.9
44/9	calc-silicate	29.9
44/9A	impure lst.	29.1
44/10	sandstone	28.3
44/11	calc-silicate	27.6
44/12	marble	27.2
44/14	mudstone	22.3
44/20	"	8.7
44/25	Whin	104.0
44/28	mudstone	107.9
44/28A	calc-silicate	108.2
44/32	mudstone	111.3

Borehole 45

45/1	contact-rock	62.3
45/5	sandstone	57.2
45/7	wollastonite	55.6
45/12	siltstone	49.7
45/13	"	47.2
45/14	sandstone	44.2
45/16	siltstone	36.0
45/17	sandstone	30.3

Borehole 46

46/2	calc-silicate	62.4
46/3	impure lst.	61.2
46/5	contact-rock	59.7
46/13	impure lst.	41.3

Borehole 47

47/1	shale	39.9
47/7	sandstone	48.6
47/8	shale	50.2
47/9	impure lst.	51.4
47/10	"	51.8
47/18	mudstone	72.2
47/19	impure lst.	72.9
47/20	"	73.4
47/22	sandstone	74.8
47/24	"	76.7

Rookhope borehole

Sample		Depth m
RB20	siltstone	206.3
RB21	mudstone	206.0
RB22	siltstone	205.7
RB23	"	204.5
RB24	"	204.8
RB25	sandstone	204.2
RB27	siltstone	203.6
RB31	"	187.1
RB32	sandstone	190.2
RB33	mudstone	191.6
RB34	siltstone	196.3
RB35	sandstone	199.3
RB37	siltstone	205.4
RB38	mudstone	194.4
RB39	"	206.7
RB41	shale	281.6
RB42	"	282.6
RB43	siltstone	287.9
RB44	mudstone	290.7
RB45	"	291.7
RB46	"	296.0
RB47	"	175.0
RB50	"	185.3
RB51	"	191.7
RB52	sandstone	194.7
RB53	"	186.2
RB54	"	197.8
RB56	limestone	367.4
RB57	"	364.2
RB59	"	360.8
RB69	"	345.6
RB72	"	315.5
RB75	"	175.9
RB78	"	142.3
RB81	"	13.3

Ninebanks borehole

L/860	Whin pegmatite	260.8
L/876	"	265.7

Falcon Clints

UT/19	Whin contact
UT/37	"

CHAPTER II

WHIN SILL AND HEAT-FLOW CALCULATIONS

Introduction

The Whin Sill, of northern England, has long been cited as one of the classic examples of a quartz-dolerite intrusive sheet. It has been the subject of intensive study for over a century and the most important works include those of Teall (1884a-b), Holmes and Harwood (1928), Tomkeieff (1929) and Smythe (1930). This work has concentrated on field characters, petrography and chemistry but little attention has been paid to the metamorphism. The present study, in contrast, concentrates on the metamorphic effect but some attention has also been given to Whin samples close to the contact, as described later.

Once the igneous character of the Whin had been established early in the last century, there was controversy as to whether the sheet was a contemporaneous flow, or an intrusive body. Hutton (1832), Sopwith (1833) and Phillips (1836) all suggested it was a lava flow. However, Sedgwick (1827), Wood (1831) and Topley and Lebour (1877) finally proved its intrusive character, owing mainly to the associated metamorphism, both above and below the sill and its variation in stratigraphical horizon.

THE WHIN SILL COMPLEX

The Whin Sill complex consists of a series of interconnected or related sills and four sets of dyke en echelons. The dyke en echelons have a ENE trend and sets are found at both the southern and northern limits of the sill-like intrusions. Holmes and

Harwood (1928) have suggested that the dykes represent feeders for the sill, with possible further concealed feeders beneath the Pennines, Fitch and Miller (1967) also support this view.

The sill does not remain at a constant stratigraphical horizon, but varies from the lowest known position in Upper Teesdale, where it intrudes the Lower Limestone Group, to the highest known position in a faulted outlier of Coal Measures at Midgeholme (Trotter and Hollingworth, 1932). The Whin Sill has been dated by the potassium-argon method (Fitch and Miller, 1967) giving a Stephanian age of 295 $\pm$ 6 My. Dunham (1948) showed that the sill gradually rises in the succession away from Upper Teesdale, but over large areas it remains at a constant horizon, migration upwards occurring at definite zones. Along with the upward rise in the succession, there is a general thinning of the sill away from Upper Teesdale where it reaches one of its greatest thicknesses of over 73 m. This Upper Teesdale section has long been the thickest known but recently a borehole at Ninebanks, West Allendale has proved a maximum of over 80 m of Whin. The sill thins to less than 8 m on the Northumberland coast at Bamburgh.

The whole complex forms a single petrographical province with quartz-dolerite dominant. The intrusion has long been regarded as a classic tholeiite on the basis of the glassy mesostasis, which consists of quartz and alkali feldspar when crystalline. Dunham and Kaye (1965) have shown, however, that when plotted on a total alkalies, silica diagram, the Whin falls in between the classic alkaline and tholeiitic basalt series. Tomkeieff (1929) and Smythe (1930) have recorded

silicic differentiates, of the Whin in Northumberland, showing some enrichment in alkalies.

The Whin petrography is very uniform, with a mineral composition, as estimated by Dunham (1948) as follows:- pyroxene 34%, plagioclase feldspar 46%, hornblende, biotite and chlorite 4½%, iron-titanium oxides 8%, quartz, orthoclase and micropegmatite 5½%. Four textural varieties have also been recognised by Dunham (1948) as follows:-

1) Tachylitic facies - a marginal rock type.
2) Fine-grained, grey dolerite.
3) Medium-grained dolerite.
4) Pegmatite-dolerite with grey and pink granophyric varieties.

Although the Whin is known through many detailed works, the author has examined contact samples and analysed three suites of samples up to the contact. This work was undertaken to record variation, if any, of the Whin up to its contact. Clough (1880) envisaged large scale assimilation of sedimentary strata by the Whin. His conclusions were based on field observation, mainly the lack of mechanical disturbance in sedimentary beds at the contact and the absence of strata in places such as Rowantree Syke, Upper Teesdale, where it was claimed approximately 6 m of sediments are missing because of assimilation by the sill. Clough's assertions are not viable according to later work and the present analyses, there is no supporting evidence for such large scale assimilation.

White Whin

White Whin, an alteration product of the original dolerite, is commonly associated with alteration produced by the northern Pennine mineralizing solutions. This alteration, of the dolerite to a carbonate-clay mineral rock, has been well described by Wager (1929a). The effect has been compared with the white traps of Scotland, which are found at the contacts of basic igneous rocks and carbonaceous shales, oil shales or coals. Such contact alteration is not seen with the Whin Sill. Although the sill cuts and comes into contact with numerous limestone horizons there is nowhere, evidence for assimilation of the country rock with subsequent production of hybrid rocks such as feldspathoidal and melilite bearing rocks. In some cases, the immediate contact rocks show inclusions of quartzose fragments but again little sign of reaction is present between these and the Whin.

Contact modifications

The tachylitic margin has been recognised in all contact specimens examined. Generally the Whin shows a sharp, clear contact with the country-rocks, but in detail it may be undulating and irregular. The actual contact is often marked by a concentration of very fine-grained magnetite-ilmenite material giving the rock a very dark colour. Set in this opaque material are phenocrysts of dominant feldspar, often in the first centimetre at the contact, showing flow orientation parallel to the contact. In the specimens examined from Teesdale, feldspar and pyroxene phenocrysts are present in the contact zone suggesting

that these were present in the magma on intrusion, indicating that the magma was probably intruded close to its liquidus temperature. Thin-sections of the contact show pyroxene dominant (UT/19), in some cases, while in others feldspar is dominant with minor pyroxene (44/28 and UT/37). The varying amounts of these two minerals present in the samples suggests that they crystallized at a similar temperature, which from Yoder and Tilley's (1962) work is suggestive of a rather low water content in the magma. The maximum water vapour pressure acting in Teesdale and West Allendale, can be estimated from probable overburden (Trotter and Hollingworth, 1932; Johnson and Dunham, 1963; Dunham and Kaye, 1965), as between 300 to 400 bars.

The feldspar laths close to the contact are usually highly sericitized, but unaltered varieties are occasionally seen with a maximum extinction angle of 29°, indicative of labradorite, An50. Pyroxenes are usually fresh with only marginal alteration. Augite is subhedral and granular showing low, second-order interference colours with a low to moderate 2V. Some crystals of orthopyroxene are also present.

CHEMICAL VARIATION

The variation in chemical composition of the Whin Sill, with distance from contact is shown in Fig. 2.1. The actual analyses used in the plots are tabulated in Appendix 2.1, along with other analyses from samples within 1.5 m of the contact.

The plot of borehole 18 (Fig. 2.1) shows results, ranging from 1.5 m up to 29.9 m from the contact, which have a

Figure 2.1 Major element variation in the Whin Sill, with distance from contact.

Country rock at contact, shown alongside each diagram.

Figure 2.2 Trace element variation in the Whin Sill, with distance from contact.

Figure 2.1

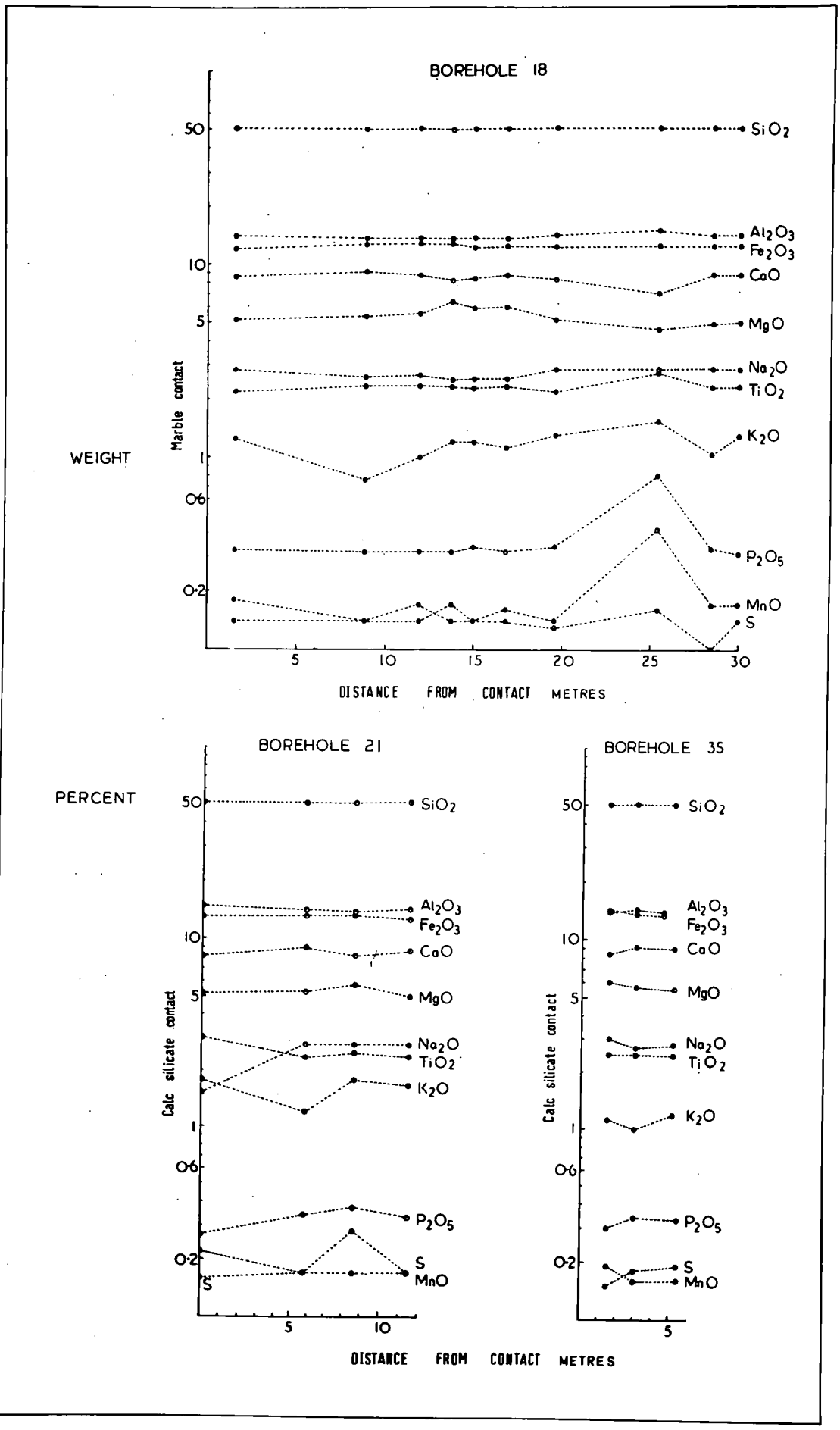
BOREHOLE 18
WEIGHT
Marble contact
50
10
5
1
0·6
0·2
SiO2
Al2O3
Fe2O3
CaO
MgO
Na2O
TiO2
K2O
P2O5
MnO
S
5
10
15
20
25
30
DISTANCE FROM CONTACT METRES
BOREHOLE 21
BOREHOLE 35
PERCENT
Calc silicate contact
DISTANCE FROM CONTACT METRES

remarkable consistency and no systematic variation is seen in any element. Samples from boreholes 21 and 35 again show no systematic variation. No similar analyses across the Whin Sill have been made for comparison, except for those across the Little Whin Sill made by Dunham and Kaye (1965). They also noted no variation in their analyses, save for an increase in the $FeO:Fe_2O_3$ ratio towards the centre of the sill. As the Fe is given as total Fe_2O_3, this variation cannot be verified in the present case.

The present analyses show a very close relationship to Holmes and Harwood's (1928) analyses, especially in the slightly higher SiO_2 and lower Al_2O_3 as compared to Smythe's (1930) results. The lower Al_2O_3 values are also supported by Harrison (1968) but his SiO_2 values are in close agreement with Smythe's. Overall, however, the analyses merely confirm the uniformity of the bulk composition of the Whin Sill.

The specimens from the chilled contact, numbers 35/3 and 21/1, which would be expected to preserve the features of the original magma, on intrusion, show only minor differences to that of 18/22 over 29 m from the contact. The two contact specimens show slightly lower SiO_2, higher Fe_2O_3 and MgO than 18/22. However, if this variation is significant it cannot represent a gradual change over the 30 m as the changes are not reflected in Fig. 2.1. The difference must, therefore, be reflected only in the immediate contact selvages represented by samples 35/3 and 21/1.

The Whin samples have also been analysed for five trace elements, Zr, Sr, Rb, Zn and Cu and the results tabulated in Appendix 2.2. As with the major element analyses, no systematic

Figure 2.2

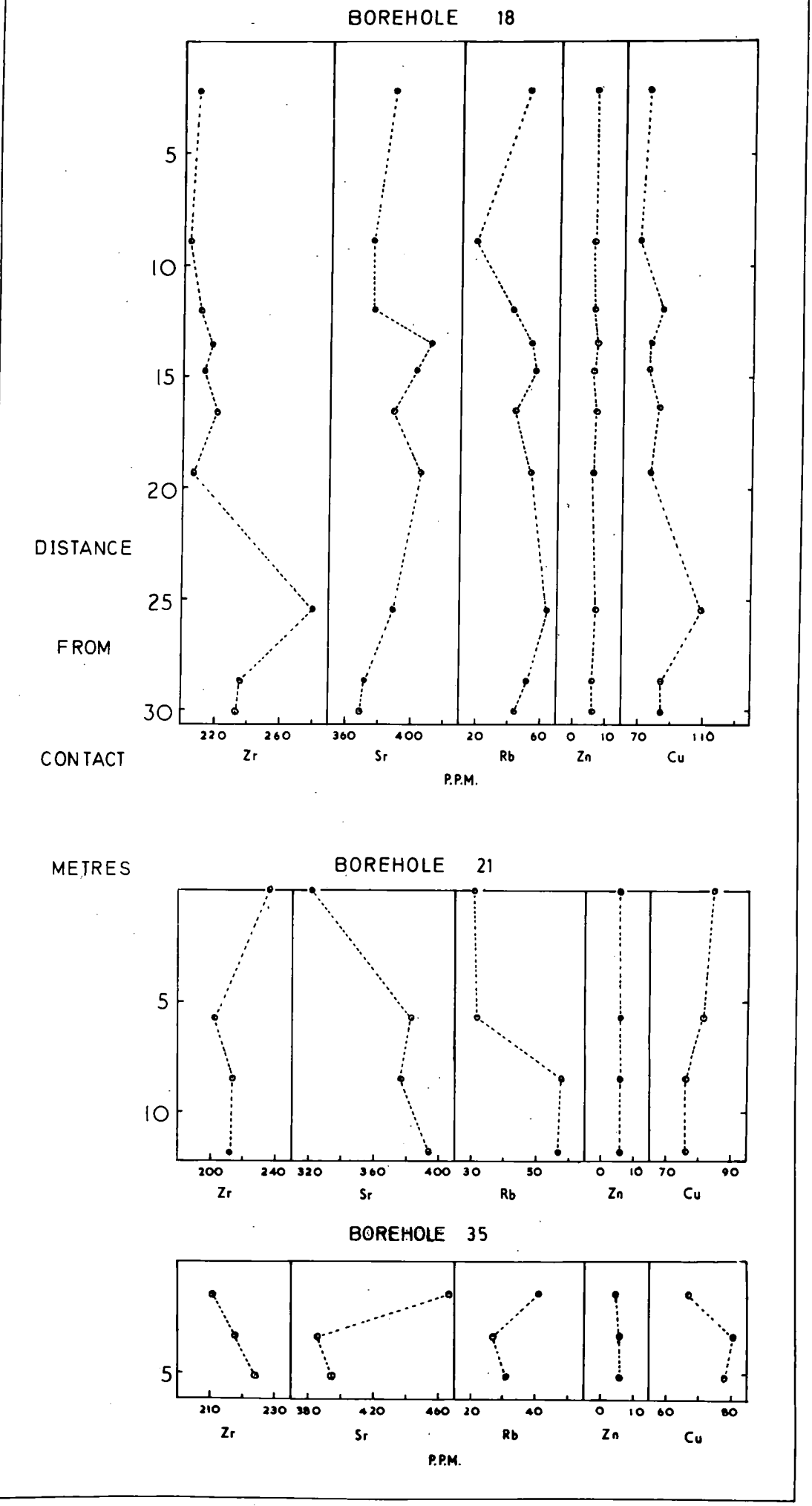
BOREHOLE 18
DISTANCE FROM CONTACT
METRES
5
10
15
20
25
30
220
260
Zr
360
400
Sr
20
60
Rb
0
10
Zn
70
110
Cu
P.P.M.
BOREHOLE 21
5
10
200
240
Zr
320
360
400
Sr
30
50
Rb
0
10
Zn
70
90
Cu
BOREHOLE 35
5
210
230
Zr
380
420
460
Sr
20
40
Rb
0
10
Zn
60
80
Cu
P.P.M.

variation can be seen away from the contact, and again the uniformity of the measurements is the noticeable point to emerge. The between section variation of the above elements is also low, as there is reasonable correspondence between the concentration of elements in all three sections

The values of Zr and Sr agree well with Harrison's (1968) bulk analysis of the Whin Sill while Cu is a factor of two higher (Appendix 2.2). The Zr and Rb values agree reasonably well with the values given by Dunham and Kaye (1965) for the Little Whin Sill. Strontium in the Little Whin Sill is significantly higher than both the average values for the Great Whin Sill, which is unusual, as Sr is usually concentrated during crystallization.

The general marked lack of chemical variation, away from the contact, both in major and trace elements suggests that the sill cannot have assimilated any sediment during intrusion, as was envisaged by Clough (1880), or suffered any marked differentiation.

One of the most notable features in thicker sections of the Whin, are the pegmatite bands. The borehole at Ninebanks recorded several of these bands. Major element analyses of two samples from these pegmatites (L/860 and L/876) are given in Appendix 2.1. Comparing these analyses with the normal Whin, there is an increase in total Fe, TiO_2 and P_2O_5 with a decrease in the MgO, Al_2O_3 and CaO contents. These pegmatites are coarse-grained with large pyroxenes and long, skeletal grains of opaques. The feldspars, of these pegmatites, are dominantly quite turbid and sericitized. Electron microprobe analyses of the feldspars are given in Appendix 5.2. Two of the crystals, L/860-1 and L/860-3 are andesine in composition, L/860-3 showing an increase of the albite

molecule from 52.4%, at the centre, to 54.5% at the crystal rim. Crystal L/860-2 is an albite, with over 96% of the albite molecule. Tomkeieff (1929) has shown that andesine is the average composition of plagioclase in the pegmatites.

Pyroxene, often altered, occurs abundantly in the pegmatites, but some fresh sections show a herring-bone structure and hour-glass zoning. A graphic intergrowth of feldspar and pyroxene is widespread. Abundant quartz is present occurring mainly in a myrmekitic intergrowth with feldspar.

Hornblende has long been recorded as an alteration rim to pyroxenes in the pegmatites. The sample L/860, however, showed euhedral, basal sections of green-brown hornblende. The euhedral outline and freshness of the crystals suggest that it is a primary phase and as such is the first recorded instance in the Whin Sill. Rarely a graphic intergrowth of green, fresh hornblende is seen with feldspar.

Apatite is very abundant throughout the samples occuring as long, slender needles. Opaque minerals occur abundantly in long, skeletal grains, the high TiO_2 content suggestive of a high percentage of the ilmenite molecule in the opaques.

For primary hornblende to crystallize from an olivine-tholeiite magma, a minimum water vapour pressure in the region of 1000 bars is suggested by Yoder and Tilley (1962). During the crystallization of the Whin magma, water must be concentrated into the pegmatite bands giving rise to an increased water pressure. An earlier estimate of maximum water pressure, based on the probable overburden, gave a value in the region of 300 to 400 bars which is significantly below the minimum value suggested by

experimental work.

Further research into these pegmatites would, therefore, be most useful in the elucidation of their petrogenesis.

Conclusions

The tachylitic margins of the Whin Sill show flow-orientated phenocrysts of feldspar in association with pyroxene which is suggestive of intrusion close to the liquidus temperature of the magma. Chemical analyses of nineteen Whin samples, for eleven major elements and five trace elements, have confirmed the overall bulk uniformity of the sill. No evidence for assimilation or differentiation could be seen from the analyses. Two samples of pegmatites from Ninebanks, West Allendale have also been analysed. Enrichment in total Fe_2O_3, TiO_2 and P_2O_5 is seen. Petrographic examination has shown the presence of primary hornblende, in these pegmatites, this being the first recorded instance from the Whin Sill.

THEORETICAL HEAT-FLOW CALCULATIONS

Calculations of theoretical metamorphic temperatures attained in the contact metamorphic aureole of the Whin Sill were undertaken at an early stage in the present investigation. These have provided some notation of the variation in temperature around the intrusion in relation to the observed metamorphism. The values obtained from the calculations are not regarded as absolute, since there is some uncertainty inherent in the mathematical model as outlined below.

A number of workers have made attempts to systematize the

cooling history of igneous intrusions. Earlier workers (Lovering, 1955; Larsen, 1945) have neglected the effect of latent heat of crystallization of the magma. This has a profound effect on the temperatures in the metamorphic aureole and for this reason Jaeger's equations (1957, 1959, and 1964), which include the effect of latent heat, have been used exclusively in the present study.

Assumptions involved and their relationship to the Whin Sill

Nature of intrusion

For simplification, in the calculations, the intrusion is assumed to be a sheet-like body of constant thickness and extending indefinitely in the horizontal plane.

The Whin Sill conforms to this pattern almost ideally. Although the sill transgresses the Carboniferous strata, it does so along definite belts (Dunham, 1948; Dunham, 1970). Between these belts the sill often remains at a constant horizon over large areas. In the main area of investigation (Upper Teesdale) the sill remains fairly constant in thickness at 73 m.

Temperature of the magma

The intrusion is assumed to have taken place rapidly, compared to the time of solidification, into rocks of zero ($0^{o}C$) temperature. The magma is also assumed to have been intruded at a constant temperature equal to its liquidus temperature.

Dunham (1948) recognised a fine-grained, tachylitic marginal facies of the Whin Sill, which is suggestive of sudden intrusion into relatively cold country rocks. The presence of phenocrysts of plagioclase and pyroxene in contact specimens suggests that

the Whin Sill was intruded close to its liquidus temperature. An estimate of the liquidus temperature may be obtained from the work of Yoder and Tilley (1962), who have shown that for a quartz-dolerite the liquidus temperature lies at approximately 1180°C, at atmospheric pressure. The solidus and liquidus temperatures used in the calculations have been adjusted to allow for the effect of water vapour pressure. A maximum water pressure in the region of 300 to 400 bars is envisaged during crystallization of the Whin Sill magma in Teesdale. This is estimated by analogy with the Coal Measures in eastern Durham, where a thickness of 1067 m of sediment is present above the Three Yard Limestone (Dunham and Kaye, 1965). In Upper Teesdale, a further 150 m of sediment is present below this limestone, giving a total cover in the region of 1200 m of strata. The actual values used in the calculations were 1150 and 1000°C for the liquidus and solidus temperatures respectively.

Heat loss from the cooling magma

For the purpose of the calculation, the magma heat loss is assumed to be by conduction only. Convective effects after emplacement, which would increase contact temperatures significantly, are not considered.

Evidence for convection in the Whin Sill, in the form of differentiation or layering is not present. Heat loss by the escape of volatiles is not considered because the heat carried by the volatiles would be dissipated over a large area and would probably not contribute significantly to the elevated temperatures in the country rocks.

Effect of latent heat

Jaeger's formulae are an advantage over earlier work, on contact metamorphic temperatures, as corrections can be made to cover the effect of the latent heat of solidification of the magma. The correction was made by an addition to the specific heat using the following equation:

$$c_1 = c + L/(T_1-T_2)$$

(symbols defined overleaf)

Thermal properties of rocks

For simplicity, the thermal properties of the country-rock and the solidified magma are assumed to be equal and independent of pressure or temperature.

The density used in the calculations was 2.9 g/cm^{-3}, a value given for the Whin Sill by Clark (1966), a density for marble was also given as 2.8 g/cm^{-3}. Little information is available on the specific heats of rocks, therefore, a value of 0.25 cal/gm/^{o}C was used, as suggested by Jaeger (1957). The thermal conductivity values, used in the calculations, are from the work of Dr. J. Weilden, Imperial College, London, who made several determinations on samples from the Rookhope borehole. A thermal conductivity value of 0.007 cal/cm sec^{o}C was used for calculations representative of the intrusion in Teesdale. A value of 0.005 cal/cm sec^{o}C was used for the models of Rookhope and Ninebanks, where there is a greater amount of shale and siltstone, close to the intrusion, as compared to Teesdale. Little is known on the latent heat of solidification of magmas and a value of 80 cal/gm was used as suggested by Jaeger (1957).

Formulae used for computation

The basic formula used in the calculations is from Jaeger (1964) and is given below:-

$$T = \frac{1}{2}\left[\operatorname{erf}\frac{\xi+1}{2\tau^{\frac{1}{2}}} - \operatorname{erf}\frac{\xi-1}{2\tau^{\frac{1}{2}}}\right] \qquad \text{——— 1}$$

$$\xi = x/d \qquad \text{——— 2}$$

$$\tau = kt/d^2 \qquad \text{——— 3}$$

$$k = K/\rho c \qquad \text{——— 4}$$

T = temperature of country rock.

x = distance from the central plane of the igneous body.

d = $\frac{1}{2}$ thickness of intrusive sheet.

t = time after intrusion (seconds).

ρ = density of rocks.

c = specific heat of rocks

c_1 = specific heat corrected for latent heat of solidification.

K = thermal conductivity of rocks.

k = diffusivity of rocks.

L = latent heat of solidification of magma.

T_1 = liquidus temperature of magma.

T_2 = solidus temperature of magma.

τ = fourier number.

Equations 2 and 3 give the dimensionless quantities of ξ and τ which are substituted in the main equation, 1. A corrected value for specific heat, taking into account the latent heat, is used as shown previously (p.25).

As calculations proved lengthy, the computation has been achieved by means of a small programme written in PL1, by M.J. Reeves.

Figure 2.3 Theoretically calculated temperatures for Whin Sill aureole.

Solid line shows values for the intrusion in Upper Teasdale.

Dash-dot line represents temperatures for the Rookhope intrusion.

Dash-double dot line represents temperatures for the Ninebanks intrusion.

Figure 2.3

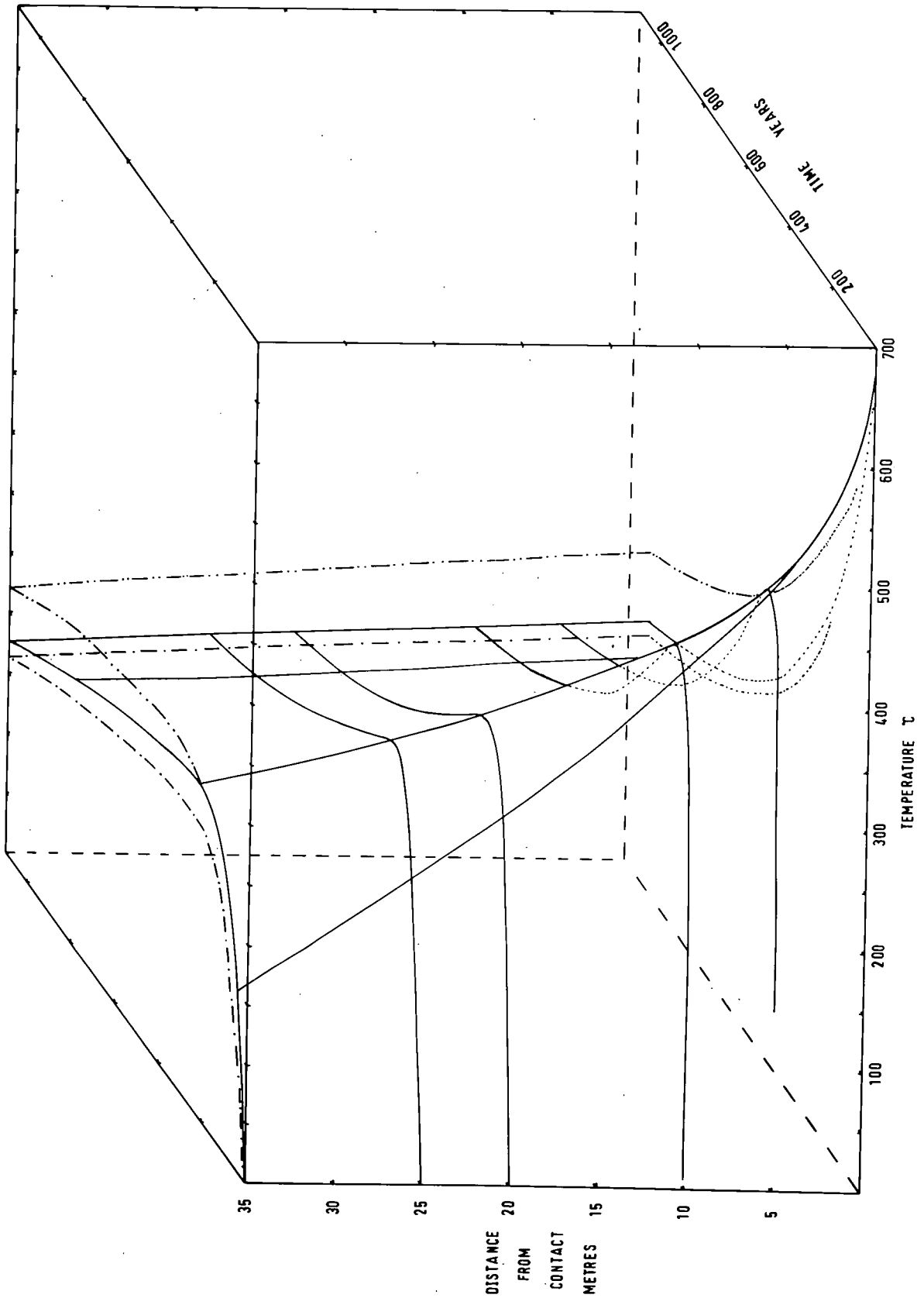
TIME YEARS
200
400
600
800
1000
TEMPERATURE τ
100
200
300
400
500
600
700
DISTANCE FROM CONTACT METRES
35
30
25
20
15
10
5

Results of calculations

Temperature curves have been plotted in the form of a three-dimensional diagram (Fig. 2.3). The solid lines of the graph indicate calculated temperatures for the aureole in Upper Teesdale, the dash-dot line and the dash-double dot line show the calculated temperatures at Rookhope and Ninebanks, respectively. The horizontal curves show the change in temperature, at a constant distance from the contact, with time. Close to the contact the temperature rises rapidly to a maximum, then drops rapidly to a state, after some 600 years, where there appears to be a gradual, linear decrease in the temperature. Away from the contact the sharp apex of the maximum temperature is no longer evident. A vertical curve shows the variation in temperature with distance from the contact, at a particular time after intrusion, the gradient of which is most steep, immediately after the intrusion. With an increase in time after the intrusion, the slope of the curve decreases such that the temperatures become more even and there is only a difference of some 50°C between the contact and a point 35 m from the contact, after 1000 years.

The results for Rookhope are lower than for Upper Teesdale as would be expected since the sill is only 58 m thick compared with 73 m in Upper Teesdale. The Ninebanks section, with 80 m of Whin recorded, shows the maximum theoretical temperatures. Thus from theoretical considerations the maximum metamorphism, associated with the Whin Sill, might be expected at Ninebanks. This, however, is contrary to the known geological observations and this anomaly is considered in Chapter VI.

Appendix 2.1 Whin Sill major element analyses.

	18/11	18/12	18/13	18/14	18/16	18/17	18/19
SiO_2	51.54	51.16	50.99	50.54	51.15	51.10	51.56
Al_2O_3	14.19	13.78	13.83	13.67	13.81	13.68	14.35
$^+Fe_2O_3$	12.16	12.81	12.97	12.92	12.31	12.53	12.38
MgO	5.21	5.40	5.59	6.40	5.97	6.00	5.18
CaO	8.68	9.23	8.87	8.28	8.54	8.83	8.41
Na_2O	2.86	2.62	2.67	2.53	2.52	2.54	2.85
K_2O	1.26	0.76	1.02	1.20	1.20	1.12	1.32
TiO_2	2.21	2.34	2.35	2.33	2.27	2.33	2.21
MnO	0.18	0.14	0.17	0.14	0.14	0.16	0.14
S	0.14	0.15	0.14	0.17	0.14	0.14	0.13
P_2O_5	0.33	0.32	0.32	0.32	0.34	0.32	0.34
Total	98.76	98.71	98.98	98.50	98.39	98.75	98.87

	18/20	18/21	18/22	21/1	21/24	21/17	21/18
SiO_2	51.20	51.60	51.15	51.03	50.13	50.33	50.87
Al_2O_3	12.51	14.14	14.17	14.74	14.00	13.80	14.13
$^+Fe_2O_3$	14.97	12.44	12.58	13.05	13.07	13.12	12.53
MgO	4.56	4.91	4.99	5.20	5.27	5.69	4.98
CaO	7.10	8.89	8.83	8.16	8.98	8.08	8.56
Na_2O	2.81	2.87	2.86	1.51	2.73	2.78	2.73
K_2O	1.71	1.31	1.28	1.76	1.19	1.76	1.64
TiO_2	2.72	2.31	2.31	3.00	2.33	2.46	2.34
MnO	0.18	0.17	0.17	0.22	0.17	0.17	0.17
S	0.16	0.10	0.14	0.16	0.18	0.28	0.17
P_2O_5	0.42	0.33	0.31	0.27	0.34	0.37	0.33
Total	98.34	99.07	98.79	99.10	98.39	98.84	98.45

	35/3	35/2	35/1	17/20	22/5	L/860	L/876
SiO_2	49.93	50.20	49.92	49.92	49.78	51.24	49.84
Al_2O_3	13.84	14.25	13.78	13.45	13.85	11.21	11.32
$^+Fe_2O_3$	14.07	13.50	13.35	14.07	13.26	14.80	16.00
MgO	6.03	5.64	5.47	8.60	5.46	4.81	4.58
CaO	8.42	9.12	8.88	7.13	8.31	6.12	8.75
Na_2O	3.02	2.68	2.78	1.60	2.87	2.48	2.01
K_2O	1.12	0.99	1.19	0.26	1.37	1.47	0.87
TiO_2	2.45	2.46	2.44	2.36	2.37	3.72	3.92
MnO	0.19	0.16	0.16	0.16	0.16	0.14	0.14
S	0.15	0.18	0.19	0.18	0.17	0.30	0.20
P_2O_5	0.30	0.34	0.33	0.24	0.32	0.36	0.45
Total	99.52	99.52	98.49	97.97	97.92	96.65	98.08

(+), Total iron

Appendix 2.2 Whin Sill trace element determinations ppm.

	Zr	Sr	Rb	Zn	Cu
18/11	209	389	36	6	75
18/12	204	376	20	6	70
18/13	211	377	31	6	84
18/14	218	412	37	7	77
18/16	213	403	38	6	76
18/17	221	389	32	7	82
18/19	207	406	37	6	77
18/20	280	389	42	7	109
18/21	236	372	36	6	84
18/22	233	369	32	6	84
21/1	236	322	31	6	85
21/24	203	383	34	6	83
21/17	214	377	58	6	75
21/18	212	394	57	6	76
35/3	211	467	41	5	67
35/2	218	386	27	6	81
35/1	224	395	31	6	78
17/20	225	326	11	4	84
22/5	191	505	44	6	78
Average	219	391	36	6	80
*Little Whin Sill Average	203	449	20	109	59
+Great Whin Sill Woodland	200	370			45

* Dunham and Kaye (1965)

\+ Harrison (1968)

CHAPTER III

PETROLOGY OF METAMORPHOSED SEDIMENTS

METAMORPHISM OF SHALES

The shales in the Whin Sill aureole have not been greatly affected by the metamorphism. There has usually been just a simple recrystallization of the original clay minerals, to a fine-grained, sericitic material and for this reason X-ray diffraction has been used extensively in studies of the shales.

The normal, unmetamorphosed Carboniferous shales of the region are fine-grained and dark in colour, with well developed bedding. The main minerals present are quartz and illite, with some chlorite and kandite-type minerals.

Spotting in the shales is well developed on metamorphism, Dunham et al. (1965) recorded spotting to over 36 m from the contact in the Rookhope borehole and similar distances have been recorded in Upper Teesdale. These spots vary in size from 0.05 to 0.45 mm and show a concentration of semi-opaque, brownish-grey material, possibly of bituminous matter. Some of the spot areas were removed and X-rayed by powder photography. Only quartz, illite and chlorite were recorded. Dunham's (1948) record of andalusite in clear spots in the shales has not been confirmed in the present survey.

Close to the contact, the shales are converted to porcellanites, due to the recrystallization of the clay minerals, in which the bedding is destroyed. These porcellanites are cream in colour, in contrast to the dark colour of the normal shales, the difference probably being due to the loss or recrystallization

of organic material on heating.

Petrographic examination has been of little value in the examination of the shales, as the metamorphism has not been extensive enough to cause large scale generation of muscovite and biotite from the clay minerals. Extensive recrystallization can often be seen in samples within 10 m of the contact, but the material is a very fine-grained sericite.

X-ray diffraction studies

Illite has been the only clay mineral examined, because of its dominance in the Carboniferous shales. Chlorite is not present in all the shales and occurs in much smaller amounts, as compared to illite. Prior to diffraction, the samples were separated as described in Appendix 3.1. The conditions used during the diffraction runs are shown in Appendix 3.2.

Two main aims were in mind during this study, (1) to show if there is any variation in the illite clay-mineral polymorph towards the contact, and (2) to trace any change in crystallinity as shown by the 10 Å peak of the illite.

Variation in polymorphism

The minerals of the mica group (including illite) occur in several polymorphs resulting from differences in arrangement of the atomic planes. Three main polymorphs are known (Yoder and Eugster, 1955):

1. The two-layer, monoclinic polymorph 2M
2. The one-layer, monoclinic polymorph 1M
3. The one-layer, disordered monoclinic polymorph 1Md

Yoder and Eugster observed a transformation from the 1Md form

to 1M and 2M with increasing temperature and suggested that this was the sequence involved during metamorphism. They found that the 2M structure was the stable form in the range 200 to 350°C, at 15000 psi water pressure. The actual identification of the polymorph, in the present study, is somewhat subjective, especially when there is, in some cases, a mixture of two varieties together with chlorite.

The polymorphs have been differentiated using the presence and strengths of reflections as shown in Table 3.1, which is based on the work of Yoder and Eugster (1955) and the A.S.T.M. index. The strength of the 004 reflection at 5.0 Å is a useful guide, as it is weak and ragged in the 1Md variety but increases in height and sharpness in the 1M and 2M varieties.

Table 3.1 Identification of illite polymorph

1Md		1M		2M	
Å	Strength	Å	Strength	Å	Strength
10.1	100	10.1	100	10.0	100
5.0	20	5.0	37	5.0	55
4.5	50	4.5	90	4.5	55
		4.4.	27	4.4	26
				4.3	21
		4.1	16	4.1	14
				4.0	12
				3.9	37
		3.7	60	3.7	32
3.4	100	3.4	100	3.4	100
		3.2	50	3.2	47
				3.0	47
		2.9	6	2.9	35
		2.8	16	2.8	22
2.6	40	2.6	50	2.6	50

Harbord (1962) has shown that the dominant illite polymorph in the shales of the Yoredale Series, of Upper Teesdale, is the 1Md variety with some occasional admixed 2M varieties.

The dominant polymorphs recorded from samples ranging from 30 m up to the contact, are shown in Fig. 3.1A. The samples are from a number of boreholes and the calibration data are shown in Appendix 3.3. The unmetamorphosed shales, greater than 25 m from the contact, consist dominantly of the 1Md variety except for one sample with the 2M polymorph. There is a change in the type of illite polymorph towards the contact, the 1Md form becoming superceded by the 1M and 2M varieties. This change has occurred solely in response to an increase in temperature, pressure having been low and most probably of constant value over the whole aureole. Experimental work and previous geological research (Yoder and Eugster, 1955; Maxwell and Hawer, 1967) has tended to suggest that pressure plays an important role in these transformations but the current work suggests that temperature alone is sufficient to produce polymorphic transformation.

Variation in crystallinity

It is known that the crystallinity of illite increases with temperature, pressure being of no significance (Kubler, 1966; Winkler, 1970). Kubler measured the width of the 10 Å peak at half peak-height and found that this value (i.e. crystallinity) decreases with an increase in metamorphic temperature. This measurement has been made on the present samples and is shown in Fig. 3.1B. There is a trend from larger peak-widths, at 30 m from the contact, to smaller values close to the contact, as shown in Fig. 3.1B by the dashed line. A reduction in the peak-width of approximately 40% is seen but there is quite a marked scatter of points about the dashed line. Associated with this decrease in

Figure 3.1 Variation in illite crystallinity and polymorphism, with distance from contact.

3.1A Variation in the ratio peak-height:width, with distance from contact. The dominant polymorph recorded is shown against each sample.

1Md one-layer, disordered monoclinic polymorph.

1M one-layer, monoclinic polymorph.

2M two-layer, monoclinic polymorph.

The two dashed lines define upper and lower limits, in the present case, to the change in the peak-height:width ratio of illite towards the contact.

3.1B Variation in the illite 10 Å peak-width with distance from contact.

Dashed line shows trend towards a norrower peak-width close to the contact.

Figure 3.1

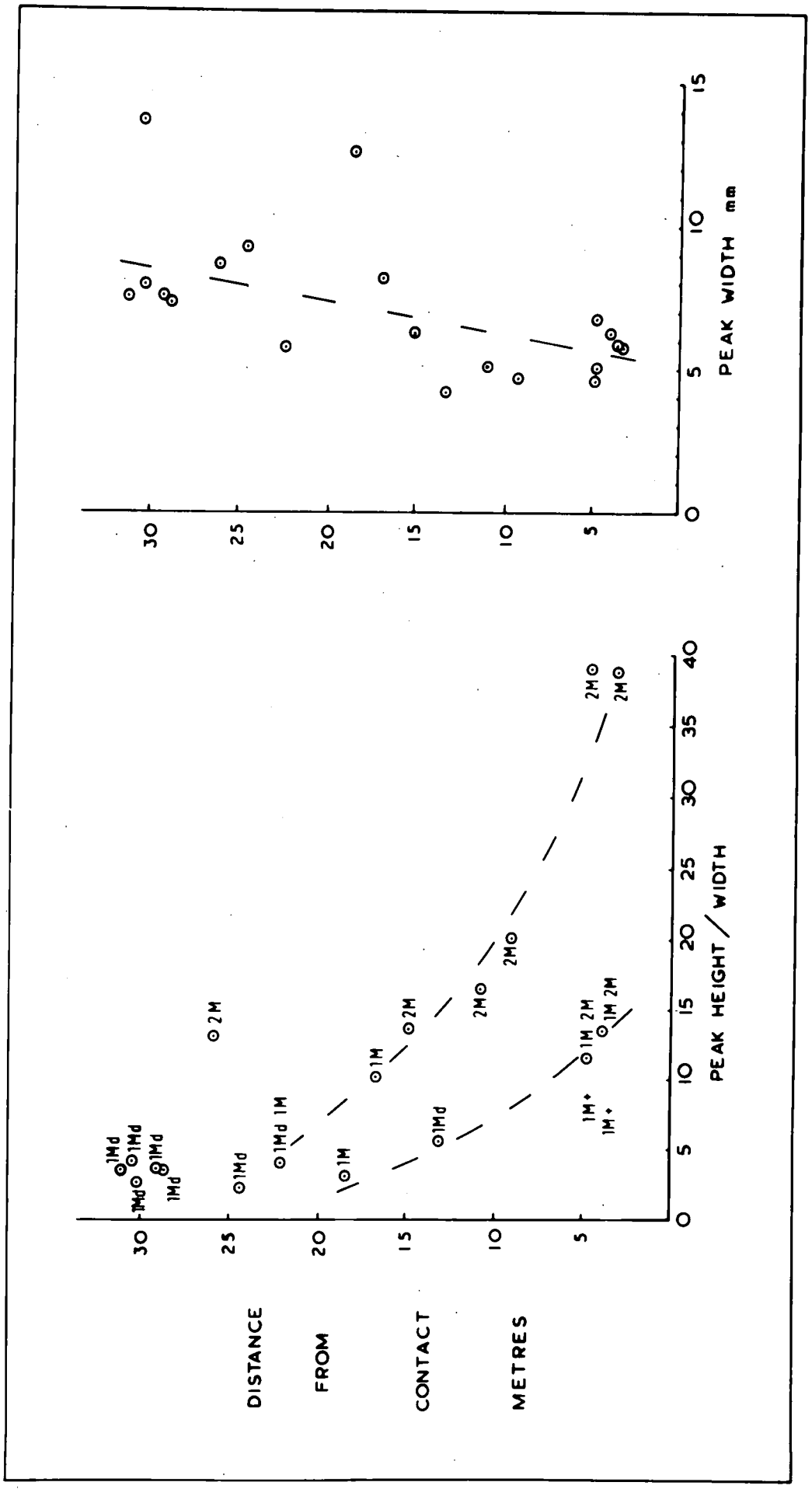
3.1A
3.1B
DISTANCE FROM CONTACT METRES
PEAK HEIGHT / WIDTH
PEAK WIDTH mm
0
5
10
15
20
25
30
35
40

peak-width, there is a marked increase in the peak-height of the 10 Å, 001 reflection. The peak-height by itself is indicative of a change in the crystallinity but it is also affected by features such as the proportion of illite present and preferred orientation. The ratio of peak-height against peak-width has, therefore, been plotted against distance from contact as shown in Fig. 3.1A.

As shown by the dashed lines, there is a well defined increase in this ratio towards the contact. At distances greater than 20 m from the contact the index appears to remain constant between the values 2 and 4, for the six samples plotted. This is suggestive of a 'background index' for the illite, prior to metamorphism, where the 10 Å peak is relatively broad and weak. One value is significantly higher than this constant index, the sample being a siltstone with abundant, large mica flakes on the bedding planes. Thus it seems this higher index must represent a 'remanent' value because the mica has not been completely weathered. At distances less than 18 m from the contact there is an increase in the peak-height:width ratio as the clay minerals recrystallize to a more complex structure. There is no simple linear increase in the ratio, it is a rather broad, but significant trend with a maximum index of almost 39 reached less than 6 m from the contact. The two points marked by crosses are results from very pure sandstones in which the clay mineral content was minimal and difficult to concentrate.

Conclusions

Petrographic examination has been of little use in examination of the shales but X-ray diffraction studies have proved

most useful. These have shown that metamorphism can be recognised in the shales, at a distance of approximately 18 m from the contact. There is a systematic increase in the peak-height: width ratio of the 10 Å illite peak, towards the contact, with a sympathetic change in the illite polymorph also. These changes have resulted from temperature alone, as pressure has been low and of constant value.

METAMORPHISM OF PURE LIMESTONES

Metamorphism of the pure limestones of Upper Teesdale causes marmorization to a saccharoidal marble, the alteration resulting in the obliteration of all the sedimentary features including the bedding. The marbles consist of rounded to dodecahedral grains of calcite, decreasing in grain-size away from the contact, which have a granular texture and grain-boundaries meeting in triple-points. The abundance of straight grain-boundaries and triple-points, in the marbles, is suggestive of a low-energy, equilibrium configuration being reached (Spry, 1969).

Saccharoidal marbles are very restricted in their occurrence in Britain; they are known mainly from Teesdale but there are some minor occurrences in Derbyshire. Fine-grained, sacchoroidal marble for instance, is developed at the immediate contact of an olivine-dolerite, intrusive into S_2 limestones, near the village of Peak Forest, Derbyshire.

Grain-size measurements

The grain-size of calcite crystals has been measured on ten thin-sections of saccharoidal marble, from three boreholes (17, 18 and 33). An average of just under 500 grains per

section were measured.

The original measurements were made using a graduated eye-piece and then corrections were applied, to these data using matrix algebra after Rose (1968). For the purpose of the measurements and corrections, it was assumed that the calcite grains were spherical. The mathematical treatment, of Rose, corrects for the fact that the plane of the thin-section does not intersect the true diameter of all the grains in the section. Uncorrected, therefore, this effect would give rise to an apparently smaller grain-size than is actually present. The corrected grain-size measurements are shown in various plots in Fig. 3.2.

The variation in average grain-size with distance from the Whin Sill contact is shown in Fig. 3.2A. The straight line represents a linear regression drawn through the plotted points (correlation coefficient 0.94). This line gives a good fit to all the points, except for the value closest to the contact. This linear plot would probably represent the variation expected if a simple relationship existed between the grain-size and maximum temperature reached in the aureole. Temperature will play a major role in determining grain-size but other factors such as time, crystal-strain and the presence of impurities, will contribute towards the final grain-size reached and also to the spread of results obtained in any one section. For these reasons, the dashed curve is believed to represent a better estimate, of the variation in average grain-size, in the present case.

Previous work has shown that the grain-size of calcite in marble and quartz in hornfels, increases exponentially towards igneous contacts, (Grigorev, 1965, p.179; Edwards and Baker, 1944). The present measurements, in contrast, show a sharp rise

Figure 3.2 Calcite grain-size distributions in saccharoidal marble.

3.2A Variation in average grain-size with distance from Whin Sill contact.

Symbols refer to boreholes 17, 18 and 33 as shown. Straight line represents a linear regression fitted to the points.

3.2B Grain-size variation with distance from contact.

The lower line and triangles represent modal values, the upper line and circles represent the higher grain-size value, at one quarter of the modal peak-height. The two diagrams show hand-drawn curves, and linear regression lines fitted to the points.

3.2C Grain-size frequency distribution of samples from borehole 18.

The distance from the contact (m) of each specimen is shown near the peak of each curve.

Figure 3.2

3.2A

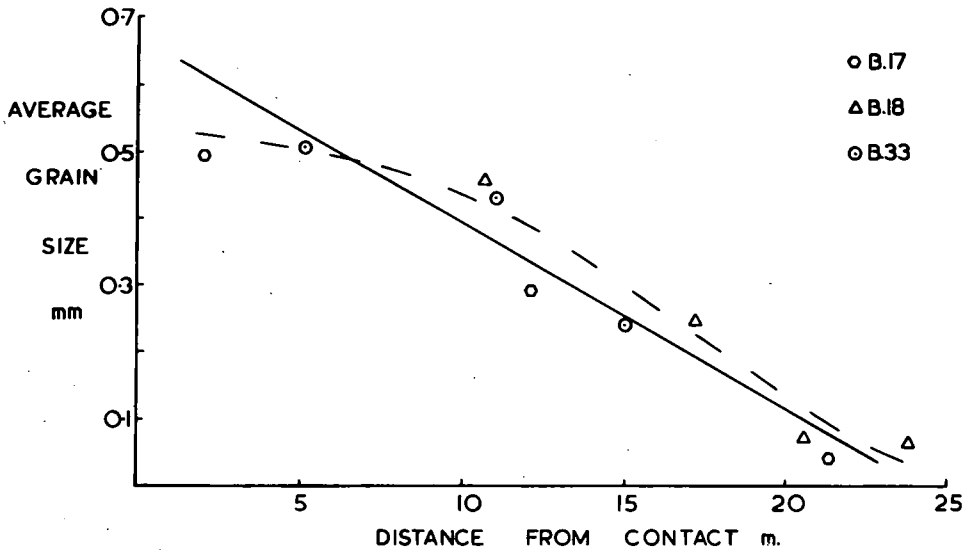

3.2B

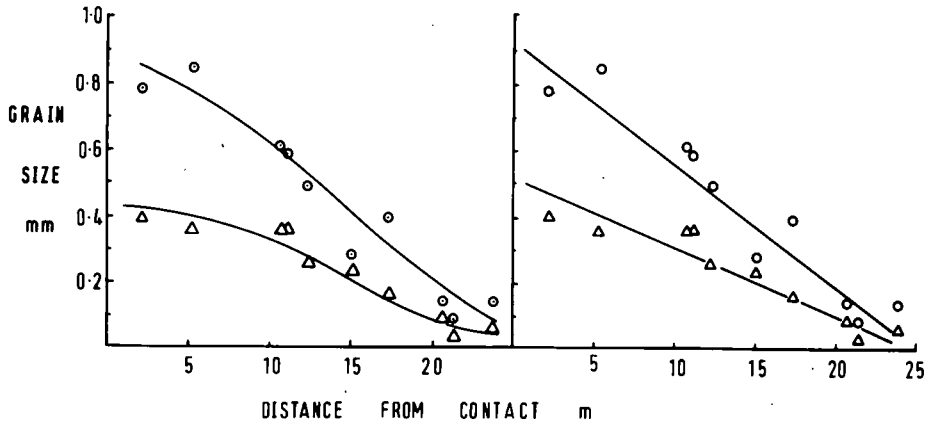

3.2C

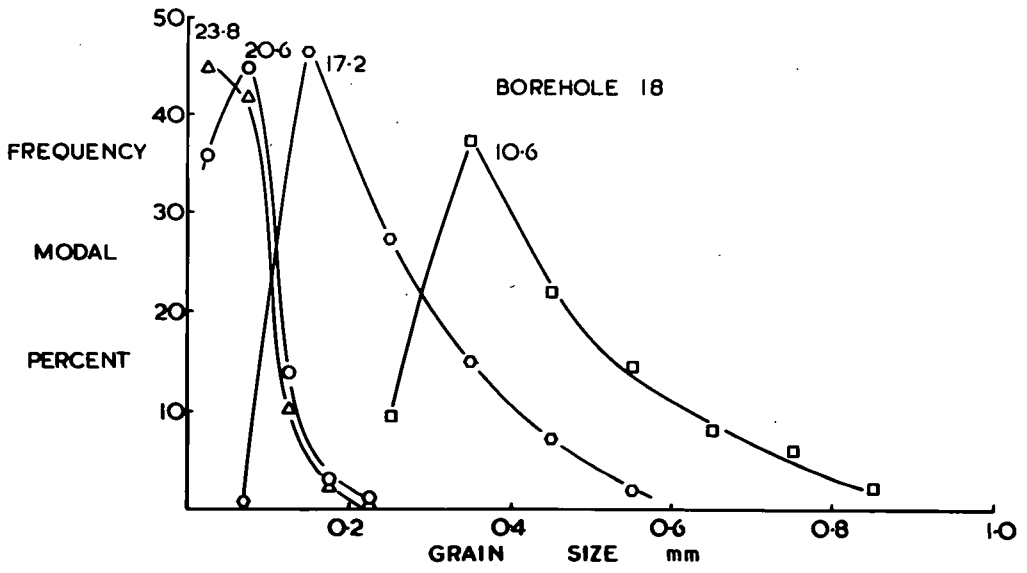

in grain-size between 25 and 5 m from the contact (Fig. 3.2A), above which a marked flattening in the slope is seen. This variance between the present curve, of grain-size against distance from contact, and the results of previous workers, is probably a reflection of the small time interval available for recrystallization. Figure 2.3 (p.27) shows the calculated temperatures, for the Whin Sill aureole. At distances between 0 and 10 m, from the contact, there is a relatively short period of time during which the temperatures, at these distances, are significantly higher than the rest of the aureole. As a result, there is probably insufficient time available, close to the contact, to allow the grain-size to equilibriate with these higher temperatures, resulting in the decrease in the slope of the curve observed in Fig. 3.2A.

Figure 3.2C shows the grain-size distribution in four samples from borehole 18. The distribution curves are not Gaussian but asymmetrical to the lower grain-sizes. Correspondingly the modal values of the grain-size distribution curves, are lower than the average grain-sizes, as shown by comparison of Fig. 3.2A and 3.2B. The curves in Fig. 3.2B, reflect the asymmetrical nature of the grain-size distribution curves. The divergence of the lines, towards the contact, indicates a higher percentage of larger grain-sizes close to the contact.

Process of recrystallization

For recrystallization to procede in a monomineralic rock, without phase change, either or both of the forces, lattice-strain and grain-boundary energies are involved (Spry, 1969). The heat of metamorphism is not a force in itself, it is rather

an initiating process for the actual energies involved in the process. In Upper Teesdale deformation of the strata, prior to metamorphism, would have been negligible, strain-energy, therefore, will have been of minor importance in the present study.

In order to provide sufficient ionic mobility for grain-boundary movement to occur, the limestones must have been heated to at least the Tamman temperature (Spry, 1969). This temperature is approximately half the melting temperature of calcite, in degrees Kelvin. Wyllie and Tuttle (1960) suggest a melting temperature for calcite, in the presence of water vapour at low pressures, in the region of 800°C. The Tamman temperature would, therefore, be of the order of 500 to 550°C. Griggs et al. (1958) showed, however, that a temperature of 800°C was required for recrystallization to occur in an unstrained sample of the Solenhofen limestone, at five kilobars. Temperatures of 800°C, in the presence of water vapour are, however, most likely to generate melts (Wyllie and Tuttle, 1960). Skeletal grains suggestive of a melt are not present in any of the limestones examined and temperatures of this order seem unlikely for the present study.

If the value of 500°C is accepted as the minimum temperature for recrystallization, then this value must have been attained at the limit of marmorization, which is approximately 27 m from the contact but the theoretical values (Fig. 2.3) show only a maximum temperature in the order of 350 to 375°C at 25 m from the contact. A second discrepancy is, therefore, noted in which geological observations do not agree with the calculated metamorphic temperatures, and this is considered in the final Chapter of this thesis.

The saccharoidal marbles, as mentioned earlier, are virtually restricted to Upper Teesdale, where the Whin Sill intrudes the Lower Limestone Group. Elsewhere the sill is found intruded mainly in the Middle Limestone Group in which dark-coloured limestones are dominant. The organic carbon in these limestones (Chapter IV) inhibits recrystallization as shown by Robinson (1971).

A copy of the paper by the writer (Robinson, 1971) is enclosed with this thesis.

Specific points in the above paper are shown in the following Plates.

The fine-grained calcite mud, with abundant carbonaceous matter, as characteristic of dark-coloured limestones, is shown in Plate 3.1. A dark limestone is also shown in Plate 3.2 but in which individual grains of calcite can be seen, with rims of carbonaceous material around the grain-boundaries. A dark, unrecrystallized limestone, is illustrated in Plate 3.3, in which the relatively carbon-free areas are recrystallized.

Conclusions

Pure limestones in Upper Teesdale are marmorized to saccharoidal marbles, which are virtually restricted, in Britain, to Upper Teesdale. Grain-size measurements on ten thin-sections show a variation in average grain-size of calcite, from 0.5 mm, at the contact, to 0.05 mm at distances greater than 20 m from the contact. Work already published (Robinson, 1971), has shown that carbon in dark limestones inhibits recrystallization by the prevention of grain-boundary movement. Temperatures in excess

Plate 3.1 Sample 40/13. Fine-grained calcite mud with abundant carbonaceous material. (x200)

Plate 3.2 Sample 40/13. Calcite grains with rims of carbonaceous material around grain-boundaries. (x150)

Plate 3.3 Sample 40/13. Groundmass of dark, fine-grained calcite mud, with lighter areas of relatively carbon-free material, which has suffered recrystallization. (x90)

Plate 3.1

Plate 3.2

Plate 3.3

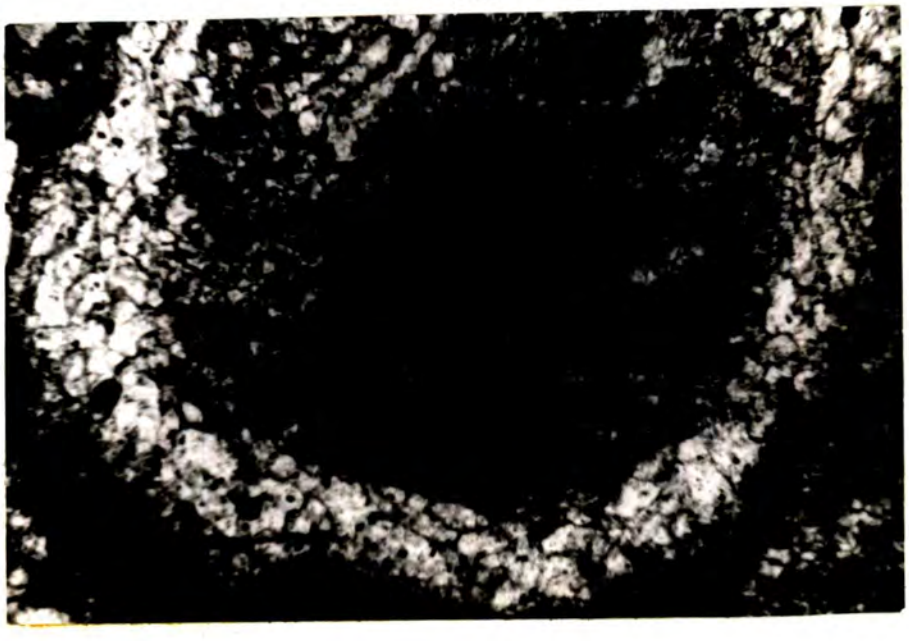

of 500°C are thought necessary in order to promote recrystallization of the limestones.

METAMORPHISM OF IMPURE LIMESTONES AND CALCAREOUS SHALES

Impure limestones and calcareous sediments have been the most susceptible to the metamorphism. A wide range of metamorphic minerals is developed, up to 25 m from the Whin Sill contact, in the calc-silicate rocks examined. The most abundant minerals found are grossular garnet, plagioclase feldspar and epidote.

Macroscopic features

General mineral identification is difficult, or not possible in the majority of samples of the metamorphosed sediments because of their fine-grained nature. Sedgwick (1827), however, noted the presence of garnets in impure limestones close to the contact in Upper Teesdale. Similarly garnets have been recognised in hand-specimens from borehole samples. Idioblastic, pinkish-red garnets are present in sample 43/22, a calcareous shale, and white, massive garnet is present in sample 35/4, a banded, calc-silicate contact-rock. Wollastonite has been recognised for the first time in hand-specimen, from three boreholes. A wollastonite-rich rock, up to 50 cms thick, is present at the junction between the Lower Robinson Limestone and underlying sandstone, The wollastonite occurs as white, radiating crystals up to 4 mm in length and is present in samples 40/7, 41/3 and 45/7. Pyrite is present in many samples and is probably a recrystallization of original sedimentary material. Small pockets of haematite have been recognised in one sample, 19/9, where it occurs in association with fine-grained feldspar.

In Upper Teesdale, these minerals are the only readily identifiable minerals to be seen in hand-specimen but at Barrasford quarry, Northumberland, elongate grains of pinkish-brown idocrase up to 4 mm in length, can be recognised from material in a sedimentary raft included in the Whin Sill (Randall, 1959).

Although no new minerals can be seen in the majority of the samples, the rocks have obviously undergone recrystallization. A banded, calc-silicate contact rock which is shown in Plate 3.4 has been extensively recrystallized, although no definite new minerals can be identified, in the hand-specimen. When metamorphosed, calcareous shales take on a creamy colour, become porcellaneous in appearance and are quite hard and flinty. Many of these rocks contain, or consist of red-orange coloured, adinole-like masses, which are illustrated in Plates 3.4 and 3.5.

Argillaceous bands and lenses in limestone are also metamorphosed to calc-silicate rocks as shown in Plate 3.5 The calc-silicate band is seen in a medium-grained, saccharoidal marble, the junction between the two materials is quite sharp but irregular. The band consists dominantly of green, recrystallized chlorite and calcite, in which are set the red-coloured adinole masses mentioned above. Because of their hardness and porcellaneous nature, these calc-silicate lenses have been misidentified by earlier workers. Knill (1966) and Kennard and Knill (1969) have erroneously identified metamorphosed argillaceous horizons interbedded with limestone, in boreholes 18 and 19 at depths of 31 and 21 m respectively, as thin leaves of the Whin Sill, with limestone inclusions. The calc-silicate lenses (Plate 3.5) were identified by Knill (1966) as mixed Whin Sill

Plate 3.4 Sample 35/4. Calc-silicate specimen, the lower boundary of which is the actual contact with the Whin. Red-coloured areas are cryptocrystalline aggregates of feldspar and quartz. White and cream areas consist mainly of massive garnet, while remaining areas consist dominantly of calcite and epidote with some clinopyroxene and prehnite. (Width of specimen, 6 cms)

Plate 3.5 Sample 19/4. Irregular, calc-silicate lens in medium-grained, saccharoidal marble illustrated at eastern side of plate. The majority of lens consists of recrystallized chlorite, with epidote, throughout the lens but especially in north-west corner of the plate. (Length of specimen, 11.5 cms)

Plate 3.6 Sample 40/7. Showing large elongate grains of wollastonite. (x50)

Plate 3.4

Plate 3.5

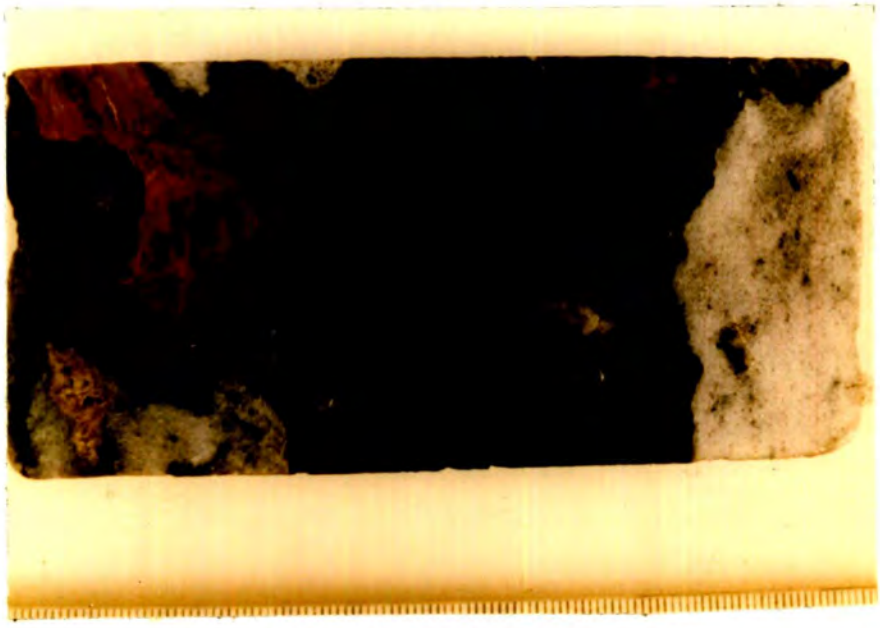

Plate 3.6

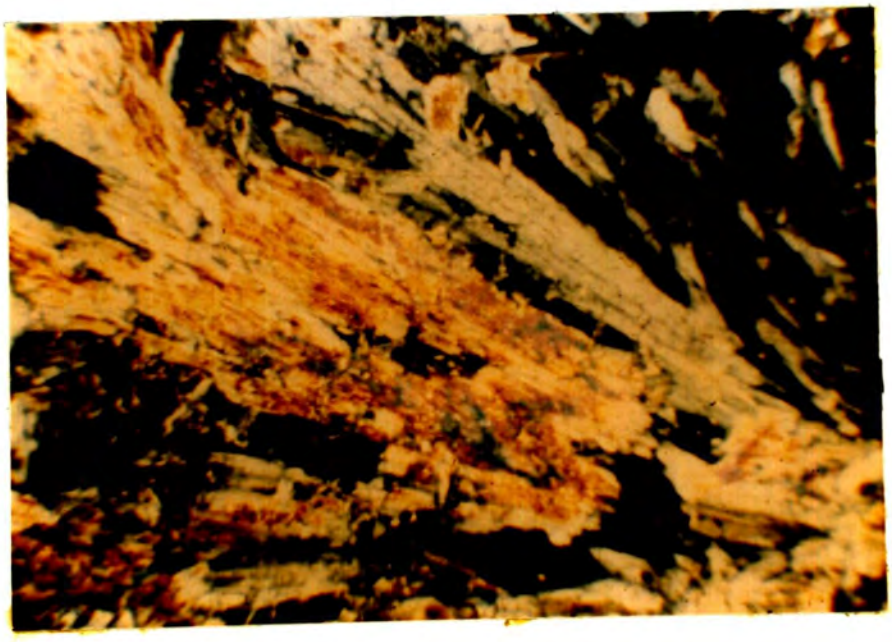

and limestone and he described them as the products of 'intimate mixing of the sugary limestone and Whin to form a skarn rock banded in dark green, red and grey'. Petrographic examination, as described later, has shown that these calc-silicate rocks are in fact, metamorphosed, argillaceous bands in the limestone.

An interesting feature of specimens from the upper contact of the Whin in a number of the Cow Green boreholes, is the occurrence of a hard, flinty, siliceous rock. Basically this rock consists of quartz and feldspar with abundant sulphides and some calcite and it has been recognised in boreholes 41, 43, 44 and 46 (samples 41/36, 43/2, 44/5 and 46/5). A similar feature was also recorded by Harrison (1968), with the development of a siderite-pyrite-silica unit at the upper contact of the Great Whin Sill, in the Woodland borehole. Harrison attributes the development of this unit to a final residuum of the Whin, which has metasomatized the immediate country rock. Petrographic examination of the Cow Green samples shows that these contact rocks were originally calcareous sediments, which have been metamorphosed. In boreholes 43, 44 and 46 the Whin is intruded at or within 0.5 m of a limestone horizon. It is possible that the Whin has intruded at the junction between a limestone and sandstone, a plane of greater weakness, and these siliceous contact specimens represent small wafers of sediment caught at the top of the sill on intrusion.

Petrographic description

Limestones, where pure, are recrystallized to a saccharoidal marble, as described earlier. The alteration patterns developed in impure limestones depend upon the amount and nature

of impurities. One of the simplest impurities in limestone is quartz and where this is present, wollastonite is to be expected if temperatures reached a sufficiently high level. A wollastonite-rich rock has been found at a limestone-sandstone junction and in borehole 40 this rock reaches 50 cms in thickness and consists mainly of wollastonite, calcite and some minor clinopyroxene. The wollastonite occurs as long, radiating crystals up to 5 mm in length (Plate 3.6). An association of quartz, calcite and wollastonite needles is illustrated in Plate 3.7, the wollastonite actually growing into the quartz at position A. This wollastonite-rich rock is found in boreholes 40, 41 and 45, occuring at 5.8, 7.2 and 7.1 m from the contact respectively. Wollastonite has been recorded previously from the contact rocks of the Whin Sill but Hutchings (1898) noted that it was only of rare occurrence.

Where limestones contain small wisps and pockets of clay minerals rather than quartz, the development of garnet is found. This is seen in sample 43/21, a fine-grained, saccharoidal marble, 21 m from the contact, which contains thin, grey-green, irregular wisps of argillaceous material. In thin-section the wisps, which are full of carbonaceous material, are a dull, earthy-brown colour and consist of fine-grained, recrystallized sericitic material. Garnets are abundant in these wisps and range up to 1 mm in size, they are usually concentrated around the edges of the thin wisps of material (Plate 3.8). Where the garnets abut against the argillaceous wisps, they are usually xenoblastic, full of inclusions and have abundant fractures.

A medium-grained, saccharoidal limestone 6 m from the

Plate 3.7 Sample 40/7. Showing quartz, (clearer grains) and calcite with thin, radiating grains of wollastonite. Wollastonite replacing quartz at A. (x100)

Plate 3.8 Sample 43/21. Showing junction between fine-grained, argillaceous horizon and saccharoidal marble with xenoblastic garnets at the junction. (x50)

Plate 3.9 Sample 44/12. Small xenoblastic datolite crystals set in a medium-grained, saccharoidal marble. (x100)

Plate 3.7

Plate 3.8

Plate 3.9

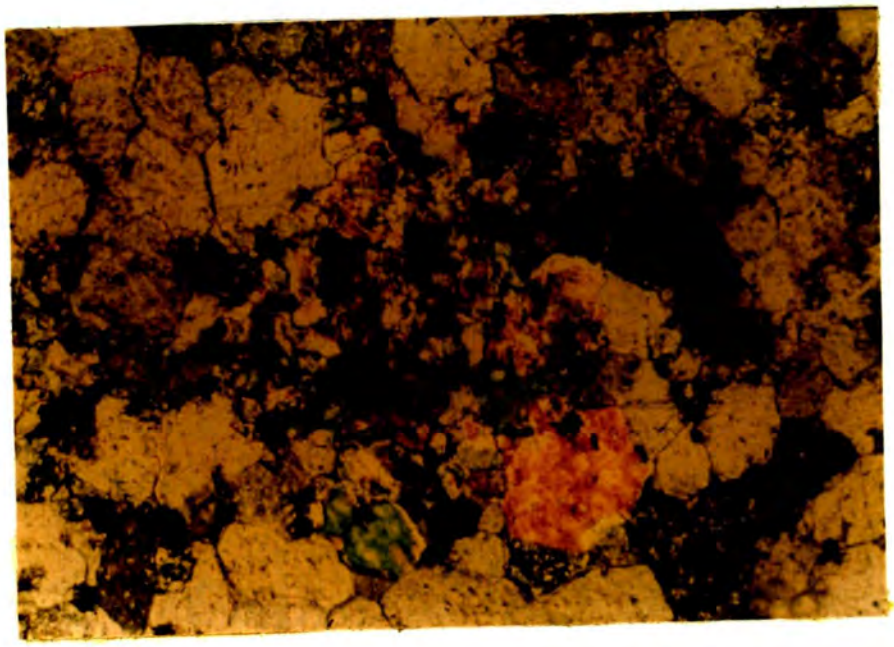

contact, with only small amounts of impurities, has clusters of small, granular, xenoblastic crystals ranging in size from <0.05 to 0.25 mm in size. These crystals are readily distinguishable from the surrounding calcite because of their low-order interference colours (Plate 3.9) and were initially thought to be monticellite. Further optical and electron mincroprobe work suggests that they are datolite, this being the first recorded instance of this mineral from the contact rocks of the Whin Sill aureole.

Calc-silicate lenses in marbles

Calc-silicate lenses, as seen in Plate 3.5, are well developed in the Melmerby Scar Limestone, in boreholes 18, 19, 43 and 44. These lenses vary from a few millimetres up to several centimetres in thickness, when the rocks grade into calcareous shales. In the majority of cases the lenses have a sharp but irregular junction with the enclosing saccharoidal marble. Knill (1966) described these calc-silicate rocks as the products of the mixing of limestone and the Whin magma but petrographic examination shows them to be simply argillaceous horizons which have been metamorphosed. The equivalent unmetamorphosed material is present towards the edge of the metamorphic aureole,as seen in borehole 47, where unaltered wisps and lenses of shale are present in grey limestone over 25 m from the sill contact. In some specimens closer to the contact, the original character of this material may also be seen. Sample 43/6, 1.5 m from the contact, is a calc-silicate band included in a saccharoidal marble, consising dominantly of greenish-coloured, recrystallized chlorite in which is set a hard, red-coloured adinole band.

In thin-section the red adinole band consists of corroded quartz, set in a fine-grained, cloudy groundmass, which electron microprobe analysis (Chapter V) has shown to be sodic feldspar. A portion of the red band is shown in Plate 3.10, where quartz grains are set in a fine-grained matrix of feldspar. The original character of the feldspar matrix is rarely seen but in places fine-grained sericite is visible and represents the original illite matrix. An area of sericite surrounded by fine-grained feldspar is shown in Plate 3.11. The hard, flinty character of the red bands is the result of cementing of the quartz grains by the formation of the fine-grained feldspar.

Normally, the original illitic material, in these lenses, is completely altered as in sample 43/6. In this specimen, the red-coloured material consists dominantly of very fine-grained feldspar and quartz, barely resolved using x100 magnification. This cryptocrystalline mixture of feldspar and quartz is a typical adinole. Coarser-grained feldspar is present in some areas as shown in Plate 3.12, here the north-east corner consists of fine-grained feldspar, while the rest of the field of view shows coarser feldspar with minor quartz. All the feldspar has a reddish-colour which is especially seen in plane-polarised light, although areas of a deepish red colour may be seen in Plate 3.12. Rarely, feldspar laths up to 1.5 mm in length showing albite twinning may be seen, as in Plate 3.13. These feldspars are also red in colour but in this Plate, individual, irregular grains of haematite are present, with translucent red edges.

Associated with the red adinole bands in hand-specimen are

Plate 3.10 Sample 43/6. Showing corroded quartz grains set in a matrix of fine-grained feldspar. (x100)

Plate 3.11 Sample 43/3. Central area of light-coloured, fine-grained sericite, surrounded by darker, fine-grained feldspar and quartz. (x80)

Plate 3.12 Sample 43/3. Consisting dominantly of red-coloured feldspar, with fine-grained material in the north-east corner. (x100)

Plate 3.10

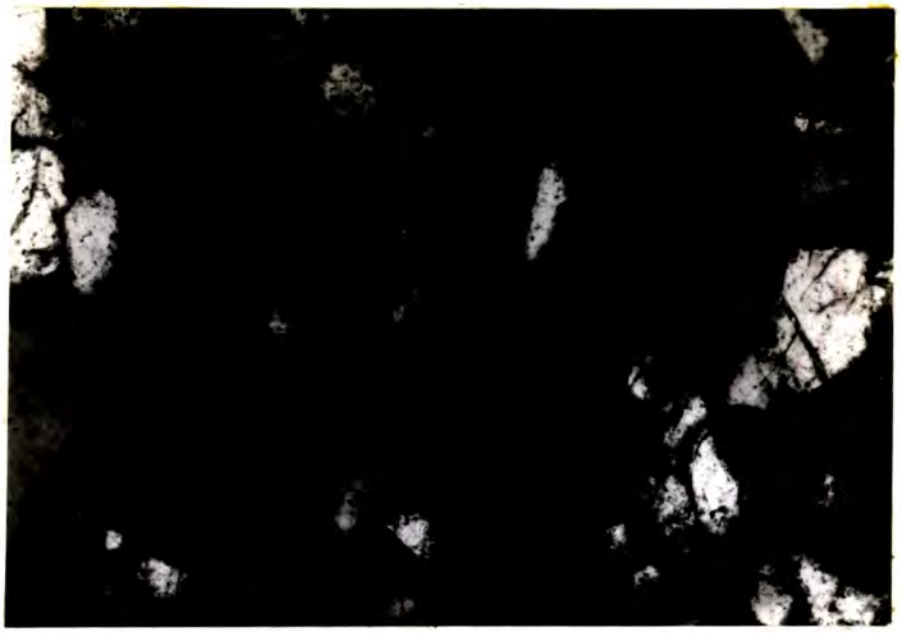

Plate 3.11

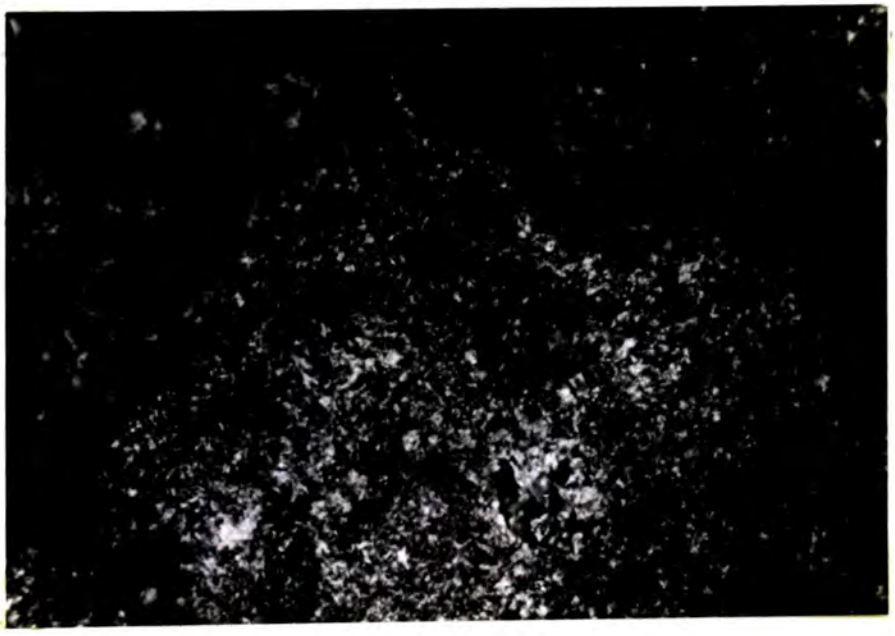

Plate 3.12

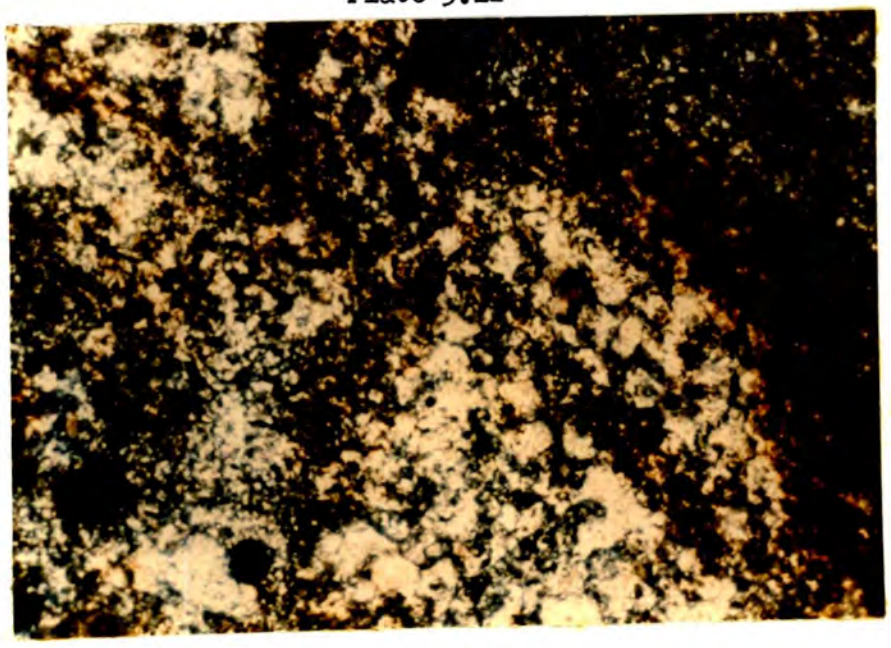

large areas of material which is fine-grained and green in colour. These areas have a varied mineralogy, the dominant minerals present are fine-grained chlorite, garnet and calcite. The chlorite constitutes the general groundmass, ranging from very fine-grained material to radiating clumps of crystals up to 4 mm in length (Plate 3.14). This chlorite must represent original sedimentary chlorite which has recrystallized in response to the metamorphism. Intergrown with this chlorite, as in sample 43/3, are crystals of possible amphibole, although exact identification is difficult because of the fine-grained nature of the material. Garnet appears abundantly in this chlorite matrix, showing a great variety in form and grain-size. It often forms large, granular masses due to the coalescence of numerous single grains. The garnets are usually crowded with inclusions of quartz, calcite and carbonaceous material. Where individual garnet grains have not coalesced completely, a variety of interstitial minerals may be present. An area of fine-grained chlorite with idioblastic epidote crystals, surrounded by massive garnet crowded with inclusions, is shown in Plate 3.15. Garnet always forms as a rim to the adinole areas described above, as shown in Plate 3.16, here the garnet is seen to border very fine-grained feldspar in the north of the Plate. The same feature is shown in Plate 3.17, where a small lens of coarser-grained feldspar 1 mm long, is surrounded by a narrow rim (0.04 mm) of xenoblastic garnet. The whole lens is set in a matrix of radiating chlorite with crystals of calcite and sub-idioblastic garnets. A mineral always occurring as an interstitial phase to garnet is prehnite, which is shown in the southern part of Plate 3.16. Garnets included in the prehnite or growing into it (Plate 5.2), have

Plate 3.13 Sample 44/9. Feldspar laths, showing albite twinning, associated with irregular grains of haematite. Opaque grains are haematite. (x100)

Plate 3.14 Sample 43/22. Showing radiating grains of chlorite associated with epidote and set in a fine-grained chloritic matrix. (x100)

Plate 3.15 Sample 43/3. Idioblastic epidote crystals in a fine-grained chloritic matrix, surrounded by massive garnet crowded with inclusions. (x100)

Plate 3.13

Plate 3.14

Plate 3.15

idioblastic outlines whereas the edges abutting against the fine-grained feldspar area, show non-rational boundaries. This record of prehnite, is the first occurence in the Whin Sill aureole.

Occasionally minor amounts of other minerals such as idocrase and wollastonite are seen in calc-silicate lenses in the marble.

Calcareous shales

Calcareous shales are particularly developed at limestone-shale junctions and show similar alteration patterns to the calc-silicate lenses described above. Differences are present, mainly in the proportion of sulphide material present, due to its concentration at limestone-shale junctions. A mudstone band 1 m from the contact, in the Melmerby Scar Limestone (44/11), shows the development of a calc-silicate band with abundant sulphides. The sulphide is mainly pyrite, although some pyrrhotite is present in sample 44/28. The junction between the shale and limestone is marked by sub-idioblastic garnets which are relatively free of inclusions. Red-coloured adinole bands are also present in these calcareous shales and are usually set in a chloritic groundmass heavily charged with carbonaceous matter. Elongate needles of apatite are usually abundant and are often seen growing into garnet (Plate 5.3). Small calcite nodules, in these shales, usually show the main mineral development. A calcite nodule, from sample 43/22, in which new mineral growth is seen, is illustrated in Plate 3.18. Idioblastic grains of epidote up to 1.2 mm in length are set in calcite and are associated with radiating crystals of chlorite and sub-idioblastic garnets which show anisotropism. Where the shale and carbonate

Plate 3.16 Sample 43/3. Fine-grained feldspar occupying central and northern areas of the plate, with a narrow rim of garnet, associated with prehnite, in the very south of the plate. (x150)

Analyses 43/-4 to 9 Fine-grained feldspar, 6 points (Appendix 5.2).

Plate 3.17 Sample 43/3. Small lens of feldspar rimmed by garnet and set in radiating chlorite with crystals of calcite and sub-idioblastic garnet. (x100)

Plate 3.18 Sample 43/22. Elongate grains of idioblastic epidote in a calcite matrix, with associated radiating chlorite and anisotropic garnet. (x50)

Plate 3.16

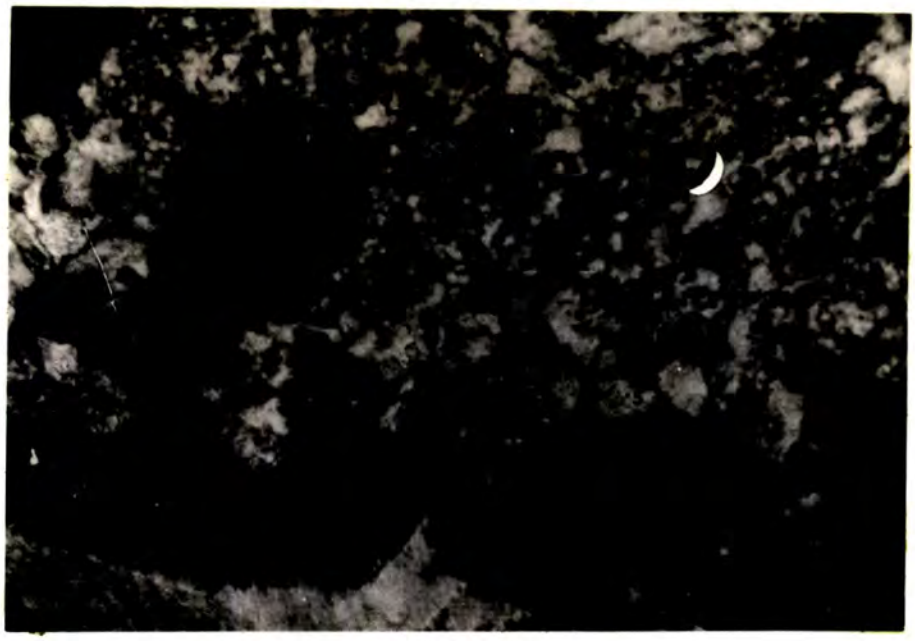

Plate 3.17

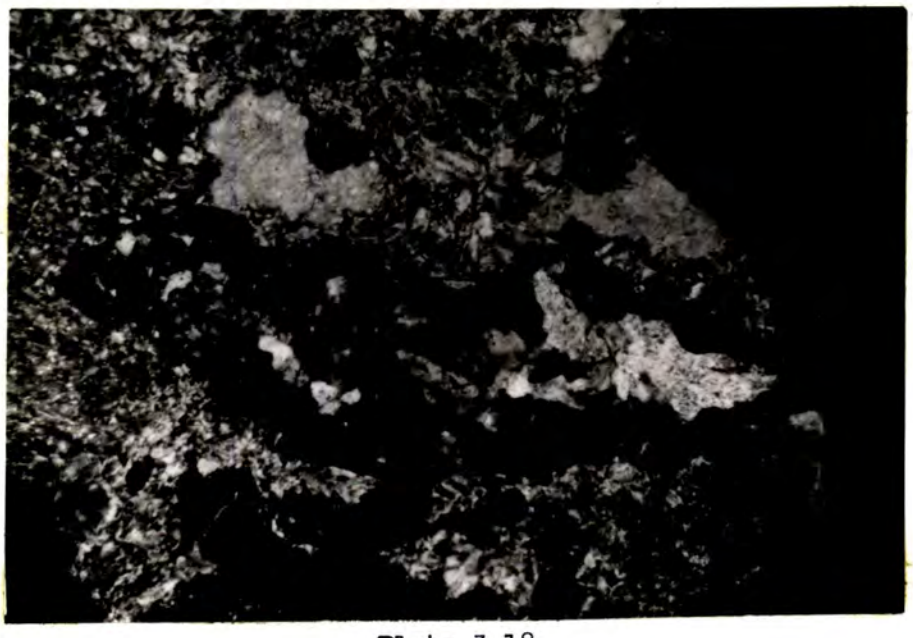

Plate 3.18

fraction have been more admixed there is the development of a cryptocrystalline mixture of feldspar and quartz, associated with fine-grained, granular epidote as illustrated in Plate 3.19.

An unusual development of a banded, calc-silicate rock 6 cms thick, is seen at the Whin contact in borehole 35. A polished surface of this specimen (35/4) is illustrated in Plate 3.4, which shows the banded nature of the sample. The lower darkened surface is the actual contact with the Whin; this and the red-coloured material consist of a cryptocrystalline mixture of quartz and feldspar. The white-greyish bands consist of massive garnet, which is full of inclusions of quartz and calcite. Various minerals are found interstitial to the garnet, small grains of xenoblastic pyroxene with some prehnite and included needles of apatite are present in sample 35/4. The greenish and faint purple coloured bands (Plate 3.4) consist of various mixtures of fine-grained epidote, calcite with some pyroxene. Epidote is very abundant, Plate 3.20 shows fine-grained, xeno-blastic epidote which is in optical continuity. No original sedimentary material was seen in this particular sample, which is unusual as chlorite is usually present in most samples.

SPATIAL DISTRIBUTION OF MINERALS FROM WHIN SILL CONTACT

The spatial distribution of minerals in the Whin Sill aureole, Upper Teesdale, is shown in Fig. 3.3.

Epidote is the most widely distributed mineral in the aureole and extends to over 25 m from the contact. The actual distance to which it extends is not known because in boreholes 46 and 47 the upper contact of the Whin was not entered. The extent of metamorphism and the presence of a hard, quartzo-

Plate 3.19 Sample 44/5. Fine-grained mixture of feldspar and quartz with granular, fine-grained epidote. (x100)

Plate 3.20 Sample 35/4. Fine-grained, xenoblastic epidote in optical continuity. (x50)

Plate 3.19

Plate 3.20

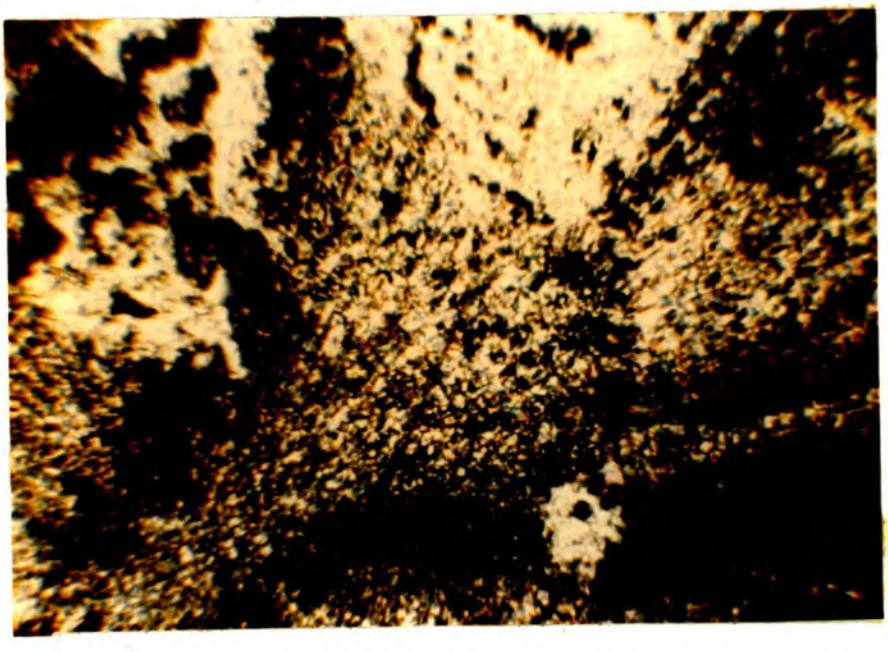

feldspathic rock, at the base of borehole 46 is, however, suggestive that the sill is quite close in this borehole.

Garnet extends almost as far as epidote and is found to almost 23 m from the contact. This appears to mark a fairly well defined limit to the formation of garnet, as the appropriate rock type is seen in samples 47/10 and 47/9 but no garnet is developed. There appears to be a break in occurence of these two minerals between 10 and 20 m, but it is more apparent than real because of the lack of samples of appropriate composition over this range.

Feldspar is recorded from the contact to almost 11 m distant, but its actual limit is not known, although it is not recorded from the samples greater than 20 m from the contact.

The remaining minerals, as shown in Fig. 3.3, are restricted to within 8 m of the contact. This restriction is real, as samples of appropriate bulk composition are found between 8 and 10 m and greater than 20 m from the contact, but these minerals are not recorded at these distances. The restriction of prehnite to within 8 m from the contact is unusual because it is a low-temperature mineral and might have been expected at greater distances from the contact.

WHIN SILL METAMORPHISM IN AREAS OUTSIDE UPPER TEESDALE

The metamorphic effects described in the preceding pages are those found particularly in sediments from above the upper contact of the Whin Sill, in the Cow Green area of Upper Teesdale. In this area metamorphism is at a maximum, elsewhere the metamorphism associated with the sill is very restricted.

The Barrasford area, Northumberland, shows the second

Figure 3.3 Spatial distribution of minerals from Whin Sill contact.

Sample numbers for typical examples are shown against each line, dotted line indicates absence of a mineral due to lack of specimens of appropriate composition.

Figure 3.3

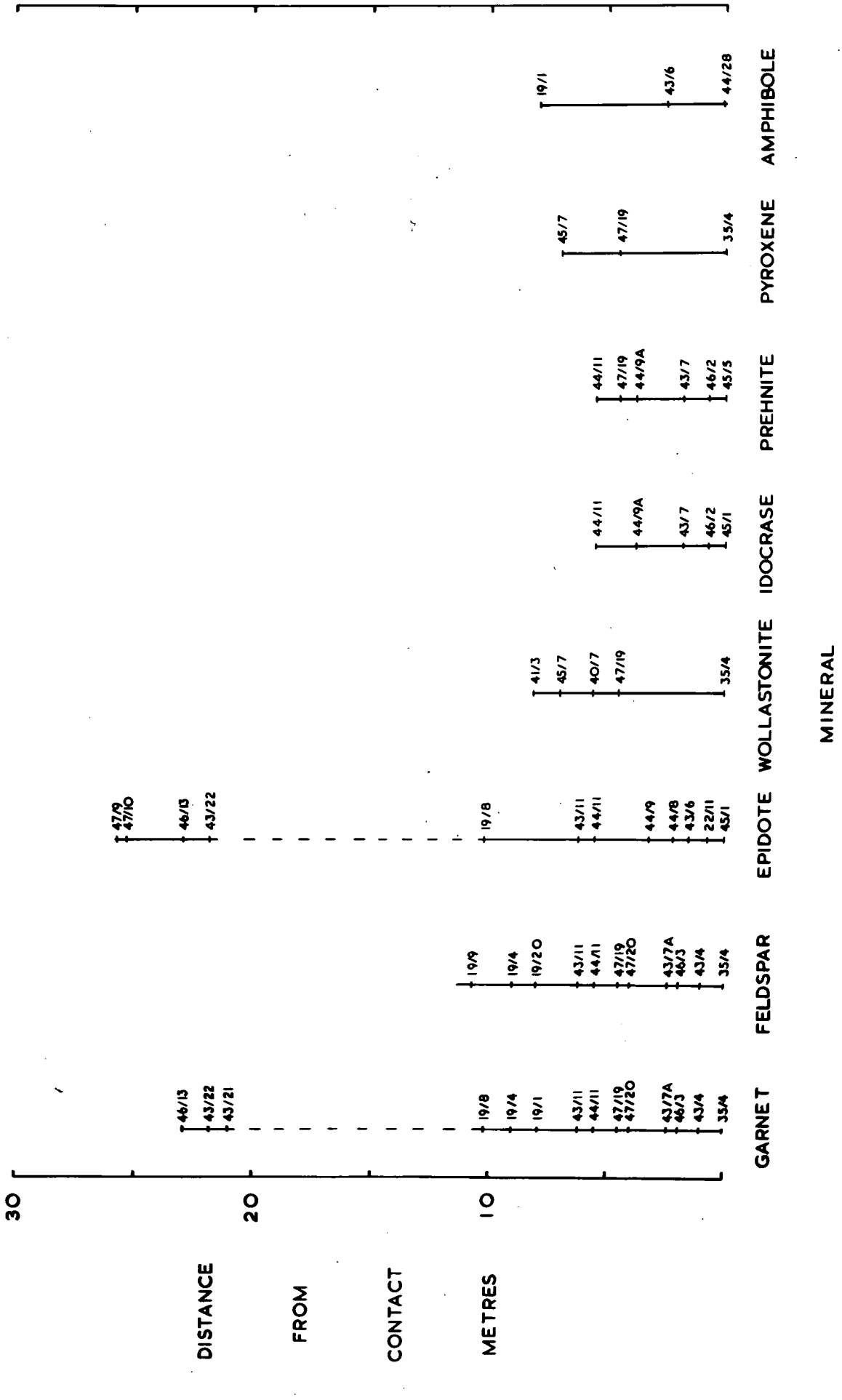
DISTANCE FROM CONTACT METRES
30
20
10
GARNET
FELDSPAR
EPIDOTE
WOLLASTONITE
IDOCRASE
PREHNITE
PYROXENE
AMPHIBOLE
MINERAL
46/13 43/22 43/21
19/8 19/4 19/1
43/11 44/11
47/19 47/20
43/7A 46/3 43/4 35/4
19/9 19/4 19/20
43/11 44/11
47/19 47/20
44/9 44/8 43/6 22/11 45/1
47/9 47/10 46/13 43/22
19/8
43/11 44/11
44/9 44/8 43/6 22/11 45/1
41/3 45/7 40/7 47/19 35/4
44/11 44/9A 43/7 46/2 45/1
44/11 47/19 44/9A 43/7 46/2 45/5
45/7 47/19 35/4
19/1 43/6 44/28

greatest metamorphic effect, with the development of idocrase, garnet and pyroxene in impure limestones and iron-rich bands, as described by Smythe (1950) and Randall (1959). Much of this mineral development, however, is seen in a limestone raft included in the sill, but mineral development is also recorded from impure limestones adjacent to the sill, with garnet and idocrase developed within 1 m of the contact (Smythe, 1950).

In the Rookhope and Woodland boreholes (Dunham et al., 1965; Harrison, 1968) metamorphism is virtually non-existent, in comparison. Induration of the sediments has occurred, and spotting is developed up to 40 m from the contact. Similarly in the Ninebanks borehole, spotting and induration has occurred but a small, calcareous nodule 4 m from the lower contact, shows the presence of recrystallized chlorite and idioblastic quartz.

Samples from close to the contact in the Throckley borehole, Northumberland, have been examined by kind permission of Dr. A. C. Dunham. In these samples, development of minor garnet is seen in an impure limestone less than 1 m from the contact.

COMPARISONS WITH OTHER DOLERITE INTRUSIONS

The mineralogy developed in the contact aureole of the Whin Sill is quite similar to that described recently by Van Houten (1971), associated with diabase sills in the New Jersey area. Calc-silicate hornfels is developed within 50 m of a sill and contains diopside-hedenbergite, andradite, grossular, prehnite, datolite, idocrase and wollastonite. Major metamorphic effects are detectable to about 134 and 200 to 240 m above 90 and 250 to 300 m sills respectively. The metamorphism is more extensive than that associated with the Whin Sill, as

metamorphic mineral assemblages are only detectable to approximately 25 m from the 73 m intrusion in Upper Teesdale. The diabase sills of the New Jersey area are, however, part of the Palisade intrusion, in which differentiation, possibly due to convective circulation of the magma (Van Houten, 1969) is well developed. The association of a number of thick sills showing convective circulation, probably accounts for the greater metamorphism seen in the New Jersey area, as compared to the Whin Sill aureole.

Phemister and MacGregor (1942) recorded grossular/andradite garnet and datolite in an impure limestone, within 10 m of a thick sill of quartz-dolerite near Kirkcaldy, Fife.

Conclusions

In the Whin Sill aureole, calcareous sediments show the greatest metamorphic effect and new mineral assemblages are developed over 25 m from the contact. Calc-silicate lenses, found in marbles, have been derived from the metamorphism of argillaceous lenses in the limestones and are not formed as a result of the mixing of Whin magma and limestone.

The main minerals developed are as follows:- garnet, sodic feldspar, epidote, wollastonite, idocrase, clinopyroxene, amphibole, prehnite and datolite. Of these minerals prehnite and datolite and recorded for the first time in the Whin aureole.

Wollastonite, which has been found previously in only small amounts, occurs in places at the junction of the Lower Robinson and underlying sandstone, in a band up to 50 cms thick. The sodic feldspar occurs in cryptocrystalline, red-coloured adinole masses, which are found in the calc-silicate lenses.

Garnet and epidote are both found over 20 m from the contact, epidote extending to over 25 m. The remaining minerals mentioned above, are restricted mainly to within 10 m from the contact.

Appendix 3.1 Separation of clay-fraction

In order to obtain reasonable peaks and easier identification, all the samples X-rayed for clay mineral polymorph and crystallinity were separated as follows.

Samples were initially crushed using a roll-jaw crusher and then the sample was coned and quartered. The sample was then further crushed using a tungsten-carbide ball-mill. This method was preferred to the Tema disc-mill which would possibly have resulted in the deformation and alteration of the crystal lattice. The resultant powder from the ball-mill was centrifuged in water for 2 to 4 minutes, and then the upper layer, consisting mainly of clay minerals, was removed with a spatula and dried gently in an oven at 80°C. This powder, on X-raying, proved sufficiently pure for the purpose of polymorph identification.

An estimate of the purity achieved using this method was obtained by the quantitative measurement of quartz present in the sample. This was done by a differential thermal analysis method (D.T.A.) involving the measurement of the quartz inversion peak (β to α) on the cooling curve of the D.T.A. analysis. Known amounts of quartz were diluted with alumina, which was also used as the reference material. The displacement of the quartz inversion peak from the base-line was measured for each concentration and averaged over two runs before a calibration curve was plotted.

Using this calibration curve, a normal sample of shale 21/8 was separated in the above manner and then run on the D.T.A. to obtain a cooling curve. The original unseparated sample averaged over two runs gave a value of 40% quartz while the samples run

after centrifuging gave a value of less than 5%. A reduction in quartz, amounting to over 80% of the original amount, has been achieved in a very small time (2 to 4 minutes). For normal work this method proves itself superior to the time-consuming suspension method of clay separation.

Appendix 3.2 X-ray diffraction of separated clay-fractions

The samples were run on a Phillips PW 1130 generator of 2KW rating, with a Co X-ray tube. The conditions for analysis are given below:

Rating	2KW	Scatter slit	1^{o}
Target	Co	Attenuation	1 volt
Filter	Fe	Window	12 volts
KV	60	Rate meter	4
MA	30	Time constant	4
Divergence slit	1^{o}	Scanning speed	$\frac{1}{2}^{o}2\theta$/minute
Receiving slit	0.1^{o}	Chart speed	80 cm per hour

Proportional counter with discriminator, was used throughout. The chart speed used, was that giving the largest peaks consistent with reproducibility.

Cavity mounts were used rather than smear mounts which tend to produce some orientation of layered silicates. Each sample was oscillatory scanned over the range 8 to 12 $\mathring{A}$, for three readings and then a second cavity mount, of the same sample, was scanned three times and the calibration data (Appendix 3.3) are based on the average of the six readings.

Appendix 3.3 Calibration data for crystallinity and polymorphism of illite

Sample	Distance from contact (m)	10 Å peak-width (mm)	10 Å peak-height (mm)	Peak-height : width	Polymorph
43/30	31.0	7.6	27	3.6	1Md
40/26	30.2	13.7	37	2.7	1Md
43/28	30.2	8.0	34	4.2	1Md
43/27	29.1	7.6	28	3.7	1Md
40/25	28.6	7.4	26	3.5	1Md
40/23	25.9	8.7	114	13.1	2M
44/20	24.4	9.3	21	2.3	1M, 1Md
43/23	22.1	5.8	24	4.1	1M, 1Md
40/16	18.4	12.4	38	3.1	1M
41/15	16.8	8.2	84	10.2	1M
40/15	14.9	6.3	86	13.7	2M
43/16	13.2	4.3	24	5.6	1Md
44/14	10.8	5.1	84	16.5	2M
40/11	9.1	4.7	95	20.2	2M
44/10	4.8	4.6	53	11.5	1M, 2M
40/6	4.7	6.8	60	8.8	1M
43/9	4.7	5.1	199	39.0	2M
44/32	3.9	6.3	85	13.5	1M, 2M
40/5	3.5	5.9	46	7.8	1M
43/8	3.2	5.8	225	38.8	2M

CHAPTER IV

WHOLE ROCK GEOCHEMISTRY

ARGILLACEOUS SEDIMENTS - MAJOR ELEMENTS

A suite of argillaceous sediments, from boreholes at Rookhope and Upper Teesdale, have been analysed for eleven major elements by X-ray fluorescence. The results of the analyses are tabulated in Appendix 4.1. One of the main aims of the study was to examine equivalent metamorphosed and unmetamorphosed beds to establish whether any redistribution of major elements had occurred during the metamorphism. The samples of unaltered sediments were obtained from the Lower Limestone Group of the Rookhope borehole, which are stratigraphically equivalent to the metamorphosed beds of Upper Teesdale.

Particular emphasis was placed on the alkali (Na_2O,K_2O) content of the sediments, in order to re-examine Hutchings's proposal (1895, 1898) that there has been a metasomatic transfer of alkalies from the Whin Sill to the metamorphosed sediments.

Results of alkali determinations

Plots of Na_2O and K_2O weight percent in samples are shown against borehole depth in Figs. 4.1 and 4.2. The first Rookhope borehole section shows the concentration of the two oxides in sediments from the unmetamorphosed Lower Limestone Group. In these, Na_2O is consistently below 1%, K_2O is more variable ranging from 4 to 7%. These values are typical for 'normal' shales with K_2O in excess of Na_2O, which is usually less than 1%. The remaining five sections show plots of samples from various

Figure 4.1 Variation in Na_2O and K_2O concentrations in the argillaceous sediments.

Borehole depth shown adjacent to each section. The table beneath the first borehole section shows Na_2O and K_2O values for individual samples from boreholes not illustrated.

Legend

	Limestone
	Argillaceous and arenaceous sediments
	Whin Sill
ROOKHOPE	Rookhope borehole
B.40 B.41 B.43 B.44	Cow Green boreholes
M.S.L.	Melmerby Scar Limestone
L.RO.	Lower Robinson Limestone
U.RO.	Upper Robinson Limestone
PE.	Peghorn Limestone
SM.	Smiddy Limestone
T.BO.	Tyne Bottom Limestone
S.PO.	Single Post Limestone
⊙	Na_2O values
⊙	K_2O values
△	separated Na_2O values
+	separated K_2O values

Figure 4.1

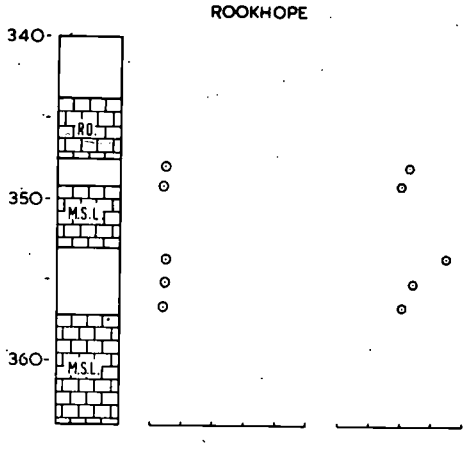

SAMPLE	Na_2O	K_2O	DISTANCE FROM CONTACT
17_{41}	1·95	8·64	3·35 m
19_4	5·25	2·38	9·02
19_9	2·18	1·02	10·74
19_{19}	1·00	4·85	8·20
20_2	1·52	5·17	0·15
35_4	3·47	4·26	0
47_{24}	1·65	0·83	0·69

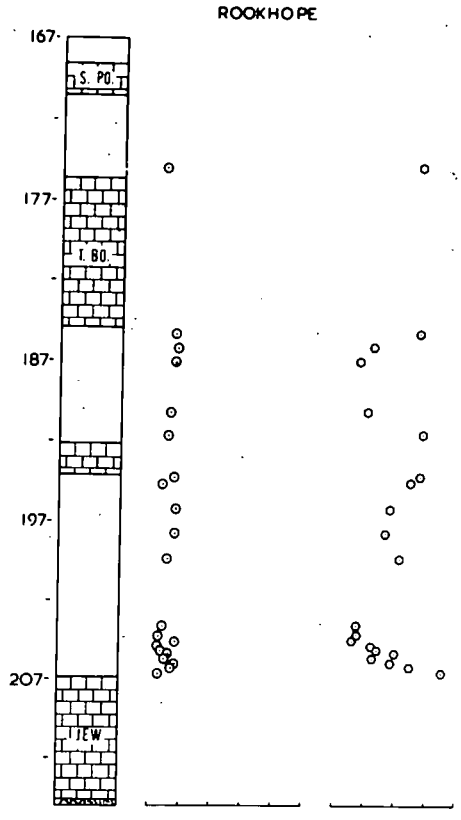

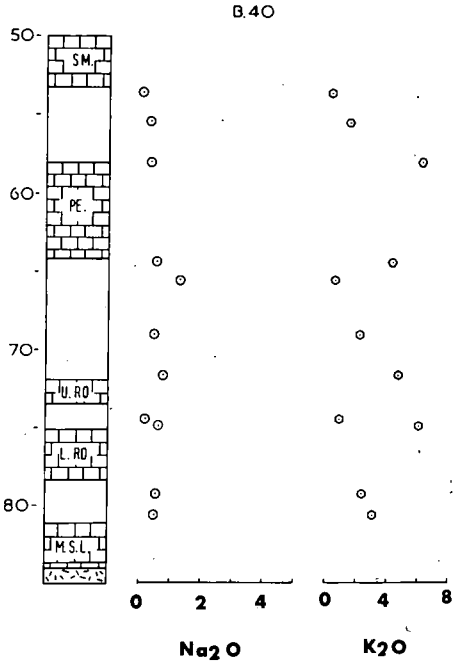

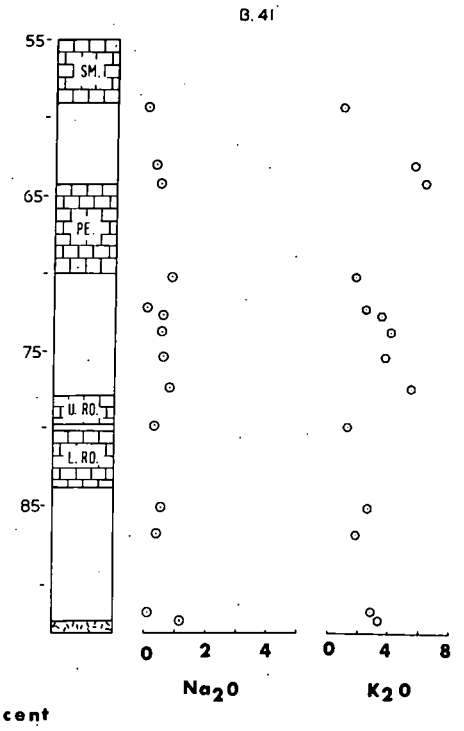

Weight Percent

boreholes up to 45 m from the Whin Sill contact.

In the second Rookhope borehole section (Fig. 4.1), above the Great Whin Sill, Na_2O remains below 1% for all samples. K_2O is more variable, ranging mainly from 2 to 6% but no particular variation is seen. Borehole 40, from Cow Green, also shows Na_2O below 1% except for one sample (40/16) with 1.3% Na_2O. Similarly in borehole 41 only one sample (41/36) has a Na_2O value higher than 1%, and in this case is at the virtual contact. Boreholes 43 and 44, however, show samples with widely varying Na_2O content. In these sections (Fig. 4.2), sediments up to 10 m from the contact have Na_2O less than 1%, while samples closer to the contact show a large variation

In borehole 43, a maximum Na_2O content of almost 4% is seen in a calcareous shale (43/10), at a depth of 48.9 m. The two shale samples 43/9 and 43/8, below 43/10, show low Na_2O of 0.5% and 0.4%, respectively. A horizon of the Melmerby Scar Limestone is present in borehole 43, for a distance of 2.5 m from the contact, in which are several thin, calc-silicate bands (described in Chapter III). Specimens of this material have been separated from the carbonate matrix and analysed. The material separated from these lenses shows a high Na_2O content, in samples 43/4 and 43/5, of 3.1% and 2.2% respectively. A similar relationship of high Na_2O content from calc-silicate lenses in limestone is seen in borehole 44. Samples 44/7S and 44/9S, at depths of 31.7 and 29.9 m respectively, are separated samples containing 3.6% and 5.1% Na_2O. In the centre of a shale horizon, less than 2 m above sample 44/9S, the sample 44/10 (at a depth of 28.3 m) shows less than 1% Na_2O, while at the upper junction of this shale horizon

Figure 4.2 Variation in Na_2O and K_2O concentrations of sediments in boreholes 43 and 44.

Borehole depth shown adjacent to each section. Symbols, ornamentation and abbreviations as given in legend to Figure 4.1.

Figure 4.2

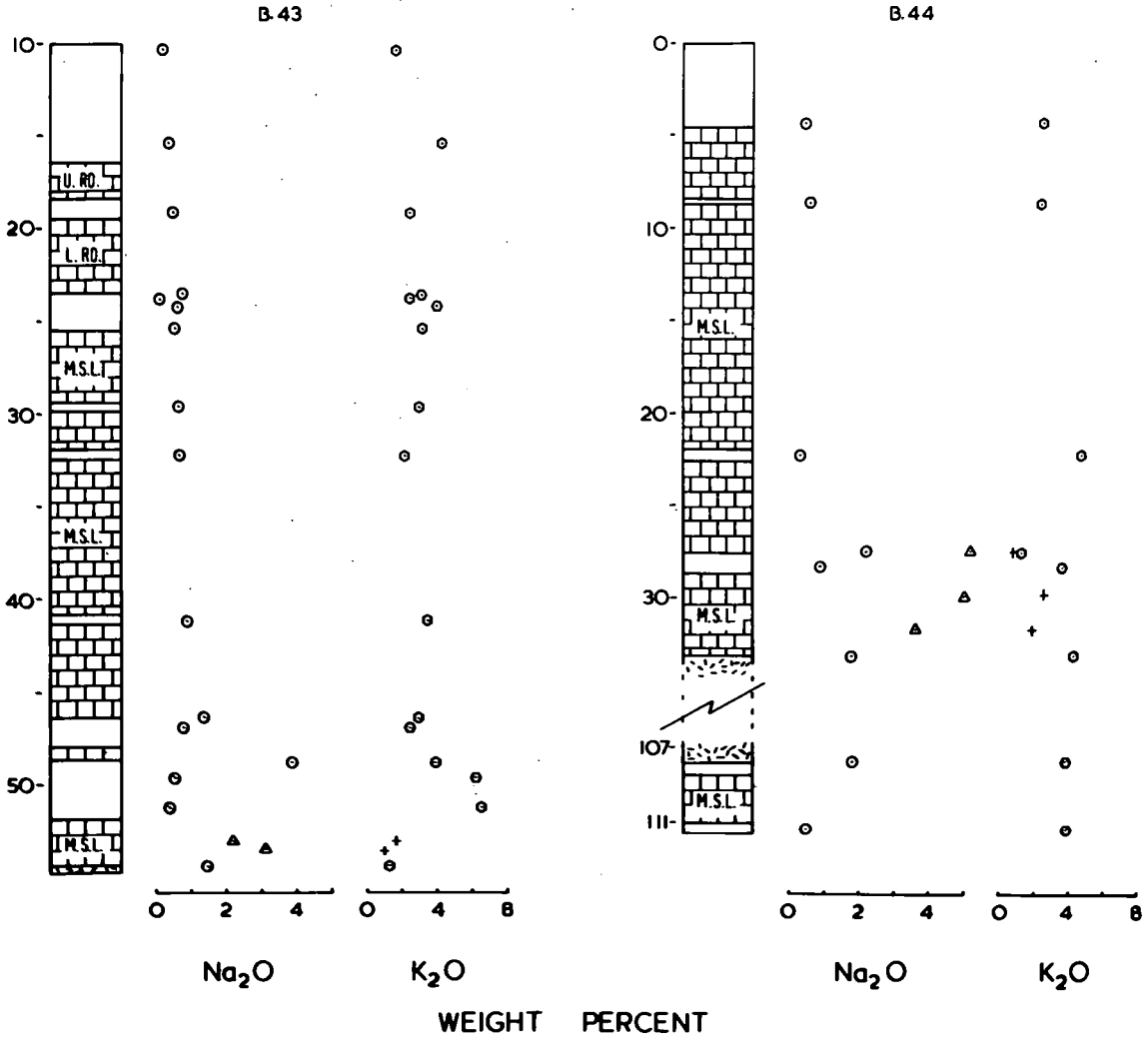
B.43
B.44
10
20
30
40
50
U. RO.
L. RO.
M.S.L.
M.S.L.
M.S.L.
M.S.L.
0
10
20
30
107
111
M.S.L.
M.S.L.
M.S.L.
M.S.L.
0 2 4
0 4 8
0 2 4
0 4 8
Na_2O
K_2O
Na_2O
K_2O
WEIGHT PERCENT

with a limestone, sample 44/11 contains over 2% Na_2O. In this specimen a thin, red flinty band was carefully separated and on analysis gave almost 5.3% of Na_2O. An increase of Na_2O is also seen in beds below the sill, as seen in borehole 44.

There appears to be no consistent change in K_2O content in relation to the variation in Na_2O content. In a few instances K_2O appears depleted when Na_2O is increased. This is seen in samples 43/4 and 43/5, at depths of 53.5 and 53.1 m, where K_2O is 1.0% and 1.7% which is unusually low for these sediments. In other samples there appears to be little change, as in sample 44/9S, which has a K_2O content of 2.6%. The depletion of K_2O in some cases may be explained by the reaction of illite with Na to form sodic feldspar, in which most of the Na is found, with the resultant release of inter-layer K, which is then subsequently concentrated to form potassic feldspar. Electron microprobe analysis (Chapter V) has shown the presence of fine-grained, potassic feldspar in narrow veinlets within some of these calc-silicate lenses.

Also shown in Fig. 4.1 is a table with several alkali determinations of Na_2O-rich beds from other boreholes.

Significance of alkali determinations

The analyses show that there has been patchy addition of Na to argillaceous sediments in the aureole of the sill. There is no steady increase of Na_2O towards the sill but the affected sediments lie mainly within 10 m of the contact. This increase was observed by Hutchings (1898) who noted the irregular pattern but was unable to explain its nature. In the present investigation, a definite correlation exists between the Na_2O content

and environment of the sample. The samples showing high Na_2O in boreholes 43 and 44 occur as calc-silicate lenses within limestones or as calcareous shales at shale-limestone junctions. Shales free from calcareous material do not show any change in alkali content from unaltered sediments.

Conclusions

Sodium is found to be increased in the metamorphosed sediments of the Whin Sill aureole. The increase appears to be confined to calcareous shales or calc-silicate lenses in limestone, mainly within 10 m of the contact. Potassium does not increase but in a few cases it is depleted probably due to breakdown of illite to form sodic feldspar, with the release of the interlayer K.

FACTOR ANALYSIS OF MAJOR ELEMENTS

The relationship between the alkali content of sediments and the metamorphism has been discussed above. To examine what, if any, effect the metamorphism has had on the distribution of the remaining major elements, the data have been processed using R-mode factor analysis. By this method, a complex pattern of variables is reduced to a series of united factors which are more readily interpreted than the raw data.

Twelve variables have been used in the analysis, eleven of which are the normal major elements. The other variable is the distance of each sample from the Whin contact, which provides some hypothetical notation of metamorphic effect. The factor analysis has been achieved using a computer programme written by M.J. Reeves and described by Reeves and Saadi (1971). All data

were transformed to logarithms before analysis, because distribution of elements in nature approaches lognormal rather than normal.

The eigenvalues, cumulative percentages and factor matrices determined are given in Table 4.1, which shows that there are four main factors accounting for over 90% of the observed chemical variance. On passing from the varimax (Table 4.1B) to the promax (Table 4.1C) solution, it is seen that the minor loadings in factors 2 and 4 are removed while many of the strong loadings are increased.

Interpretation of factors

Four main factors are extracted, representing some 90% of the total variance of the data. Over 40% of the variance is explained by factor 4.

Factor 1

This factor accounts for the variance in Na_2O content and distance from contact. The distance has a negative loading against the positive Na_2O variable. Thus as distance from the contact decreases, there is an increase in Na_2O content. This factor is interpreted as a metamorphic feature which has been described previously. There is also a small positive loading for TiO_2, but as this only lies slightly above the significance level of 0.25, it is of doubtful significance.

Factor 2.

Positive loadings are present for Fe_2O_3, MgO, MnO and S. Although MnO and S show high loadings their significance is

Table 4.1 Factor analysis - major elements

A

Eigenvalue	Cumulative percentage
0.210	
0.359	9.03
0.743	19.68
1.031	33.26
1.709	55.76
3.360	100.00

B

Varimax factor matrix

Factor	1	2	3	4
SiO_2		-0.334		-0.714
Al_2O_3				0.938
Fe_2O_3		0.720		0.384
MgO		0.602		0.336
CaO			0.833	
Na_2O	0.663			
K_2O				0.740
TiO_2	0.287			0.734
MnO		0.666		
S		0.400		
P_2O_5			0.824	
Distance from contact	-0.524			

C

Promax oblique factor matrix, K min = 5

Factor	1	2	3	4
SiO_2				-0.676
Al_2O_3				1.012
Fe_2O_3		0.695		
MgO		0.587		
CaO			0.825	
Na_2O	0.696			
K_2O				0.765
TiO_2	0.268			0.731
MnO		0.772		-0.375
S		0.425		
P_2O_5			0.856	
Distance from contact	-0.551			

Loadings less than 0.250 omitted

doubtful because of the low concentrations of these elements. The loadings for Fe_2O_3 and MgO suggest this factor is due to variation in chlorite content of the samples, while the small negative loading for SiO_2 (Varimax) is suggestive of a fall in quartz content with increase in chlorite.

Factor 3

This factor is bipolar with positive loadings for CaO and P_2O_5. The high loading for P_2O_5 is again suspect due to low concentration. The large single loading remaining is probably indicative of variation due to carbonate content.

Factor 4

Positive loadings are present for Al_2O_3, K_2O and TiO_2 (promax) with a negative loading against SiO_2. The high loadings for Al_2O_3, K_2O and TiO_2 point to illite content accounting for the observed variation. As the illite clay fraction increases the quartz content decreases, explaining the negative loading on SiO_2.

Conclusions

R-mode factor analysis has shown that four factors account for over 90% of the observed chemical variation. Of these factors, 2, 3 and 4 are sedimentary features. Factor 4 is dominant, with the change in illite percentage accounting for more than 40% of the variation.

Factor 1, correlating Na_2O with distance from content, is interpreted as a metamorphic feature and as such is the only variation in major element geochemistry of the sediments which

can be explained by the contact metamorphism. This factor only accounts for just over 10% of the chemical variation and, therefore, is of minor volumetric importance compared to the other factors.

ARGILLACEOUS SEDIMENTS - TRACE ELEMENTS

Thirty-one argillaceous sediments, from two boreholes, have been analysed for eight trace elements as follows:- Zn, Cu, Ni, Ba, Zr, Y, Sr and Rb. The results of the analyses are tabulated in Appendix 4.2. No previous determinations of trace element contents, in the sediments adjacent to the Whin Sill, have been made. Trace element variation in other contact aureoles has, however, been examined by various workers including Ghose (1965), Joyce (1970) and Wodzicki (1971).

One of the problems in the investigation of trace element variation, around igneous bodies, is the assumption that the original sediments were homogenous. This assumption is most valid where one particular unit can be traced from outside the aureole up to the igneous contact. This method was followed by Joyce (1970) who noted an enrichment in Y and La, with a decrease in B, towards an intrusive, granitic body. Ghose (1965) and Wodzicki (1971) both studied areas in which regional metamorphic rocks had been intruded by granitic bodies. Of the seven trace elements determined in the present survey, Ghose examined five (Cu, Ni, Ba, Y and Sr) and Wodzicki three (Zn, Cu and Ni). Ghose found a decrease, in pelitic hornfelses towards the contact, of all the five elements except Y which increased. Wodzicki showed a depletion in Cu and Zn at the outer edge of the

Table 4.2 Summary statistics and correlation coefficients - trace elements

Summary statistics

	Zn	Cu	Ni	Ba	Zr	Y	Sr	Rb
Mean	92.8	41.5	75.9	580.7	346.0	81.3	259.5	182.4
Variance	1278.3	188.2	1325.7	4870.3	3251.7	1961.1	6308.2	9559.1
Standard deviation	106.2	13.7	36.4	620.4	152.5	44.3	310.3	139.9
Maximum	415	88	180	3341	748	194	1800	619
Minimum	n.d.	23	26	51	n.d.	15	n.d.	n.d.

Correlation coefficients

	Zn	Cu	Ni	Ba	Zr	Y	Sr	Rb	Distance
Zn	1.000								
Cu	0.133	1.000							
Ni	0.268	0.340	1.000						
Ba	0.040	0.146	0.318	1.000					
Zr	0.201	-0.219	0.100	0.299	1.000				
Y	0.394	0.338	0.635	0.366	0.233	1.000			
Sr	-0.165	0.155	0.171	0.135	-0.269	-0.015	1.000		
Rb	0.250	0.508	0.578	0.386	0.131	0.848	0.011	1.000	
Distance from contact	0.258	0.112	0.173	0.230	0.229	0.384	0.026	0.418	1.000

n.d., not detected

aureole, followed by a rise in concentration which decreased adjacent to the intrusion.

In the present study, a single argillaceous horizon cannot be traced from outside the aureole up to the contact because of the generally conformable sill-like nature of the intrusion. The assumption of initial homogenity is, therefore, less accurate in the present case, where different stratigraphical horizons have been sampled.

The trace element values are presented in Appendix 4.2, and the summary statistics and correlation coefficients in Table 4.2. The summary statistics show that Cu occurs in the lowest concentrations with a standard deviation of 13.7 ppm, while Ba occurs in the highest concentrations. The correlation coefficients show that no single element has a strong correlation with distance from the contact; the only strong correlation seen is that between Y and Rb.

FACTOR ANALYSIS OF TRACE ELEMENTS

Nine variables in thirty-one samples have been processed using R-mode factor analysis. The nine variables include the eight trace elements, listed above, and the distance of each sample from the contact. The eigenvalues, cumulative percentages and factor matrices are given in Table 4.3 and these show that four main factors account for nearly 98% of the observed variance of data. On passing from the varimax (Table 4.3B) to the promax oblique solution (Table 4.3C), most of the higher loadings are increased while some minor loadings are removed.

Table 4.3 Factor analysis - trace elements

A

Eigenvalue	Cumulative percentage
0.102	2.05
0.398	8.50
0.761	20.87
1.584	46.20
3.318	100.00

B

Varimax factor matrix

Factor	1	2	3	4
Zn	0.564			
Cu			-0.511	
Ni			-0.800	
Ba	0.566	0.262	-0.408	0.433
Zr		0.783		
Y	0.432	0.400	-0.618	0.389
Sr				0.983
Rb				0.964
Distance from contact	0.652			

C

Promax oblique factor matrix, K min = 7

Factor	1	2	3	4
Zn	0.717			
Cu		-0.276	-0.706	
Ni			-1.082	
Ba	0.458			0.259
Zr		1.021	0.284	
Y		0.315	-0.556	
Sr				1.138
Rb				1.034
Distance from contact	0.922			

Loadings less than 0.250 omitted

Interpretation of factors

Factor 1

This factor shows strong positive (promax) loadings for Zn and distance from the contact with a moderate positive loading for Ba. This is the only factor to show a significant loading for distance from the contact. It is suggestive of a metamorphic origin with a decrease of Zn and Ba towards the contact. It is probable that Zn, in the argillaceous sediments, is associated with chlorite, replacing Mg and Fe^{2+} ions. Recrystallization of the chlorite would possibly lead to the loss of Zn from the lattice, due to its volatility. This factor, however, is rather insignificant, accounting for less than 7% of the total variation of the data.

Factor 2.

Positive loadings for Zr and Y are shown with a low negative loading for Cu. The strong loading for Zr suggests that the resistate fraction of the sediments controls this factor. Most of the Zr is probably found in detrital zircon. The small loading for Y, which has decreased from varimax to promax solution, is probably explained by its incorporation into zircon or apatite crystals. The negative loading for Cu is of doubtful significance due to it being just above the significance level of 0.250.

Factor 3

Strong negative loadings are seen for Cu, Ni and Y, with a small positive loading for Zr. The interpretation of this factor has proved difficult, although Ni may well be associated with Mg in the chlorite structure.

Factor 4

This factor accounts for over 50% of the observed variance. Strong positive loadings are seen for Sr and Rb, while a minor positive loading is present for Ba. The strong loading for Rb suggests that this factor is associated with the hydrolysate fraction of the sediments, the Rb exchanging for K in the inter-layer position in illite. In sediments, Sr is often introduced by secondary infiltration (Goldschmidt, 1954) and is fixed in the clay-fraction by base exchange. Both elements, therefore, support the interpretation that factor 4 is explained by the variation in the clay-fraction content.

Conclusions

R-mode factor analysis has extracted four main factors, accounting for almost 98% of the trace element data variance.

A decrease in Zn and Ba towards the contact may be interpreted from factor 1 but is only of minor significance. Factor 4 is most important, accounting for over 50% of the variance. This is interpreted as variation due to changes in the hydrolysate fraction of the sediment. A decrease in Zn towards the contact agrees with the results of Ghose (1965) and Wodzicki (1971), although they found decreases in other elements, as mentioned earlier. An increase in Y, as recorded by Ghose and Wodzicki was not seen in the present survey. It was not possible to examine the trace element variation within a single horizon, versus distance from the contact, in the present study. Thus the comments made on factor 1 may not be dependable as it is probable that much of the variation is due to changes in the lithology of the sediments.

LIMESTONE GEOCHEMISTRY

The limestones of the northern Pennines are relatively pure and contain only minor quantities of argillaceous and carbonaceous impurities. Frost (1969) has shown that the CaO content of limestones from the Lower Limestone Group of Otterburn, Northumberland, is in the narrow range of 53 to 55%. For this reason, in the examination of limestones, emphasis was directed towards the trace element content. Strontium is of particular interest, as it is known that even diagenetic recrystallization of limestones results in the loss of Sr from the crystal lattice of calcite (Kulp et al., 1952). Little work, however, appears to have been undertaken on the variation in trace element content of limestones subjected to thermal metamorphism. Ghose (1965) noted an increase in Ba and Cu and a decrease in Sr in regional metamorphosed limestones, from the contact aureole of a granitic body.

Trace element analysis

Thirty-six limestone samples, from five boreholes, were analysed by X-ray fluorescence for seven trace elements as follows: Zr, Cu, Zn, Ni, Ba, Sr and Rb. A further thirty-one samples have also been analysed for Sr and Ba only. In the first series, Zr, Zn, Ni and Rb were found to be present in low concentrations (close to or below the detection limits of the method of analysis, Table 1.1). Of the remaining elements, Sr has proved of greatest value and interest. The data for the trace elements, determined in the limestones, are given in Appendix 4.3.

Results of strontium determinations

For comparative purposes, Sr has been determined in limestones

from the Rookhope borehole and these results are given in Table 4.4.

Table 4.4. Strontium and C determinations in limestones from the Rookhope borehole

Sample	Limestone horizon	Type of limestone	Depth m	Sr ppm	C wt. %
RB56	Melmerby Scar Limestone	Light-grey, pseudobrecciated	367.4	465	0.21
RB57	Melmerby Scar Limestone	Light-grey, pseudobrecciated	364.2	432	0.39
RB59	Melmerby Scar Limestone	Light-grey, pseudobrecciated	360.8	878	0.16
RB69	Robinson Limestone	Light-grey	345.6	1114	0.49
RB72	Upper Smiddy Limestone	Dark-blue, grey	315.5	2181	0.63
RB75	Tyne Bottom Limestone	Dark-grey	175.9	2881	0.69
RB78	Scar Limestone	Light-grey	142.3	1120	0.14
RB81	Great Limestone	Light-grey	13.3	1633	0.31

The Melmerby Scar Limestone shows low concentrations of Sr (RB56, 57 and 59). These limestones, however, have suffered extensive diagenetic recrystallization and appear to be brecciated (Dunham et al., 1965). Light-grey limestones, similar to the Melmerby Scar Limestone but in which diagenetic recrystallization is not so evident, have higher Sr values, in the region of 1100 to 1600 ppm (RB69, 78 and 81). The low values of Sr in the pseudobrecciated limestones may, therefore, be attributed to their extensive recrystallization.

Dark-grey limestones usually have Sr values greater than

2000 ppm. Samples RB72 and RB75 have 2181 and 2881 ppm, respectively. From these results, it is feasible to suggest 'background values' for Sr in the light and dark-grey limestones, in the region of 1100 to 1600 and 2000 to 3000 ppm, respectively. Ineson (1969) obtained an average value of 1750 ppm Sr in the grey, Great Limestone of the northern Pennines. It is probable that both types of limestones had, originally, comparable Sr concentrations. Kulp et al. (1952) have shown that the Sr content in a limestone is dependent on the Sr/Ca ratio of the sea-water during deposition. The fossils in the limestone contain Sr a factor of two higher than the carbonate matrix. As both types of limestone are bioclastic, it seems likely that the difference in 'background values' of Sr is a result of a diagenetic recrystallization (Johnson and Dunham, 1963) in the light-coloured limestones.

Figures 4.3 and 4.4 show Sr values, in Teesdale boreholes, up to 35 m from the Whin Sill contact. Boreholes 17, 18, 21, 22 and 35 are dominated by the light-grey Melmerby Scar and Robinson Limestones. The saccharoidal marble from boreholes 17, 18, 22 and 35 shows consistently low Sr contents, with concentrations below 500 ppm. Boreholes 17 and 18 show values constant around 300 ppm, up to 27 m from the contact. At distances greater than 27 m from the contact, in these boreholes, the Sr concentration rises to between 1000 and 1200 ppm in non-saccharoidal limestone. These concentrations are consistent with the values obtained for unmetamorphosed limestones. It appears, therefore, that there is a limit to metamorphic Sr loss, from the limestones, in the region of 27 m from the contact. Figures 3.2A and 3.2B (p.37), showing the grain-size distributions of calcite in saccharoidal marbles,

Figure 4.3 Strontium variation in limestones from the Cow Green boreholes.

Abbreviations as given in legend to Figure 4.1

Figure 4.4. Strontium variation in limestones from the Cow Green boreholes.

Ornamentation as given in Figure 4.3 and abbreviations as given in legend to Figure 4.1.

Figure 4.3

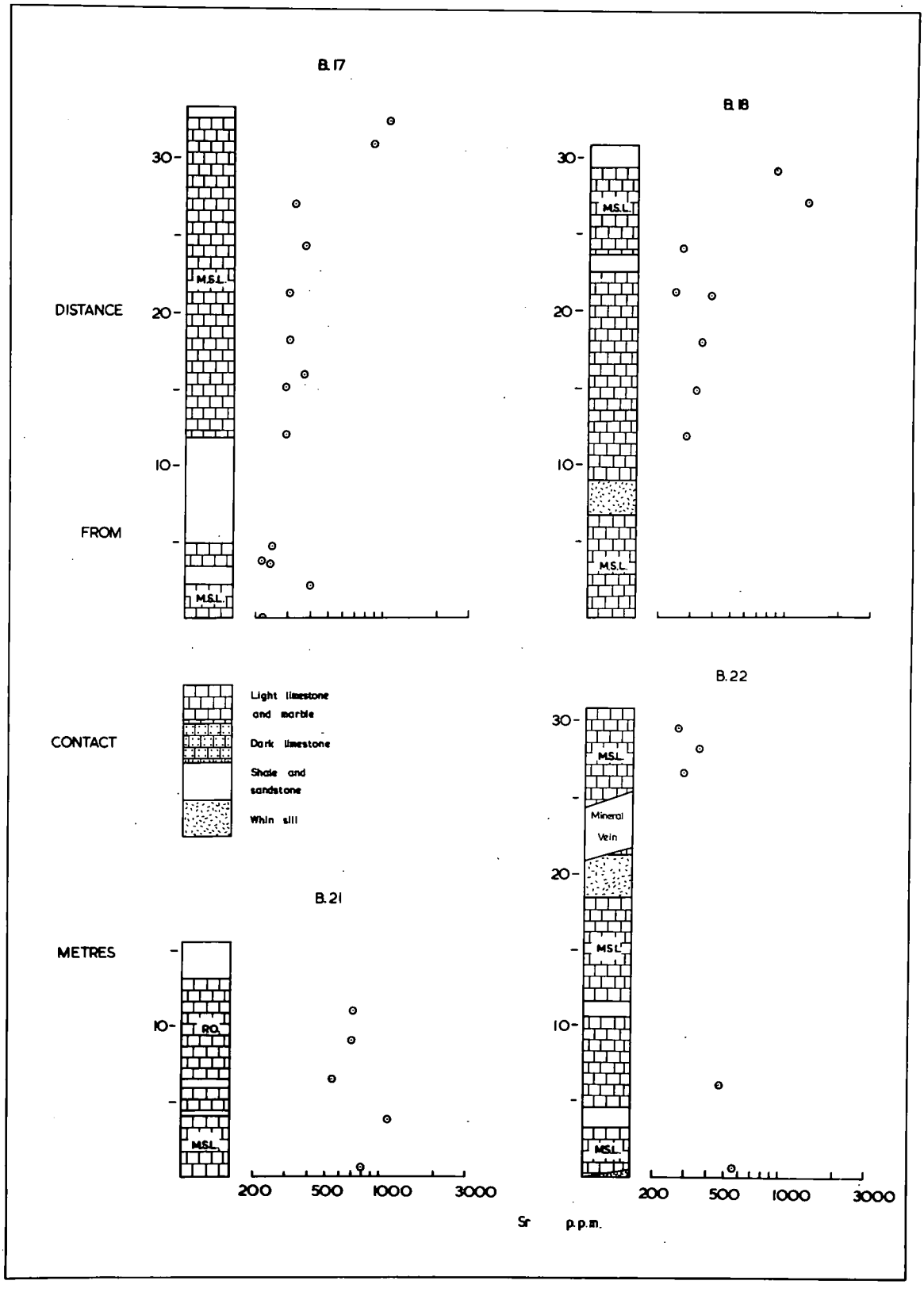
B.17
B.18
B.21
B.22
DISTANCE
FROM
CONTACT
METRES
30-
20-
10-
M.S.L.
RQ.
Light limestone and marble
Dark limestone
Shale and sandstone
Whin sill
Mineral Vein
200
500
1000
3000
Sr p.p.m.

show a decrease in the slope of the curves in the region of 25 m from the contact. This marks the effective limit of marmorization, which correlates well with the rise in Sr concentration, to a 'background value' in the region of 27 m from the contact.

Borehole 22 shows low values of Sr extending up to 30 m from the contact. In this case the mineral vein, shown in Fig. 4.3, is believed to have caused the extra depletion. Ineson (1969) has shown that Sr is depleted in limestones up to 9 m around mineral veins.

An interesting feature of the marbles is that there is a relatively constant value for Sr, over a distance of 25 m from the contact. Boreholes 17 and 18 show consistent Sr concentrations in the region of 300 ppm. A decrease in Sr towards the contact might have been expected as a result of increasing grain-size in the marble. This Sr decrease is not seen, and suggests that an approach to total recrystallization of the original limestone occurs even in the production of fine-grained, saccharoidal marble.

Boreholes 39, 40 and 41 (Fig. 4.4) show stratigraphical sections in which limestones above the Melmerby Scar are dominant. In these sections, dark limestones occur in equal abundance with light-coloured limestones. The dark limestones show Sr in concentrations usually greater than 2000 ppm. However, the majority of the samples analysed lie within the limit of marmorization, recognised previously as 25 m from the contact. Dark limestones, with high Sr, are also intercalated with marbles containing low Sr. The Peghorn Limestone (borehole 40) shows this feature with two dark lenses of limestone interbedded with marbles. The two

Figure 4.4

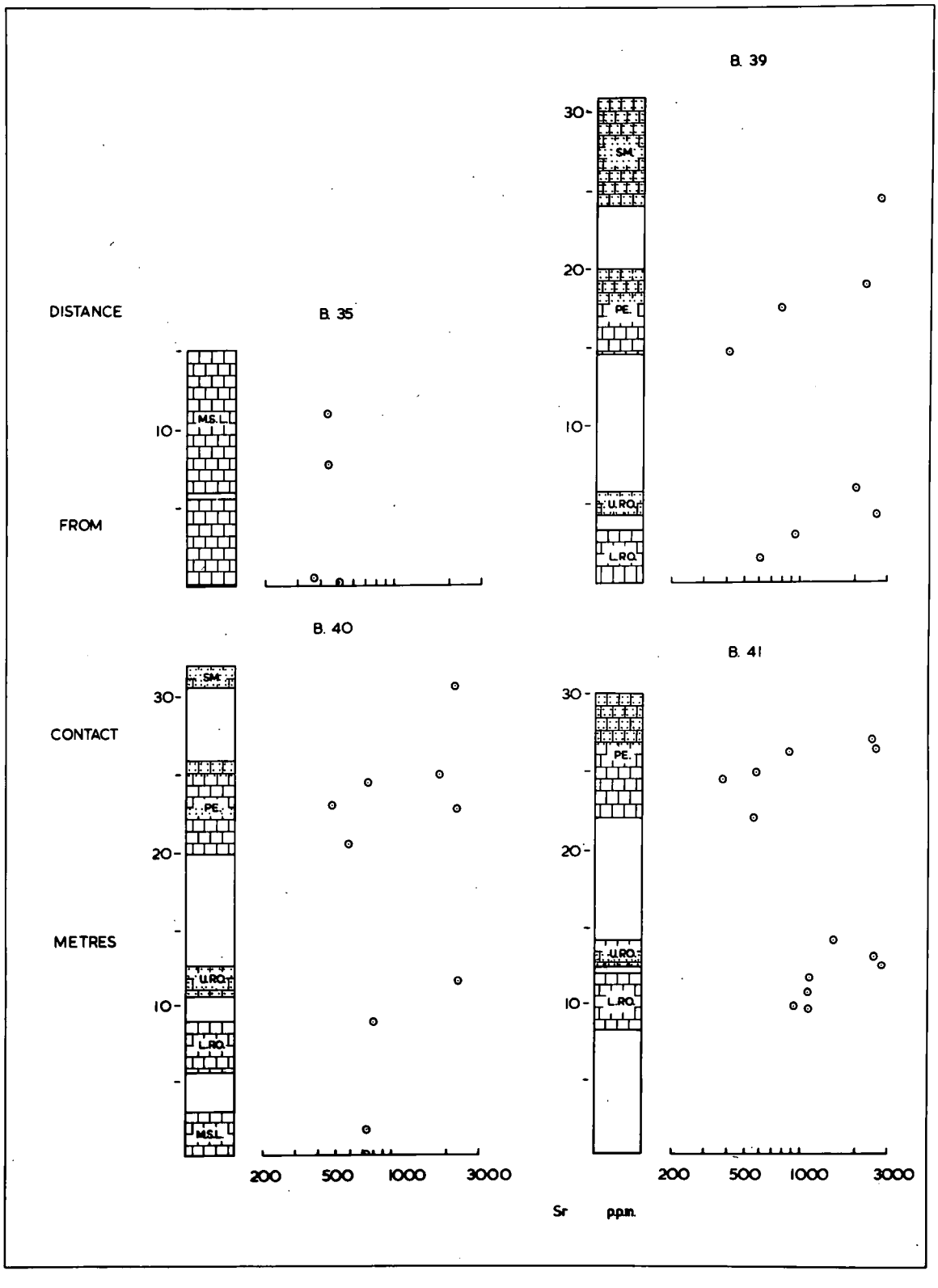
B. 39
B. 35
B. 40
B. 41
DISTANCE
FROM
CONTACT
METRES
SM.
PE.
U.RO.
L.RO.
M.S.L.
30
20
10
200
500
1000
3000
Sr ppm.

dark limestones have 1801 and 2257 ppm Sr respectively (40/22 and 40/19), while the marbles have values of 741, 474 and 581 ppm Sr (40/21, 40/20 and 40/18). Petrographic examination has shown that the dark limestones, even close to the contact, are virtually unrecrystallized. The absence of recrystallization is a result of the inhibiting effect of the organic carbon in these dark limestones, as explained previously by the writer (Robinson, 1971).

Barium and Cu determinations

The Ba and Cu results are given in Appendix 4.3, Ba has an average value of 53 ppm but values range from non-detectable to 228 ppm. Copper values are lower, with an average concentration of 7 ppm and ranging from non-detectable to 23 ppm. No particular pattern of variation could be detected for these two elements.

Conclusions

The results of seven trace elements determinations have shown that Sr is of most value; of the remaining six, only Ba and Cu were consistently above the detection limit of analysis. The marmorization of light-coloured limestones has resulted in a loss of Sr, from a 'background' concentration of 1200 to 1600 ppm, to values mainly in the range of 200 to 400 ppm. Strontium, in boreholes 17 and 18, is depleted to an average value of 301 ppm (std. dev. 58 ppm), up to 25 m from the contact. At distances greater than 25 m, from the contact, the Sr values rise to their 'background values'. Strontium is not depleted in dark-coloured limestones because these sediments have not suffered recrystallization.

FACTOR ANALYSIS OF TRACE ELEMENTS

Five variables in th irty-six limestone samples have been examined using factor analysis. The five variables used were concentrations of Sr, Ba and Cu; distance from contact and an integer representing marble (1), light, unaltered limestone (2) or unrecrystallized, dark limestone (3).

Only two main factors were obtained, as shown in Table 4.5.

Table 4.5. Factor Analysis - Limestones.

Eigenvalue	Cumulative percentage
0.117	
0.212	19.68
1.345	100

Varimax factor matrix

Factor	1	2
Sr		0.800
Ba		
Cu	-312	
Distance from contact	0.340	
Type of limestone		0.790

Promax oblique factor matrix, K min = 2

Factor	1	2
Sr		0.800
Ba		
Cu	-0.318	
Distance from contact	0.336	
Type of limestone		0.792

Loadings less than 0.250 omitted.

Interpretation of factors

Factor 1

This factor is bipolar with a positive loading for distance from contact and a negative loading for Cu. The loadings are both, however, relatively low and as the Cu concentration is low

and near the detection limit, this factor is of doubtful significance.

Factor 2

This factor shows strong positive leadings for both Sr and type of limestone. This factor is interpreted as explaining the variance in the data, as a result of metamorphic recrystallization of the limestones. The positive loadings for both variables show that Sr increases in the unrecrystallized limestones, distance from the contact showing no significant loading.

A second analysis was made using sixty-seven limestone samples, omitting the Cu values. In this analysis only one main factor was extracted, corresponding to factor 2 above. In this case, the loadings on Sr and type of limestone were significantly increased to 0.887 and 0.862 respectively, at K min = 2.

Conclusions

Factor analysis has confirmed the earlier conclusion that metamorphic recrystallization explains the variation in Sr. This factor explaining the majority (80%) of the variation seen. No particular significance can be attributed to the concentrations of Ba or Cu, nor is there any significant variation in these elements with distance from the contact.

ORGANIC CARBON DETERMINATIONS

Two types of limestone were recognised by Johnson and Dunham (1963) in the northern Pennines. Light and dark-coloured limestones constitute the two types, the difference in colour being attributed to the presence of bituminous, organic material

and terrigeneous impurities. In order to confirm the above conclusion, and to give quantitative values to the organic material present, a series of organic carbon determinations have been conducted. (Carbon was determined by an absorption train method after correction for CO_2). Samples from borehole 40 were used, as they showed interbedding of dark limestones and saccharoidal marbles. The results of these carbon analyses have been published (Robinson, 1971). A series of samples from the Rookhope borehole were also analysed for comparative purposes; these results are shown in Table 4.4. These values show that in the unmetamorphosed limestones, the light-coloured limestones have low carbon content, less than 0.4% by weight. The dark limestones (RB72 and 75) have C greater than 0.6%. This relationship is also seen in borehole 40, the carbon acting as an inhibitor to recrystallization as described by Robinson (1971).

APPENDIX 4.1 MAJOR ELEMENT ANALYSES

	RB20	RB21	RB22	RB23	RB24	RB25	RB27	RB31	RB32	RB33
PERCENT										
SIO2	68.68	74.93	83.30	85.48	84.06	86.99	85.30	67.53	84.11	50.88
AL2O3	20.39	15.61	8.75	8.77	9.28	5.13	5.43	24.51	11.02	13.88
+FE2O3	1.30	1.10	1.27	0.89	1.05	1.17	2.65	1.33	0.73	3.62
MGO	0.64	0.54	0.45	0.40	0.35	0.38	0.57	0.92	0.43	1.00
CAO	1.85	1.97	1.66	1.14	1.45	3.83	2.19	2.61	0.47	15.59
NA2O	0.71	0.83	0.37	0.27	0.36	0.83	0.39	0.70	0.58	0.53
K2O	4.86	3.72	2.46	2.44	2.77	1.19	1.36	1.26	1.96	5.45
TIO2	0.96	0.75	0.55	0.52	0.56	0.37	0.39	1.00	0.49	0.77
MNO	0.01	0.01	0.01	0.01	0.01	0.01	0.02	0.01	0.01	0.02
S	0.58	0.52	1.13	0.05	0.08	0.04	1.66	0.10	0.11	1.62
P2O5	0.02	0.03	0.04	0.04	0.02	0.06	0.04	0.02	0.09	0.02

	RB34	RB35	RB37	RB38	RB39	RB41	RB42	RB43	RB44	RB45
PERCENT										
SIO2	69.48	68.96	69.99	62.53	59.41	59.39	59.36	68.22	59.33	59.37
AL2O3	17.86	23.23	20.68	25.34	21.54	24.75	26.28	20.86	27.21	27.32
+FE2O3	3.64	1.03	1.12	2.17	2.51	5.77	4.19	1.54	3.77	2.60
MGO	0.51	0.49	0.51	0.94	1.01	1.73	1.74	0.10	1.16	1.05
CAO	1.24	0.45	2.02	1.11	7.02	0.83	0.60	0.96	0.84	0.86
NA2O	0.80	0.53	0.61	0.70	0.31	0.82	0.59	1.11	0.84	0.73
K2O	3.48	4.19	3.86	5.37	6.95	4.93	6.06	4.50	5.42	6.15
TIO2	0.81	1.02	0.87	0.99	0.96	1.06	1.05	1.04	1.23	1.14
MNO	0.01	0.01	0.01	0.01	0.03	0.01	0.01	0.01	0.01	0.01
S	2.12	0.01	0.30	0.83	0.24	0.69	0.09	1.64	0.16	0.73
P2O5	0.05	0.09	0.03	0.02	0.02	0.02	0.04	0.03	0.03	0.05

+ = Total Fe as Fe_2O_3

APPENDIX 4.1 MAJOR ELEMENT ANALYSES

	RB46	RB47	RB50	RB51	RB52	RB53	RB54	RB66	RB67	17/4
PERCENT										
SIO2	60.71	52.78	61.27	62.25	61.72	68.93	76.34	55.38	68.80	56.29
AL2O3	28.07	23.87	26.88	20.22	26.46	21.45	16.11	25.11	23.56	33.90
+FE2O3	1.17	2.07	1.57	2.16	3.31	0.81	0.86	10.62	0.62	2.21
MGO	0.73	0.90	0.89	1.02	0.72	0.46	0.44	2.67	0.54	0.71
CAO	0.94	10.82	1.47	6.22	0.98	0.94	0.37	0.68	0.30	1.17
NA2O	1.08	0.70	0.72	0.41	0.34	0.80	0.77	0.28	0.42	0.73
K2O	5.58	5.27	5.26	5.78	4.58	2.31	3.23	3.91	4.38	3.10
TIO2	1.34	0.93	1.04	0.94	1.07	0.56	1.08	1.08	1.17	1.55
MNO	0.01	0.02	0.01	0.01	0.02	0.01	0.01	0.02	0.04	0.01
S	0.36	0.12	0.88	0.96	0.72	3.65	0.71	0.12	0.10	0.25
P2O5	0.02	0.03	0.02	0.02	0.07	0.09	0.08	0.14	0.06	0.07

	17/7	17/8	17/10	17/10A	17/11	17/15	17/35	17/41	19/4	19/9
PERCENT										
SIO2	61.97	72.05	55.44	79.99	63.35	53.38	71.04	59.69	66.91	62.97
AL2O3	25.41	17.27	22.42	8.22	18.36	34.80	18.37	22.54	15.24	9.55
+FE2O3	4.22	4.11	5.21	3.16	2.78	1.03	5.32	3.36	1.34	6.79
MGO	0.53	0.61	0.61	0.79	0.48	0.44	0.94	0.67	1.24	2.23
CAO	1.31	1.46	2.17	2.70	2.19	2.47	0.51	0.98	6.46	10.22
NA2O	2.41	0.39	1.95	3.63	10.86	0.50	0.31	1.95	5.25	2.18
K2O	2.96	3.41	8.96	0.58	0.82	5.17	2.77	8.64	2.38	1.02
TIO2	1.08	0.60	1.47	0.46	0.87	1.75	0.68	1.37	1.05	0.61
MNO	0.01	0.02	0.03	0.02	0.02	0.00	0.02	0.19	0.03	0.07
S	0.01	0.00	1.71	0.36	0.20	0.41	0.00	0.54	0.00	0.00
P2O5	0.10	0.08	0.04	0.08	0.07	0.05	0.04	0.07	0.09	0.07

APPENDIX 4.1 MAJOR ELEMENT ANALYSES

	19/10	19/19	20/2	35/4	40/5	40/6	40/11	40/12	40/14	40/15
PERCENT										
SIO2	58.56	67.83	53.21	67.81	60.92	77.84	58.08	91.03	60.46	61.53
AL2O3	24.49	19.34	23.18	15.98	24.66	17.42	28.40	4.95	21.08	16.25
+FE2O3	10.01	3.06	12.17	2.70	7.19	0.28	4.21	1.14	6.31	11.33
MGO	1.01	1.93	0.32	0.70	1.41	0.00	1.42	0.47	2.38	2.73
CAO	0.83	0.92	0.99	3.27	1.18	0.93	0.00	1.14	2.48	0.99
NA2O	0.40	1.00	1.52	3.47	0.47	0.53	0.62	0.19	0.79	0.46
K2O	3.52	4.85	5.17	4.26	3.07	2.39	6.06	0.86	4.69	2.15
TIO2	1.12	0.95	1.26	1.40	0.99	0.58	1.15	0.11	0.99	0.73
MNO	0.02	0.03	0.73	0.30	0.06	0.00	0.04	0.08	0.08	0.13
S	0.00	0.03	1.40	0.05	0.00	0.00	0.02	0.00	0.55	3.50
P2O5	0.04	0.05	0.05	0.05	0.05	0.03	0.00	0.04	0.20	0.19

	40/16	40/17	40/23	40/25	40/26	41/1	41/10	41/14	41/15	41/16
PERCENT										
SIO2	90.37	66.28	61.85	87.71	96.46	61.02	76.26	63.02	65.00	68.09
AL2O3	5.19	25.87	26.52	8.36	2.03	22.69	15.50	22.11	20.97	20.75
+FE2O3	1.24	0.44	1.56	0.79	0.18	7.09	1.89	4.46	5.32	3.35
MGO	0.61	0.25	1.05	0.76	0.00	0.44	0.73	1.98	2.19	1.68
CAO	0.34	1.40	0.73	0.16	0.91	3.57	3.35	1.14	1.05	0.55
NA2O	1.30	0.57	0.36	0.34	0.04	0.50	0.38	0.77	0.56	0.50
K2O	0.55	4.33	6.15	1.51	0.34	2.58	1.18	5.32	3.60	3.87
TIO2	0.23	0.82	1.33	0.26	0.00	1.51	0.52	0.95	0.97	1.02
MNO	0.07	0.00	0.04	0.01	0.02	0.07	0.06	0.06	0.06	0.02
S	0.08	0.00	0.26	0.00	0.00	0.49	0.08	0.04	0.15	0.04
P2O5	0.03	0.05	0.15	0.09	0.03	0.05	0.04	0.15	0.14	0.14

APPENDIX 4.1 MAJOR ELEMENT ANALYSES

	41/17	41/18	41/19	41/27	41/28	41/31	41/32	41/35	41/36	43/2
PERCENT										
SIO2	67.99	73.26	86.80	60.72	62.53	60.17	83.73	38.87	65.59	70.21
AL2O3	20.30	17.56	9.01	19.22	20.98	1.87	11.88	12.41	17.35	8.35
+FE2O3	4.66	4.32	0.19	3.45	5.96	4.43	1.66	6.89	3.18	8.13
MGO	1.49	1.17	0.01	1.79	1.30	0.13	0.22	6.48	0.90	1.12
CAO	0.37	0.43	1.19	6.43	1.69	20.40	0.41	21.52	7.06	5.29
NA2O	0.56	0.09	0.83	0.41	0.25	0.07	0.38	0.09	1.16	1.50
K2O	3.34	2.29	1.58	6.10	5.40	0.71	1.82	2.88	3.36	1.33
TIO2	0.91	0.56	0.35	1.02	0.98	0.11	0.50	0.60	1.28	0.70
MNO	0.06	0.06	0.01	0.14	0.18	0.22	0.06	0.22	0.05	0.07
S	0.23	0.21	0.00	0.56	0.62	1.96	0.00	0.08	0.00	3.25
P2O5	0.09	0.05	0.03	0.15	0.12	0.10	0.04	0.09	0.06	0.06

	43/4	43/5	43/8	43/9	43/10	43/12	43/13	43/16	43/23	43/25
PERCENT										
SIO2	85.46	69.57	59.41	57.06	56.51	67.76	62.80	51.38	63.84	48.49
AL2O3	7.69	12.47	28.56	28.19	22.31	25.95	25.12	34.72	29.58	30.24
+FE2O3	0.21	3.41	3.16	5.36	4.07	0.85	3.96	4.34	1.26	7.75
MGO	0.00	4.48	0.63	0.93	0.90	0.00	0.21	0.46	0.12	1.50
CAO	2.20	5.33	0.49	0.38	6.21	0.83	1.40	1.21	0.87	6.18
NA2O	3.12	2.20	0.36	0.53	3.98	0.77	1.37	0.89	0.60	0.62
K2O	0.96	1.67	6.50	6.18	3.96	2.54	2.92	3.35	2.08	2.90
TIO2	0.31	0.66	0.83	1.32	1.46	1.22	1.13	1.57	1.58	1.85
MNO	0.01	0.07	0.02	0.00	0.11	0.00	0.03	0.07	0.00	0.12
S	0.00	0.07	0.00	0.00	0.41	0.04	1.02	1.96	0.00	0.29
P2O5	0.03	0.06	0.04	0.05	0.08	0.04	0.03	0.06	0.07	0.07

APPENDIX 4.1 . MAJOR ELEMENT ANALYSES

	43/27	43/28	43/29	43/30	43/33	43/35	43/36	44/5	44/7S	44/9S
PERCENT										
SIO2	68.60	57.69	52.69	63.66	77.15	64.78	81.59	63.83	50.21	70.34
AL2O3	22.98	28.85	25.96	26.85	16.40	21.55	14.66	18.24	15.67	14.97
+FE2O3	1.40	5.54	13.90	0.86	1.08	4.11	0.60	4.84	5.30	1.93
MGO	0.32	0.39	2.08	0.18	0.13	1.28	0.25	2.48	4.59	1.64
CAO	1.57	1.40	1.18	3.13	1.62	2.05	0.59	3.35	12.28	2.63
NA2O	0.51	0.60	0.09	0.70	0.46	0.32	0.17	1.80	3.62	5.05
K2O	3.08	3.98	2.46	3.11	2.37	4.24	1.64	4.36	1.86	2.59
TIO2	1.03	1.25	1.11	1.46	0.60	0.92	0.40	0.97	1.20	0.79
MNO	0.04	0.11	0.10	0.01	0.03	0.04	0.01	0.05	0.06	0.03
S	0.37	0.13	0.39	0.00	0.12	0.56	0.05	0.02	0.00	0.00
P2O5	0.10	0.06	0.05	0.04	0.03	0.16	0.04	0.05	0.09	0.04

	44/10	44/11	44/11S	44/14	44/20	44/22	44/28	44/28A	44/32	45/5
PERCENT										
SIO2	65.25	63.03	63.62	54.72	55.80	66.66	68.21	70.12	60.59	67.44
AL2O3	25.85	21.32	15.80	33.61	30.39	25.66	17.97	15.81	22.37	24.53
+FE2O3	1.00	2.88	4.90	2.18	1.86	1.78	2.95	2.85	7.27	2.35
MGO	0.15	0.21	0.10	0.87	0.44	0.66	2.46	2.09	0.90	1.01
CAO	1.73	6.87	5.46	1.03	5.33	0.85	1.67	2.11	0.52	0.52
NA2O	0.93	2.21	5.27	0.37	0.64	0.52	1.82	2.34	0.49	0.51
K2O	3.76	1.41	0.92	4.84	3.62	2.78	3.88	3.70	3.93	2.58
TIO2	1.29	1.43	1.28	1.73	1.73	1.05	0.95	0.80	1.07	1.02
MNO	0.00	0.01	0.03	0.05	0.06	0.00	0.03	0.11	0.03	0.00
S	0.00	0.56	2.57	0.56	0.07	0.00	0.00	0.00	2.78	0.00
P2O5	0.03	0.06	0.05	0.05	0.06	0.03	0.06	0.06	0.04	0.03

APPENDIX 4.1 MAJOR ELEMENT ANALYSES

	45/12	45/13	45/14	45/16	45/17	47/1	47/7	47/8	47/18	47/19
PERCENT										
SIO2	60.99	67.29	82.44	62.83	89.79	64.33	71.35	60.75	57.40	60.04
AL2O3	20.85	20.25	5.69	20.19	7.89	22.39	21.29	24.16	31.46	24.40
+FE2O3	7.26	4.52	2.04	4.64	0.25	4.50	0.90	7.10	2.12	1.70
MGO	2.82	1.85	2.02	2.43	0.07	1.59	0.05	1.43	0.61	1.59
CAO	1.00	0.86	6.04	2.46	0.31	1.35	2.68	1.62	1.09	4.24
NA2O	0.79	0.45	0.82	0.37	0.29	0.38	0.45	0.37	0.49	0.55
K2O	4.06	3.40	0.52	5.12	1.16	4.04	1.02	3.44	4.07	6.11
TIO2	0.89	1.00	0.16	0.96	0.18	0.99	2.01	1.03	1.58	1.21
MNO	0.46	0.04	0.04	0.05	0.00	0.04	0.00	0.03	0.00	0.03
S	0.69	0.19	0.19	0.80	0.00	0.24	0.23	0.00	1.15	0.09
P2O5	0.18	0.16	0.04	0.15	0.07	0.16	0.03	0.06	0.04	0.04

	47/22	47/24
PERCENT		
SIO2	57.95	35.37
AL2O3	27.71	7.66
+FE2O3	6.17	14.35
MGO	0.76	2.32
CAO	0.68	25.57
NA2O	0.37	1.65
K2O	5.04	0.83
TIO2	1.26	0.78
MNO	0.00	0.08
S	0.00	0.02
P2O5	0.06	0.09

Appendix 4.2 Trace element determinations - argillaceous sediments (ppm).

Sample	Zn	Cu	Ni	Ba	Zr	Y	Sr	Rb
17/4	182	60	125	989	376	194	333	619
17/7	66	34	86	402	384	64	372	144
17/8	n.d.	36	41	91	128	53	76	167
17/10	108	88	84	1000	265	132	419	450
17/11	n.d.	36	33	93	276	22	181	9
17/13	5	31	26	97	150	15	82	13
17/14	7	23	26	67	199	16	67	26
17/17	5	28	107	171	440	74	96	109
17/24	37	36	47	886	368	136	289	434
17/25	60	37	41	992	446	77	169	146
17/29	166	69	89	892	251	113	210	247
17/30	82	38	180	1638	366	155	406	405
17/34	9	48	62	156	347	92	361	127
17/36	41	56	68	51	134	22	n.d.	n.d.
17/37	17	32	44	236	174	41	20	94
17/38	6	58	87	817	312	77	132	182
17/43	64	32	69	482	415	71	408	114
21/5	75	34	69	238	674	80	225	138
21/6	35	36	112	652	368	104	462	228
21/7	296	24	78	668	330	168	196	100
21/8	14	34	67	3341	544	55	474	126
21/13	41	44	86	543	372	106	197	272
21/14	130	42	51	357	339	88	147	202
21/15	296	32	27	284	339	39	95	98
21/16	83	35	31	241	748	39	99	48
21/19	111	44	97	516	403	97	160	242
21/20	317	54	146	658	461	101	163	243
21/21	167	26	71	369	533	81	116	173
21/22	38	45	126	424	251	94	139	244
21/22A	415	46	100	520	333	91	152	232
21/23	5	47	77	130	n.d.	22	1800	23

n.d. = not detected.

Appendix 4.3 Trace element determinations - limestones (ppm).

Sample	Sr	Ba	Cu	Sample	Sr	Ba	Cu
17/18	219	23	4	35/11	440	22	12
17/15	400	60	11	35/13	438	63	7
17/14	366	112	n.d.	39/3	605	89	-
17/9	242	31	5	39/4	941	38	-
17/40	216	11	5	39/7	2632	66	-
17/39	247	31	7	39/8	2022	191	-
17/6	293	12	23	39/17	409	123	-
17/5	291	19	7	39/19	786	95	-
17/3	307	26	5	39/20	2275	228	-
17/2	304	n.d.	10	39/25	2701	24	-
17/1	374	19	20	40/2	728	36	-
17/31	327	37	6	40/3	729	98	-
17/28	875	22	9	40/10	800	40	-
17/26	1090	100	11	40/13	2302	79	-
18/10	285	36	n.d.	40/18	581	52	-
18/9	322	12	8	40/19	2257	131	-
18/8	341	24	7	40/20	474	59	-
18/7	382	5	10	40/21	741	66	-
18/6	242	25	8	40/22	1801	42	-
18/4	264	30	11	40/27	2193	51	-
18/3	1298	35	9	41/5	1133	33	-
18/2	870	56	13	41/7	937	54	-
21/2	797	16	5	41/8	1110	32	-
21/4	1124	40	10	41/9	1143	29	-
21/9	549	59	9	41/11	2780	68	-
21/11	702	26	n.d.	41/12	2545	176	-
21/12	716	29	15	41/13	1536	85	-
22/11	558	31	10	41/20	561	42	-
22/7	470	34	9	41/21	382	76	-
22/1	286	22	n.d.	41/22	578	46	-
22/2	348	45	10	41/23	871	50	-
22/3	266	22	n.d.	41/24	2619	76	-
35/5	506	25	5	41/25	2496	74	-
35/6	367	65	7				

n.d. = not detected.

- = not determined.

CHAPTER V

MINERALOGY OF CONTACT ROCKS

Introduction

A wide range of metamorphic minerals has been developed in calcareous rocks within 25 m from the Whin Sill contact (Fig. 3.3). Because of the fine-grained nature of the metamorphic products, specific mineral identification is difficult, even with detailed petrographic examination of the samples. Early work on the contact rocks of the Whin Sill, involving mineral identification, should be treated with caution.

Electron microprobe analysis has proved of great value in the examination of the mineralogy of fine-grained contact rocks and the majority of this Chapter is based upon such work although X-ray diffraction has also proved useful for mineral identification. The chemical analyses presented are the first to be recorded of any minerals in the Whin Sill aureole.

GARNETS

Garnet is the most abundant and ubiquitous mineral appearing in the metamorphic aureole. Although no previous analyses of the garnets have been made, Dunham (1948) and Smythe (1950) suggested that they were grossular on the basis of refractive index measurements. Electron microprobe analyses of 129 points have been made on nineteen garnet crystals from seven samples and these are presented in Appendix 5.1. The grossular molecule is dominant in the analyses (total Fe assumed as Fe_2O_3) with 90% of the points analysed having a grossular molecule component of between 70 and 98.6%.

Eighteen of the point analyses have a grossular molecular content of between 95 and 98.6% and are some of the purest recorded grossulars (Deer, Howie and Zussman, 1962). The unit formulae and end-member compositions presented in Appendix 5.1 are those derived using the method proposed by Rickwood (1968) and a computer programme written by Dr. A. Peckett of the Dept. of Geology, University of Durham. Andraditic garnet is recorded for the first time, in sample 46/13, with an andradite component of over 60% (Appendix 5.1).

Garnets are only rarely seen in hand-specimen (Chapter III) but petrographic examination reveals their relative abundance. Where seen in hand-specimen they are typically red-brown in colour (43/22). The presence of white to buff-coloured, massive garnet in sample 35/4 (Plate 3.4) could have been indicative of hydrogrossular and for this reason cell-size determinations were undertaken (p.90). The garnet crystals vary greatly in form and size, ranging from <0.01 to over 1 mm in diameter. A variety of forms are seen in the crystals, depending on the matrix material. Where the garnet is set in a matrix of calcite, chlorite or prehnite, idioblastic and sub-idioblastic outlines are present (Plates 5.1, 3.17 and 5.2). Where the grains abut against feldspar areas (Plate 5.2), non-rational, serrated outlines are developed. An idioblastic outline is, however, present on the side adjacent to the prehnite. Many of the garnets, as is common in the ugrandite series, show slight anisotropism, the maximum is seen in sample 43/22 (Plate 5.1) with areas of first-order yellow interference colours. Sector twinning is occasionally seen in the garnets, with up to 12 pyramids present,

Plate 5.1 Sample 43/22. Idioblastic to sub-idioblastic garnets set in a calcite matrix. Sector twinning is well developed in these garnets, which also show marked anisotropism. (x50)

Plate 5.2 Sample 43/3. Very fine-grained feldspar, which has a rim of garnet, is present in the northern third of the Plate. The lower half is dominantly prehnite with garnets. The garnets in the prehnite, or abutting against it, have idioblastic outlines whereas those edges abutting against feldspar have non-rational boundaries. (x250)

Analysis 43/3-2 Garnet rim to feldspar. 3 points, 2A-2C

Analysis 43/3-3 Garnet rim to feldspar. 7 points, 3A-3G

Analysis 43/3-8 Garnet set in prehnite. 6 points, 8A-8F

Plate 5.3 Sample 44/11. Idioblastic garnet surrounded by pyrite and penetrated by needles of apatite. Well developed, concentric optical zoning is visible. (x200)

Analysis 44/11-1 Garnet in pyrite. 12 points, 1A-1L

Plate 5.1

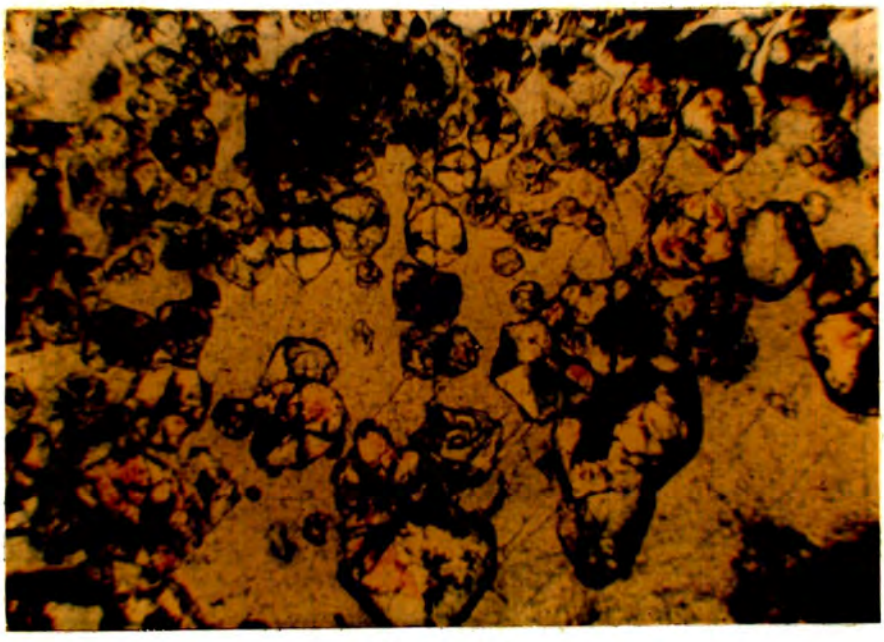

Plate 5.2

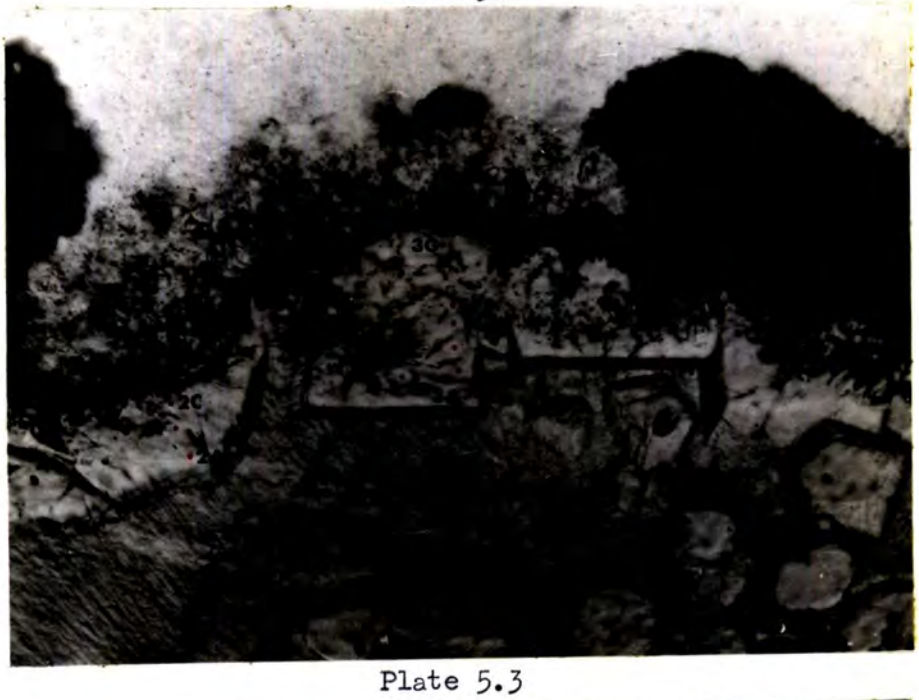

Plate 5.3

the vertices meeting in the centre of the crystals (Plate 5.1). Optical zoning is seen in some garnets (Plates 5.3 and 5.4) suggestive of chemical zoning which is examined in a later section. Inclusions of quartz, calcite and carbonaceous material, are abundant in many of the garnets. Normally the inclusions are arranged haphazardly (Plate 3.15) but, rarely, inclusions arranged in a regular pattern are present (Plate 5.5).

Cell-size determinations

Cell-size measurements have been made on garnets from five samples, using an 11.460 cm diameter, Debye Scherrer camera with Cu radiation and a Ni filter, at 40 KV and 20 Ma. The samples were crushed using a tungsten-carbide ball-mill and then the carbonate fraction was removed by digestion of the sample in oxalic acid. The residues were separated using Clerici's solution and were finally hand-picked under the microscope.

The cell-size computations were made by using a computer programme held by A. Hall of the Dept. of Geology, University of Durham. The results of the determinations are given in Table 5.1 below:-

Table 5.1 Grossular cell-size determinations

Average Mol.% grossular	Sample	Cell-size (Å)	Std. Dev.
-	19/5	11.821	0.012
96.18	35/4	11.811	0.012
-	43/7	11.871	0.008
93.31	43/21	11.842	0.032
69.97	43/22	11.858	0.017

(-), not determined

Plate 5.4 Sample 43/22. Sub-idioblastic garnets, in calcite matrix, showing twinning and optical zoning. Tabular epidote and radiating chlorite are visible at western edge of Plate. (x100)

Plate 5.5 Sample 43/3. Garnet showing inclusions of dominant quartz and calcite arranged in a regular manner parallel to the crystal edges. (x250)

Plate 5.6 Sample 43/3. Garnet associated with coarse feldspar in north-east part of Plate. Fine-grained chlorite matrix with garnets in south-west part. (x200)

Analysis 43/3-1 Garnet crystal. 7 points, 1A-1G

Analysis 43/3-4 Garnet rim to feldspar. 4 points, 4A-4D

Analysis 43/3-1 Carlsbad twinned feldspar. 3 points, 1A-1C

Analysis 43/3-2 Untwinned feldspar crystal.

Analysis 43/3-3 Untwinned feldspar crystal.

Plate 5.4

Plate 5.5

Plate 5.6

The cell-sizes recorded in Table 5.1 are somewhat lower than the values given by Deer, Howie and Zussman (1962). They give a value of 11.851 Å for grossular, while garnet from sample 35/4, with 96% of the grossular molecule, has a cell-size of 11.811 Å. Of the above five samples, chemical analyses of the garnets are available for 35/4, 43/21 and 43/22 (Appendix 5.1). In these the smallest cell-edge, 35/4 is associated with the highest molecular % of grossular and vice versa (Table 5.1). No evidence appears to be forthcoming, from these results, to suggest the presence of hydrogrossular.

Electron microprobe studies

Analyses of 129 points within garnets have been made, to determine the general composition of the crystals and to examine possible compositional zoning which is suggested by petrographic examination (Plate 5.3). Zoned garnets are well known from contact and regional metamorphic areas through the work of Hollister (1969), Leake (1967) and Atherton and Edmunds (1966). In the garnets studied there is a general enrichment of Mn and Ca in the cores and Mg, Fe and Ti in the rims of crystals, the zoning not being related to the metamorphic conditions. No microprobe studies, however, appear to have been undertaken on garnets dominant in the grossular molecule, besides those presented here.

The garnet point analyses are shown in diagrammatic form in Figs. 5.1 to 5.4. Photomicrographs of twelve of the crystals are shown in Plates 5.2, 5.3, 5.6, 5.7, 5.8 and 5.9 as described in the explanation to each Figure. Each garnet was analysed for seven elements, except for 44/9A and 44/11-2 in which Ti and Mn,

Plate 5.7 Sample 43/3. Sub-idioblastic garnets in prehnite matrix, with clouded feldspar visible at edges of Plate. (x100)

Analysis 43/3-5 Garnet set in prehnite. 6 points, 5A-5F

Analysis 43/3-6 Garnet set in prehnite. 5 points, 6A-6E

Analysis 43/3-7 Garnet rim to feldspar. 3 points, 7A-7C

Plate 5.8 Sample 43/22. Calcite nodule in argillaceous horizon, with sub-idioblastic garnets. (x100)

Analysis 43/22-2 Garnet at edge of calcite nodule and abutting against argillaceous material. 6 points, 2A-2F

Plate 5.9 Sample 44/9A. Idioblastic garnet set in fine-grained chlorite associated with idocrase. (x120)

Analysis 44/9A-2 Garnet set in chlorite. 7 points, 2A-2G

Plate 5.7

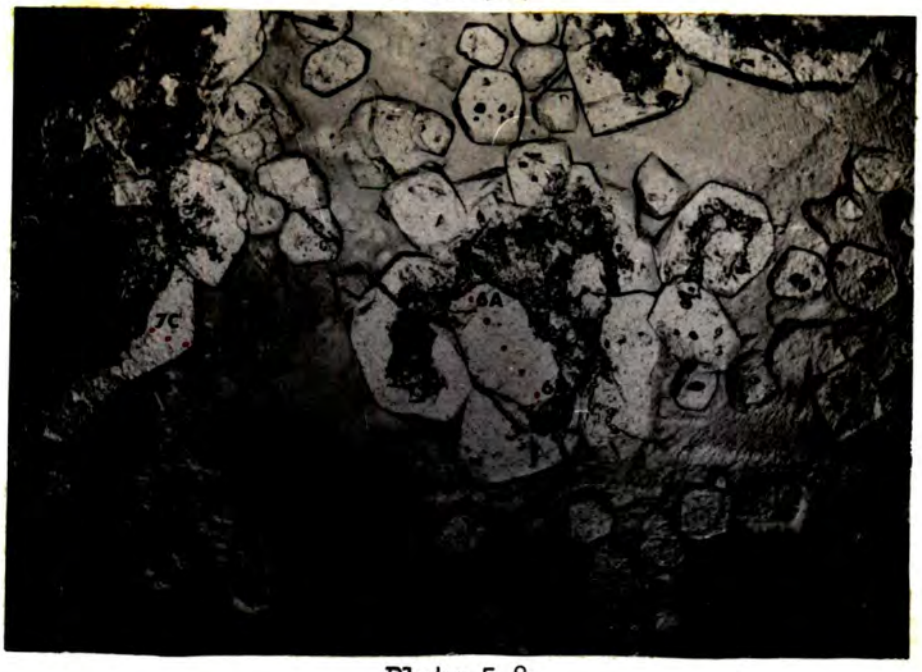

Plate 5.8

Plate 5.9

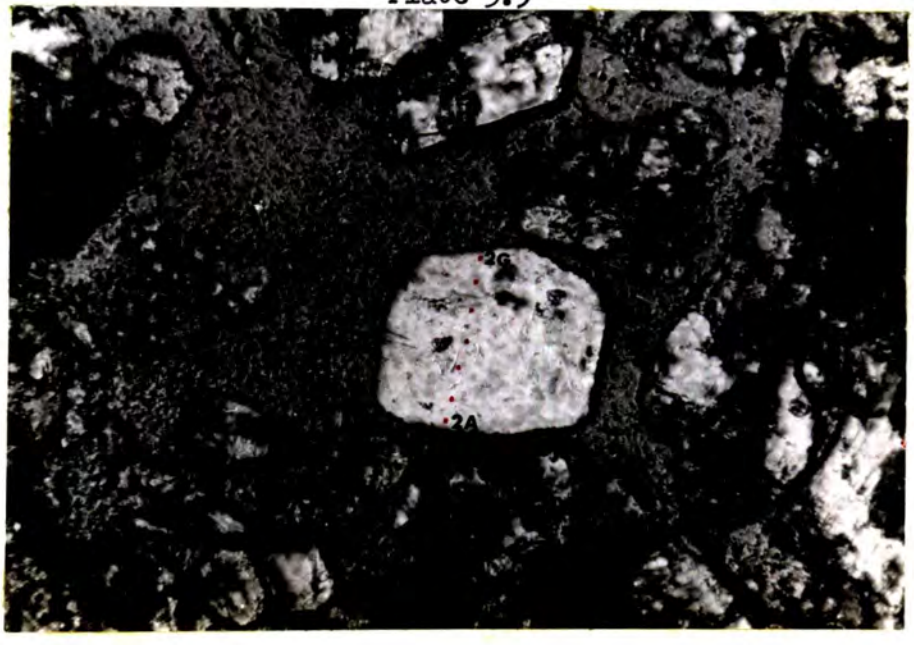

respectively, were not determined (Appendix 5.1). Of the seven oxides, TiO_2, MgO and MnO are consistently below 1%, while MnO is in several cases below 0.1%. The standard deviation of each element, for eight readings on point I of crystal 44/11-1, is given in Appendix 5.9.

Compositional zoning

Compositional zoning in the 'normal' sense (Leake, 1967; Hollister, 1969) is not well developed in garnets examined during the present study, except for the two crystals from sample 44/11 (Fig. 5.3). In both crystals, a marked decrease in Fe (total as Fe_2O_3) is seen in the core, 44/11-2 showing a small central peak of Fe. Sample 44/11-1 shows a decrease of Fe_2O_3, from 11.0%, at the rim (L) to 2.1% at the centre (F). A reciprocal change is seen in the Al_2O_3 contents of these garnets with an increase towards the centre. Variation in Al content does not appear to have been reported before but is to be expected in the grossular/andradite series. A slight increase, in the core, is also seen in both CaO and SiO_2, but TiO_2 shows a marked decrease in sympathy with Fe_2O_3. In sample 44/11-1, TiO_2 appears to have been depleted in the actual crystal rim (Fig. 5.3). Variation in MgO does not show a simple pattern but both crystals show a slight core enrichment.

Of the remaining crystals, only 43/21-2 (H-J) shows depletion of Fe_2O_3 in the core, while TiO_2 is depleted in the core of 43/3-8. Crystals 43/21-1 and 43/21-2 (A-G), (Fig. 5.2) show an increase of Fe in the core, which is a reversal of the normal zoning sequence. Thus zoning of the normal sense is only seen in sample 44/11, where the garnets are surrounded by pyrite. In

Figure 5.1 Electron microprobe garnet analyses.

Analyses 43/3-1, 43/3-4 } analysed crystals shown in Plate 5.6.

Analyses 43/3-2, 43/3-3 } analysed crystals shown in Plate 5.2.

Analyses 43/3-5, 43/3-6 } analysed crystals shown in Plate 5.7.

Figure 5.2 Electron microprobe garnet analyses.

Analysis 43/3-7, analysed crystal shown in Plate 5.7.

Analysis 43/3-8, analysed crystal shown in Plate 5.2.

Analysis 43/21-1, xenoblastic garnet crystal set in calcite, 16 points analysed along edge of crystal.

Analysis 43/21-2, sub-idioblastic garnet set at edge of argillaceous band in saccharoidal marble. Analyses 2A-2G, north-south traverse and 2H, E, I and J, east-west from contact with shale to calcite edge.

Figure 5.1

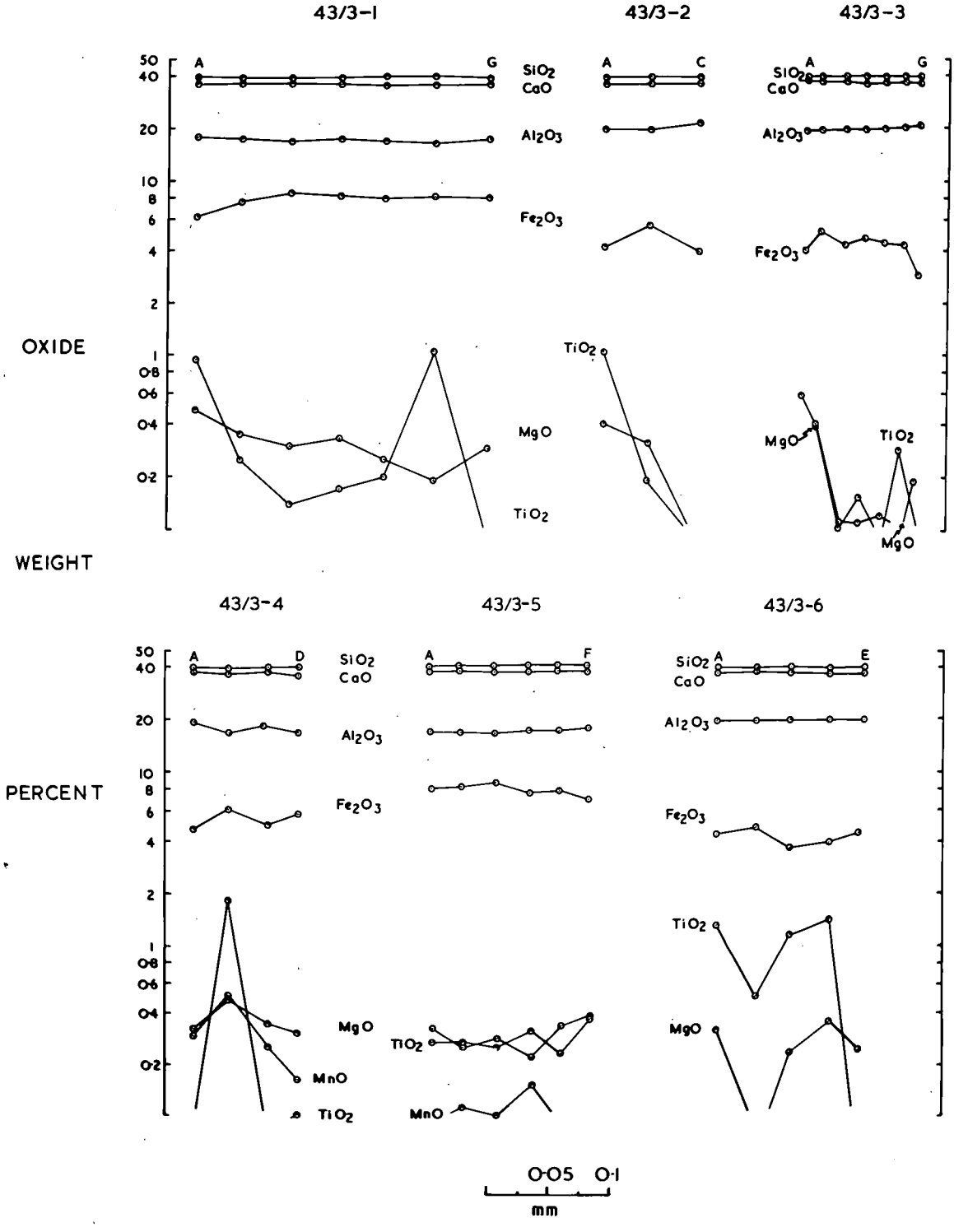
43/3-1
43/3-2
43/3-3
OXIDE
WEIGHT
PERCENT
A
G
C
SiO2
CaO
Al2O3
Fe2O3
MgO
TiO2
43/3-4
43/3-5
43/3-6
D
F
E
MnO
0·05
0·1
mm

Figure 5.2

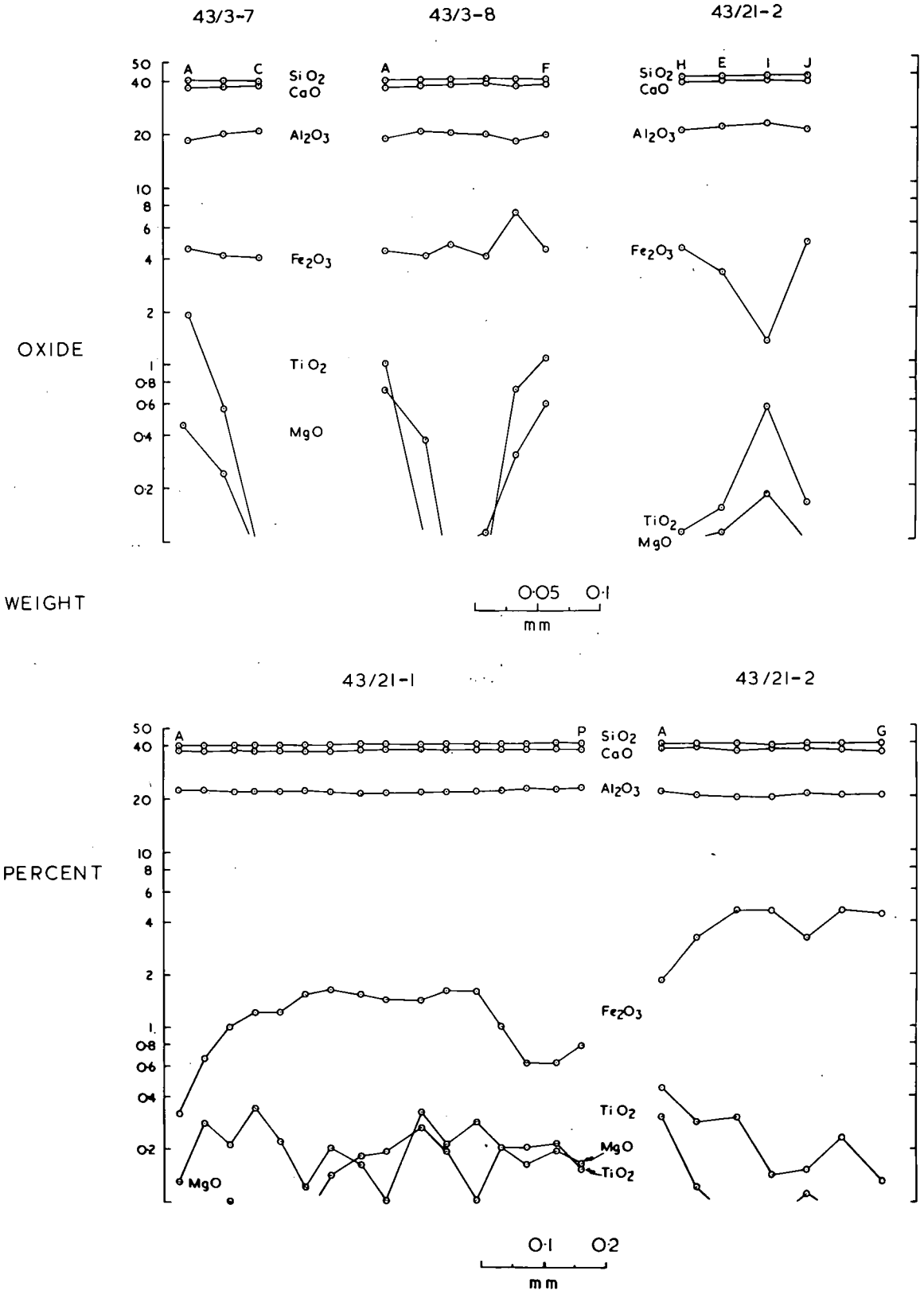
43/3-7
43/3-8
43/21-2
OXIDE
WEIGHT
PERCENT
A
C
F
H
E
I
J
G
P
SiO2
CaO
Al2O3
Fe2O3
TiO2
MgO
50
40
20
10
8
6
4
2
1
0·8
0·6
0·4
0·2
0·05
0·1
0·2
mm

this case it appears that Fe will have been relatively abundant during the growth of the garnet, while Al was relatively rare. Aluminium would then be preferentially incorporated in the lattice and, as it became depleted in the volume surrounding the garnet, so Fe was incorporated to fulfil the lattice requirements.

Although the majority of the crystals do not appear to show any regular compositional variation at first examination, some conclusions may be drawn by detailed knowledge of the particular environment in which each crystal is found. In sample 43/3, garnets nos. 2, 3, 4, 7, occur as rims around the feldspar areas (Plates 5.2, 5.6 and 5.7). In all of these crystals an increase in Al is seen towards the feldspar; 43/3-7 shows an increase from 18.1% (A) to 20.5% (C) of Al_2O_3. There is a reciprocal decrease in Fe, from 4.5% (A) to 4.0% (C) of Fe_2O_3 in the same sample. Similarly TiO_2 and MgO show a decrease towards the feldspar, except for 43/3-4 which shows an increase in these elements before decreasing at the edge of the crystal (Fig. 5.1). A decrease in TiO_2 from 1.9% (A) to 0.1% (C) is evident in crystal 43/3-7. The feldspar areas are produced by the reaction of illite with Na to form albite, excess Al, Ca and Si is available, which forms grossular as described in Chapter VI. Illite has Fe and small amounts of Ti and Mg in its structure and as these cannot be readily incorporated in the feldspar lattice, they are incorporated into the grossular. Titanium and Mg are only present in small amounts and Fe, although present in greater amounts, is still relatively low in concentration. It seems, therefore, that these 'scarcer' elements are concentrated during the initial period of growth of the crystal and as the garnets grow out from

Figure 5.3 Electron microprobe garnet analyses.

Analysis 43/22-1, sub-idioblastic crystal set in calcite.

Analysis 43/22-2, analysed crystal shown in Plate 5.8.

Analysis 44/9A-1, sub-idioblastic garnet set in calcite.

Analysis 44/9A-2, analysed crystal shown in Plate 5.9.

Analysis 44/11-1, analysed crystal shown in Plate 5.3.

Analysis 44/11-2, crystal surrounded by opaques as in 44/11-1.

Figure 5.4 Electron microprobe garnet and idocrase analyses.

Analysis 35/4, garnet crystal set in prehnite.

Analysis 46/13-1, xenoblastic garnet crystal formed at edge of argillaceous horizon in a limestone.

Analysis 46/13-2, xenoblastic garnet in centre of argillaceous band mentioned above.

Analysis 44/9A-1, idioblastic idocrase set in fine-grained chlorite, shown in Plate 5.15.

Analysis 44/9A-2, idioblastic idocrase set in fine-grained chlorite.

Analysis 45/1, sub-idioblastic idocrase in a calcite matrix.

Figure 5.3

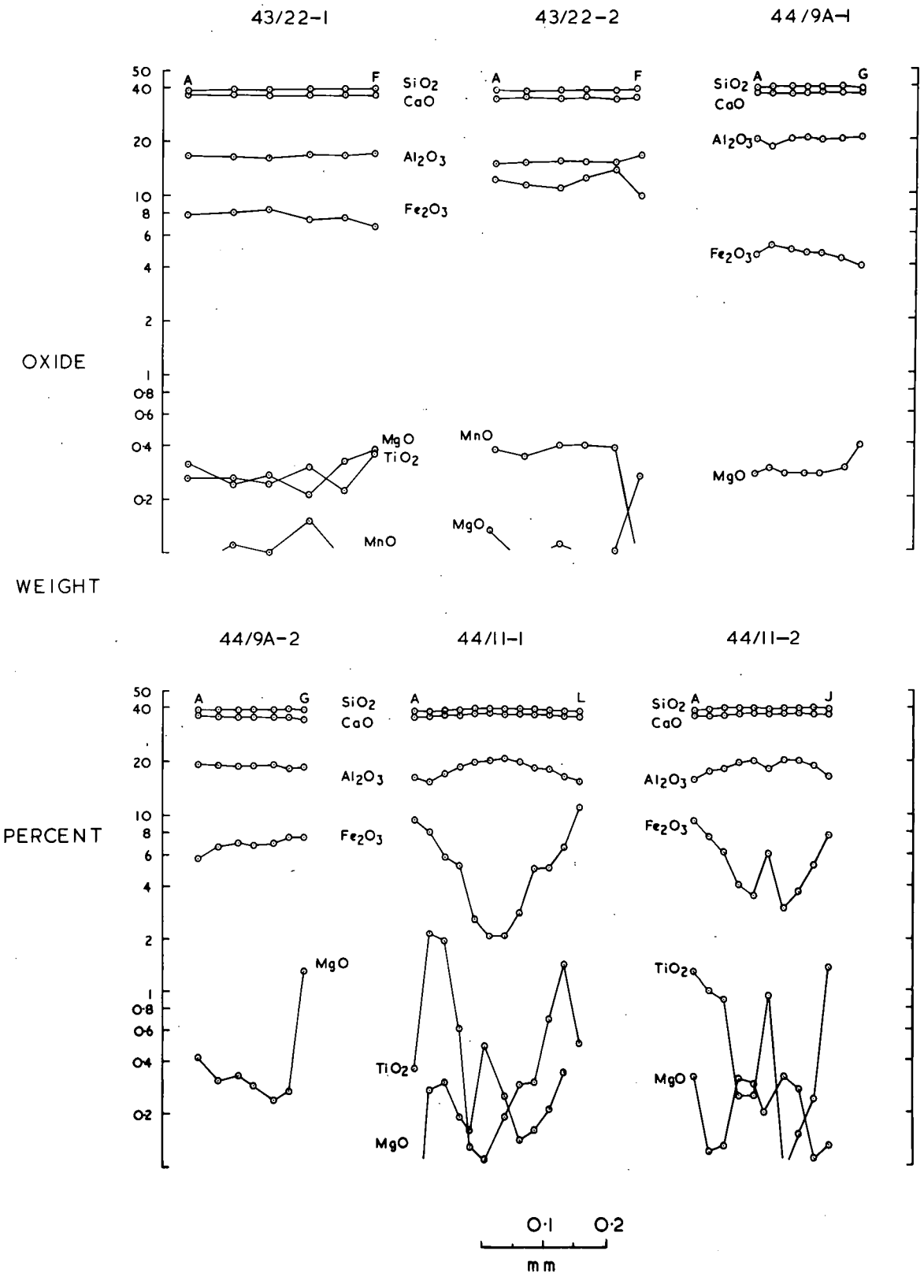
43/22-1
43/22-2
44/9A-1
OXIDE
WEIGHT
PERCENT
A
F
G
SiO2
CaO
Al2O3
Fe2O3
MgO
TiO2
MnO
44/9A-2
44/11-1
44/11-2
L
J
50
40
20
10
8
6
4
2
1
0·8
0·6
0·4
0·2
0·1
0·2
mm

Figure 5.4

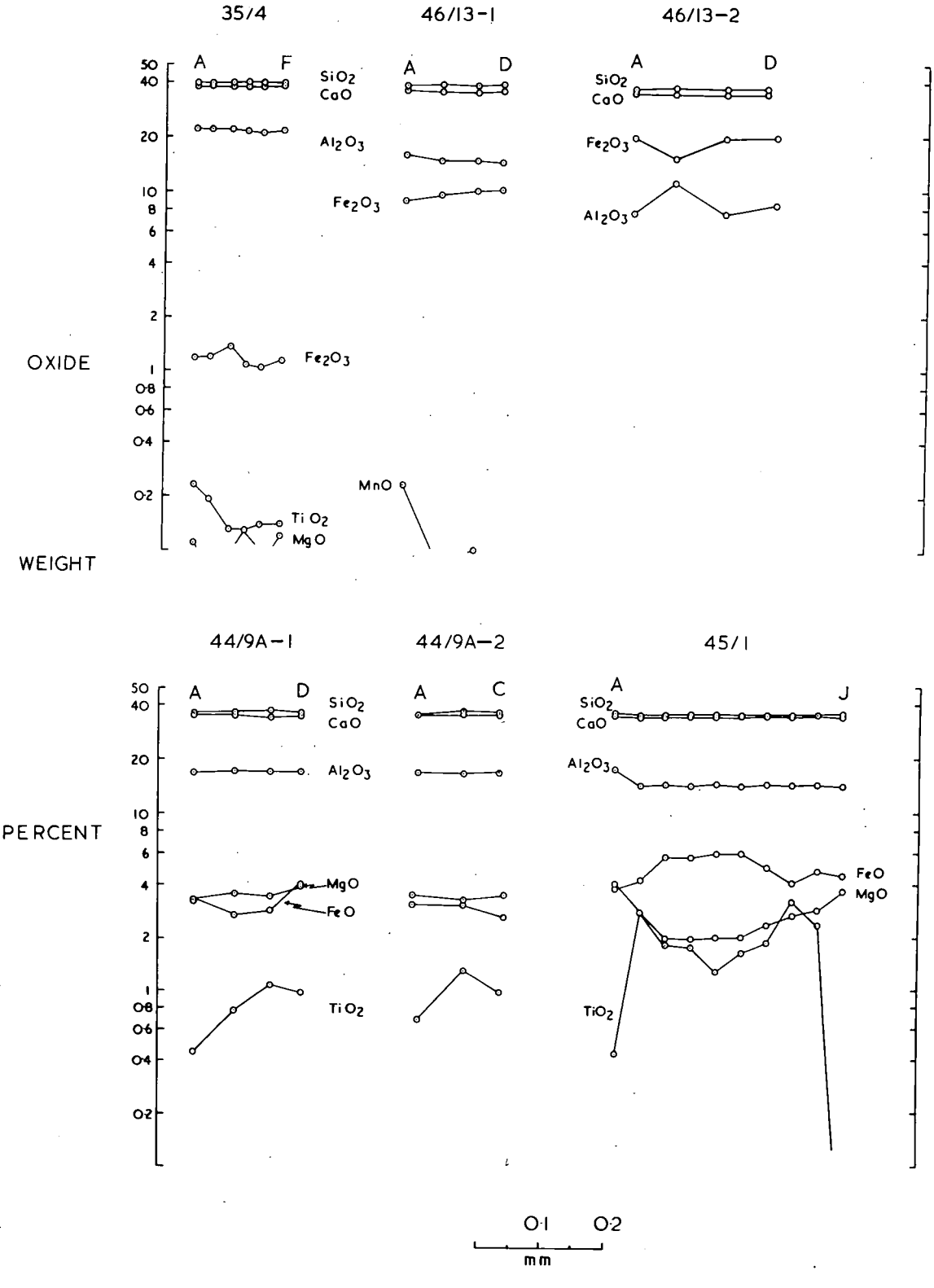
35/4
46/13-1
46/13-2
A
F
D
SiO2
CaO
Al2O3
Fe2O3
MnO
TiO2
MgO
OXIDE
WEIGHT
44/9A-1
44/9A-2
45/1
C
J
FeO
PERCENT
0·1
0·2
mm

the feldspar areas, these elements decrease in concentration. As the immediate area around the crystals becomes depleted, Al then increases in concentration to fulfil the lattice requirements.

Garnets also form as a rim to argillaceous bands in marble, as in 43/21-2 (H-J), 43/22-2 and 46/13-1 (Plate 5.8). No regular variation in composition is seen in any of these crystals, although a decrease in Fe and an increase in Ti and Mg is seen in the core of 43/21-2. A sudden decrease in Fe and Mn and increase in Al and Mg is seen, at the edge of the crystal nearest the argillaceous band, in 43/22-2 (Fig. 5.3). There is no similarity with the garnets seen around the feldspar areas, and this is probably because there has been no breakdown of illite to form albite, with subsequent release of minor amounts of mafic elements to be concentrated at the initial period of growth.

Garnets set in a matrix of calcite, as in 43/21-1, 43/21-2 (A-G), 44/9A-1, and 46/13-1 (Figs. 5.2, 5.3 and 5.4) again show no uniform variation. Iron in crystals 43/21-1 and 43/21-2 shows enrichment in the cores, rising from 0.3% in 1 (A), at the rim, to 1.6% (G) of Fe_2O_3 in the core, Al showing a slight reciprocal decrease in the core (Fig. 5.2). Crystal 43/21-2 shows a higher Fe content than 43/21-1 as it is adjacent to an argillaceous band. The TiO_2 and MgO values in these crystals appear irregular and may be due to experimental error. Standard deviation for elements are given in Appendix 5.9. No variation is seen in crystals 44/9A-1 and 46/13-1, TiO_2 and MgO on three of the point analyses were below 0.1% in crystal 46/13-1 (Figs. 5.3 and 5.4).

Similarly little variation is seen in those garnets in a

prehnite matrix, such as 43/3-5, 6 and 8 and 35/4 (Plates 5.2 and 5.7). Depletion of TiO_2 and MgO in the core of 43/3-8, and possibly in 43/3-6, is the only variation discernible (Figs. 5.1 and 5.2).

Finally the two garnets surrounded by fine-grained recrystallized chlorite, 43/3-1 (Fig. 5.1) and 44/9A-2 (Fig. 5.3), show possible slight depletion of MgO in the cores of crystals which is also mirrored by TiO_2 in 43/3-1.

The lack of compositional variation in the examples described above suggests that the elements incorporated in the structure were available in roughly equal concentrations throughout the growth of the garnet crystals. Lack of variation, in these garnets, due to homogenization by the diffusion of material through the solid crystal is unlikely, as it is widely accepted that such diffusion occurs extremely slowly, especially in low-grade metamorphism.

There is no relation between distance from contact and compositional zoning in the garnets, suggesting that temperature is of negligible importance. Garnets from sample 44/11, 5 m from the contact, show the most well developed zoning, whereas crystals in sample 43/3, 0.1 m from the contact, are relatively unzoned.

Conclusions

Garnet, rich in the grossular molecule (70-99%), is the most abundant mineral found in the metamorphic aureole. Andradite, with over 60% of the end-member molecule, has been recorded for the first time. Cell-size determinations show a range from

11.811 Å to 11.871 Å, which are somewhat lower than those given by Deer, Howie and Zussman (1962) for the grossular/andradite series. Petrographic examination reveals that the garnets vary greatly in form and size, anisotropism is usually present (Plates 5.1 and 5.4), while sector twinning is seen in some samples (Plate 5.1). Well developed optical zoning is only rarely seen (Plate 5.3). Compositional zoning, of the 'normal' type (Leake, 1967), is only well developed in two crystals, from sample 44/11, surrounded by pyrite. The majority of the garnets showing no regular zoning.

FELDSPAR

Albite feldspar is a common constituent of low-grade metamorphic rocks and is an indicator mineral of the albite-epidote hornfels facies of contact metamorphism. Albite adinoles are often developed at basic igneous contacts and are due to Na metasomatism, according to Deer, Howie and Zussman (1962). Albite is an abundant mineral in the Whin aureole, extending to over 10 m from the contact. The actual limit is unknown because of an absence of suitable samples between 10 and 20 m from the contact. Sodic feldspar has also been recorded as an abundant mineral in the aureole of the Palisade sill (Van Houten, 1971). In the present study, the adinole areas may be recognised in hand-specimen by their red colouration (Plate 3.5). In thin-section, the feldspar is usually very fine-grained (Plates 3.16 and 5.10). In plane-polarised light, the feldspar areas usually have a distinctive reddish colour (Plate 3.12). In some samples, the feldspar becomes coarser and individual, lath-shaped crystals are visible (Plates 3.13 and 5.11). Well developed laths up

Plate 5.10 Sample 35/4. Cryptocrystalline mixture of feldspar and quartz, clouded with carbonaceous material. (x250)

Analyses 35/4-1 to 6, approximate positions of feldspar analyses.

Plate 5.11 Sample 44/7. Lath-shaped, albite twinned plagioclase crystals set in calcite matrix. (x120)

Analysis 44/7-1 Albite-twinned feldspar. 3 points, 1A-1C

Plate 5.12 Sample 44/7. Albite-twinned plagioclase feldspars, set in calcite matrix. (x120)

Analysis 44/7-2 Untwinned feldspar crystal. 1 point.

Analysis 44/7-4 Albite-twinned plagioclase. 1 point.

Analysis 44/7-5 Twinned plagioclase. 2 points, 5A-5B

Analysis 44/7-6 Plagioclase feldspar. 1 point.

Analysis 44/7-7 Plagioclase feldspar. 1 point.

Plate 5.10

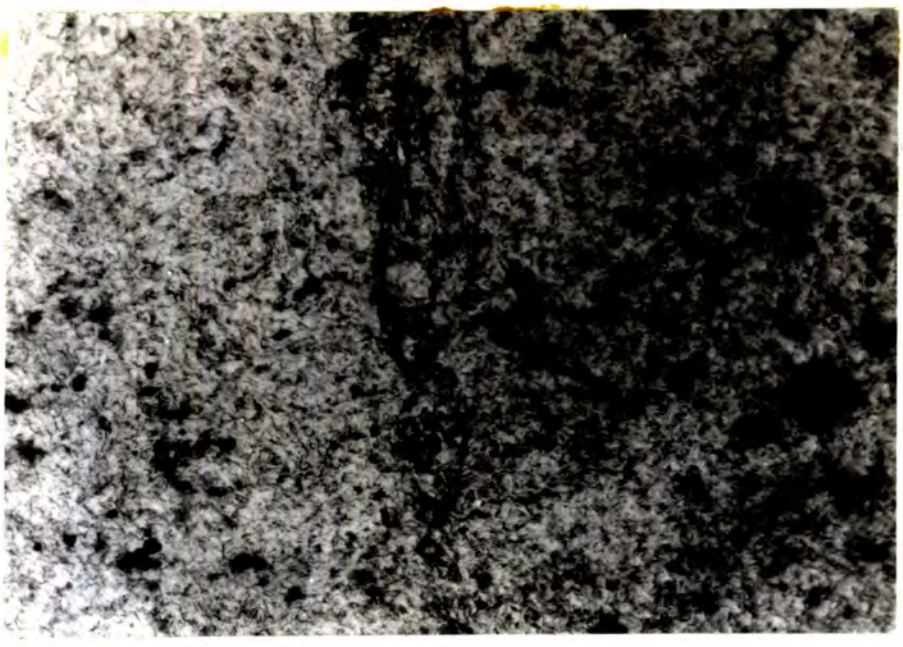

Plate 5.11

Plate 5.12

to 0.3 mm in length, showing albite twinning, are present in sample 44/7 (Plate 5.11). Albite twinning is dominant in the coarser-grained feldspar but occasionally carlsbad twins are developed (Plate 5.6). The fine-grained feldspars are highly clouded due to minute inclusions.

Electron microprobe analysis

Electron microprobe analysis has been used extensively in the examination of the feldspars, because of their fine-grained nature. The feldspar analyses, atomic proportions and end-member compositions are presented in Appendix 5.2. The end-member compositions and atomic proportions have been calculated using a computer programme written by E. B. Curran of the Dept. of Geology, University of Durham. Electron microprobe analysis of the coarser-grained feldspar proved relatively simple but the fine-grained material presented difficulties because of the difficulty in resolving individual crystals, especially in the reflected light optics of the probe. The analysis point, in this case, was chosen close to a readily identifiable inclusion, but some errors in the analysis may have arisen by the placing of the electron beam on an unseen fracture or grain-boundary.

Forty-three analyses of the contact feldspars have been undertaken and of these, three are rich in the orthoclase component and thirty-nine are plagioclases (Appendix 5.2). Of the plagioclases, over 50% are very rich in the Ab molecule with greater than 98% of the end-member, while almost 84% of the contact metamorphic plagioclases analysed have greater than Ab_{95}.

The approximate positions of the six points analysed from

sample 35/4 are shown in Plate 5.10. Three of the four analyses, close to the fracture (Plate 5.10), have greater than Or_{97}. These potassic feldspars are believed to have formed by the concentration of K, from the inter-layer position in illite into late-stage pore solutions before, crystallization along the fractures such as that seen in Plate 5.10. Analyses 43/3-1 to 43/3-3 are of points across a carlsbad twin and adjacent crystals as shown in Plate 5.6. Analyses 43/3-4 to 43/3-9 are single points of fine-grained feldspar, shown in Plate 3.16. The analyses of the carlsbad twin (Plate 5.6) show two points rich in albite (1A and 1C) and one with Or_{11} (1B) suggesting that there may be some antiperthitic intergrowth in the crystal. Of the remaining analyses from sample 43/3, six have greater than Ab_{96}, while the remaining two have compositions of Ab_{90} and Ab_{88}.

Eleven crystals of coarser-grained feldspar were analysed from sample 44/7, six of which are shown in Plates 5.11 and 5.12. Even though all the crystals are in a calcite matrix, sixteen of the seventeen points analysed showed greater than 97% of the Ab component, while analysis 44/7-8 had greater than 13% of the An component. Analyses of feldspars from sample 44/11 were of fine to medium-grained material, all of which have greater than Ab_{95}. Analysis was also made for Fe in a number of cases, especially where the feldspar was reddish in colour. A maximum of 0.9% Fe_2O_3 (total iron) was recorded in sample 43/3-6 but it is not possible to distinguish whether the Fe is present in the structure or as an oxide coating around the grains.

Feldspar composition from previous work

The present work has shown that feldspars rich in the albite

component (>95% Ab) are dominant in the aureole with only minor amounts of orthoclase and oligoclase present. Previous work, however, has suggested that a more calcic plagioclase is present. Hutchings (1898) suggested the presence of anorthite, using optical methods, while Harbord (1962) also suggested the presence of feldspar in the range labradorite to anorthite on the basis of an X-ray powder photograph. Dunham (1948) was of the belief that the feldspar was probably oligoclase.

Comparison of feldspar compositions using optical and electron microprobe methods

The optical properties of the coarser-grained plagioclases were examined, because of the variation in composition suggested by the present and previous work. The optical properties of feldspar from four samples are shown in Table 5.2. The 2V measurements were kindly made by Dr. G. Borrodaile, using a four-axis universal stage. The maximum extinction angles (Michel-Lévy) and optic signs were measured by the author.

Table 5.2 Plagioclase feldspars, optical determinations

Sample	Max. ext. angle	Optic sign	2V
19/20	10	-	n.d.
43/11	12	-	n.d.
44/7-1	10	-	79±4
44/7-3	10	+	93±4
44/7-4	12	-	n.d.
44/7-5	8	+	n.d.
44/9	20	-	n.d.

n.d., not determined

The measurements, in samples 19/20, 43/11 and 44/9, were made on at least four crystals. The number was smaller than would have

been preferred because selection was limited due to the fine-grained nature of the material. The readings given for sample 44/7 are of individual crystals which have been analysed (Appendix 5.2). The maximum extinction angles of feldspars from samples 19/20, 43/11 and 44/7 are indicative of an oligoclase composition, the negative sign suggesting an An content of 28 to 30%. The 2V measurement of sample 44/7-3 is also compatible with oligoclase. The optical properties of feldspars from sample 44/9 are indicative of an andesine composition with as much as 38% of the An component. The optical properties of the present feldspars appear, then, largely to substantiate the oligoclase composition suggested by Dunham (1948). The electron microprobe analyses, described earlier, have shown that albite is the dominant feldspar: only two oligoclase compositions were recorded, with a maximum An content of 13.2%. The microprobe results are, therefore, at variance with the results obtained by optical methods.

Although the structural state of the present feldspars has not been determined, it seems without doubt that they must belong to the low-albite series. It has been recently shown that in the low-albite series, there is a compositional break between An_1 and An_{24} (Barth, 1969). Over this compositional range there is no solid solution; instead, the crystals are unmixed into separate sodic and calcic phases (peristerites). Of the thirty-nine plagioclase analyses, twenty-five lie in the compositional field of the peristerites, the remaining fifteen having greater than Ab_{99}. In analysing peristerites, the composition determined will be dependant upon the size of the intergrowth and the proportions of the sodic and calcic phases excited by the electron

beam. Thus the analyses very rich in the Ab component may represent areas where no calcium phase is present and the oligoclase compositions, 43/3-4 and 44/7-8, areas where a calcium phase is present in greater proportion.

Barth (1969) shows that the low-temperature plagioclases have extremely complicated optical and crystallographic properties, which change in a very irregular manner with composition. The anomalies noted above between the optical and microprobe results seem, therefore, attributable to the irregular variation of optical and crystallographic properties in the peristerites. Plagioclases lying above the peristerite range have also been examined, to determine the relationship between the optical properties and electron microprobe results of these feldspars.

Plagioclase from the normal Whin Sill dolerite (44/25) and pegmatite (L/860) has been analysed and the results are given in Appendix 5.2. The dolerite feldspars are sodic-labradorite and calcic-andesine, with a difference of An content of over 2% between the centre (1A) and the rim (1B) of crystal 44/25-1. Three plagioclases were analysed from the pegmatite, two of which are also andesine in composition (L860-1 and L/860-3), while analysis L/860-2 is of an albite composition. The optical measurements taken on these two samples are given in Table 5.3. The composition of crystal 44/25-1, using the carlsbad-albite method, is An_{55}, agreeing extremely well with the microprobe average analysis of $An_{54.5}$. The maximum extinction angle recorded, from a number of readings, from sample 44/25 is 22° and indicative of An_{41}. While not in agreement with analysis 44/25-1, it shows close agreement with analysis 44/25-2, which

Table 5.3 Optical measurements on Whin Sill plagioclase.

Sample	Ext. angles	Optic sign
44/25-1	15 and 30^{x}	+
44/25	22^{+}	-
L/860	9^{+}	-

(x), Carlsbad-albite twin

(+), Michel-Lévy method

has an An content of 42.2%. Only a few crystals could be examined in the pegmatite because of sericitization. The extinction angle obtained is indicative of an An content of 27%, but this may not be representative of the sample. The microprobe results for the pegmatite show two crystals with An greater than 40% and one analysis with An less than 4%. Finally, four point-analyses have been made on plagioclase from an allivalite sample of Dr. C.H. Emeleus, Dept. of Geology, University of Durham. The analysis of CHE 1 shows a variation from $An_{90.1}$, at the core, to $An_{83.6}$ at the rim of the crystal. The second crystal (CHE 2) shows a similar but not so marked difference. The average of the analyses, 86.8% An, agrees quite well with the optical determination of An_{84} given by Dr. Emeleus.

Conclusions

Feldspar is a common constituent of the altered calcareous sediments of the Whin aureole. It is usually very fine-grained and reddish coloured, probably due to the presence of fine-grained haematite. Electron microprobe analysis has shown that plagioclase

feldspar, rich in the Ab molecule (>95%), but ranging from Ab_{100} to Ab_{87}, is dominant. Small quantities of potassic feldspar have been recorded, for the first time, close to fractures. Coarser grained, lath-shaped crystals are occasionally developed whose composition, determined optically, is in the oligoclase range. The disparity between the optical and microprobe determinations is suggested to be the result of complications produced by the unmixing of two phases in the peristerite range. Barth (1969) having shown that the optical properties of the peristerites vary irregularly with composition.

EPIDOTE

Epidote is a common mineral seen in thermal aureoles and its presence is typical of the albite-epidote hornfels facies. It is a common mineral in the Whin aureole and was originally recognised by Hutchings (1898). It is the mineral which occurs the greatest distance from the contact and is found at 25.7 m from the base of borehole 47, which did not penetrate the Whin Sill.

Petrographic description

The epidote crystals occur in a great variety of form and size. Fine-grained, (<0.01 mm) granular epidote often occurs, associated with fine-grained feldspar, close to the contact (Plate 3.19). Coarser-grained, granular epidote occurs in optical continuity in sample 35/4 (Plate 3.20). Idioblastic and sub-idioblastic epidote is often seen in a calcite or chlorite matrix (Plates 3.18 and 3.15). Plate 3.15 shows a cross-section of an epidote in which only simple (001), (100) and (101) forms appear to be developed. In plane-polarised light, the epidotes are often

slightly coloured and pleochroic with X = colourless, Y = pale green-yellow, and Z = pale green. Interference colours range from first to upper-second order and anomalous blues and greenish-yellows are often seen. A biaxial, negative interference figure, with a large 2V, was obtained from the crystals. The optical properties agree with those of the type epidote.

Electron microprobe analysis

Nineteen partial point analyses on sixteen epidote crystals from six samples are presented in Appendix 5.3. These results confirm the optical identification as epidote, by the presence of Fe in all the crystals analysed. The Fe_2O_3 (total Fe) content ranges from 6.6 to 12.7%, which is not especially high as epidote with up to 23% Fe_2O_3 has been recorded, (Deer, Howie and Zussman, 1962). The crystals analysed in samples 41/36 and 44/5 are shown in Plates 5.13 and 5.14. The Mn content is quite low in the twelve crystals analysed for this element. Calcium and Si appear rather high in some of the analyses from samples 35/4, 41/36 and 43/3 as compared with those quoted by Deer, Howie and Zussman (1962). Two of the analyses, with the lowest (35/4) and highest (44/11-1B) Fe contents, have been recalculated to end-member compositions, assuming H_2O^+ as 2%, on the basis of 13 (O, OH). The Fe shows a range from 16 to 26 mol. % Fe_2O_3, placing the analyses in the pistacite compositional range. Iron-rich epidotes (pistacite) can form at quite low temperatures in burial metamorphism (Winkler, 1968) but in the greenschist facies it is usually a variety with low Fe content, a zoisite or clinozoisite (Winkler, 1968). Little, however, appears to be recorded on the composition of epidotes in contact aureoles and it is,

Plate 5.13 Sample 41/36. Sub-idioblastic epidote crystals with recrystallized quartz in a fine-grained adinole matrix. (x50)

Analyses 41/36-1 and 2 Epidote crystal. 2 points.

Plate 5.14 Sample 44/5. Granular epidote in adinole matrix. (x100)

Analyses 44/4-1 and 2 Epidote crystal. 2 points.

Plate 5.15 Sample 44/9A. Idocrase crystal, showing longitudinal section, set in a fine-grained matrix of chlorite. (x120)

Analysis 44/9A-1 Idocrase crystal. 4 points.

Plate 5.13

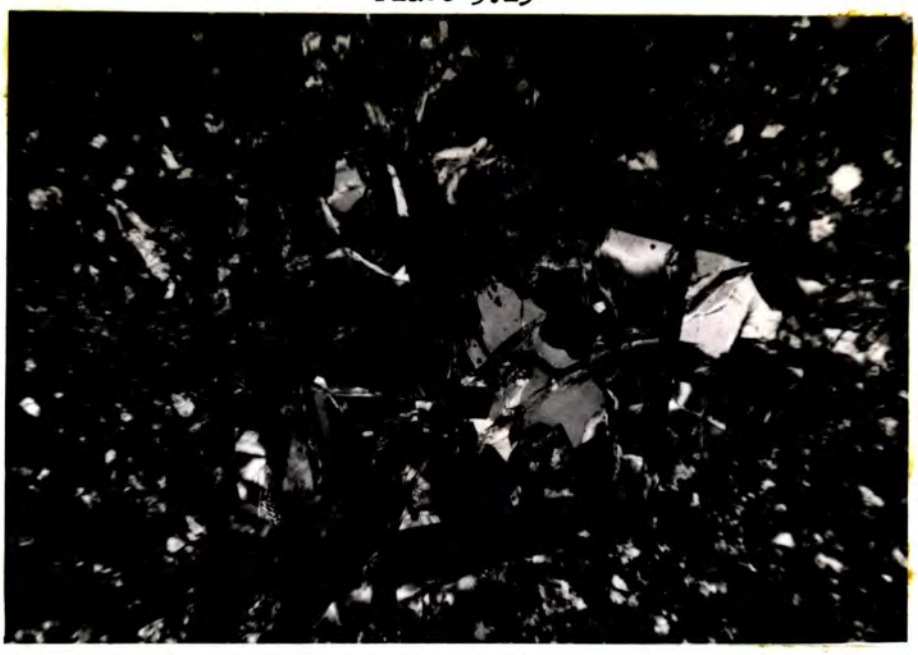

Plate 5.14

Plate 5.15

therefore, difficult to establish if the moderate Fe content of the epidote, recorded in the present study, is typical for contact environments.

Conclusions

Epidote is a common mineral in the Whin aureole, occurring at the greatest distances (>25 m), from the contact, of any mineral. Idioblastic crystals are often present, the optical properties of which suggest epidote, sensu stricto. Electron microprobe analysis has confirmed the optical identification, showing Fe_2O_3 (total Fe) contents ranging from 6.6 to 12.7%.

IDOCRASE

Idocrase was first recorded in the Whin aureole by Hutchings (1898) and was found in great abundance by Randall (1959). It also occurs in greater abundance, in Upper Teesdale, than was originally thought (Robinson, 1970) and extends to just over 5 m from the Whin contact.

Petrographic description

The idocrase usually forms idioblastic to sub-idioblastic crystals. Those found in a raft at Barrasford quarry, Northumberland (Randall, 1959) often show anomalous blue interference colours. The idocrase recorded from the boreholes at Cow Green is often set in a matrix of fine-grained chlorite. Longitudinal sections are often present (Plate 5.15), showing well developed faces, probably (110), (111) and (001). Longitudinal sections up to 0.31 m long and basal sections up to 0.1 mm wide have been recorded. Basal sections showing probable (110) and small, (100) faces are shown in Plate 5.16. In plane-polarised light in

sample 45/1, the idocrase crystals are a yellowish-brown colour and slightly pleochroic, but in other samples are colourless. Anomalous colours have not been recorded in the Teesdale samples. Small crystals from sample 44/11 gave biaxial positive interference figures with a low 2V.

Electron microprobe analysis

Twenty-one partial analyses of five crystals, in four samples have been made and are presented in Appendix 5.4. The analyses of crystals 43/7 and 45/1 appear to have low totals, which may be due to Al_2O_3 being slightly too low. There is a reasonable similarity between the garnet and idocrase analyses, although MgO occurs in significantly higher concentrations in the idocrase. This is probably because it is usually found in a matrix of chlorite. Analyses have been made across three crystals to establish if any zoning is present. Diagrams showing the variation are given in Fig. 5.4.

A small increase of TiO_2 is seen in the cores of crystals from sample 44/9A, while 45/1 also shows an increase away from the rim which is followed by a depletion effect. The latter specimen also shows a depletion of MgO in the core, from 4 to 1.8%, while a reciprocal increase in FeO (total Fe) is seen from 3.8 to 6.0%. Besides a slight core depletion of FeO in the core of 44/9A-1, no other variation is seen.

Conclusions

Idocrase has been recorded to just over 5 m from the Whin Sill contact. It occurs dominantly in idioblastic to sub-idioblastic crystals, often in a matrix of fine-grained chlorite.

Electron microprobe analyses agree satisfactorily with those quoted by Deer, Howie and Zussman (1962). Slight zoning is seen in some crystals, in the elements Fe, Mg and Ti.

CLINOPYROXENE

Diopsidic pyroxene is a particularly common mineral in contact metamorphic, calcareous sediments. Clinopyroxene has been recorded in four samples, extending up to 7 m from the contact. It is most abundant in sample 35/4 at the immediate contact, where it is found in association with grossular, epidote, prehnite and calcite. The idioblastic to sub-idioblastic form has only been recorded from specimen 35/4, where a small group of crystals occur surrounded by grossular. Elongate grains, up to 0.5 mm in length, are dominant, although a sub-idioblastic basal section is present showing the two pyroxene cleavages. Normally the pyroxene occurs in fine-grained granular crystals, often associated with epidote. The crystals are colourless and have first to second-order interference colours. The crystals from 35/4 give a biaxial positive interference figure with a moderate 2V and an extinction angle (Z:c) of 49°. Specific identification of the clinopyroxene was not possible from simple optical work but was achieved with microprobe analysis.

Electron microprobe analysis

Nine point analyses of eight pyroxene crystals, from two samples, have been undertaken and the results given in Appendix 5.5. The atomic proportions and end-member compositions are also given in the Appendix and were determined using a computer programme written by E.B. Curran, Dept. of Geology, University of Durham.

The compositions of the pyroxenes from the two samples are quite different, as shown in Fig. 5.5. All analyses lie close to the diopside-hedenbergite join, sample 45/1 having an average of over 52 atomic percent Ca, while 35/4 has an average of just under 50%. The analyses of 35/4 are Fe rich, each point having over 48 atomic percent Fe^{2+} + Mn and these fall virtually at the end-member composition for hedenbergite, with less than 2 atomic percent Mg recorded in all cases. This record of hedenbergite is the first from the Whin Sill aureole. The compositions of crystals from 45/1 lie strictly above the diopside-hedenbergite series (Deer, Howie and Zussman, 1962) but should still be regarded as belonging to the series. The compositions fall approximately on the diopside-salite boundary, the crystals having an average Ca:Mg:Fe ratio of 53:37:10 (Appendix 5.5). Normally, however, minerals from the diopside-hedenbergite series have low Al_2O_3 and TiO_2 contents of between 1 to 3% and below 1% respectively. In the present analyses Al_2O_3 and TiO_2 are low in 35/4 but in 45/1, Al_2O_3 is considerably higher, ranging from 5.8 to 9.6% while TiO_2 values vary from 0.4 to 3.4%. These values are more compatible with the augite analyses quoted by Deer, Howie and Zussman (1962), while TiO_2 in 45/1-2 approaches values seen in titanaugite. Deer, Howie and Zussman, however, do quote diopside-hedenbergite analyses with Al_2O_3 and TiO_2 values approaching those in the present study. An Al_2O_3 content of 8.3% and TiO_2 of 3.0% have been quoted and thus it seems reasonable to classify the 45/1 analyses as diopside-salite.

These clinopyroxenes are distinctive in that they are the

Figure 5.5 Distribution of pyroxene analyses, with respect to Ca, Mg and Fe^{2+} + Mn atoms.

Electron microprobe analyses (Appendix 5.5), with total Fe as Fe^{2+}.

Figure 5.5

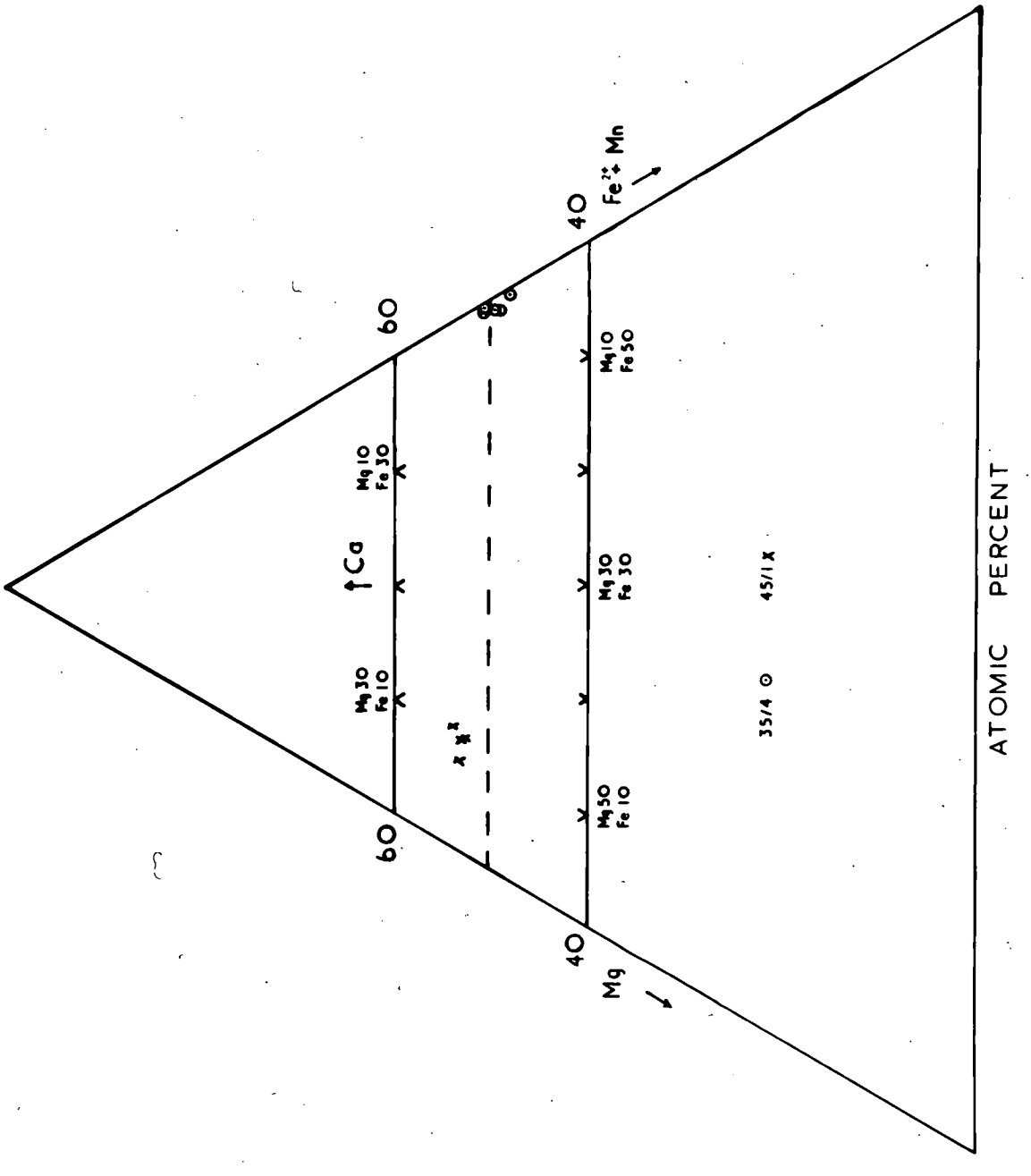
60
40
Fe2+ Mn
60
40
Mg
↑Ca
Mg10 Fe30
Mg30 Fe10
Mg10 Fe50
Mg30 Fe30
Mg50 Fe10
35/4 ⊙
45/1 x
ATOMIC PERCENT

only phases developed, in the Whin aureole, which are rich in Fe^{2+} and Mg. Ferrous iron, although not determined separately from Fe^{3+}, is probably relatively low in the other minerals. Previously, idocrase has shown the highest MgO content with a maximum of 4.0% in sample 45/1, whereas in the pyroxene analysis 45/1-3, 13.7% MgO has been recorded. The two samples with the most pyroxene are found at the immediate contact and in sample 35/4, chlorite is notably absent. It is possible that close to the contact, temperatures were elevated for long enough to allow some breakdown of chlorite, which would then release Fe^{2+} and Mg to be incorporated in the pyroxenes. The absence of Mg in 35/4 is puzzling, unless, however, it was derived from the breakdown of an especially Fe-rich chlorite. Hedenbergite is often found in limestone skarns, the Fe^{2+} being derived from an adjacent intrusion (Harker, 1932). This introduction of Fe^{2+} is not believed to have taken place in the present case, as it usually occurs in the vicinity of granitic bodies. The hedenbergite is not abundant and its association with grossular rather than andradite is also evidence against the introduction of Fe from the intrusion.

Conclusions

Clinopyroxene has been recorded from four samples up to 7 m from the contact. Normally the pyroxene occurs as fine-grained, granular crystals, but idioblastic sections are present in sample 35/4. Electron microprobe analysis has shown the presence of two distinct pyroxenes in the two samples analysed. Diopside-salite and hedenbergite compositions have been recorded. These minerals show the highest Fe^{2+} and Mg content of the metamorphic

minerals in the aureole and may be due to the breakdown of chlorite releasing these elements.

PREHNITE

Prehnite often occurs as a hydrothermal mineral in igneous rocks and as a common constituent of rocks subjected to burial metamorphism (Winkler, 1968). It is also found in metamorphosed limestones (Deer, Howie and Zussman, 1962), although records of such occurrences seem rather rare. Van Houten (1971) has recorded it in the aureole of the Palisade sill and it has also been recorded, for the first time, in the present study of the Whin aureole. The prehnite has been recorded in nine samples, extending up to 5.5 m from the sill contact.

Petrographic examination

The prehnite usually occurs in small pockets and lenses surrounded by grossular and having small, sub-idioblastic garnets set in it, as shown in Plates 5.2 and 5.7. In plane-polarised light the prehnite is colourless and only rarely shows cleavage. In crossed polars, first-order, grey interference colours are dominant but low, second-order are also seen, and anomalous first-order blues. A characteristic feature of the prehnite is its undulatory and indistinct extinction, seen in Plate 5.17. A biaxial positive interference figure was obtained from the crystals, with a variable 2V from low to moderate. A small sample of the prehnite was removed from a polished thin-section of 43/3 and an X-ray powder photograph taken, the results of which are given in Table 5.4.

Table 5.4 X-ray diffraction of prehnite

43/3 Å	Strength	A.S.T.M. Å	Strength
		5.28	10
4.58	VW	4.60	20
		4.15	10
3.52	VVW	3.53	10
3.43	MS	3.48	90
3.26	M	3.28	60
3.06	S	3.08	100
2.80	W	2.81	30
		2.62	5
2.56	S	2.55	100
2.33	M	2.37	40
		2.31	40
		2.18	5
		2.13	10
		2.07	20
1.90	W	1.93	30
1.80	W	1.84	20
1.72	M	1.77	70
1.65	VW	1.69	5
		1.66	20

S, strong. MS, medium strong. M, medium. W, weak. VW, very weak. VVW, very, very weak.

The lines recorded in the sample from 43/3 show good agreement with those given in the A.S.T.M. index, although some of the weaker lines have not been recorded from the sample.

Electron microprobe analysis

Partial analyses of the prehnite (Plates 5.17 and 5.18) have been undertaken by electron microprobe, using a defocussed electron beam to minimize volatilization. These analyses are presented in Appendix 5.6, H_2O^+ was not determined but analyses quoted by Deer, Howie and Zussman (1962) suggest that between 4 and 4.5% H_2O^+ is present. Accepting this value, some of the analyses appear slightly low and are most likely due to some volatilization, although the

Plate 5.16 Sample 44/9A. Sub-idioblastic, basal section of idocrase set in chlorite groundmass. (x150)

Plate 5.17 Sample 43/3. Prehnite crystal, surrounded by garnet, showing characteristic irregular extinction. (x100)

Analysis 43/3-1 Prehnite crystal. 4 points, 1A-1D

Plate 5.18 Sample 43/3. Prehnite crystal surrounded by garnet. (x100)

Analysis 43/3-2 Prehnite crystal. 2 points, 2A-2B

Plate 5.16

Plate 5.17

Plate 5.18

standard deviation of the elements, on four repeat readings, is low (Appendix 5.9). The CaO, Al_2O_3 and Fe_2O_3 (total Fe) weight percent oxides have been recalculated and plotted on a triangular diagram (Fig. 5.6). As shown, there is quite a wide variation from an almost ideal composition (shown by the arrow) in sample 44/11-B, to over 15% weight percent Fe_2O_3 in sample 43/3-2B. The two analyses with the almost ideal compositions (44/11) are found some 5 m from the contact while of the remaining ten analyses eight are Fe-rich and are found within 0.1 m of the contact.

It was thought that prehnite did not show appreciable substitution of Fe^{3+} for Al, the analyses quoted by Deer, Howie and Zussman (1962) showing a maximum Fe_2O_3 content of 1.4%. A maximum of 8.3% Fe_2O_3 (total Fe) has been recorded in the present analyses. The analyses for 43/3-2B and 44/11-B have been recalculated to atomic proportions (Table 5.5), on the basis of 24(O, OH) and assuming the remainder of the analyses are H_2O^+.

Table 5.5 Atomic proportions, on the basis of 24(O, OH), for 2 prehnite crystals

	43/3-2B			44/11-B	
Si	5.83	6.0	Si	6.12	
Al	0.17		Al	3.89	
Al	3.11		Ca	4.02	4.05
Fe^{3+}	0.89	4.04	Na	0.03	
Mg	0.04		OH	3.76	
Ca	4.03	4.09			
Na	0.06				
OH	3.98				

The recalculation shows that on the assumptions made, over 22% substitution of Al by Fe^{3+} has occurred, between the two theoretical end-members, $Ca_2Al_2Si_3O_{10}(OH)_2$ and $Ca_2Fe^{3+}_2Si_3O_{10}(OH)_2$.

Figure 5.6 Distribution of prehnite analyses with respect to Al_2O_3, CaO and Fe_2O_3, weight percent.

Electron microprobe analyses (Appendix 5.6), with total Fe as Fe_2O_3. The arrow on side of triangle represents the ideal composition, $Ca_2Al_2Si_3O_{10}(OH)_2$. The square represents the average composition of the most Fe-rich crystal recorded by Surdam (1969).

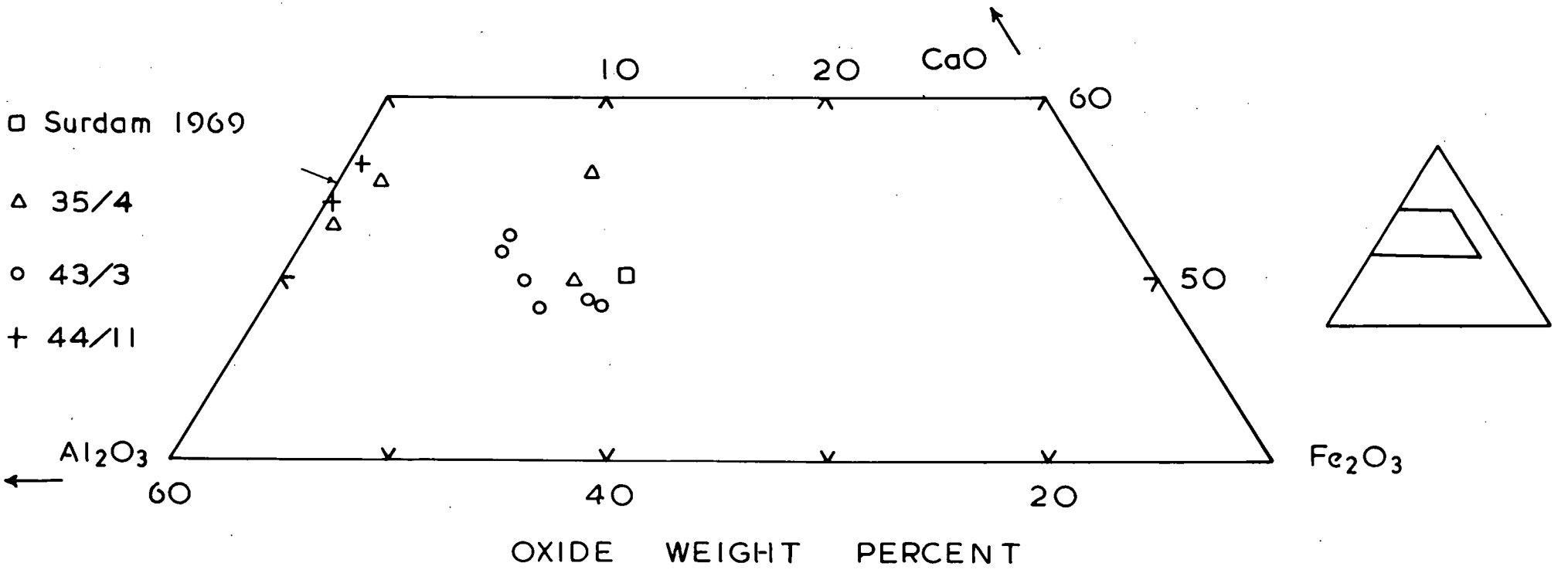
Surdam 1969
35/4
43/3
44/11
10
20
CaO
60
50
Al_2O_3
60
40
20
Fe_2O_3
OXIDE WEIGHT PERCENT

Figure 5.6

The present microprobe analyses agree extremely well with those of Surdam (1969), who undertook 612 point analyses, on 18 prehnite samples, from metavolcanics on Vancouver Island, British Columbia. His analyses showed an average range of Fe_2O_3 from 0.1 to 8.2%, although a maximum of 10.8% was recorded in one analysis. The square in Fig. 5.6 shows the composition of the most Fe-rich crystal, averaged from several point analyses, recorded by Surdam (1969). By comparison, the present analyses show a range from <0.05 to 8.3%. Hasimoto (1968) suggested that less than 20% substitution of Al by Fe^{3+} occurred in prehnite. The present analyses show that this figure can be exceeded while Surdam (1969) suggests that the limit of substitution may be at least 30%.

Paragenesis

Early work on the stability of prehnite suggested that it only formed rapidly, at low temperatures, when pressures were above 3Kb (Fyfe et al., 1958). The environment under study is, however, one of low pressure, well below 1Kb. Recent work has, however, resulted in the synthesis of prehnite at 1Kb (Liou, 1971), where it was suggested that its stability field may extend to lower pressures, but only in an environment approaching its own bulk composition. In the present study, prehnite always appears to be filling small pockets surrounded by garnet (Plates 5.7, 5.17 and 5.18). These pockets may, therefore, represent small areas remaining after the development of feldspar and grossular, whose bulk composition closely approached that of prehnite, resulting in its formation. Liou (1971) also showed that prehnite reacts to form zoisite, grossular, quartz and fluid at approximately 400°C at 3Kb. If this is applicable at

lower pressures, it also suggests that the prehnite may have formed after the formation of grossular and feldspar during cooling of the aureole. If prehnite forms in this manner, it would have been expected to occur in association up to the limit of feldspar occurrence but it has only been recorded up to 5.5 m from the contact. This limitation may not be real, as its formation at low pressures appears dependant on a pocket of material of appropriate bulk composition which may not have been available in all the specimens examined.

Conclusions

Prehnite has been recorded in several samples up to 5.5 m from the Whin contact. It occurs in small pockets, surrounded by garnet and shows characteristic irregular extinction. Electron microprobe analysis has shown compositions ranging from almost ideal, to a composition showing over 22% substitution of Al by Fe^{3+} (Fig. 5.6). The results agree extremely well with those of Surdam (1969) and both sets of analyses show Fe^{3+} substitution occurring to an extent not recorded previously.

CHLORITE

Chlorite is a common mineral in the sedimentary rocks of Teesdale (Harbord, 1962) but is not present in all the samples examined. It appears to be particularly common in the calc-silicate lenses in the marbles, where it is often fine-grained but recrystallized. Fine-grained chlorite, as a matrix to epidote, is illustrated in Plate 3.15, while medium-grained crystals are shown in Plate 3.17. Coarse-grained crystals up to 3 mm in length are often seen in calc-silicate nodules (Plate 3.18) showing green and anomalous blue interference colours.

Electron microprobe analysis

Four point analyses have been made on green, radiating chlorite, similar to that shown in Plate 3.18, and these are presented in Appendix 5.7. The totals are low but are to be expected because of the high H_2O^+ content in chlorites and possible volatilization during the analysis. In order to classify the chlorites, using the system adopted by Deer, Howie and Zussman (1962) and to allow comparisons to be made, the analyses have been recalculated to atomic proportions. For the purpose of recalculation, total Fe is given as FeO, (OH) has been assumed as 16.00, and the formula has been derived on the basis of 28 oxygen equivalents, ignoring H_2O. These atomic proportions are also shown in Appendix 5.7, the number of 'Y' ions per formula unit is quite low in the first two analyses and slightly high in the second two analyses. On the basis of the assumptions made, the analyses of 43/3 fall in the diabanite field and those from 43/22 in the ripidolite field, in comparison to the aphrosiderite, near daphnite, recorded by Dunham (1948), which is less Mg-rich than those recorded here.

A notable feature of the analyses is the high content of CaO, ranging from 2% to over 11%. In contrast, the analyses quoted by Deer, Howie and Zussman (1962) only show a maximum CaO content of 1.2%, much of which they regard as impurities present in the chlorite. It is possible that during the analysis the calcite, which was present as a matrix to the chlorite, was excited by the electron beam, to give rise to a spurious CaO value. It is also possible, however, that in a Ca-rich environment, some additional Ca may be incorporated into the chlorite

structure.

Chlorite is present in most of the calc-silicate samples examined and is only notably absent in sample 35/4. It is a mineral typical of the albite-epidote hornfels and is stable, in the presence of quartz, to temperatures only slightly in excess of 500°C (Winkler, 1968). Temperatures of this magnitude are believed to have been attained in the aureole (Chapter III) but little evidence is seen for the breakdown of chlorite. In the majority of cases it only appears to have suffered recrystallization, suggesting that temperatures were not held at elevated levels long enough to allow the breakdown of the mineral. This, in turn, explains the virtual absence of Mg and Fe^{2+} phases in the contact mineralogy, as most of the Mg and Fe^{2+} remains bound in the chlorite structure.

Conclusions

Chlorite is a common constituent of the calc-silicate rocks, varying from fine-grained material to radiating clusters of crystals up to 3 mm in length. Four partial analyses have been made and after recalculation into atomic proportions, using assumptions described above, the analyses plot into the diabanite and ripidolite fields. The chlorite has suffered recrystallization as a result of the metamorphism but has not broken down, thus accounting for the general absence of Mg and Fe^{2+}-rich mineral phases in the aureole.

DATOLITE

Datolite is common as a secondary mineral in cavities and veins in basic igneous rocks. It has been recorded from the Dartmoor aureole, in an impure limestone, and in a similar

setting, to the present occurrence by Phemister and MacGregor (1942). They recorded it in an impure limestone overlying a thick sill of dolerite in Fife, Scotland. In the present study the mineral was only recorded in one sample (44/12), an impure saccharoidal marble, 5.8 m from the contact. The crystals are readily distinguishable from calcite because of their relatively low-order interference colours (Plate 3.9). The datolite occurs in small, granular crystals (0.05 to 0.25 mm), xenoblastic to sub-idioblastic in form. A biaxial interference figure was obtained from several of the crystals, with a 2V recorded from two crystals of 79 to 81° and 80 to 83°. (Optic axial angles were determined by Dr. G. Borrodaile, Dept. of Geology, University of Durham). An extinction angle of 5° (Z:c) was recorded on two crystals.

Electron microprobe analysis

Six point analyses have been undertaken on two crystals and the results given in Appendix 5.8. The analyses show SiO_2 and CaO dominant with totals consistently in the range 72 to 73%. The optical properties and partial analyses suggested datolite and for confirmatory purposes, access was given to a Geoscan instrument at the Dept. of Physics, University of Newcastle-upon-Tyne. This microprobe is equipped with a lead stearate crystal, allowing boron to be detected. No standard was available, so a qualitative 2θ scan was made to establish the presence of B, a peak was recorded at 84° 55', some 15' of arc away from the value given in the 2θ tables. Comparison of the analyses presented here with those quoted by Deer, Howie and Zussman (1962) shows good agreement with the SiO_2 and CaO

values for datolite. Only minor amounts of other elements were detected, namely Al_2O_3 (0.3%), Fe_2O_3 (0.2%) total Fe as Fe_2O_3, and TiO_2 (0.1%), as is the case in the analyses quoted by Deer et al. (1962).

The genesis of the datolite poses a problem, as it is quite rich in B and where it has been found previously in metamorphosed limestones, B-rich volatile action has been invoked (Phemister and MacGregor, 1942). The mineral has, however, only been recorded from one sample, and it is difficult to equate B-rich volatiles invading the sediments, with the rarity of its development.

HAEMATITE

The feldspar areas described in Chapter III are red-coloured in hand-specimen (Plate 3.5). In thin-section, these areas are highly red-stained, especially in plane-polarised light (Plate 3.12). Occasionally the material becomes coarser-grained, as shown in Plate 5.19. Here the material can be recognised as haematite, showing red, translucent crystal edges in transmitted light. The haematite in sample 19/9 is concentrated into small pockets, where sufficient was present to separate and prepare a powder X-ray diffraction photograph. The pattern obtained from the diffraction is shown in Table 5.6.

The pattern obtained from the haematite sample 19/9 is virtually identical with that given in the A.S.T.M. index. This haematite is always associated with the feldspars, and up to 0.9% Fe_2O_3 has been recorded in the feldspar analyses. Whether this Fe^{3+} occurs as a substitution for Al in the feldspar structure

Plate 5.19 Sample 44/9. Elongate, lath-shaped feldspar crystals with irregular grains of haematite showing red, translucent edges. (x100)

Plate 5.20 Sample 44/5. Sub-idioblastic crystal of sphene set in an argillaceous matrix, with radiating chlorite. (x100)

Plate 5.19

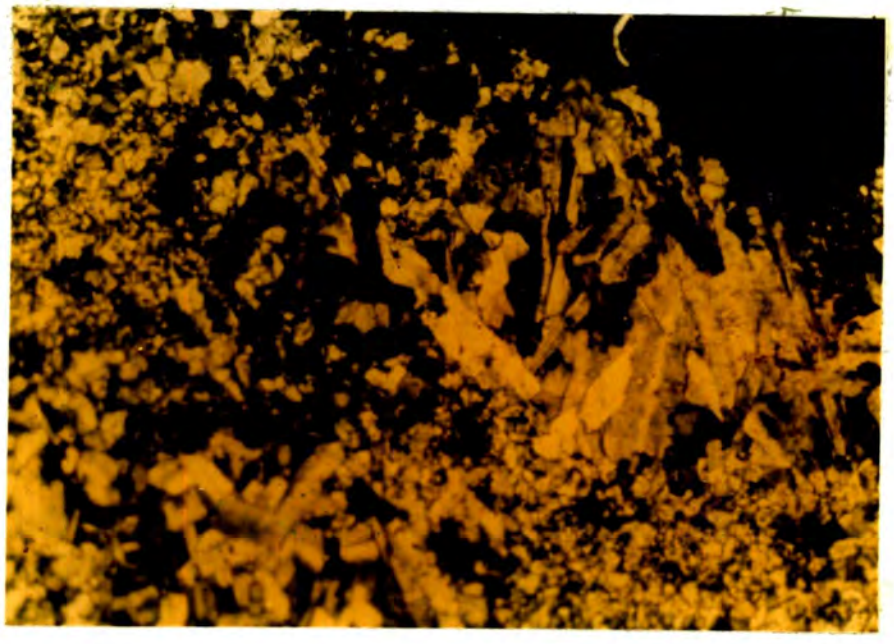

Plate 5.20

Table 5.6 X-ray diffraction of haematite

19/9 Å		A.S.T.M. Haematite Å	
3.70	M	3.66	25
2.69	VS	2.69	100
2.51	S	2.51	50
2.27	VVW	2.29	2
2.20	M	2.20	30
2.09	VVW	2.07	2
1.83	M	1.84	40
1.69	S	1.69	60
		1.63	4
1.60	MW	1.60	16
1.48	M	1.48	35
1.45	M	1.45	35

or as a haematite pigment around crystal grains, in the present examples, is problematical. The haematite is formed during the breakdown of illite to form feldspar and calc-silicate minerals. The Fe^{3+} ions cannot readily be incorporated into the plagioclase lattice and only some is incorporated into grossular, leaving the remainder to form haematite. The Fe_2O_3 content of an illite is given as 5.0%, in one variety quoted by Deer, Howie and Zussman (1962). Thus substantial amounts of Fe^{3+} may be released by the breakdown of the illite material.

WOLLASTONITE

Wollastonite is a common constituent of contact metamorphosed impure limestones, where temperatures of 600°C have been achieved (Winkler, 1968). In the present study, wollastonite has been recorded in several boreholes to more than 8 m distant from the contact. The most spectacular development is seen in borehole 40, where a wollastonite-rich rock, up to 50 cm thick, is recorded. No electron microprobe analyses have been made of the wollastonite,

although its identification was confirmed by X-ray diffraction.

The wollastonite has, without doubt, formed by the reaction: calcite + quartz $\rightleftharpoons$ wollastonite + CO_2. An association of wollastonite, calcite and quartz is seen in Plate 3.7, where the above reaction has not proceeded to completion. The halting of this reaction suggests that either the elevated temperatures fell below those required for the reaction, before completion of the reaction, or that the mole fraction of CO_2 rose to such a value as to prevent the reaction occurring at the temperatures prevalent. The work of Harker and Tuttle (1956) suggests that a minimum temperature of some 450°C is required to initiate the reaction, at a low mole fraction of CO_2, in the environment under study. Winkler (1968) is of the opinion that temperatures in excess of 600°C are required for the formation of wollastonite. Thus it seems probable that temperatures in the order of 550°C were required for the formation of the wollastonite rock in the present case. Examination of the theoretical temperature curves (Fig. 2.3) indicates that temperatures in the order of only 450°C are reached at 8 m distance from the contact. This temperature is, however, a maximum and will only be held for a very limited length of time. Thus, as described earlier, the theoretically derived temperatures are at variance with those suggested by geological observation.

AMPHIBOLE

Amphiboles are common constituents of contact metamorphosed impure limestones and appear in the lowest grades of metamorphism. Hutchings (1898) recorded hornblende, tremolite and

orthoamphibole from the contact-rocks of the Whin Sill aureole. In the present survey, amphibole has only been recorded in three samples up to 8 m from the contact, and no orthoamphibole has been recorded. Hutchings (1898) record of orthoamphibole must be viewed with caution, as in a highly calcareous environment it seems unlikely that an amphibole relatively devoid in Ca would form. The record of tremolite is also doubtful, as it is usually formed by the reaction of dolomite + quartz + H_2O, and dolomite is not known from the Carboniferous limestones of Upper Teesdale.

In the petrographic examination, the amphibole is seen to be very fine-grained and is distinguished from chlorite by its higher relief and cleavage. The optical properties are too imprecise to allow specific identification, and as no electron microprobe analyses have been made it seems reasonable to assume that the mineral is probably a Ca hornblende. The relative lack of amphibole is most likely due to the non-breakdown of chlorite mentioned previously.

ACCESSORY MINERALS

A number of minerals are described here, which occur only in relatively small amounts and which have not been studied in detail.

Pyrite

Pyrite occurs abundantly in places, usually at limestone-argillaceous horizons. It is recrystallized and in certain cases forms late rims around garnet (Plate 5.3). The material is probably recrystallized from original sedimentary pyrite,

which is common in the Carboniferous argillaceous sediments of Teesdale (Harbord, 1962).

Pyrrhotite

Pyrrhotite has been recognised in one sample (45/1) by an X-ray diffraction analysis. This mineral was recorded in a contact sample and is probably derived from metamorphism of the pyrite.

Sphene

Small crystals of sphene have been recorded in several samples but in sample 44/5 a small (0.2 mm), sub-idioblastic, rhombic section was present (Plate 5.20), showing moderate pleochroism from colourless to red-brown.

Apatite

Elongate needles of apatite are commonly seen in the calcareous shales. Needle-shaped crystals are shown with garnet in Plate 5.3, and small needles are often seen included in prehnite.

Rutile

Minute needles of possible rutile occur in some shales, showing high relief and a faint yellowish colour.

APPENDIX 5.1 ELECTRON MICROPROBE GARNET ANALYSES

	35/4 A	35/4 B	35/4 C	35/4 D	35/4 E	35/4 F	43/3 1A	43/3 1B
SI1.02.	39.48	39.36	39.53	39.98	39.67	39.61	39.06	39.05
TI1.02.	0.23	0.19	0.13	0.13	0.09	0.12	0.93	0.25
AL2.03.	21.98	21.85	21.87	21.24	20.87	20.04	17.86	17.43
+FE2.03.	1.17	1.18	1.36	1.07	1.03	1.13	6.23	7.57
MN1.01.	0.03	0.02	0.03	0.10	0.02	0.0	0.07	0.07
MG1.01.	0.11	0.07	0.0	0.13	0.14	0.14	0.48	0.35
CA1.01.	37.34	37.80	37.46	37.72	37.57	39.91	35.97	36.23
TOTAL	100.34	100.47	100.38	100.37	99.39	100.95	100.60	100.95
UNIT FORMULA								
SI	5.934	5.919	5.944	6.012	6.025	5.976	5.954	5.960
TI	0.026	0.021	0.015	0.015	0.010	0.014	0.107	0.029
AL	3.894	3.873	3.876	3.764	3.736	3.564	3.209	3.136
FE	0.132	0.134	0.154	0.121	0.118	0.128	0.715	0.870
MN	0.004	0.003	0.004	0.013	0.003	0.0	0.009	0.009
MG	0.025	0.016	0.0	0.029	0.032	0.031	0.109	0.080
CA	6.013	6.091	6.035	6.077	6.114	6.452	5.875	5.925
O	24.000	24.000	24.000	24.000	24.000	24.000	24.000	24.000
GARNET MOLECULES (RICKWOOD(1968))								
ANDRADIT	2.89	3.01	3.63	3.12	3.05	3.47	18.21	21.30
PYROPE	0.41	0.26	0.0	0.50	0.55	0.57	1.85	1.33
SPESSART	0.06	0.04	0.06	0.22	0.04	0.0	0.15	0.15
GROSSULA	96.19	96.32	96.06	96.17	96.35	95.96	79.78	76.74
SCHORLOM	0.44	0.36	0.25	0.0	0.00	0.00	0.0	0.48
PERCENTAGE CATIONS ASSIGNED	99.16	98.66	99.14	96.95	96.12	91.36	98.23	99.77

+ = Total Fe as Fe_2O_3

APPENDIX 5.1 ELECTRON MICROPROBE GARNET ANALYSES

	43/3 1C	43/3 1D	43/3 1E	43/3 1F	43/3 1G	43/3 2A	43/3 2B	43/3 2C
SI1.02.	38.82	39.04	39.69	39.53	39.40	38.90	39.07	39.62
TI1.02.	0.14	0.17	0.20	1.05	0.0	1.04	0.19	0.05
AL2.03.	16.95	17.29	16.98	16.43	17.27	19.65	19.51	21.26
++FE2.03.	8.51	8.21	7.90	8.12	8.07	4.21	5.56	3.94
MN1.01.	0.08	0.07	0.07	0.10	0.06	0.10	0.11	0.04
MG1.01.	0.30	0.33	0.25	0.19	0.29	0.40	0.31	0.09
CA1.01.	36.27	35.90	35.11	35.77	35.80	35.52	35.90	36.00
TOTAL	101.07	101.01	100.20	101.19	100.89	99.82	100.65	101.00
UNIT FORMULA								
SI	5.942	5.961	6.080	6.022	6.012	5.924	5.926	5.940
TI	0.016	0.020	0.023	0.120	0.0	0.119	0.022	0.006
AL	3.058	3.112	3.066	2.950	3.106	3.527	3.488	3.757
FE	0.980	0.943	0.911	0.931	0.927	0.482	0.635	0.444
MN	0.010	0.009	0.009	0.013	0.008	0.013	0.014	0.005
MG	0.068	0.075	0.057	0.043	0.066	0.091	0.070	0.020
CA	5.948	5.873	5.763	5.839	5.853	5.796	5.835	5.783
O	24.000	24.000	24.000	24.000	24.000	24.000	24.000	24.000
GARNET MOLECULES (RICKWOOD(1968))								
ANDRADIT	24.41	23.75	23.43	23.99	23.45	12.27	16.08	11.48
PYROPE	1.15	1.26	0.98	0.74	1.11	1.54	1.18	0.35
SPESSART	0.17	0.15	0.16	0.22	0.13	0.22	0.24	0.09
GROSSULA	74.00	74.84	75.43	75.05	75.30	85.98	82.49	88.09
SCHORLOM	0.27	0.00	0.00	0.0	0.0	0.00	0.00	0.00
PERCENTAGE CATIONS ASSIGNED								
	99.15	99.34	97.71	97.53	98.96	98.62	98.71	97.08

APPENDIX 5.1 ELECTRON MICROPROBE GARNET ANALYSES

	43/3 3A	43/3 3B	43/3 3C	43/3 3D	43/3 3E	43/3 3F	43/3 3G	43/3 4A
SI1.02.	38.55	39.06	39.32	39.63	39.55	39.64	39.63	39.09
TI1.02.	0.57	0.39	0.10	0.15	0.05	0.28	0.05	0.01
AL2.03.	19.04	19.25	19.64	19.46	19.86	20.02	20.73	19.06
+ FE2.03.	3.97	5.12	4.25	4.72	4.44	4.30	2.91	4.65
MN1.01.	0.09	0.05	0.05	0.07	0.04	0.08	0.08	0.29
MG1.01.	0.58	0.37	0.11	0.11	0.12	0.09	0.19	0.32
CA1.01.	36.85	36.51	36.77	35.73	36.50	36.55	36.09	37.26
TOTAL	99.65	100.75	100.24	99.87	100.56	100.96	99.68	100.68
UNIT FORMULA								
SI	5.911	5.924	5.976	6.030	5.984	5.972	6.009	5.946
TI	0.066	0.044	0.011	0.017	0.006	0.032	0.006	0.001
AL	3.441	3.441	3.518	3.490	3.542	3.555	3.705	3.417
FE	0.458	0.584	0.486	0.540	0.506	0.487	0.332	0.532
MN	0.012	0.006	0.006	0.009	0.005	0.010	0.010	0.037
MG	0.133	0.084	0.025	0.025	0.027	0.020	0.043	0.073
CA	6.054	5.934	5.988	5.825	5.917	5.900	5.863	6.073
O	24.000	24.000	24.000	24.000	24.000	24.000	24.000	24.000
GARNET MOLECULES (RICKWOOD(1968))								
ANDRADIT	11.75	13.94	11.99	13.84	12.75	12.33	8.42	13.48
PYROPE	2.27	1.40	0.42	0.43	0.45	0.34	0.73	1.22
SPESSART	0.20	0.11	0.11	0.15	0.09	0.17	0.17	0.63
GROSSULA	85.79	83.80	87.30	85.58	86.71	87.16	90.68	84.67
SCHORLOM	0.0	0.75	0.19	0.00	0.00	0.00	0.00	0.0
PERCENTAGE CATIONS ASSIGNED								
	97.03	99.37	99.72	98.04	99.24	98.99	98.81	98.25

APPENDIX 5.1 ELECTRON MICROPROBE GARNET ANALYSES

	43/3 4B	43/3 4C	43/3 4D	43/3 5A	43/3 5B	43/3 5C	43/3 5D	43/3 5E
SI1.02.	39.00	39.35	39.76	38.78	39.30	38.85	39.35	39.36
TI1.02.	1.80	0.03	0.10	0.26	0.26	0.24	0.30	0.22
AL2.03.	16.58	18.23	16.72	16.61	16.33	16.11	16.72	16.63
+FE2.03.	6.01	4.91	5.64	7.75	7.97	8.30	7.28	7.44
MN1.01.	0.50	0.25	0.16	0.04	0.11	0.10	0.15	0.05
MG1.01.	0.47	0.34	0.30	0.31	0.24	0.27	0.21	0.32
CA1.01.	36.27	37.44	36.30	36.37	36.63	36.10	36.19	36.28
TOTAL	100.63	100.55	98.98	100.12	100.84	99.97	100.20	100.30
UNIT FORMULA								
SI	5.970	6.002	6.153	5.984	6.025	6.012	6.048	6.046
TI	0.207	0.003	0.012	0.030	0.030	0.028	0.035	0.025
AL	2.991	3.277	3.050	3.021	2.951	2.939	3.029	3.011
FE	0.692	0.564	0.657	0.900	0.919	0.967	0.842	0.860
MN	0.065	0.032	0.021	0.005	0.014	0.013	0.020	0.007
MG	0.107	0.077	0.069	0.071	0.055	0.062	0.048	0.073
CA	5.949	6.119	6.020	6.013	6.017	5.986	5.960	5.971
O	24.000	24.000	24.000	24.000	24.000	24.000	24.000	24.000
GARNET MOLECULES (RICKWOOD(1968))								
ANDRADIT	18.79	14.67	17.72	22.95	23.76	24.75	21.75	22.22
PYROPE	1.94	1.34	1.24	1.21	0.94	1.06	0.83	1.26
SPESSART	1.17	0.56	0.38	0.09	0.25	0.22	0.34	0.11
GROSSULA	78.09	83.42	80.66	75.75	75.05	73.96	77.08	76.41
PERCENTAGE CATIONS ASSIGNED								
	92.20	95.58	92.78	97.87	96.69	97.59	96.89	96.81

APPENDIX 5.1 ELECTRON MICROPROBE GARNET ANALYSES

	43/3 5F	43/3 6A	43/3 6B	43/3 6C	43/3 6D	43/3 6E	43/3 7A	43/3 7B
SI1.02.	39.34	39.14	39.03	39.53	39.05	39.60	39.85	39.51
TI1.02.	0.35	1.27	0.59	1.13	1.38	0.0	1.90	0.56
AL2.03.	17.01	19.23	19.27	19.52	19.67	19.61	18.12	19.84
+FE2.03.	6.63	4.24	4.70	3.58	3.86	4.40	4.53	4.12
MN1.01.	0.04	0.11	0.05	0.06	0.03	0.01	0.12	0.08
MG1.01.	0.37	0.41	0.04	0.23	0.45	0.34	0.45	0.24
CA1.01.	36.05	36.13	36.92	36.65	36.03	36.39	35.98	36.16
TOTAL	99.79	100.53	100.60	100.70	100.47	100.35	100.95	100.51
UNIT FORMULA								
SI	6.053	5.931	5.929	5.968	5.909	6.002	6.014	5.973
TI	0.041	0.145	0.067	0.128	0.157	0.0	0.216	0.064
AL	3.085	3.434	3.450	3.473	3.508	3.503	3.223	3.535
FE	0.768	0.483	0.537	0.407	0.440	0.502	0.514	0.469
MN	0.005	0.014	0.006	0.008	0.004	0.001	0.015	0.010
MG	0.085	0.093	0.009	0.052	0.102	0.077	0.101	0.054
CA	5.944	5.866	6.010	5.928	5.842	5.910	5.818	5.857
O	24.000	24.000	24.000	24.000	24.000	24.000	24.000	24.000
GARNET MOLECULES (RICKWOOD(1968))								
ANDRADIT	19.93	12.34	12.60	10.48	10.92	12.57	13.76	11.87
PYROPE	1.47	1.58	0.15	0.89	1.71	1.28	1.81	0.91
SPESSART	0.09	0.24	0.11	0.13	0.06	0.02	0.27	0.17
GROSSULA	78.52	85.84	86.27	88.50	87.09	86.12	84.16	87.04
SCHORLOM	0.0	0.0	0.88	0.00	0.22	0.0	0.0	0.00
PERCENTAGE CATIONS ASSIGNED								
	96.44	98.16	99.64	97.22	98.94	99.83	94.02	98.93

APPENDIX 5.1 ELECTRON MICROPROBE GARNET ANALYSES

	43/3 7C	43/3 8A	43/3 8B	43/3 8C	43/3 8D	43/3 8E	43/3 8F	43/21 1A
SI1.02.	39.05	39.05	39.10	39.45	39.56	39.28	39.05	39.99
TI1.02.	0.02	1.00	0.05	0.0	0.04	0.70	1.06	0.08
AL2.03.	20.47	18.29	20.12	19.70	19.29	17.62	19.00	22.37
+ FE2.03.	4.00	4.29	4.03	4.66	4.02	7.04	4.34	0.32
MN1.01.	0.01	0.10	0.07	0.07	0.06	0.08	0.07	0.02
MG1.01.	0.03	0.70	0.37	0.07	0.11	0.30	0.58	0.13
CA1.01.	36.87	35.40	36.34	36.67	36.94	35.82	36.71	37.47
TOTAL	100.45	98.83	100.08	100.62	100.02	100.84	100.81	100.38
UNIT FORMULA								
SI	5.917	6.014	5.941	5.976	6.024	5.981	5.915	5.985
TI	0.002	0.116	0.006	0.0	0.005	0.080	0.121	0.009
AL	3.656	3.320	3.604	3.517	3.462	3.163	3.392	3.946
FE	0.456	0.497	0.461	0.531	0.461	0.807	0.495	0.036
MN	0.001	0.013	0.009	0.009	0.008	0.010	0.009	0.003
MG	0.007	0.161	0.084	0.016	0.025	0.068	0.131	0.029
CA	5.986	5.841	5.917	5.952	6.027	5.845	5.958	6.008
O	24.000	24.000	24.000	24.000	24.000	24.000	24.000	24.000
GARNET MOLECULES (RICKWOOD(1968))								
ANDRADIT	11.52	13.02	11.53	13.33	11.74	20.43	12.73	0.91
PYROPE	0.11	2.81	1.41	0.26	0.42	1.15	2.25	0.49
SPESSART	0.02	0.23	0.15	0.15	0.13	0.17	0.15	0.04
GROSSULA	88.31	83.94	86.82	86.25	87.70	78.25	84.87	98.57
SCHORLOM	0.04	0.00	0.10	0.0	0.0	0.00	0.0	0.00
PERCENTAGE CATIONS ASSIGNED								
	98.50	95.66	98.99	99.59	98.00	99.00	97.05	99.45

APPENDIX 5.1 ELECTRON MICROPROBE GARNET ANALYSES

	43/21 1B	43/21 1C	43/21 1D	43/21 1E	43/21 1F	43/21 1G	43/21 1H	43/21 1I
SI1.02.	40.17	40.14	40.22	40.04	40.06	40.00	40.35	40.04
TI1.02.	0.10	0.05	0.04	0.0	0.0	0.14	0.18	0.19
AL2.03.	22.25	21.87	22.05	21.94	21.99	21.67	21.03	21.29
+ FE2.03.	0.66	0.96	1.21	1.21	1.52	1.62	1.52	1.41
MN1.01.	0.0	0.05	0.02	0.06	0.08	0.0	0.0	0.0
MG1.01.	0.28	0.21	0.34	0.22	0.12	0.20	0.16	0.10
CA1.01.	37.02	37.46	37.05	37.00	36.76	36.82	37.04	37.29
TOTAL	100.48	100.74	100.93	100.47	100.53	100.45	100.28	100.32
UNIT FORMULA								
SI	6.001	5.999	5.993	5.996	5.996	5.996	6.060	6.017
TI	0.011	0.006	0.004	0.0	0.0	0.016	0.020	0.021
AL	3.918	3.852	3.873	3.873	3.879	3.829	3.723	3.771
FE	0.074	0.108	0.136	0.136	0.171	0.183	0.172	0.159
MN	0.0	0.006	0.003	0.008	0.010	0.0	0.0	0.0
MG	0.062	0.047	0.076	0.049	0.027	0.045	0.036	0.022
CA	5.926	5.998	5.915	5.937	5.895	5.914	5.961	6.005
O	24.000	24.000	24.000	24.000	24.000	24.000	24.000	24.000
GARNET MOLECULES (RICKWOOD(1968))								
ANDRADIT	1.86	2.73	3.39	3.41	4.33	4.60	4.41	4.06
PYROPE	1.04	0.79	1.26	0.82	0.45	0.75	0.61	0.38
SPESSART	0.0	0.11	0.04	0.13	0.17	0.0	0.0	0.0
GROSSULA	97.10	96.38	95.30	95.64	95.05	94.65	94.98	95.56
SCHORLOM	0.0	0.0	0.01	0.0	0.0	0.0	0.0	0.0
PERCENTAGE CATIONS ASSIGNED								
	99.85	98.91	99.90	99.90	99.00	99.42	97.54	98.29

APPENDIX 5.1 ELECTRON MICROPROBE GARNET ANALYSES

	43/21 1J	43/21 1K	43/21 1L	43/21 1M	43/21 1N	43/21 1O	43/21 1P	43/21 2A
SI1.02.	39.77	40.03	40.09	39.94	40.03	40.25	40.00	39.51
TI1.02.	0.26	0.19	0.10	0.20	0.20	0.21	0.15	0.44
AL2.03.	21.33	21.50	21.58	21.87	22.36	22.02	22.53	21.37
+ FE2.03.	1.40	1.59	1.57	0.99	0.51	0.51	0.67	1.81
MN1.01.	0.0	0.0	0.0	0.01	0.0	0.03	0.02	0.04
MG1.01.	0.42	0.21	0.28	0.20	0.16	0.19	0.16	0.30
CA1.01.	37.08	37.07	37.13	37.02	37.17	37.30	36.88	37.01
TOTAL	100.26	100.59	100.75	100.23	100.43	100.51	100.41	100.48
UNIT FORMULA								
SI	5.981	5.997	5.996	5.993	5.984	6.015	5.978	5.940
TI	0.029	0.021	0.011	0.023	0.022	0.024	0.017	0.050
AL	3.781	3.797	3.805	3.868	3.940	3.879	3.969	3.787
FE	0.158	0.179	0.177	0.112	0.057	0.057	0.075	0.205
MN	0.0	0.0	0.0	0.001	0.0	0.004	0.003	0.005
MG	0.094	0.047	0.062	0.045	0.036	0.042	0.036	0.067
CA	5.975	5.951	5.951	5.952	5.954	5.973	5.906	5.962
O	24.000	24.000	24.000	24.000	24.000	24.000	24.000	24.000
GARNET MOLECULES (RICKWOOD(1968))								
ANDRADIT	4.02	4.51	4.44	2.81	1.35	1.46	1.90	4.34
PYROPE	1.59	0.79	1.05	0.75	0.60	0.72	0.60	1.12
SPESSART	0.0	0.0	0.0	0.02	0.0	0.06	0.04	0.09
GROSSULA	94.38	94.70	94.52	96.42	97.97	97.76	97.46	93.66
SCHORLOM	0.00	0.00	0.0	0.0	0.09	0.0	0.00	0.79
PERCENTAGE CATIONS ASSIGNED								
	98.37	99.45	99.52	99.54	99.87	98.44	99.17	99.69

APPENDIX 5.1 ELECTRON MICROPROBE GARNET ANALYSES

	43/21 2B	43/21 2C	43/21 2D	43/21 2E	43/21 2F	43/21 2G	43/21 2H	43/21 2I
SI1.02.	39.82	39.73	38.67	39.44	39.30	39.52	39.61	39.78
TI1.02.	0.28	0.30	0.14	0.15	0.23	0.13	0.11	0.55
AL2.03.	20.29	19.88	19.84	20.72	20.15	20.19	19.91	21.44
FE2.03.	3.20	4.54	4.54	3.18	4.57	4.36	4.37	1.30
MN1.01.	0.04	0.10	0.06	0.04	0.0	0.08	0.05	0.03
MG1.01.	0.12	0.08	0.06	0.11	0.05	0.06	0.06	0.18
CA1.01.	36.94	36.13	37.40	37.01	36.46	35.48	36.79	37.32
TOTAL	100.69	100.76	100.71	100.65	100.76	99.82	100.90	100.60
UNIT FORMULA								
SI	5.998	5.993	5.875	5.946	5.937	6.002	5.976	5.965
TI	0.032	0.034	0.016	0.017	0.026	0.015	0.012	0.062
AL	3.602	3.535	3.553	3.682	3.588	3.614	3.541	3.790
FE	0.363	0.515	0.519	0.361	0.520	0.498	0.496	0.147
MN	0.005	0.013	0.008	0.005	0.0	0.010	0.006	0.004
MG	0.027	0.018	0.014	0.025	0.011	0.014	0.013	0.040
CA	5.962	5.840	6.088	5.979	5.902	5.774	5.948	5.997
O	24.000	24.000	24.000	24.000	24.000	24.000	24.000	24.000
GARNET MOLECULES (RICKWOOD(1968))								
ANDRADIT	9.15	13.17	12.95	8.79	13.18	12.89	12.47	3.73
PYROPE	0.45	0.31	0.23	0.41	0.19	0.23	0.23	0.68
SPESSART	0.09	0.22	0.13	0.09	0.0	0.18	0.11	0.06
GROSSULA	90.31	86.31	86.42	90.42	86.63	86.70	87.20	95.53
SCHORLOM	0.00	0.00	0.27	0.29	0.0	0.00	0.00	0.00
PERCENTAGE CATIONS ASSIGNED								
	99.20	98.16	97.74	99.30	98.65	97.07	99.50	98.38

APPENDIX 5.1 ELECTRON MICROPROBE GARNET ANALYSES

	43/21 2J	43/22 1A	43/22 1B	43/22 1C	43/22 1D	43/22 1E	43/22 1F	43/22 2A
SI1.02.	39.45	38.78	39.19	38.85	39.35	39.36	39.34	38.39
TI1.02.	0.16	0.26	0.26	0.24	0.30	0.22	0.35	0.01
AL2.03.	19.77	16.61	16.33	16.11	16.72	16.63	17.01	14.71
FE2.03.	4.66	7.75	7.96	8.28	7.28	7.44	6.63	12.02
MN1.01.	0.07	0.04	0.11	0.10	0.15	0.05	0.04	0.37
MG1.01.	0.03	0.31	0.24	0.27	0.21	0.32	0.37	0.13
CA1.01.	36.62	36.37	36.63	36.10	36.19	36.28	36.05	34.22
TOTAL	100.76	100.12	100.72	99.95	100.20	100.30	99.79	99.85
UNIT FORMULA								
SI	5.966	5.984	6.017	6.013	6.048	6.046	6.053	6.001
TI	0.018	0.030	0.030	0.028	0.035	0.025	0.041	0.001
AL	3.524	3.021	2.955	2.939	3.029	3.011	3.085	2.710
FE	0.530	0.900	0.920	0.964	0.842	0.860	0.768	1.414
MN	0.009	0.005	0.014	0.013	0.020	0.007	0.005	0.049
MG	0.007	0.071	0.055	0.062	0.048	0.073	0.085	0.030
CA	5.934	6.013	6.026	5.987	5.960	5.971	5.944	5.731
O	24.000	24.000	24.000	24.000	24.000	24.000	24.000	24.000
GARNET MOLECULES (RICKWOOD(1968))								
ANDRADIT	13.37	22.95	23.73	24.71	21.75	22.22	19.93	36.50
PYROPE	0.11	1.21	0.95	1.06	0.83	1.26	1.47	0.52
SPESSART	0.15	0.09	0.25	0.22	0.34	0.11	0.09	0.84
GROSSULA	86.37	75.75	75.07	74.01	77.08	76.41	78.52	62.14
PERCENTAGE CATIONS ASSIGNED								
	99.23	97.87	96.77	97.54	96.89	96.81	96.44	97.23

APPENDIX 5.1 ELECTRON MICROPROBE GARNET ANALYSES

	43/22 2B	43/22 2C	43/22 2D	43/22 2E	43/22 2F	44/9A 1A	44/9A 1B	44/9A 1C
SI1.02.	37.90	38.28	38.25	38.19	38.93	38.99	39.57	39.47
TI1.02.	0.0	0.09	0.03	0.02	0.02	0.0	0.0	0.0
AL2.03.	14.96	15.26	15.14	14.86	16.34	20.05	19.82	20.04
+ FE2.03.	11.17	10.81	12.18	13.62	9.65	4.48	5.11	4.86
MN1.01.	0.34	0.39	0.39	0.38	0.09	0.04	0.09	0.06
MG1.01.	0.09	0.11	0.04	0.10	0.26	0.27	0.29	0.27
CA1.01.	35.09	34.23	34.95	33.73	34.72	36.63	36.23	35.98
TOTAL	99.55	99.17	100.98	100.90	100.01	100.46	101.11	100.68
UNIT FORMULA								
SI	5.950	6.003	5.926	5.926	6.015	5.916	5.962	5.963
TI	0.0	0.011	0.003	0.002	0.002	0.0	0.0	0.0
AL	2.768	2.821	2.765	2.718	2.976	3.586	3.520	3.569
FE	1.320	1.276	1.420	1.590	1.122	0.512	0.579	0.553
MN	0.045	0.052	0.051	0.050	0.012	0.005	0.011	0.008
MG	0.021	0.026	0.009	0.023	0.060	0.061	0.065	0.061
CA	5.903	5.751	5.802	5.608	5.748	5.955	5.849	5.824
O	24.000	24.000	24.000	24.000	24.000	24.000	24.000	24.000
GARNET MOLECULES (RICKWOOD(1968))								
ANDRADIT	33.27	32.83	36.33	41.99	28.92	12.97	14.67	14.06
PYROPE	0.35	0.44	0.16	0.41	1.03	1.03	1.10	1.03
SPESSART	0.76	0.89	0.87	0.88	0.20	0.09	0.19	0.13
GROSSULA	65.62	65.84	62.63	56.72	69.85	85.91	84.04	84.77
PERCENTAGE CATIONS ASSIGNED								
	99.12	97.52	97.85	95.18	97.39	98.39	98.84	98.36

APPENDIX 5.1 ELECTRON MICROPROBE GARNET ANALYSES

	44/9A 1D	44/9A 1E	44/9A 1F	44/9A 1G	44/9A 2A	44/9A 2B	44/9A 2C	44/9A 2D
SI1.02.	39.37	39.33	39.59	38.62	39.01	39.01	39.00	39.40
AL2.03.	20.30	19.69	20.08	20.35	19.33	19.04	18.78	19.03
+ FE2.03.	4.64	4.60	4.28	3.92	5.73	6.64	7.05	6.81
MN1.01.	0.08	0.04	0.11	0.06	0.04	0.06	0.06	0.04
MG1.01.	0.27	0.27	0.29	0.39	0.42	0.31	0.33	0.29
CA1.01.	36.30	36.77	36.31	36.43	36.28	35.84	35.63	35.49
TOTAL	100.96	100.70	100.66	99.77	100.81	100.90	100.85	101.06
UNIT FORMULA								
SI	5.934	5.955	5.978	5.892	5.918	5.922	5.928	5.961
AL	3.606	3.514	3.574	3.659	3.457	3.407	3.365	3.394
FE	0.526	0.524	0.486	0.450	0.654	0.759	0.806	0.775
MN	0.010	0.005	0.014	0.008	0.005	0.008	0.008	0.005
MG	0.061	0.061	0.065	0.089	0.095	0.070	0.075	0.065
CA	5.862	5.966	5.875	5.955	5.898	5.830	5.803	5.754
O	24.000	24.000	24.000	24.000	24.000	24.000	24.000	24.000
GARNET MOLECULES (RICKWOOD(1968))								
ANDRADIT	13.31	13.20	12.25	11.46	16.58	19.26	20.55	19.97
PYROPE	1.02	1.02	1.10	1.51	1.60	1.19	1.27	1.12
SPESSART	0.17	0.09	0.24	0.13	0.09	0.13	0.13	0.09
GROSSULA	85.50	85.69	86.42	86.91	81.73	79.42	78.05	78.82
PERCENTAGE CATIONS ASSIGNED								
	98.89	99.10	99.28	97.87	98.47	98.49	98.19	97.35

APPENDIX 5.1 ELECTRON MICROPROBE GARNET ANALYSES

	44/9A 2E	44/9A 2F	44/9A 2G	44/11 1A	44/11 1B	44/11 1C	44/11 1D	44/11 1E
SI1.02.	39.06	39.66	39.04	38.21	38.02	38.21	38.70	39.31
TI1.02.	0.0	0.0	0.0	0.36	2.16	1.94	0.61	0.13
AL2.03.	19.26	18.23	18.60	16.21	15.30	16.93	18.59	19.73
+ FE2.03.	6.99	7.04	7.47	9.37	7.97	5.75	5.17	2.60
MN1.01.	0.09	0.14	0.13	0.12	0.05	0.04	0.01	0.0
MG1.01.	0.24	0.27	1.31	0.0	0.27	0.30	0.19	0.16
CA1.01.	35.44	35.41	34.37	35.22	35.74	36.10	36.15	37.13
TOTAL	101.08	100.75	100.92	99.49	99.51	99.27	99.42	99.06
UNIT FORMULA								
SI	5.916	6.026	5.919	5.953	5.922	5.919	5.952	6.022
TI	0.0	0.0	0.0	0.042	0.253	0.226	0.071	0.015
AL	3.438	3.265	3.324	2.977	2.809	3.091	3.370	3.563
FE	0.797	0.805	0.852	1.099	0.934	0.670	0.598	0.300
MN	0.012	0.018	0.017	0.016	0.007	0.005	0.001	0.0
MG	0.054	0.061	0.296	0.0	0.063	0.069	0.044	0.037
CA	5.751	5.765	5.584	5.880	5.965	5.992	5.957	6.095
O	24.000	24.000	24.000	24.000	24.000	24.000	24.000	24.000
GARNET MOLECULES (RICKWOOD(1968))								
ANDRADIT	20.54	20.66	21.68	27.95	24.96	17.82	15.07	7.76
PYROPE	0.93	1.05	5.02	0.0	1.12	1.23	0.73	0.63
SPESSART	0.20	0.31	0.28	0.27	0.12	0.09	0.02	0.0
GROSSULA	78.33	77.98	73.01	71.78	73.81	80.86	84.17	91.61
SCHORLOM	0.0	0.0	0.0	0.00	0.00	0.0	0.01	0.0
PERCENTAGE CATIONS ASSIGNED								
	97.15	97.77	98.32	98.47	93.86	94.20	99.25	96.37

APPENDIX 5.1 ELECTRON MICROPROBE GARNET ANALYSES

	44/11 1F	44/11 1G	44/11 1H	44/11 1I	44/11 1J	44/11 1K	44/11 1L	44/11 2A
SI1.02.	39.53	39.59	39.57	39.16	38.91	38.13	38.06	38.42
TI1.02.	0.11	0.19	0.29	0.30	0.68	1.41	0.50	1.28
AL2.03.	20.16	20.79	19.83	18.34	18.02	16.37	15.35	15.73
+ FE2.03.	2.06	2.06	2.81	4.94	5.04	6.48	11.04	9.20
MN1.01.	0.04	0.0	0.0	0.05	0.0	0.05	0.09	0.0
MG1.01.	0.48	0.25	0.14	0.16	0.21	0.34	0.0	0.32
CA1.01.	37.22	36.63	36.80	36.45	36.36	35.87	35.27	35.96
TOTAL	99.60	99.51	99.44	99.40	99.22	98.65	100.31	100.91
UNIT FORMULA								
SI	6.011	6.007	6.032	6.020	5.999	5.957	5.918	5.912
TI	0.013	0.022	0.033	0.035	0.079	0.166	0.058	0.148
AL	3.613	3.718	3.563	3.323	3.275	3.014	2.813	2.853
FE	0.236	0.235	0.322	0.572	0.585	0.762	1.292	1.065
MN	0.005	0.0	0.0	0.007	0.0	0.007	0.012	0.0
MG	0.109	0.057	0.032	0.037	0.048	0.079	0.0	0.073
CA	6.065	5.955	6.011	6.004	6.007	6.005	5.877	5.929
O	24.000	24.000	24.000	24.000	24.000	24.000	24.000	24.000
GARNET MOLECULES (RICKWOOD(1968))								
ANDRADIT	6.12	5.95	8.30	14.67	15.15	20.17	32.91	27.19
PYROPE	1.88	0.95	0.55	0.63	0.83	1.40	0.0	1.25
SPESSART	0.09	0.0	0.0	0.11	0.0	0.12	0.20	0.0
GROSSULA	91.90	93.10	91.16	84.59	84.02	78.31	66.89	71.56
PERCENTAGE CATIONS ASSIGNED								
	95.92	98.87	97.18	97.39	96.53	94.47	98.32	98.08

APPENDIX 5.1 ELECTRON MICROPROBE GARNET ANALYSES

	44/11 2B	44/11 2C	44/11 2D	44/11 2E	44/11 2F	44/11 2G	44/11 2H	44/11 2I
SI1.02.	39.13	40.03	39.77	39.59	39.06	39.95	39.49	40.00
TI1.02.	0.91	0.88	0.25	0.25	0.93	0.05	0.15	0.24
AL2.03.	17.50	18.04	19.53	20.04	18.09	20.14	20.04	18.74
+FE2.03.	7.52	6.09	4.04	3.49	6.02	2.98	3.68	5.19
MG1.01.	0.12	0.13	0.31	0.29	0.20	0.32	0.27	0.11
CA1.01.	35.69	36.05	36.87	36.99	36.63	36.76	37.07	36.40
TOTAL	100.87	101.22	100.77	100.65	100.93	100.20	100.70	100.68
UNIT FORMULA								
SI	5.963	6.043	6.004	5.976	5.939	6.037	5.964	6.056
TI	0.104	0.100	0.028	0.028	0.106	0.006	0.017	0.027
AL	3.144	3.210	3.475	3.566	3.242	3.587	3.567	3.344
FE	0.862	0.692	0.459	0.396	0.689	0.339	0.418	0.591
MG	0.027	0.029	0.070	0.065	0.045	0.072	0.061	0.025
CA	5.828	5.832	5.964	5.983	5.968	5.952	5.999	5.905
O	24.000	24.000	24.000	24.000	24.000	24.000	24.000	24.000
GARNET MOLECULES (RICKWOOD(1968))								
ANDRADIT	22.09	17.73	11.67	10.01	17.52	8.63	10.25	15.02
PYROPE	0.47	0.50	1.18	1.10	0.77	1.22	1.02	0.42
GROSSULA	77.44	81.77	87.15	88.90	81.71	90.14	88.49	84.55
SCHORLOM	0.00	0.0	0.00	0.00	0.00	0.0	0.24	0.00
PERCENTAGE CATIONS ASSIGNED								
	98.02	98.13	98.35	98.96	98.34	98.20	99.48	98.71

APPENDIX 5.1 ELECTRON MICROPROBE GARNET ANALYSES

	44/11 2J	46/13 1A	46/13 1B	46/13 1C	46/13 1D	46/13 2A	46/13 2B	46/13 2C
SI1.02.	39.06	38.47	38.98	38.56	38.95	36.88	37.58	37.02
TI1.02.	1.35	0.21	0.06	0.09	0.05	0.05	0.04	0.06
AL2.03.	16.33	15.94	14.73	14.74	14.52	7.59	11.34	7.49
+ FE2.03.	7.65	8.82	9.57	10.07	10.13	19.90	15.42	19.75
MN1.01.	0.0	0.13	0.06	0.10	0.09	0.07	0.09	0.05
MG1.01.	0.13	0.0	0.0	0.0	0.0	0.0	0.12	0.01
CA1.01.	36.35	36.21	35.71	35.33	35.97	35.04	34.80	34.20
TOTAL	100.87	99.78	99.11	98.89	99.71	99.53	99.39	98.58
UNIT FORMULA								
SI	5.979	5.984	6.106	6.064	6.082	6.008	6.004	6.070
TI	0.155	0.025	0.007	0.011	0.006	0.006	0.005	0.007
AL	2.946	2.922	2.720	2.732	2.672	1.457	2.136	1.448
FE	0.881	1.032	1.128	1.192	1.190	2.440	1.854	2.437
MN	0.0	0.017	0.008	0.013	0.012	0.010	0.012	0.007
MG	0.030	0.0	0.0	0.0	0.0	0.0	0.029	0.002
CA	5.962	6.035	5.994	5.953	6.018	6.116	5.957	6.009
O	24.000	24.000	24.000	24.000	24.000	24.000	24.000	24.000
GARNET MOLECULES (RICKWOOD(1968))								
ANDRADIT	23.02	26.10	29.32	30.37	30.82	62.60	46.47	62.74
PYROPE	0.52	0.0	0.0	0.0	0.0	0.0	0.48	0.04
SPESSART	0.0	0.29	0.14	0.23	0.21	0.17	0.20	0.12
GROSSULA	76.46	73.61	70.54	69.40	68.98	37.23	52.85	37.10
PERCENTAGE CATIONS ASSIGNED								
	95.97	98.78	96.42	98.31	96.69	97.20	99.76	97.23

APPENDIX 5.1 ELECTRON MICROPROBE GARNET ANALYSES

	46/13 2D
SI1.02.	37.10
TI1.02.	0.11
AL2.03.	8.39
+ FE2.03.	19.96
MN1.01.	0.06
CA1.01.	34.65
TOTAL	100.27

UNIT FORMULA	
SI	5.980
TI	0.013
AL	1.594
FE	2.421
MN	0.008
CA	5.984
O	24.000

GARNET MOLECULES (RICKWOOD(1968))	
ANDRADIT	60.39
SPESSART	0.14
GROSSULA	39.26
SCHORLOM	0.21

PERCENTAGE CATIONS ASSIGNED
99.87

APPENDIX 5.2 ELECTRON MICROPROBE FELDSPAR ANALYSES

	35/4 1	35/4 2	35/4 3	35/4 4	35/4 5	35/4 6	43/3 1A	43/3 1B
OXIDE WEIGHT PERCENTAGE								
SIO2	63.9	63.9	69.7	65.0	69.5	68.3	69.5	69.1
AL2O3	18.2	18.2	19.7	18.4	19.6	18.8	19.6	19.4
°FE2O3	0.0T	0.0T	0.1	0.2	0.1	0.1	0.1	0.1
CAO	0.0+	0.0T	0.3	0.0+	0.2	0.2	0.3	0.2
NA2O	0.3	0.2	10.2	0.2	10.3	11.2	10.9	9.2
K2O	16.0	16.5	0.1	16.5	0.3	0.2	0.0T	1.8
TOTAL	98.4	98.8	100.1	100.3	100.0	98.8	100.4	99.8
ATOMIC PROPORTIONS ON THE BASIS OF 32 OXYGENS								
SI	11.99	11.98	12.08	11.99	12.07	12.06	12.04	12.09
AL	4.03	4.02	4.03	4.00	4.01	3.91	4.00	4.00
FE3	0.00	0.00	0.01	0.03	0.01	0.01	0.01	0.01
CA	0.00	0.00	0.06	0.00	0.04	0.04	0.06	0.04
NA	0.11	0.07	3.43	0.07	3.47	3.84	3.66	3.12
K	3.83	3.95	0.02	3.88	0.07	0.05	0.00	0.40
END MEMBER COMPOSITIONS								
AB	2.8	1.8	97.8	1.8	97.1	97.9	98.5	87.7
AN	0.0	0.0	1.6	0.0	1.0	1.0	1.5	1.1
OR	97.2	98.2	0.6	98.2	1.9	1.1	0.0	11.3

T = trace, + = not detected, ¤ = not determined
o = Total Fe as Fe_2O_3

APPENDIX 5.2 ELECTRON MICROPROBE FELDSPAR ANALYSES

	43/3 1C	43/3 2	43/3 3	43/3 4	43/3 5	43/3 6	43/3 7	43/3 8
OXIDE WEIGHT PERCENTAGE								
SIO2	68.3	69.0	67.4	68.6	70.2	69.6	69.7	69.3
AL2O3	19.5	19.6	17.7	18.0	18.6	18.5	19.9	19.6
°FE2O3	0.1	0.1	0.1	0.7	0.2	0.9	0.1	0.2
CAO	0.2	0.2	2.3	2.8	0.5	0.6	0.6	0.5
NA2O	11.7	10.4	11.9	11.2	10.6	10.8	9.6	10.6
K2O	0.0T	0.0T	0.0T	0.1	0.1	0.1	0.1	0.1
TOTAL	99.8	99.3	99.4	101.4	100.2	100.5	100.0	100.3
ATOMIC PROPORTIONS ON THE BASIS OF 32 OXYGENS								
SI	11.96	12.06	11.97	11.95	12.18	12.10	12.07	12.03
AL	4.03	4.04	3.70	3.70	3.81	3.79	4.06	4.01
FE3	0.01	0.01	0.01	0.09	0.03	0.12	0.01	0.03
CA	0.04	0.04	0.44	0.52	0.09	0.11	0.11	0.09
NA	3.97	3.53	4.10	3.78	3.57	3.64	3.23	3.57
K	0.00	0.00	0.00	0.02	0.02	0.02	0.02	0.02
END MEMBER COMPOSITIONS								
AB	99.1	98.9	90.3	87.4	96.9	96.5	96.0	96.9
AN	0.9	1.1	9.6	12.1	2.5	3.0	3.3	2.5
OR	0.0	0.0	0.0	0.5	0.6	0.6	0.7	0.6

APPENDIX 5.2 ELECTRON MICROPROBE FELDSPAR ANALYSES

	43/3 9	44/7 1A	44/7 1B	44/7 1C	44/7 2A	44/7 2B	44/7 3A	44/7 3B
OXIDE WEIGHT PERCENTAGE								
SIO2	69.7	68.6	67.9	67.3	67.0	66.6	67.7	68.2
AL2O3	19.9	19.4	19.7	19.6	19.9	19.9	19.5	19.8
FE2O3	0.1	0.0*	0.0*	0.0*	0.0*	0.0*	0.0*	0.0*
CAO	0.6	0.0T	0.0T	0.0T	0.1	0.2	0.1	0.2
NA2O	9.6	11.7	12.0	11.9	12.2	11.9	11.7	12.0
K2O	0.1	0.0T	0.0T	0.0T	0.1	0.1	0.1	0.1
TOTAL	100.0	99.7	99.6	98.8	99.3	98.7	99.1	100.3
ATOMIC PROPORTIONS ON THE BASIS OF 32 OXYGENS								
SI	12.07	12.00	11.92	11.91	11.83	11.82	11.94	11.90
AL	4.06	4.00	4.08	4.09	4.14	4.17	4.06	4.07
FE3	0.01	0.00	0.00	0.00	0.00	0.00	0.00	0.00
CA	0.11	0.00	0.00	0.00	0.02	0.04	0.02	0.04
NA	3.23	3.97	4.09	4.09	4.18	4.10	4.00	4.06
K	0.02	0.00	0.00	0.00	0.02	0.02	0.02	0.02
END MEMBER COMPOSITIONS								
AB	96.0	100.0	100.0	100.0	99.0	98.5	99.0	98.6
AN	3.3	0.0	0.0	0.0	0.4	0.9	0.5	0.9
OR	0.7	0.0	0.0	0.0	0.5	0.5	0.6	0.5

APPENDIX 5.2 ELECTRON MICROPROBE FELDSPAR ANALYSES

	44/7 3C	44/7 4	44/7 5A	44/7 5B	44/7 6	44/7 7	44/7 8	44/7 9
OXIDE WEIGHT PERCENTAGE								
SIO2	68.0	67.9	68.4	67.7	68.8	68.8	68.6	70.6
AL2O3	19.3	19.7	19.3	19.5	18.3	19.8	19.4	19.3
°FE2O3	0.0*	0.0*	0.0*	0.0*	0.0*	0.0*	0.6	0.1
CAO	0.1	0.4	0.1	0.1	0.3	0.3	2.5	0.1
NA2O	12.1	12.1	11.6	11.9	11.6	11.8	8.8	10.8
K2O	0.0T	0.0T	0.2	0.4	0.0T	0.0+	0.4	0.1
TOTAL	99.5	100.1	99.6	99.6	99.0	100.7	100.3	101.0
ATOMIC PROPORTIONS ON THE BASIS OF 32 OXYGENS								
SI	11.96	11.88	12.00	11.92	12.13	11.94	11.95	12.14
AL	4.00	4.07	3.99	4.05	3.80	4.05	3.98	3.91
FE3	0.00	0.00	0.00	0.00	0.00	0.00	0.08	0.01
CA	0.02	0.08	0.02	0.02	0.06	0.06	0.47	0.02
NA	4.13	4.11	3.95	4.06	3.97	3.97	2.97	3.60
K	0.00	0.00	0.04	0.09	0.00	0.00	0.09	0.02
END MEMBER COMPOSITIONS								
AB	99.5	98.2	98.4	97.4	98.6	98.6	84.3	98.9
AN	0.5	1.8	0.5	0.5	1.4	1.4	13.2	0.5
OR	0.0	0.0	1.1	2.2	0.0	0.0	2.5	0.6

APPENDIX 5.2 ELECTRON MICROPROBE FELDSPAR ANALYSES

	44/7 10	44/7 11	44/11 1	44/11 2	44/11 3	44/11 4	44/11 5A	44/11 5B
OXIDE WEIGHT PERCENTAGE								
SIO2	69.0	69.9	68.0	68.9	67.9	68.6	68.5	68.9
AL2O3	19.3	19.6	19.3	19.1	19.3	18.9	19.4	18.5
°FE2O3	0.1	0.0T	0.0*	0.0*	0.0*	0.4	0.4	0.3
CAO	0.3	0.1	0.4	0.4	0.3	1.0	0.4	0.3
NA2O	11.3	11.6	11.1	11.4	12.5	11.7	11.3	11.6
K2O	0.1	0.1	0.1	0.1	0.0+	0.0T	0.0T	0.0T
TOTAL	100.1	101.3	98.9	99.9	100.0	100.6	100.0	99.6
ATOMIC PROPORTIONS ON THE BASIS OF 32 OXYGENS								
SI	12.03	12.03	11.99	12.04	11.91	11.96	11.97	12.08
AL	3.97	3.98	4.01	3.93	3.99	3.89	4.00	3.83
FE3	0.01	0.00	0.00	0.00	0.00	0.05	0.05	0.04
CA	0.06	0.02	0.08	0.07	0.06	0.19	0.07	0.06
NA	3.82	3.87	3.80	3.86	4.25	3.96	3.83	3.95
K	0.02	0.02	0.02	0.02	0.00	0.00	0.00	0.00
END MEMBER COMPOSITIONS								
AB	98.0	99.0	97.5	97.5	98.7	95.5	98.1	98.6
AN	1.4	0.5	1.9	1.9	1.3	4.5	1.9	1.4
OR	0.6	0.6	0.6	0.6	0.0	0.0	0.0	0.0

APPENDIX 5.2 ELECTRON MICROPROBE FELDSPAR ANALYSES

	44/11 6A	44/11 6B	44/11 7	44/25 1A	44/25 1B	44/25 2	L/860 1	L/860 2
OXIDE WEIGHT PERCENTAGE								
SIO2	69.0	68.7	69.1	54.8	55.7	59.9	60.6	67.8
AL2O3	19.3	19.1	19.3	27.7	27.6	27.1	27.1	20.1
°FE2O3	0.2	0.1	0.4	0.0*	0.0*	0.0*	0.0*	0.0*
CAO	0.6	0.2	0.3	11.8	12.3	6.6	6.8	0.7
NA2O	11.3	11.7	11.8	5.0	5.8	4.8	5.3	10.4
K2O	0.0T	0.0+	0.0+	0.2	0.3	0.3	0.4	0.0T
TOTAL	100.4	99.8	100.9	99.5	101.7	98.7	100.2	99.0
ATOMIC PROPORTIONS ON THE BASIS OF 32 OXYGENS								
SI	12.00	12.02	11.98	9.95	9.95	10.67	10.66	11.92
AL	3.96	3.94	3.95	5.93	5.81	5.69	5.62	4.17
FE3	0.03	0.01	0.05	0.00	0.00	0.00	0.00	0.00
CA	0.11	0.04	0.06	2.30	2.35	1.26	1.28	0.13
NA	3.81	3.97	3.97	1.76	2.01	1.66	1.81	3.55
K	0.00	0.00	0.00	0.05	0.07	0.07	0.09	0.00
END MEMBER COMPOSITIONS								
AB	97.1	99.1	98.6	42.9	45.3	55.5	56.9	96.4
AN	2.8	0.9	1.4	56.0	53.1	42.2	40.3	3.6
OR	0.0	0.0	0.0	1.1	1.5	2.3	2.8	0.0

APPENDIX 5.2 ELECTRON MICROPROBE FELDSPAR ANALYSES

	L/860 3A	L/860 3B	CHE 1A	CHE 1B	CHE 2A	CHE 2B
OXIDE WEIGHT PERCENTAGE						
SIO2	57.7	56.3	46.1	45.8	46.0	46.6
AL2O3	26.3	25.5	34.1	33.7	33.6	33.5
°FE2O3	0.0*	0.0*	0.0*	0.0*	0.0*	0.0*
CAO	8.4	10.0	18.2	18.2	18.4	18.3
NA2O	5.4	7.0	1.1	1.9	1.4	1.6
K2O	0.4	0.5	0.0T	0.1	0.1	0.0T
TOTAL	98.2	99.3	99.5	99.7	99.5	100.0
ATOMIC PROPORTIONS ON THE BASIS OF 32 OXYGENS						
SI	10.47	10.26	8.52	8.49	8.53	8.59
AL	5.62	5.48	7.43	7.37	7.35	7.28
FE3	0.00	0.00	0.00	0.00	0.00	0.00
CA	1.63	1.95	3.61	3.62	3.66	3.61
NA	1.90	2.48	0.39	0.68	0.50	0.57
K	0.09	0.12	0.00	0.02	0.02	0.00
END MEMBER COMPOSITIONS						
AB	52.4	54.5	9.9	15.8	12.0	13.7
AN	45.0	43.0	90.1	83.6	87.4	86.3
OR	2.6	2.6	0.0	0.5	0.6	0.0

Appendix 5.3 Electron microprobe epidote analyses

	35/4	41/36 1	41/36 2	43/3 1A	43/3 1B	43/3 2	43/22 1
SiO_2	41.37	38.03	37.93	41.83	41.43	42.78	37.62
Al_2O_3	22.28	26.57	25.95	18.10	20.48	20.09	25.30
*Fe_2O_3	6.61	9.37	10.90	10.31	9.19	7.52	10.84
MgO	n.d.	0.04	0.77	0.98	n.d.	1.05	n.d.
CaO	26.42	23.75	21.70	25.78	25.83	25.97	23.41
MnO	n.d.	0.04	0.08	0.13	0.09	0.12	0.11
Total	96.68	97.80	97.33	97.13	97.02	97.53	97.28

	43/22 2	43/22 3	43/22 4	44/5 1	44/5 2	44/11 1A
SiO_2	38.29	40.81	38.49	37.57	38.27	37.42
Al_2O_3	22.31	23.59	25.90	27.04	25.40	23.34
*Fe_2O_3	12.52	10.78	10.98	10.24	9.89	12.62
MgO	n.d.	0.05	n.d.	n.d.	0.18	-
CaO	24.01	22.18	22.18	23.37	23.86	23.34
MnO	0.08	0.22	0.40	0.02	0.20	-
Total	97.51	97.63	97.95	98.42	97.80	96.72

	44/11 1B	44/11 2	44/11 3	44/11 4A	44/11 4B	44/11 5
SiO_2	37.84	37.97	37.78	37.65	37.11	37.24
Al_2O_3	23.10	24.94	25.36	24.37	25.58	25.35
*Fe_2O_3	12.65	11.52	11.11	11.25	11.72	10.77
CaO	23.82	23.49	23.61	23.64	23.28	23.94
Total	97.41	97.92	97.86	96.91	97.69	97.30

(*), Total iron as Fe_2O_3.
(n.d.), not detected.
(-), not determined.

Appendix 5.4 Electron microprobe idocrase analyses

	43/7 1	43/7 2	44/9A 1A	44/9A 1B	44/9A 1C	44/9A 1D	44/9A 2A
SiO_2	35.36	34.85	36.63	36.75	37.41	36.60	35.28
Al_2O_3	14.49	14.19	16.96	17.27	17.03	17.18	16.91
+FeO	3.69	4.02	3.32	2.72	2.87	4.04	3.09
MgO	1.32	2.70	3.29	3.59	3.46	3.88	3.50
CaO	35.09	35.67	35.91	35.65	34.57	35.21	35.70
TiO_2	3.23	1.87	0.45	0.77	1.07	0.97	0.68
MnO	0.10	0.03	0.04	0.06	0.08	0.05	0.05
Total	93.28	93.33	96.59	96.81	96.48	97.94	95.21

	44/9A 2B	44/9A 2C	44/11 1	44/11 2	45/1 A	45/1 B	45/1 C
SiO_2	36.70	36.68	38.73	37.79	36.25	35.47	35.51
Al_2O_3	16.81	17.01	21.06	19.29	17.49	14.34	14.44
+FeO	3.06	2.62	0.16	0.15	3.78	4.19	5.68
MgO	3.28	3.49	0.34	2.16	4.00	2.78	1.98
CaO	35.06	35.59	37.10	36.12	34.76	34.72	34.84
TiO_2	1.30	0.97	0.05	0.05	0.43	2.75	1.81
MnO	0.05	0.08	0.42	1.57	0.18	0.01	0.03
Total	96.26	96.44	97.86	97.13	96.89	94.26	94.29

	45/1 D	45/1 E	45/1 F	45/1 G	45/1 H	45/1 I	45/1 J
SiO_2	35.71	35.65	35.55	35.55	35.52	35.35	35.75
Al_2O_3	14.20	14.47	14.25	14.49	14.33	14.41	14.15
+FeO	5.65	5.96	5.94	4.99	4.07	4.75	4.47
MgO	1.75	2.02	2.08	2.35	2.67	2.87	3.64
CaO	34.73	34.58	34.89	35.01	34.94	35.11	35.48
TiO_2	1.75	1.27	1.65	1.88	3.21	2.37	0.01
MnO	0.04	0.05	0.03	0.01	0.03	0.02	0.03
Total	93.82	93.99	94.39	94.27	94.77	94.87	93.52

(+), Total Fe as FeO

APPENDIX 5.5 ELECTRON MICROPROBE PYROXENE ANALYSES

	35/4 1	35/4 2	35/4 3	35/4 4	35/4 5	45/1 1A	45/1 1B	45/1 2	45/1 3
OXIDE WEIGHT PERCENTAGE									
SIO2	48.48	48.53	49.49	47.37	47.65	47.30	45.80	43.06	48.66
TIO2	0.05	0.03	0.03	0.0 *	0.0 *	0.43	1.16	3.42	0.75
AL2O3	0.24	0.54	0.26	1.38	0.48	6.56	7.30	9.62	5.75
o FEO	27.16	27.32	28.08	27.46	27.63	6.33	6.09	6.32	4.69
MNO	1.05	0.57	0.70	0.47	0.51	0.11	0.12	0.09	0.12
MGO	0.14	0.26	0.15	0.33	0.40	12.83	12.75	11.67	13.68
CAO	22.82	22.63	20.97	21.98	21.95	25.15	25.16	24.76	25.39
NA2O	0.00+	0.02	0.04	0.07	0.07	0.02	0.03	0.03	0.00+
K2O	0.00+	0.00+	0.00+	0.0 *	0.0 *	0.0 *	0.0 *	0.0 *	0.0 *
TOTAL	99.94	99.90	99.72	99.06	98.69	98.73	98.41	98.97	99.04
ATOMIC PROPORTIONS ON THE BASIS OF 6 OXYGENS									
SI	1.996	1.993	2.029	1.964	1.987	1.792	1.745	1.639	1.822
TI	0.002	0.001	0.001	0.000	0.000	0.012	0.033	0.098	0.021
AL	0.012	0.026	0.013	0.067	0.024	0.293	0.328	0.432	0.254
FE2	0.935	0.939	0.963	0.952	0.964	0.201	0.194	0.201	0.147
MN	0.037	0.020	0.024	0.017	0.018	0.004	0.004	0.003	0.004
MG	0.009	0.016	0.009	0.020	0.025	0.724	0.724	0.662	0.763
CA	1.007	0.996	0.921	0.977	0.981	1.021	1.027	1.010	1.019
NA	0.000	0.002	0.003	0.006	0.006	0.001	0.002	0.002	0.000
K	0.000	0.000	0.000	0.000	0.000	0.000	0.000	0.000	0.000
END MEMBER COMPOSITIONS									
WO	50.66	50.55	48.04	49.68	49.35	52.37	52.70	53.83	52.71
EN	0.43	0.81	0.48	1.04	1.25	37.16	37.14	35.29	39.49
FS	48.91	48.64	51.48	49.28	49.40	10.47	10.16	10.88	7.80

+ = not detected, * = not determined
o = Total Fe as FeO

Appendix 5.6 Electron microprobe prehnite analyses.

	35/4 A	35/4 B	35/4 C	35/4 D
SiO_2	40.6	42.3	43.7	43.3
Al_2O_3	17.3	19.2	23.4	20.7
+Fe_2O_3	5.8	7.0	0.3	0.9
MgO	1.3	<0.05	<0.05	0.3
CaO	29.5	26.2	26.8	26.9
Na_2O	0.1	<0.05	<0.05	<0.05
K_2O	<0.05	<0.05	<0.05	<0.05
Total	94.6	94.7	94.2	92.1

	43/3 1A	43/3 1B	43/3 1C	43/3 1D
SiO_2	42.9	43.5	42.8	43.6
Al_2O_3	19.3	20.0	19.7	20.0
+Fe_2O_3	4.7	4.8	7.9	6.5
MgO	<0.05	<0.05	<0.05	<0.05
CaO	26.5	26.4	26.4	25.0
Na_2O	0.3	<0.05	0.3	<0.05
K_2O	<0.05	<0.05	<0.05	0.9
Total	93.7	94.7	97.1	96.0

	43/3 2A	43/3 2B	44/11 A	44/11 B
SiO_2	42.5	41.0	43.8	44.5
Al_2O_3	20.8	19.6	21.1	24.0
+Fe_2O_3	5.9	8.3	0.2	<0.05
MgO	<0.05	0.2	<0.05	<0.05
CaO	26.8	26.5	27.5	27.3
Na_2O	0.1	0.2	<0.05	0.1
K_2O	n.d.	n.d.	0.1	<0.05
Total	96.1	95.8	92.7	95.9

(n.d.), not determined.

(+), Total iron given as Fe_2O_3

Appendix 5.7 Electron microprobe chlorite analyses.

	43/3 1	43/3 2	43/22 1	43/22 2
SiO_2	35.5	35.9	24.2	22.3
Al_2O_3	13.9	14.0	18.0	17.6
+ FeO	22.7	18.8	30.6	28.7
MgO	15.2	10.7	11.4	8.6
CaO	2.0	5.4	4.1	11.6
TiO_2	0.5	0.5	0.1	0.1
MnO	0.4	0.4	0.2	0.2
Total	90.1	85.7	88.6	88.9

Number of ions*

Si	6.93	8.00	7.45	8.00	5.31	8.00	4.99	8.00
Al	1.07		0.55		2.69		3.01	
Al	2.12	10.81	2.88	10.73	1.97	12.36	1.63	12.70
Fe	3.72		3.27		5.63		5.38	
Mg	4.41		3.33		3.73		2.86	
Ca	0.42		1.20		0.97		2.78	
Ti	0.07		0.04		0.02		0.01	
Mn	0.07		0.01		0.04		0.04	
OH	16.00		16.00		16.00		16.00	

(+), Total iron given as FeO

(*), OH is taken as 16.00, and the formulae have been calculated on the basis of 28 oxygen equivalents, ignoring H_2O.

Appendix 5.8 Electron microprobe datolite analyses.

	44/12 1A	44/12 1B	44/12 1C
SiO_2	37.7	38.3	37.5
Al_2O_3	0.2	0.05	0.1
$^{+}Fe_2O_3$	0.2	0.1	0.1
MgO	n.d.	n.d.	n.d.
CaO	33.6	34.5	34.6
TiO_2	0.1	0.05	0.05
MnO	n.d.	0.05	n.d.
Total	71.8	72.9	72.3

	44/12 1D	44/12 1E	44/12 2
SiO_2	38.1	38.0	37.9
Al_2O_3	0.1	0.1	0.3
$^{+}Fe_2O_3$	0.1	n.d.	0.1
MgO	n.d.	n.d.	n.d.
CaO	34.5	33.9	34.6
TiO_2	0.05	0.05	0.1
MnO	n.d.	n.d.	n.d.
Total	72.8	72.0	72.4

(n.d.), not detected.

(+), Total iron given as Fe_2O_3

Appendix 5.9 Variance and standard deviation of electron microprobe analyses

Element	Std. dev.	Var.	No. of readings
Garnet 44/11-1(I)			
SiO_2	0.49	0.24	8
TiO_2	0.10	0.01	"
Al_2O_3	0.40	0.16	"
$^{+}Fe_2O_3$	0.26	0.07	"
MnO	0.10	0.01	"
MgO	0.14	0.02	"
CaO	0.53	0.28	"
Pyroxene 45/1			
SiO_2	0.56	0.31	8
TiO_2	0.22	0.05	"
Al_2O_3	0.33	0.11	"
^{x}FeO	0.35	0.12	"
MnO	0.10	0.01	"
MgO	0.45	0.20	"
CaO	0.44	0.19	"
Feldspar 43/3			
SiO_2	0.7	0.42	4
Al_2O_3	0.5	0.27	"
$^{+}Fe_2O_3$	0.3	0.13	"
CaO	0.3	0.13	"
Na_2O	0.6	0.35	"
K_2O	0.1	0.01	"

Element	Std. dev.	Var.	No. of readings
Idocrase 44/9A-1(A)			
SiO_2	0.45	0.20	5
TiO_2	0.22	0.05	"
Al_2O_3	0.39	0.15	"
^{x}FeO	0.25	0.06	"
MnO	0.10	0.01	"
MgO	0.27	0.07	"
CaO	0.54	0.29	"
Epidote 41/36-2			
SiO_2	0.45	0.20	5
Al_2O_3	0.41	0.17	"
$^{+}Fe_2O_3$	0.50	0.25	"
MnO	0.10	0.01	"
MgO	0.33	0.11	"
CaO	0.40	0.16	"
Prehnite 35/4			
SiO_2	0.5	0.26	4
Al_2O_3	0.4	0.19	"
$^{+}Fe_2O_3$	0.3	0.13	"
MgO	0.5	0.32	"
CaO	0.5	0.27	"
Na_2O	0.2	0.05	"

(+), total Fe as Fe_2O_3

(x), total Fe as FeO

CHAPTER VI

CONCLUSIONS AND DISCUSSION

METAMORPHIC FACIES

One of the most significant assemblages seen in the aureole is that of wollastonite + calcite, recorded in boreholes 40, 41 and 43. Winkler (1968) suggests that temperatures in the order of 600°C are required for the formation of wollastonite at 500 bars. If minimum temperatures of 500°C are accepted, as suggested, for limestone recrystallization to occur at 27 m from the contact (Chapter III), then temperatures of 600°C appear reasonable within 10 m of the contact, to which region wollastonite is restricted. Wollastonite is a mineral typical of the K feldspar-cordierite-hornfels facies, although it can occur in the highest temperature part of the hornblende-hornfels facies (Winkler, 1968). The presence of wollastonite-rich rocks, up to 25 cm thick and over 8 m from the contact, suggests that the conditions of the K feldspar-cordierite-hornfels facies may have been established, for a time, close to the contact.

Mineral assemblages typical of the hornblende-hornfels facies (Winkler, 1968) are well developed in the aureole and include grossular, diopside-hedenbergite, amphibole and idocrase. Temperatures of the order of 520 to 580°C have been suggested for this facies (Winkler, 1968), which are in agreement with those already suggested.

The minerals epidote, chlorite and albite are widespread and are typical minerals of the albite-epidote-hornfels facies, formed at temperatures of 400 to 500°C. Ideally the mineral assemblages

should form distinct zones away from the contact, representing a fall in temperature. Unfortunately such a simple zoning is not apparent and, as can be seen from Fig. 3.3, all the minerals are found over a range 0 to 10 m while only garnet and epidote extend to greater distances. All the minerals indicative of the higher temperature facies, namely idocrase, wollastonite, diopside-hedenbergite and hornblende and with the exception of grossular, are restricted to within 10 m of the contact. However, minerals indicative of the low-temperature facies, i.e. albite, chlorite and epidote, are also found in this region. The co-existence of minerals of two and possibly three facies of contact metamorphism suggests that equilibrium conditions have not been attained. Evidence of equilibrium is, however, forthcoming on a microscopic scale, namely the association of wollastonite + calcite (40/9), grossular + diopside (35/4) and chlorite + epidote (43/3). Ideally, therefore, the facies concept is difficult to relate to the present study where evidence for disequilibrium is evident, although localized equilibrium may have been attained on a microscopic scale. A point of great significance should be made at this stage. The electron microprobe results have shown the dominance of albite (>95Ab), which is compatible with the albite-epidote-hornfels facies. However, the optical determinations, in the present survey and those of Dunham (1948), are suggestive of an oligoclase composition which is compatible with the hornblende-hornfels facies (Winkler, 1968). Thus in the comparison with other work using optical determination of feldspar composition, caution must be used in the event that the feldspar composition has been erroneously identified.

The mineral assemblages examined here are those formed only

in calcareous sediments. Pure argillaceous sediments have suffered only recrystallization of the original sedimentary material, which is dominantly quartz, illite and chlorite. Chemical composition appears, therefore, to have played the major role in determining the metamorphic products seen, temperature playing a secondary role. This conclusion is similar to that reached by Van Houten (1971). His examination of the Palisade aureole showed that minor differences in composition of rocks and fluids were the controlling factors in metamorphism, temperature being of minor importance. The variation in the Whin Sill and Palisade aureoles substantiates the contention by Turner (1968) that compared with other sediments, calcareous rocks show wide variation, less regularity and obscure zoning in contact environments.

Argillaceous sediments do not show metamorphic mineral development, yet they have been subjected to the identical pressure-temperature conditions as the calcareous sediments in which a varied, new mineralogy is found. The pelitic hornfels of the Palisade aureole, Van Houten (1971) show a quite varied mineralogy including andalusite, epidote, cordierite, biotite and hornblende, with some feldspar. The only difference between the rock-types would be in the mole fraction of CO_2 in the vapour phase which would, presumably, be low in the argillaceous sediments. Quartz, illite and chlorite are present in the argillaceous lenses in limestones and in these illite has reacted to form calc-silicates, while chlorite appears to have suffered only extensive recrystallization with the formation of large radiating crystals of chlorite. It appears, therefore, that a CO_2 fraction acts as a catalyst in the breakdown of illite but not of chlorite. Turner (1968) shows

that any metamorphic reaction involves three main processes: (1) liberation of material from original crystals (i.e. breakdown of minerals), (2) diffusion of material, (3) crystal nucleation. The rate of the reaction depends upon the slowest of the above three processes. In the present study, all rock-types have undergone metamorphism under virtually identical conditions and it appears that the differences seen may be attributed to the first process, i.e. the breakdown of minerals. The lack of reaction in the argillaceous sediments is suggested to be the result of insufficient time available, at elevated temperatures, to allow the breakdown of the minerals concerned. The basic conclusion arrived at, therefore, is that the reaction rates of calc-silicate and non-calc-silicate reactions vary greatly. Yoder (1952) also invoked reaction kinetics, to explain the first appearance of garnet in regional metamorphism and not pressure-temperature conditions. This view was strongly attacked by Fyfe, Turner and Verhoogen (1958), and is probably not particularly relevant in regional metamorphism where the time-span at elevated temperatures will have been much greater than that in contact metamorphism. Turner (1968), however, states that 'reaction kinetics possibly play a significant role' where metamorphism occurs on the fringe of contact aureoles. The present work suggests that reaction rates must play a significant role, especially in the case of relatively small intrusions into areas of varying rock-type.

The limitation of the majority of the new minerals to within 10 m of the contact may, perhaps, be explained by reference to the theoretical temperature curves (Fig. 2.3). The actual values recorded are not particularly relevant in the present discussion

but rather the actual form of the curves. On intrusion of the sill, a sudden increase in temperature of the country-rocks occurs, which decreases rapidly with distance from the contact. There is in effect a 'pulse' of higher temperatures, close to the contact, before a relatively steady-state is achieved. This pulse has a sharp apex which is most pronounced between 0 and 10 m from the contact. Reaction rates increase exponentially with rising temperature (Turner, 1968) and it appears that this pulse was sufficient to promote the reactions with highest velocities, thus giving the mineral assemblages seen within 10 m of the contact. Harker (1932), in a discussion of lime-silicate rocks, hints at the effect of reaction rates in contact metamorphism by the statement 'reactions ... premised a peculiar promptitude and rapidity are only those which take place between carbonate and non-carbonate'.

The status of grossular as a mineral diagnostic of the hornblende-hornfels facies (Winkler, 1968; Turner and Verhoogen, 1960) should be viewed in a critical light in retrospect of the present study. Grossular/andradite is found up to 23 m from the contact and between 20 and 23 m it is only found in association with a relatively Fe-rich epidote. Iron-rich epidote can form at quite low temperatures and is known from burial metamorphism (Winkler, 1968). Furthermore, grossular is commonly associated with albite and in a later section of this Chapter, an idealized formula is given in which the simultaneous formation of albite and grossular is suggested. This relation is not straightforward, however, because on the basis of simple optics, the feldspars are calcic-oligoclase which would be stable with grossular in the normal sense. The role of reaction kinetics

should also be borne in mind, as explained earlier, in the elucidation of calc-silicate reactions and the status of grossular. Liou (1971) has shown the breakdown of prehnite to give zoisite + grossular + quartz, in regional metamorphism at the greenschist facies level. The presence of grossular in the greenschist facies, of which the albite-epidote-hornfels is the contact equivalent, is contributory evidence that the status of grossular/andradite should be further critically reviewed.

EXTENT OF METAMORPHISM

The work presented in this thesis is mainly devoted to the contact metamorphic effects of the Whin Sill, in Upper Teesdale. It is in this area, where the sill is at one of its thickest known horizons (73 m), that the maximum metamorphic effects are seen. In other areas the sill reaches similar thicknesses, such as at Ettersgill (73 m), Burtree Pasture mine (73 m) and the Rookhope borehole (59 m), while a recent borehole at Ninebanks, West Allendale, has proved a maximum known thickness of 80 m. However, as described in Chapter III, metamorphism is highly restricted in areas outside Upper Teesdale, and development of metamorphic minerals is seen only within 4 m of the contact, while at Cow Green, metamorphic mineral assemblages have been recorded to more than 25 m from the contact. Theoretical considerations show that assuming all heat transfer is by conduction, the maximum metamorphic effect would be expected where the sill is thickest. As shown in Fig. 2.3, the theoretical temperatures reached in the country-rocks at Ninebanks should have been some 50°C higher than in Upper Teesdale. This variation in metamorphism is, therefore, difficult to interpret on the basis of

theoretical temperature curves alone, where less than 100°C separates the country-rock temperatures at Rookhope, Cow Green and Ninebanks.

A possible contributory factor has recently been suggested by studies of coal rank on the Alston Block and adjacent areas. Ridd, Walker and Jones (1970) have suggested that the coals from the Harton borehole were raised to a high-rank prior to the intrusion of the Whin Sill, because of a high geothermal heat-flow through the Weardale granite. Further work has confirmed the results seen at Harton and a temperature of the country-rocks in the region of 100 to 150°C, is postulated for the Alston Block (Dr. B.S. Cooper, personal communication) immediately before the intrusion of the Whin Sill. The calculations made to derive the temperature curves in Fig. 2.3 were computed on the basis of country-rocks at 0°C. Any excess temperature of the country-rocks is merely added to the values determined (Jaeger, 1964). This pre-heating does not account for the disparity between Rookhope and Teesdale as both are underlain by granite at depth, and presumably were subjected to identical geothermal gradients. The pre-heating may be of importance when comparisons are made with areas lying off the Alston Block, where the geothermal gradient was lower. The Ninebanks borehole is situated off the main granite cupola (Institute of Geological Sciences, 1971) and may have been subjected to a lower geothermal gradient with resultant lower country-rock temperatures prior to the Whin Sill intrusion.

A further and possibly decisive factor in explaining the variation in metamorphism is to suggest that a source for the

Whin magma lies in Upper Teesdale. A magma source, coupled with magma flowing through the area, would significantly increase both the maximum temperatures and the period of time at which a particular temperature was prevalent, as compared to a simple case involving sudden intrusion into cold country-rocks. Previous authors (Dunham and Kaye, 1965; Hodge, 1965) have also suggested that the source for the sill may be in Upper Teesdale. This assumption was made on the basis of the sill being at its lowest stratigraphical level, attaining one of its maximum thicknesses and whose outcrops are markedly irregular on Cronkley Fell. Recently Solomon, Rafter and Dunham (1971) have also suggested a magma source, for the sill, in Upper Teesdale, with access to the surface gained via the Burtreeford disturbance. The relatively extensive metamorphism seen in Upper Teesdale is, perhaps, the most decisive evidence in suggesting a magma source in that area. This interpretation should be treated with some caution, however, because if the whole of the volume of Whin is assumed to have originated from Upper Teesdale, than a more extensive metamorphism might have been expected, associated with higher grades of metamorphism close to the contact. Mineral assemblages of the sanidinite-facies might then have been developed because the reaction rates of the relevant minerals, in carbonate rocks at the required temperatures, are very rapid (Reverdatto, 1964). It is also possible that Whin dykes have acted as feeders to parts of the complex, as suggested by Holmes and Harwood (1928). This is in part substantiated by Jones and Cooper (1970) who have shown changes in coal rank adjacent to Tertiary dykes,

which extend up to three times the width of the dykes. Whin dykes usually have much greater effects; zones of affected coal were found 2.5 km wide on either side of the Ludworth dyke (27 m), while the 34 m sill intrusion in the Throckley borehole only altered coal within 200 m of the contact.

Recently Reverdatto et al. (1970) have shown that for non-abyssal intrusions, the Ingersoll criterion (ratio of the thickness of the aureole to that of the intrusive body) cannot exceed 0.2 to 0.3. Sill-like dolerite and basic intrusions usually have Ingersoll values of 0.1. In the present case the ratio of the aureole (25 m) to the intrusion (73 m) gives a value of 0.3, which is significantly higher than that assigned to non-abyssal intrusions. This disparity may be explained by the presence of highly reactive, impure carbonate rocks and by invoking flowage of magma, thereby giving rise to anomalous conditions as compared to a simple intrusion into cold country-rocks. Similarly in the case of the Palisade intrusion (Van Houten, 1971), Ingersoll values of between 0.3 and 0.7 are found, which may be due to increased aureole temperatures because of convective circulation of the magma (Van Houten, 1969).

Reverdatto et al. (1970) classify contact metamorphism into six types, depending upon the metamorphic facies developed in the contact aureoles. Although facies cannot be strictly defined in the Whin aureole, it appears feasible to suggest that the hornblende-hornfels and albite-epidote hornfels facies conditions were most prevalent. This would place the metamorphism into Type 3 of Reverdatto et al., which is usually associated with granitic intrusions and only rarely with basic

rocks. Reverdatto et al. normally associate basic rock intrusions with metamorphism of the sanidinite and K feldspar-cordierite facies, explaining the absence of lower-temperature facies as the result of lower reaction rates in these facies. Similarly the Palisade contact metamorphism may be classified as Type 3. Thus as outlined above, the metamorphic effects seen in the contact aureoles of the Whin and Palisade intrusions, are at variance with the conclusions of Reverdatto et al. (1970). It appears that these authors are attempting to classify rigidly a system in which there are a great number of variables, such as type of igneous intrusion, depth of intrusion, thickness of intrusive body, whether convection or flowage of magma has occurred. Also in contact metamorphism, where the effects are limited to a relatively small area, the composition of the country-rock will play an important role. It seems more expedient, therefore, not to classify contact metamorphism as rigidly as Reverdatto et al. (1970) but simply as the 'facies series of contact metamorphism', as suggested by Den Tex (1971).

SODIUM METASOMATISM AND THE ORIGIN OF THE Na

Certain beds within 10 m of the Whin Sill contact show a definite increase in the amount of Na, as compared to the unmetamorphosed sediments. These changes are described in detail in Chapter IV. Electron microprobe analysis (Chapter V) has shown that most of the Na is found in albite, the majority of which occurs in red-coloured, adinole bands.

Hutchings (1898) first noted the increased Na_2O contents of certain beds close to the Whin contact. His numerous alkali determinations showed that there had been an undoubted increase,

but the effect was patchy and could not be explained. The patchy nature of the addition was confirmed in the present survey but it is shown that the increase only occurs in calcareous sediments. Sodium metasomatism and adinolization at the contacts of basic igneous rocks is a widely accepted phenomenon, the classic areas being in the Harz and north Cornwall (Harker, 1932). The igneous intrusions associated with these adinoles are usually basic rocks which have been albitized. The fluids producing the alterations have long been suggested as being derived from somewhat obscure sources in the parent magma, which then invade the country-rock causing adinolization. Turner and Verhoogen (1960) consider that the Na is more probably derived from entrapped sea-water and wet sediments, into which the intrusion was emplaced. Hutchings also attributed the increase of Na to introduction of material from the magma, a view supported by Smythe (1930).

In the case of the present study, no albitization is seen in the Whin Sill although it has suffered late-stage hydrothermal alteration along early-joints (Wager, 1929b). This alteration has resulted in a loss of SiO_2, Na_2O and CaO from the original Whin, Wager (1928) suggested that the increased Na found in the sediments, was derived from the residual portions of these hydrothermal solutions. However, pectolite is found in numerous places along joints in the Whin Sill, especially in Upper Teesdale, and it appears probable that much of the Na released during chloritization was incorporated into the pectolite, Smythe's (1930) analyses show over 7% Na_2O in a sample of pectolite from Cauldron Snout, and he suggested that

the two processes were inter-related in the statement '... pectolization and chloritization appear to be complementary'. Furthermore, extensive chemical investigations by Smythe (1930) have shown that Na_2O is not concentrated in late-stage derivatives of the Whin, suggesting that any late-stage solutions expelled from the Whin would not be Na-rich.

If the Whin Sill is not accepted, therefore, as the major source for the increased Na, seen in the metamorphosed sediments, then the only feasible assumption is to suggest that the Na was present probably as NaCl in the pore-waters of the sediments, prior to the intrusion. It is known that pore-fluids are not composed of pure water but are solutions of salt in which NaCl is dominant (M.G. Waljaschko, quoted by Althaus and Johannes, 1969). Further contributory evidence for the presence of NaCl pore solutions comes from the record of salt-pseudomorphs from basal Carboniferous beds west of the Pennines (personal communication, Dr. G.A.L. Johnson). Support for this contention is also found in relation to recent hypotheses as to the origin of the mineralizing solutions of the northern Pennines. The Whin Sill has been dated as late Coal Measures (295±6 My) by Fitch and Miller (1967), and was probably intruded only shortly before mineralization commenced. Dunham et al. (1968) have shown from their own work and that of Dr. S. Moorbath, that the earliest mineralization occurred during the period 284±40 My. As mentioned earlier, studies of coal metamorphism are indicative of a 'background' temperature of 150°C for the country rocks of the Alston Block, prior to intrusion of the Whin Sill. This is further evidence that mineralization was soon to commence. Recently,

Dunham (1970) has reviewed the increasingly accepted hypothesis that mineralizing fluids may be derived from formation waters (i.e. water that is present in the rocks prior to any drilling), which have been raised to a high temperature. He has shown that these waters are hypersaline brines which in several recorded cases have salinities well in excess of 100,000 ppm. Solomon, Rafter and Dunham (1971) have invoked such a mechanism for the development of the northern Pennine mineralization. They also suggest that the intrusion of the Whin Sill, coupled with a magma source in Upper Teesdale, gave rise to a convective circulation cell for these formation waters. Thus from the above discussion on the relationship between the intrusion of the sill, the commencement of the mineralization and the origin of the mineralizing solutions, it appears most feasible that the pore-waters of the sediments, at the time of the Whin Sill intrusion, were hypersaline in character. Sawkins (1966) has shown, from fluid inclusion studies in the northern Pennines, that the trapped solutions had between 20 to 23% equivalent weight NaCl, while up to 33% has been recorded from fluorite in Derbyshire (Dunham, 1970).

Recently Althaus and Johannes (1969) have conducted pertinent experiments in relation to reactions between NaCl aqueous solutions and clay minerals. One of their most significant reactions recorded, with regard to the present study, is as follows:

Illite + NaCl + quartz $\longrightarrow$ albite + 2M-muscovite + biotite + haematite + salts + HCl + H_2O.

This actual reaction has not been observed in the present study,

although the production of albite and haematite, from illite, has occurred as described in Chapters III and V. Newly formed muscovite and biotite is not observed. Grossular is, however, always intimately associated with the feldspar areas (Plates 3.17 and 5.2). In a carbonate-rich environment, such as that under study, with a high concentration of Ca ions, it appears that reaction will occur between these and the excess Si and Al, from the illite, to form grossular, possibly on the lines of the idealized equation given below:

2 illite + 1 quartz + 2 NaOH $\longrightarrow$ 2 albite + 3 grossular

$2\ K\ Al_4Fe^{3+}Si_7O_{20}(OH_4) + SiO_2 + 2\ NaOH \longrightarrow 2\ NaAlSi_3O_8$

$+ 3\ Ca_3Al_2Si_3O_{12}$ + fluid

In the above reaction, NaOH is suggested instead of NaCl as Turner and Verhoogen (1960) show that NaCl in aqueous solutions at high temperatures dissociates to form NaOH + HCl. The illite composition is shown with Fe^{3+} substituting for Al as is normal, up to a certain extent (Deer, Howie and Zussman, 1962). The Fe is partly incorporated into the grossular to form a certain percentage of the andradite molecule while the remainder probably enters the fluid phase and forms haematite, giving rise to the red-colouration of the feldspar areas. The K ions are also envisaged as entering the fluid phase, as was recorded by Althaus and Johannes (1969), being concentrated and then forming potassic feldspar along fractures in the feldspar areas as described in Chapter V. In order to estimate whether sufficient Na is available for the production of albite on the above basis, a simple calculation can be made as follows:

Weight percent of illite used in the generation of albite.

Illite $KAl_4Fe^{3+}Si_7O_{20}(OH)_4$	Mol.wt.%	Albite $NaAlSi_3O_8$	Mol.wt.%
$\frac{1}{2}K_2O$	47.1	$\frac{1}{2}Al_2O_3$	51.0
$2Al_2O_3$	203.9	$3SiO_2$	180.3
$\frac{1}{2}Fe_2O_3$	79.9	$\frac{1}{2}O$	8
$7SiO_2$	420.6		
$2H_2O$	36.0		239.3
	787.5		

% illite consumed in formation of albite = 30.4.

Examining 16.4 cm^3 of argillaceous material at a density of 38.1 gm/cm^3 (Kennard et al. 1967) and assuming a 50% illite content in the sample.

Weight of albite produced = 5.8 gm

Weight percent Na in albite (Ab_{98}) = 8.2

Weight of Na in 5.8 gm of albite = 0.45 gm

Assuming the material has 12.5% voids (Kennard et al. 1967), then in 16.4 cm^3, volume of void = 2.05 cc.

Using salinity values given by Sawkins (1966) and Dunham (1971), of 20 to 23 weight percent and 33 weight percent NaCl, respectively.

A 20% solution has 7.9 gm Na, 2.05 cc will have 0.2 gm

A 23% solution has 9.0 gm Na, 2.05 cc will have 0.24 gm

A 33% solution has 13.0 gm Na, 2.05 cc will have 0.4 gm

Allowance should also be made for Na already present as a constituent of the argillaceous material, which is usually in the region of 0.6% Na_2O. In the present case, if all this is used in formation of albite then approximately a further 0.1% Na is also available. Thus based on the above examples, between 0.3 and 0.5% Na is available, in a closed system, for the production of albite.

Earlier it was estimated that some 0.45 gm of Na would be required for the formation of albite, from illite, based on the proposed idealized reaction. Using the values given by Sawkins (1966) for the northern Pennines, insufficient Na is available, and this may explain situations such as illustrated in Plate 3.11. Here sample 43/6, 1.5 m from the contact, shows a central area of recrystallized illite surrounded by fine-grained feldspar. This illite, even though close to the contact, has not reacted completely to form feldspar, possibly due to a lack of Na. This feature is possibly repeated in the very fine-grained adinole areas, where it is not readily possible to resolve between quartz, feldspar and illite. The above system is envisaged as isochemical but, no doubt, once some Na is consumed in the reaction and the pore-water becomes relatively depleted, a concentration gradient will be established. This will allow replenishment from areas where Na is not being consumed, such as areas of chloritic or quartzose material.

SKARN FORMATION

Skarn deposits are usually developed at igneous contacts with marbles and consist dominantly of andradite, hornblende, diopside, quartz, wollastonite and haematite. The classic explanation for these deposits has been to invoke reactions between the carbonate and solutions, derived from the intrusion, containing Fe, Mg and Si, which invade the country-rock. This hypothesis has been suggested even when the intruded magma has been relatively depleted in one or more of the elements concentrated in the proposed invading solutions; this particular anomaly has been stressed by Harker (1932). Such skarn deposits

are of great interest because of the common occurrence of iron ores in association with them, a situation recently reviewed by Bartholomé (1970).

The mineral assemblages found in the Whin Sill aureole are very similar to those found in skarn deposits. Knill (1966) attributed the calc-silicate lenses, found in the Melmerby Scar Limestone, to a skarn development. This hypothesis is shown to be wrong, by the present work, the calc-silicate lenses being merely the product of metamorphism of originally argillaceous bands in the limestone, as described in Chapter III. The compositions of the phases developed have been shown to be largely controlled by the breakdown of illite. The present work is, therefore, of importance in relation to skarns, especially those found adjacent to intrusions which are not enriched in the elements dominant in the skarn.

Impure limestones, when metamorphosed, can give rise to a skarn-like mineralogy, which is developed as a consequence of the mineralogy of the original impurities and of the grade of metamorphism. In the present study, the impurities in the limestones have been dominantly illite, quartz and chlorite, of which only the illite and quartz have reacted, at the conditions prevalent in the aureole. This in turn has given rise to the dominance of aluminosilicate phases in the aureole. If chlorite had also broken down, then a more varied mineral assemblage would have developed, due to the release of the Mg and Fe^{2+} components. Where the original nature of the rocks has been completely destroyed by the metamorphism, it is often quite difficult to resolve whether metasomatic introduction of material,

from an igneous body, into a pure limestone, or isochemical metamorphism has occurred. This uncertainty was apparent to Bartholomé (1970) who stated that '... few decisive conclusions can be drawn as far as ferric metasomatism ... is concerned'. He is, however, of the opinion that although the metasomatic elements may have been derived from the country-rock, they have suffered remobilization by ascent through the intrusive body. This is not necessarily the case in all examples, as the skarn-like calc-silicate lenses, of the Whin Sill aureole, have formed in situ without necessity for recourse to metasomatic introduction from the Whin Sill.

The presence of haematite in the calc-silicate lenses is also of interest in relation to the genesis of iron ores, which are often found in skarn deposits. The haematite found in the present study, associated with the feldspar areas, has been suggested as derived from the Fe^{3+} released by the breakdown of illite. Thus if illite forms a substantial percentage of the impurities in contact-metamorphosed, impure limestones, there is potentially a high proportion of Fe^{3+} available to be concentrated so as to give rise to haematite. The experimental work of Althaus and Johannes (1969), on the reaction of clay minerals with NaCl aqueous solutions, showed that haematite is formed from illite, while relatively large concentrations of K and Fe were present in the fluid phase. The authors suggested that if this fluid phase left the rock system in which it was formed, then it could give rise to metasomatic deposits. Siderite or ankerite deposits would be formed, it was suggested, if these fluids came into contact with carbonate rocks. The present environment is

carbonate-rich but haematite has formed and not an Fe-carbonate, suggesting that conditions were in the haematite stability field. Garrels and Christ (1965) have shown that at one atmosphere and a temperature of 25°C, the stability field of haematite, with respect to Eh, pH and partial pressure of CO_2, is quite large. They showed that a partial pressure of log Pco_2^{-2} is required before the stability field of siderite is well established. The stability field of magnetite is quite small in the above system, the formation of haematite or magnetite being dependant upon the Eh of the system although this is highly dependant upon the pH of the solutions. The pH of the solutions involved in the pertinent reactions is difficult to estimate, as the dissociation constants of acids and water vary greatly with temperature such that the pH of solutions at high temperatures will be quite different from those of the same solutions at room temperature. It is apparent, though, that the conditions existing still allowed the formation of haematite.

BEDROCK GEOLOGY AND THE SOIL-FLORA ASSOCIATION

The Upper Teesdale region, especially the Cow Green area, has long been renowned in biological circles for its unique arctic-alpine flora. The flora association consists of a number of species of flowering plants which are rare in the British Isles and some which are unknown elsewhere in the country. The area has been the subject of a classic article by Pigott (1956), who noted the close association between the rare flora, outcrops of and soils developed on the metamorphosed Melmerby Scar Limestone. The metamorphism of this limestone has resulted in the formation of a saccharoidal marble (Chapter III), which is known

to biologists as 'sugar limestone'. The association noted by Pigott (1956) has recently been stressed by Turner (1970) and Bradshaw (1970), who showed that the bulk of the great floral rarities are found in communities confined to, or associated with the marble.

One of the aims of the present study, as outlined in Chapter I, was to examine the unique development of saccharoidal marble and its geochemistry, in this area of Upper Teesdale. This was to establish what influence, if any, geological factors have had on the sustenance of the arctic-alpine flora up to the present day.

It is highly doubtful if the limestone geochemistry will have any influence on the flora association, as little variation has been found. The limestones of the region are quite pure and contain only minor amounts of terrigenous and carbonaceous impurities. The trace element geochemistry, as described in Chapter IV is relatively uniform. Only Cu, Ba and Sr were found to be consistently above the detection limit of analysis and of these, Cu and Ba occurred only in relatively low concentrations. The only areas where possible influence by the bedrock geochemistry on the flora might occur, is in the vicinity of mineral veins, where a more varied geochemistry is present; these areas have not been studied in the present survey.

The physical aspects of the bedrock geology have, however, played a major role in sustaining the rare flora association. The intrusion of the Whin Sill into clear-water limestones produced saccharoidal marble in the Upper Teesdale area. This

marble and the associated rendzinas have produced a series of precarious habitat which have proved suitable for the survival of the arctic-alpine flora. This role has been described in greater detail in a recent joint article by the writer (Johnson, Robinson and Hornung, 1971).

A copy of the paper (Johnson et al., 1971) is enclosed with this thesis.

REFERENCES

Althaus, E. & Johannes, W. 1969 Experimental metamorphism of NaCl-bearing aqueous solutions by reaction with silicates. Am. J. Sci. 267, p.87-98.

Atherton, M.P., & Edmunds, W.M. 1966 An electron microprobe study of some zoned garnets from metamorphic rocks. Earth Planet. Sci. Letters 1, p.185-193.

Barth, T.F.W. 1969 Feldspars. New York-London-Sydney-Toronto: Wiley-Interscience.

Bartholomé, P. 1970 Minerais et skarns dans les auréoles de métamorphisme. Mineral. Deposita 5, p.345-353.

Bott, M.H.P. & Johnson, G.A.L. 1970 Structure. In: Geology of Durham County. Trans. nat. Hist. Soc. Northumb. 41, p.10-20.

Bradshaw, M. 1970 The Teesdale flora. In: Durham County and City with Teesside. p.141-152. (Brit. Assoc. Durham 1970)

Brown, G.M., Emeleus, C.H., Holland, J.G. & Phillips, R. 1970 Mineralogical, chemical and petrological features of Apollo 11 rocks and their relationship to igneous processes. Proc. Apollo 11 Lunar Science Conference. Geochim. Cosmochim. Acta 1, p.195-219.

Clark, S.P. (Editor) 1966 Handbook of Physical Constants. Geol. Soc. Amer. Mem. 97.

Clough, C.T. 1880 The Whin Sill of Teesdale as an assimilator of the surrounding beds. Geol. Mag. 7, p.433-447.

Deer, W.A., Howie, R.A. & Zussman, J. 1962 Rock-forming minerals Volumes 1 to 5. London: Longmans.

Den Tex, E. 1971 The facies groups and facies series of metamorphism, and their relation to physical conditions in the earth's crust. Lithos 4, p.23-41.

Dunham, A.C.	1970	Whin Sill and dykes. In: Geology of Durham County. Trans. nat. Hist. Soc. Morthumb. 41, p.92-100.
--- & Kaye, M.J.	1965	The Petrology of the Little Whin Sill, County Durham. Proc. Yorks. geol. Soc. 35, p.229-276.
Dunham, K.C.	1948	Geology of the northern Pennine orefield. 1, Tyrne to Stainmore. Mem. geol. Surv. G.B.
---	1970	Mineralization by deep formation waters: a review. Trans. Instn Min. Metall. (Section B: Appl. earth sci.) 79, p.127-136.
---, Dunham, A.C., Hodge, B.L. & Johnson, G.A.L.	1965	Granite beneath Viséan sediments with mineralization at Rookhope, northern Pennines. Q. Jl geol. Soc. Lond. 121, P.383-417.
---, Fitch, F.J., Ineson, P.R., Miller, J.A. & Mitchell, J.G.	1968	The geochronological significance of argon-40/argon-39 age determinations on white Whin from the northern Pennine orefield. Proc. Roy. Soc. A. 307, p.251-266.
Edwards, A.B. & Baker, G.	1944	Contact phenomena in the Morang Hills, Victoria. Proc. R. Soc. Vict. 56. p.19-26.
Fitch, F.J. & Miller, J.A.	1967	The age of the Whin Sill. J. Geol. 5, p.233-250.
Frost, D.V.	1969	The Lower Limestone Group (Viséan) of the Otterburn district, Northumberland. Proc. Yorks. geol. Soc. 37, p.277-309.
Fyfe, W.S., Turner, F.J. & Verhoogen, J.	1958	Metamorphic reactions and metamorphic facies. Geol. Soc. Am. Mem. 73.
Garrels, R.M & Ghrist, C.L.	1965	Solutions, minerals, and equilibria. New York-Evanston-London: Harper and Row. Tokyo: John Weatherhill.

Ghose, N.C. 1965 Behaviour of trace elements during thermal metamorphism and or granitization of the metasediments and basic igneous rocks. Geol. Rdsch. 55, p.608-616.

Goldschmidt, V.M. 1954 Geochemistry. Oxford: Clarendon.

Griggs, D. T., Patterson, M.S., Heard, H.C. & Turner, F.J. 1958 Annealing recrystallization in calcite crystals and aggregates. In: Rock deformation. Geol. Soc. Amer. Mem. 79, p.21-37.

Grigorev, D.P. 1965 Ontogeny of Minerals. Israel Program for Scientific Translations, Jerusalem.

Harbord, N.H. 1962 Mineralogy of Yoredale Series rocks in upper Teesdale with special reference to clay minerals. Unpublished Ph.D. thesis, University of Durham.

Harker, A. 1932 Metamorphism. London: Methuen.

--- & Tuttle, O.F. 1956 Experimental data on the P_{CO_2}-T curve for the reaction: calcite+quartz $\rightleftharpoons$ wollstonite+ carbondioxide. Am. J. Sci. 254, p.239-256.

Harrison, R.K. 1968 Petrology of the Little and Great Whin Sills in the Woodland borehole, Co. Durham. Bull. geol. Surv. G.B. 28, p.38-54.

Hasimoto, M. 1964 The chemistry and optics of prehnite. J. Geol. Soc. Jap. 70, p.180-183.

Hodge, B.L. 1965 In discussion to Durham & Kaye, 1965.

Holland, J.G. & Brindle, D.W. 1966 A self-consistent mass absorption correction for silicate analysis by X-ray fluorescence. Spectrochim. Acta 22, p.2083-2093.

Hollister, L.S. 1969 Contact Metamorphism in the Kwoiek area of British Columbia: an end member of the metamorphic process. Bull. geol. Soc. Am. 80, p.2465-2494.

Holmes, A. & Harwood, H.F. 1928 The age and composition of the Whin Sill and the related dykes of the north of England. Mineralog. Mag. 21, p.493-542.

Hutchings, W.M. 1895 An interesting contact-rock with notes on contact-metamorphism. Geol. Mag. 2, p.121-124.

--- 1898 The contact rocks of the Great Whin Sill. Geol. Mag. 5, p.69-82 and p.123-135.

Hutton, W. 1832 On the stratiform basalt associated with the Carboniferous formation of the north of England. Q. Jl geol. Soc. Lond. 2, p.368-405.

Ineson, P.R. 1969 Trace-element aureoles in limestone wallrocks adjacent to lead-zinc-barite-fluorite mineralization in the northern Pennine and Derbyshire ore fields. Trans. Instn Min. Metall. (Section B: Appl. earth sci.) 78, p.29-40.

Institute of Geological Sciences 1970 Annual Report, p.33.

Jaeger, J.C. 1957 The temperature in the neighborhood of a cooling intrusive sheet. Am. J. Sci. 255, p.306-318.

--- 1959 Temperatures outside a cooling intrusive sheet. Am. J. Sci. 257, p.44-54.

--- 1964 Thermal effects of intrusions. Geophys. Rev. 2, p.443-466.

Johnson, G.A.L. 1970a Introduction. In: Geology of Durham County. Trans. nat. Hist. Soc. Northumb. 41, p.5-9.

Johnson, G.A.L.	1970b	Carboniferous. In: Geology of Durham County. Trans. nat. Hist. Soc. Northumb. 41, p.23-42.
--- & Dunham, K.C.	1963	The geology of Moor House. Nature Conservancy Monograph No. 2. London: H.M.S.O.
---, Robinson, D. & Hornung, M.	1971	Unique bedrock and soils associated with the Teesdale flora. Nature Lond. 232, p.453-456.
Jones, J.M. & Cooper, B.S.	1970	Coal. In: Geology of Durham County. Trans. nat. Hist. Soc. Northumb. 41, p.43-65.
Joyce, A.S.	1970	Chemical variation in a pelitic hornfels. Chem. Geol. 6, p.51-58.
Kennard, M.F., Knill, J.L. & Vaughan, P.R.	1967	The geotechnical properties and behaviour of Carboniferous shale at the Balderhead dam. Q. Jl Engin. Geol. 1, p.3-24.
---, ---	1969	Reservoirs on limestone, with particular reference to the Cow Green scheme. J. Instn Wat. Engrs. 23, p.87-136.
Knill, J.L.	1966	The geology of the proposed Cow Green Reservoir. Tees Valley and Cleveland Water Board. Unpublished.
Kubler, B.	1966	La cristallinité de illite et les zones tout a fait supérieures du métamorphisme. In: Étages tectoniques. Colloque de Neuchâtel. p.105-122.
Kulp, J.L., Turekian, K. & Boyd, D.W.	1952	Strontium content of limestones and fossils. Bull. geol. Soc. Am. 63, p.701-716.
Larsen, E.S.	1945	Time required for the crystallization of the great batholith of southern and lower California. Am. J. Sci. 243, p.399-416.

Leake, B.E. 1967 Zoned garnets from the Galway granite and its aplites. Earth Planet. Sci. Letters 3, p.311-316.

Liou, J.G. 1971 Synthesis and stability relations of prehnite, $Ca_2Al_2Si_3O_{10}(OH)_2$. Am. Miner. 56, p.507-531.

Lovering, T.S. 1955 Temperatures in and near intrusions. Econ. Geol. 50, p.249-281.

Maxwell, D.T. & Hower, J. 1967 High-grade diagenesis and low-grade metamorphism of illite in the precambrian belt series. Am. Miner. 52, p.843-857.

Phemister, J. & MacGregor, A.G. 1942 Note on datolite and other minerals in a contact-altered limestone at Chapel quarry, near Kirkcaldy, Fife. Mineralog. Mag. 26, p.275-282.

Phillips, J. 1836 Illustrations of the geology of Yorkshire. Pt.II, The Mountain Limestone District. London.

Pigott, C.D. 1956 The vegetation of Upper Teesdale in the north Pennines. J. Ecol. 44, p.545-586.

Randall, B.A.O. 1959 Intrusive phenomena of the Whin Sill, East of the R. North Tyne. Geol. Mag. 96, p.385-392.

Reeves, M.J. 1971 Geochemistry and mineralogy of British Carboniferous seatearths from northern coalfields. Unpublished Ph.D. Thesis. University of Durham.

--- & Saadi, T.A. 1971 Factors controlling the deposition of some phosphate bearing strata from Jordan. Econ. Geol. 66, p.451-465.

Reverdatto, V.V. 1964 Paragenetic analysis of carbonate rocks of the spurrite-merwinite facies. Geochem. Internat. 5, p.1038-1053.

Reverdatto, V.V., Sharapov, V.N. & Melamed, V.G.	1970	The controls and selected peculiarities of the origin of contact metamorphic zonation. Contr. Mineral. Petrol. 29, p.310-337.
Rickwood, P.C.	1968	On recasting analyses of garnet into end-member molecules. Contr. Mineral. Petrol. 18, p.175-198.
Ridd, M.F., Walker, D.B. & Jones, J.M.	1970	A deep borehole at Harton on the margin of the Northumbrian trough. Proc. Yorks. geol. Soc. 38, p.75-103.
Robinson, D.	1970	Metamorphic rocks. In: Geology of Durham County. Trans. nat. Hist. Soc. Northumb. 41, p.119-123.
---	1971	The inhibiting effect of organic carbon on contact metamorphic recrystallization of limestones. Contr. Mineral. Petrol. 32, p.245-250.
Rose, H.E.	1968	The determination of the grain-size distribution of a spherical granular material embedded in a matrix. Sedimentology 10, p.293-309.
Rucklidge, J. & Gasparrini, E.L.	1969	Empadr VII. Specifications of a computer program for processing electron micro-probe analytical data. Dept. of Geology, University of Toronto.
Sawkins, F.J.	1966	Ore genesis in the north Pennine orefield, in the light of fluid inclusion studies. Econ. Geol. 61, p.385-401.
Sedgwick, A.	1827	On the association of trap rocks with the Mountain Limestone formation in High Teesdale. Trans. Camb. phil. Soc. 2, p.140-196.

Smythe, J.A. 1930 A chemical study of the Whin Sill. Trans. nat. Hist. Soc. Northumb. 7, p.16-150.

--- 1950 Metamorphism of sedimentary rocks by the Great Whin Sill. Proc. Univ. Durham phil. Soc. 10, p.541-546.

Solomon, M., Rafter, T.A. & Dunham, K.C. 1971 Sulphur and oxygen isotope studies in the northern Pennines in relation to ore genesis. Trans. Instn Min. Metall. (Section B: Appl. earth sci.) 80, p.259-275.

Sopwith, T. 1833 An account of the mining district of Alston Moor, Weardale and Teesdale in Cumberland and Durham. Alnwick.

Spry, A. 1969 Metamorphic Textures. Oxford-New York-London-Paris: Pergamon Press.

Surdam, R.C. 1969 Electron microprobe study of prehnite and pumpellyite from the Karmutsen Group, Vancouver Island. British Columbia. Am. Miner. 54, p.256-266.

Sweatman, T.R. & Long, J.V.P. 1969 Quantitative Electron -probe Microanalysis of Rock-forming Minerals. J. Petrology 10, p.332-379.

Teall, J.J.H. 1884a Petrological notes on some north of England dykes. Q. Jl. geol. Soc. Lond. 40, p.209-247.

--- 1884b On the chemical and microscopical characters of the Whin Sill. Q. Jl. geol. Soc. Lond. 40, p.640-657.

Tomkeieff, S.I. 1929 A contribution to the petrology of the Whin Sill. Mineralog. Mag. 22, p.100-120.

Topley, W. & Lebour, G.A. 1877 On the intrusive character of the Whin Sill of Northumberland. Q. Jl. geol. Soc. Lond. 33, p.406-421.

Trotter, F.M. & Hollingworth, S.E. 1932 The geology of the Brampton district. Mem. Geol. Surv. G.B. London: H.M.S.O.

Turner, F.J. 1968 Metamorphic Petrology. New York-San Francisco-St.Louis-London-Toronto-Sydney: McGraw-Hill.

--- & Verhoogen, J. 1960 Igneous and Metamorphic Petrology. New York-Toronto-London: McGraw-Hill.

Turner, J. 1970 Vegetation. In: Durham County and City with Teesside. p.123-133. (Brit. Assoc. Durham 1970)

Van Houten, F.B. 1969 Late Triassic Newark Group, north central New Jersey and adjacent Pennsylvania and New York. In: Geology of selected areas in New Jersey and eastern Pennyslvania. New Brunswick. Rutgers. Un. Press.

--- 1971 Contact metamorphic mineral assemblages, Late Triassic Newark Group, New Jersey, Contr. Mineral. Petrol. 30, p.1-14.

Wager, L.R. 1928 A metamorphosed nodular shale previously described as a 'spotted' metamorphic rock. Geol. Mag. 65, p.88-91.

--- 1929a Metasomatism in the Whin Sill of the north of England. Part 1. Metasomatism by lead vein solutions. Geol. Mag. 66, p.97-110.

--- 1929b Metasomatism in the Whin Sill of the north of England. Part 2. Hydrothermal alteration by juvenile solutions. Geol. Mag. 66, p.221-238.

Winkler, H.G.F. 1967 Petrogenesis of metamorphic rocks. 2nd ed. Berlin-Heidelberg-New York: Springer-Verlag.

Winkler, H.G.F.	1970	Abolition of metamorphic facies, introduction of the four divisions of metamorphic stage, and of a classification based on isograds in common rocks. Neues Jb. Miner. Mh. 5, p.189-248.
Wodzicki, A.	1971	Migration of trace elements during contact metamorphism in the Santa Rosa Range, Nevada, and its bearing on the origin of ore deposits associated with granitic intrusions. Mineral. Deposita 6, p.49-64.
Wood, N.	1831	On the geology of part of Northumberland and Cumberland. Trans. nat. Hist. Soc. Northumb. 1, p.302-334.
Wyllie, P.J. & Tuttle, O.F.	1960	The system $CaO-CO_2-H_2O$ and the origin of carbonatites. J. Petrology 1, p.1-46.
Yoder, H.S.	1952	The $MgO-Al_2O_3-SiO_2-H_2O$ system and the related metamorphic facies. Am. J. Sci. Bowen Volume p.569-627.
--- & Eugster, H.P.	1955	Synthetic and natural muscovites. Geochim. cosmochim. Acta 8, p.225-280.
--- & Tilley, C.E.	1962	Origin of basalt magmas: an experimental study of natural and synthetic rock systems. J. Petrology 3, p.342-532.

Teesdale supported by the Natural Environment Research Council.

Received July 12, 1971.

1 Pigott, C. D., *J. Ecol.*, 44, 545 (1956).
2 Bellamy, D. J., Bridgewater, P., Marshall, C., and Tickle, W., *Nature*, 222, 238 (1969).
3 Turner, J., in *Durham County and City with Teesside*, 123 (Brit. Assoc., Durham, 1970).
4 Bradshaw, M., in *Durham County and City with Teesside*, 141 (Brit. Assoc., Durham, 1970).
5 Johnson, G. A. L., *Trans. Nat. Hist. Soc. Northumb.*, 41, 5 (1970).
6 Dunham, K. C., *The Geology of the Northern Pennine Orefield*, 1 (Mem. Geol. Surv. Gt. Brit., 1948).
7 Dunham, A. C., *Trans. Nat. Hist. Soc. Northumb.*, 41, 92 (1970).
8 Dunham, K. C., Firch, F. J., Ineson, P. R., Miller, J. A., and Mitchell, J. G., *Proc. Roy. Soc.*, A, 307, 215 (1968).
9 Robinson, D., *Trans. Nat. Hist. Soc. Northumb.*, 41, 119 (1970).
10 Robinson, D., *Cont. Min. Pet.* (in the press, 1971).
11 Welch, D., and Rawes, M., *Trans. Nat. Hist. Soc. Northumb.*, n.s., 17, 57 (1969).
12 Johnson, G. A. L., and Dunham, K. C., *Geology of Moor House* (Nature Conservancy Monograph No. 2), 158 (1963).

Transitive Inferences and Memory in Young Children

P. E. BRYANT
Department of Experimental Psychology, University of Oxford

T. TRABASSO
Department of Psychology, Princeton University

Contrary to the conclusions of Piaget, young children can make transitive inferences if precautions are taken to prevent deficits of memory from being confused with inferential deficits.

For some time, it has been believed that young children are unable to form transitive inferences about quantity until they pass the stage of logical preoperations at about 7 yr old[1,2]. This argument has been very widely accepted[3,4]. Piaget and his colleagues propose that the young child cannot infer, for example, that A > C from the information that A > B and B > C. They assert that the child is unable to coordinate the first two, separate items of information in order to reach the correct inferential conclusion about A and C. If true, this claim has important educational implications, for a child who cannot combine this information must also be unable to understand the most elementary principles of measurement.

We report two experiments which show that the claim is unjustified. The experiments demonstrate that 4 yr old children can make transitive inferences about quantity, provided that they can remember the items of information which they are asked to combine.

One must ensure that the child has retained the comparisons which he has to combine, if one is to infer whether or not he can make transitive inferences. Otherwise, an error might simply be due to a failure in memory and have nothing to do with inferential ability. Yet experiments in which it is reported that children cannot make inferential judgments lack this elementary precaution. One can control for forgetting by taking two precautions. First, teach the child the initial comparisons (A > B and B > C) very thoroughly. Second, test for memory of these comparisons at the same time as one asks the inferential question about A and C. The first precaution ensures retention of the initial comparisons and the second checks for this retention during the inferential problem.

We found it necessary to introduce another control in our experiments. This was against the transfer of "absolute" responses. The general procedure in prior experiments has been to use three quantities (A, B and C). If only three are used, the correct response to the two extreme quantities must be the same in both the inferential problem and in the initial direct comparisons. The quantity A is the "larger" when compared with B, and C is the "smaller" when compared with B, in the initial direct comparisons. Yet "larger" is the correct response to A and "smaller" is the correct response to C in the inferential AC comparisons. Thus a child who produces the correct response when asked the AC question may do so by parroting a verbal label picked up during the initial comparisons, and not, as has always been assumed, by making a genuine inference through the combination of two separate comparisons.

The correct control is to introduce more stimuli and thus more direct comparisons. If there are as many as five stimuli (in descending order of size they are A, B, C, D and E) four initial direct comparisons are possible, A > B, B > C, C > D, and D > E. Note that B, C, and D all feature in two of these comparisons and that each of them is the larger in one comparison and the smaller in the other. This means that no one absolute response can be transferred to any one of these three quantities, and it therefore follows that the crucial transitive comparison will be between B and D. This indirect comparison cannot be solved by transfer of absolute responses, since B and D were both larger and smaller in the initial direct comparisons.

Our experiments thus involved first a thorough training period with four direct comparisons, followed by a test period in which the children were tested for their ability to make transitive judgments *and* to remember the initial comparisons. In the first experiment, sixty children in three age groups of twenty each participated. The mean ages of the groups were

the surface at the bedrock drift or mineral soil interface. At the surface a hardened crust tends to form on the marble and erosion may be relatively slow except near to the Whin contact where the coarsely crystalline rock is often readily attacked by subaerial weathering processes. At the subsurface junction of bedrock marble and overlying drift or soil, percolating ground water causes solution weathering leading to loss of cohesion between calcite grains in the marble. Sections through the drift-marble interface show rotten saccharoidal marble or calcite sand deposits 0.25 to 3.0 m thick. The thickness of the layer and the rate of weathering of the marble are dependent on the amount of ground-water movement. Subsurface erosion sufficient to produce hollows in the land surface has taken place as the rotted marble is removed in solution.

From these observations it follows that the unconsolidated calcite sand, known to a succession of biologists as "sugar limestone", is chiefly a subsurface weathering product of saccharoidal marble formed beneath a cover of drift and soil. Its presence at the surface today is caused by contemporary erosion of the soil and drift cover. Calcite sand is a most unstable surface deposit which tends to erode by rain and wind action at any place where the protective drift, soil or vegetation cover is removed. A cycle consisting of subsurface weathering below thin soil followed by erosion of unstable calcite sand may have taken place on crystalline marble outcrops on Widdybank and Cronkley fells during much of the post-glacial time. This would provide a succession of open habitats suitable for the survival of the arctic–alpine flora. Because of its instability and secondary origin it is unlikely that calcite sand deposits were present on these outcrops during the period of initial plant colonization in late-glacial times.

Soil Development

The presence or absence and thickness of drift cover have been important factors in determining the soils developed over crystalline marble on Widdybank and Cronkley fells. Under continuous drift, more than 60 cm thick, the limestone acts chiefly as a platform on which soil formation takes place in the upper layers of the drift cover. The limestone exerts some influence on soil formation by maintaining free drainage in the subsoil and lower drift, even though the latter is often of heavy texture. Peaty gleyed podzols or deep peat are the resultant soils. Where the superficial drift cover is thinner (30 to 60 cm) the limestone maintains free drainage, but also exerts an influence on the chemistry of the soil so that brown earths or brown calcareous soils result. Where there is only a thin layer of superficial material, less than 30 cm thick, the bedrock marble dominates soil formation and rendzinas are the resulting soils.

The rendzinas form part of a complex in which three subtypes, for the purpose of this paper called α, β and γ, occur in association with small areas of brown earth soils. The brown earths are found over patches of deeper superficial material. The rendzinas are characterized by alkaline reaction and excessive drainage such that even short dry periods cause a water deficit[11]. Rendzina α is the simplest and forms *in situ* from rotten crystalline marble. The profile is divisible into a dark grey, humic but sandy surface horizon (A or A_h) which has a dense mat of fibrous roots, and an underlying C horizon of white or cream coloured calcite sand. Formation of α rendzinas requires the prior removal of any superficial drift with exposure of the underlying marble to subaerial erosion and soil forming processes.

Rendzina β is the most widespread in the rendzina complexes. It develops over crystalline marble bedrock in regions where drift parent materials play an important part in profile formation. A typical profile is composed of a thin horizon (up to 10 cm) of dark brown or reddish brown clay or silt loam over calcite sand resting on relatively unaltered marble. The colour and texture of the surface layer vary considerably. Colour variation reflects a number of factors but bright coloured reddish variants have a high content of total iron present as hydroxides. The bright red soils overlie marble cut by fine siderite veins which oxidize to hydroxides of iron including goethite. The soils inherit their coluration and high iron content from the vein material, fragments of which are normally present in the soils. Textural variation depends on changes in the proportions of sand and clay with the silt fraction remaining fairly constant. The soils also contain small stones which have been derived from the surrounding drift. The loam is clearly of mixed origin containing contributions from the drift and the underlying marble; mixing probably took place during pedogenesis.

Rendzina subtype γ is a closely related group of soils which have aeolian erosion and depositional characteristics as a uniting feature. They form a small part of the total rendzina complexes and show much variation in detailed profile morphology. These rendzinas are particularly well developed in the Thistle Green area, Cronkley fell, where they are associated with and abut against bare areas of calcite sand. Profiles of rendzina γ almost always contain a number of buried surface horizons and clear evidence of surface accretion. Observation on a windy day immediately demonstrates that aeolian movement and deposition are active and sufficient to produce profile accretion. These soils were formed under conditions of periodic erosion, aeolian transport and deposition of calcite sand. Readily identifiable old surface horizons within the rendzina γ profiles support an origin by periodic deposition rather than continuous accretion. Periodic erosion of limestone sand would produce areas available for plant colonization and would aid the survival of the Teesdale flora.

The typical rendzina profiles differ markedly from soils developed over unaltered Carboniferous limestone though the rendzina β subtype grades imperceptively into normal limestone soils away from the Whin Sill contact as the bedrock changes from coarse to fine grained marble. The marble rendzinas, though distinctive, form only a relatively small part of the soils of the botanically significant region of Upper Teesdale. The brown earths, brown calcareous soils and the various gleys developed on drift and other parent materials are also important.

Bedrock–Soil–Flora Association

The combination of lower Carboniferous clear water limestone, late Carboniferous Earth movements and the injection of the Whin Sill produced coarse grained crystalline marble in Upper Teesdale. Tertiary and recent erosion with the Quaternary glaciation exposed this unusual bedrock at the surface. Rendzinas developed on outcropping marble by soil forming processes. A geological setting of this type is unknown outside Upper Teesdale in Britain and comparable rendzinas are similarly restricted. In the vicinity of this narrow geological and pedological setting the Teesdale flora has survived since shortly after the end of the Quaternary glaciation. It is our contention that the survival of the relict flora in association with unique geology and soils is not coincidental. The inherent instability and excessive drainage of the calcite sand soils have provided a continuous series of precarious habitats suitable for the survival of the alpine plants. In the vicinity of these soils elements of the flora have colonized restricted adjacent regions of differing soil type giving the plant distribution found today. Other factors have clearly played their part in sustaining the flora over the period of about 10,000 years. Two factors are particularly noteworthy; first, the severe climate of the Teesdale fells provides a suitable environment, and second, continuous grazing of the small areas of limestone grassland from prehistoric times[12] to the present day has tended to maintain the required more open habitats.

We thank Drs W. A. Clark, A. W. Davison, J. Turner and D. F. Ball who have read the manuscript and offered helpful advice. This research forms part of a survey of Upper

and the overlying crystalline marbles outcrop extensively though often masked by superficial glacial drift. The morainic drift and peat deposits, formed during Quaternary glacial and post-glacial times, have also played a significant part in the formation of the biologically important soils.

Whin Sill and Metamorphism

On Widdybank and Cronkley fells metamorphism of the Melmerby Scar Limestone and associated sediments occurs above and below the Great Whin Sill. The limestone is recrystallized for more than 25 m from the contact and the metamorphic effect can be detected to almost 40 m above and below the sill on the basis of spotting in shales. Elsewhere in northern England, where the sill is thinner, the effect of metamorphism is restricted to beds close to the contact, at a distance of 18 m above. The dark pigmented limestones, found principally in the Middle Limestone Group, are not recrystallized because the carbonaceous organic matter causes the suppression of marmarization[10]. Thus where dark limestones are found near the Whin contacts very little or no crystalline marble is found.

The formation of marble in Upper Teesdale is clearly the result of three factors combining to form a bedrock formation unique in northern England. First, the Whin Sill is near maximum thickness and lowest stratigraphical horizon.

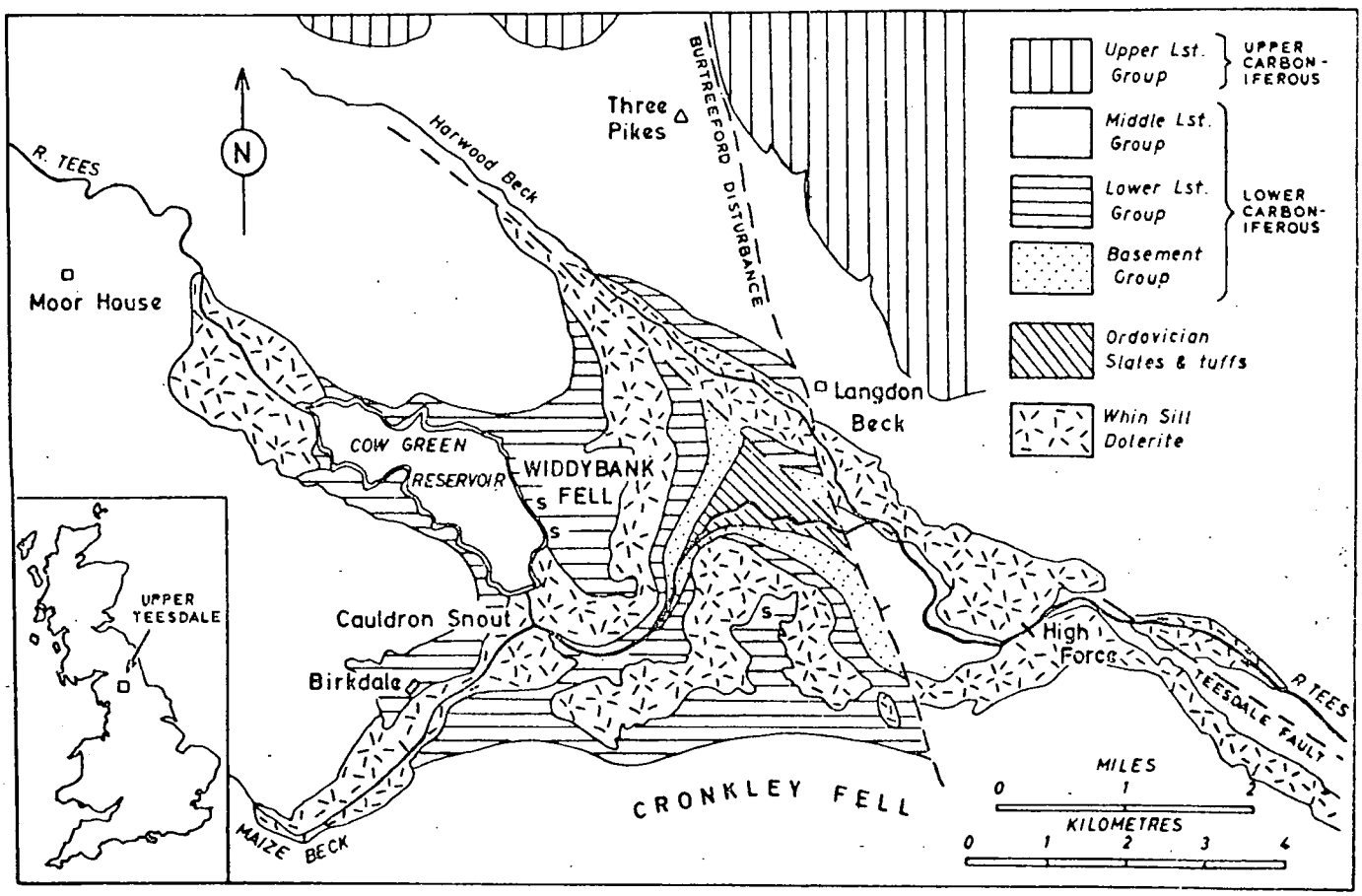

Fig. 1 Geological sketch map of part of Upper Teesdale showing the outcrop of the Great Whin Sill and the principal groups of sedimentary rocks. *S*, Well developed rotten marble and calcite sand rendzinas.

The alteration of pure limestones is limited to simple recrystallization. Impure limestones close to the contact form calc-silicate rocks in which a wide variety of minerals are present. Shales adjacent to the Whin Sill are converted into hard porcellaneous rocks (whetstones) in which the bedding is lost. Further from the contact spotted shales are commonly developed. Pure sandstones are converted into white quartzite at the contact and impure sandstones develop alteration patterns depending on the amounts of argillaceous or calcareous material present. The mineralogy of contact rocks associated with the Whin Sill in Teesdale has been described recently by Robinson[9].

The pure Melmerby Scar Limestone of Widdybank and Cronkley fells is recrystallized by the Whin Sill to a saccharoidal marble for about 25 m from the upper contact; a small thickness of marble is also present below the sill. The marble consists of dodecahedral to rounded grains of calcite varying in average grain size from 0.5 mm at the contact to 0.05 mm

Second, the sill is injected into the thickest limestone in the Carboniferous succession of the region, the Melmerby Scar Limestone. Finally, the low carbon content of this pure, light coloured limestone allowed metamorphic recrystallization to take place readily, with the development of thick marble formations.

Weathering of Crystalline Marble

The marble outcrop is partly masked by patches and tongues of glacial drift on Widdybank and Cronkley fells. This is a pattern of exposure that has not changed greatly from the early post-glacial period when continuous vegetation cover stabilized the unconsolidated drift slopes. Since then peat has developed over impervious deposits, particularly the clay drifts, and thin soils have formed over exposed bedrock.

Weathering of bedrock crystalline marble takes place both at the surface, by processes of subaerial erosion, and below

example. This gradient would theoretically give a high enough temperature to allow for the formation of the wollastonite rock of the Cow Green area, upper Teesdale.

The development of abundant soda feldspar in shales near the whin contact implies addition of alkalies to the country rocks. The phenomena of soda metasomatism is well known at basic igneous rock contacts. Hutchings's work (1895; 1898) contains numerous alkali determinations and shows that many of the altered sediments display an undoubted increase in soda, at the whin contact, which in a number of cases exceeds the potassium content. The soda (Na_2O) content of some rocks reaches 6-7%. Hutchings's work showed that the metasomatism was an erratic feature, however, with some altered beds near the whin showing no increase in soda. Wager (1928) suggested that the soda was derived from late stage alkaline carbonate solutions, produced by alteration of early joints in the whin by late stage magmatic waters. This alteration probably occurred soon after solidification of the magma, the temperatures at this time, over most of the aureole, although falling, would most likely be high enough to allow growth of albite in which the majority of the soda is found.

ACKNOWLEDGEMENT

Permission to study the Cow Green borings, upper Teesdale, was kindly granted to the author by the Tees Valley and Cleveland Water Board to whom he expresses his grateful thanks.

REFERENCES

DUNHAM, A. C. and KAYE, M. J. (1965). The petrology of the Little Whin Sill, Co. Durham. *Proc. Yorks. geol. Soc.* **35**, 229.

DUNHAM, K. C. (1948). Geology of the northern Pennine orefield. **1**, Tyne to Stainmore. *Mem. geol. Surv. G.B.*

DUNHAM, K. C., DUNHAM, A. C., HODGE, B. L., and JOHNSON, G. A. L. (1965). Granite beneath Viséan sediments with mineralization at Rookhope, northern Pennines. *Q. Jl geol. Soc. Lond.* **121**, 383.

EASTWOOD, T., HOLLINGWORTH, S. E., ROSE, W. C. C. and TROTTER, F. M. (1968). Geology of the country around Cockermouth and Caldbeck. *Mem. geol. Surv. G.B.*

HARRISON, R. K. (1968). Petrology of the Little and Great Whin Sills in the Woodland borehole, Co. Durham. *Bull. geol. Surv. G.B.* **28**, 38.

HUTCHINGS, W. M. (1895). An interesting contact-rock, with notes on contact-metamorphism. *Geol. Mag.* **2**, 1.

(1898). The contact rocks of the Great Whin Sill. *Geol. Mag.* **5**, 69 and 123.

JAEGER, J. C. (1964). Thermal effects of intrusions. *Geophys. Rev.* **2**, 443.

JOHNSON, G. A. L. and DUNHAM, K. C. (1963). *The geology of Moor House.* Nature Conservancy Monograph No. 2. London: H.M.S.O.

MILLS, D. A. C., HULL, J. H. and RAMSBOTTOM, W. H. C. (1968). The Geological Survey borehole at Woodland, Co. Durham. *Bull. geol. Surv. G.B.* **28**, 1.

RANDALL, B. A. O. (1959). Intrusive phenomena of the whin sill, east of the R. North Tyne. *Geol. Mag.* **96**, 385.

SEDGWICK, A. (1827). On the association of trap rocks with the Mountain Limestone formation in high Teesdale. *Trans. Camb. phil. Soc.* **2**, 140.

WAGER, L. R. (1928). A metamorphosed nodular shale previously described as a 'spotted' metamorphic rock. *Geol. Mag.* **65**, 88.

WINKLER, H. G. F. (1967). *Petrogenesis of metamorphic rocks.* 2nd ed. New York: Springer-Verlag.

WOOLACOTT, D. (1923). On a boring at Roddymoor colliery, near Crook, Co. Durham. *Geol. Mag.* **60**, 50.

developed and occurs at great distances from the contact as in the Rookhope borehole. Normally these spots consist of chlorite with minor quartz and illite. Dunham (1948) recorded andalusite from clear spots in some shales. The metamorphism has not resulted in any large scale generation of muscovite, but has been limited to a simple recrystallization of the clay minerals to give a sericitic material, with a loss of organic material. Some of the shales near the contact have been converted into adinole-like rocks consisting of crypocrystalline mixtures of quartz and soda feldspar. This development of feldspar, seen in many instances, is suggestive of the addition of alkalies to the rock. Calcareous shales develop similar minerals as in the impure limestones, the most common being garnet, epidote, idocrase and feldspar. A borehole core often shows well-developed euhedral garnets in lens-like bodies within the calcareous shale. In thin section the garnets show weak birefringence and are twinned with the development of sector twins composed of six or twelve pyramids with vertices meeting in the centre of the crystal. The calcareous shales may show a banded hornsfelsic structure with lenses of red feldspathic material, white fine-grained garnet (hydrogrossular?) with darker lenses of epidote. Thin sections show smaller concentrations of wollastonite, diopside and abundant calcite.

Pure sandstones at the contact, are converted into white quartzite. Impure shaly sandstones show similar alteration patterns to shales and limy sandstones to impure limestones; these rocks have been discussed previously.

Metamorphic facies. The whin sill intrusion was not of sufficient size to allow a well-defined series of metamorphic mineral assemblages to be developed and definite zones of different hornsfels facies cannot be delimited in the area, but from the mineral assemblages present, it is possible to draw some conclusions about the metamorphic facies. Wollastonite is one of the highest temperature minerals seen in the whin aureole. At low pressures it forms only in the highest part of the hornblende-hornsfels facies, but is more usually characteristic of the potassium feldspar-cordierite-hornsfels facies (Winkler, 1967). The presence of a wollastonite rock over 25 ft. (7·6 m.) from the contact suggests that the potassium feldspar-cordierite facies was established for a time close to the contact. The presence of idocrase also points to this facies, but is mainly recorded from a limestone raft within the whin. Abundant evidence showing that the hornblende-hornsfels facies was well developed is indicated by the presence of garnet, diopside, plagioclase and andalusite. The low temperature albite-epidote-hornsfels facies is also well exhibited, generally at greater distances from the contact, with epidote, albite, chlorite and sericite as the main minerals. Using Jaeger's (1964) formula, theoretical values for the heat-flow through the country rocks have been calculated to give estimates of the temperatures reached in the metamorphic aureole. The temperature at any point will, of course, vary with time after the intrusion, but a maximum temperature curve after 25 years would give a contact temperature in the region of 720°C with a decrease, away from the contact, at approximately 5°C/ft. (17°C/m.). An increase or decrease of the time interval after the intrusion will cause the temperature gradient to become respectively shallower or steeper, relative to the above

cuts through and alters many beds of limestone no evidence of assimilation or reaction, between the magma and carbonate rocks, to form hybrid feldspathoidal and melilitic rocks has been recorded. However, it is interesting to note that where a thin leaf of whin sill is in contact with calcareous beds, as in the Rookhope and Woodland boreholes, there has been a local development of White Whin at both contacts (Dunham and Kaye, 1965; Harrison, 1968).

Impure limestones show the highest degree of alteration when found adjacent to the whin sill. They are converted into calc-silicate rocks yielding a wide variety of minerals. One of the simplest impurities is quartz, as developed at limestone sandstone junctions. In the Cow Green reservoir boreholes a wollastonite rock has been found, over a restricted area, at the junction between the Lower Robinson Limestone and the underlying sandstone. The rock is between 3 to 18 ins. (80 to 460 mm.) in thickness and shows white radiating crystals of wollastonite with only minor amounts of calcite and diopside. Hutchings (1898) recorded wollastonite from a limestone at Dunstanburgh, but it is of infrequent occurrence. The development of a wollastonite rock up to 27 ft. (8·2 m.) from the whin sill contact is unusual as the assemblage quartz-calcite is stable up to quite high temperatures. Although the relevant reaction is bivariant and should not be used as a temperature indicator, Winkler (1967) states that wollastonite is not found where maximum temperatures have been below 500°C. Considering the shallow nature of the intrusion, giving a pressure in the region of 350 to 400 bars and a high value for the mole fraction of CO_2, the presence of wollastonite suggests that temperatures in the region of 550°C were attained in this position. Impure limestones containing clay minerals as well as quartz allow sufficient alumina, magnesia, iron and alkalies for the development of an extensive range of minerals. These include garnet, feldspar, chlorite, epidote, idocrase and diopside. Garnet is the most abundant along with chlorite. Hutchings records that the garnets are small and vary in colour from neutral to yellow and green. The present survey by the author confirms the widespread occurrence of garnets which are often euhedral and zoned with isotropic cores and slightly anisotropic rims. Feldspar has also been previously noted and similar identifications have been made on borehole material where it occurs in much greater abundance as quartzo-feldspathic lenses within the limestone. Hutchings recorded augite as occurring with garnet, but present work only shows diopside with wollastonite in small amounts. Idocrase has not been found in Teesdale, but Randall (1959) records idocrase in abundance with garnet from a raft within the whin sill, at Barrasford. The idocrase occurs in both euhedral and anhedral grains showing some low interference colours and in other grains anomalous blues. Other minerals noted by Hutchings are only of rare occurrence and include amphibole and sphene.

The alteration products of shales adjacent to the whin sill vary greatly, mainly dependent on the distance from the whin sill contact. The normal Carboniferous shales are usually dark coloured and well bedded, and under maximum alteration are converted into smooth, much lighter coloured, hard porcellaneous rocks in which the bedding is lost; they are often known as whetstones. Spotting of the shales is well

effect is even wider in the shales. In the Rookhope borehole (Dunham *et al.*, 1965) the metamorphic effect could be traced to almost 130 ft. (39·6 m.) above and below the contacts on the basis of spotting in the shales. Where the whin is thinner, as along the Pennine escarpment, the metamorphism is very restricted and generally only affects the beds close to the contact.

In the Cow Green, Cronkley and Widdybank Fell areas of upper Teesdale the whin sill is found in the Lower Limestone Group, the position being 90 ft. (27·4 m.) below the top of the Melmerby Scar Limestone. To the north, the whin trangresses into the Middle Limestone Group in the Moor House National Nature Reserve (Johnson and Dunham, 1963). The whin sill proved in boreholes in Durham county shows it to be intruded into the Middle Limestone Group (text-fig. 18). At Rookhope it is found between the Lower Little and Jew limestones while in the Roddymoor boring at Crook it is intruded into the Scar Limestone. The Woodland borehole (Mills *et al.*, 1968) proved the Great Whin Sill just below the upper part of the Three Yard Limestone. In the Harton borehole, near South Shields, the whin sill is found to consist of three leaves, the upper and lower leaves are the thickest and are found at the base of the Great Limestone and above the Robinson Limestone respectively.

Mineralogy of contact rocks. The effect of the whin sill on pure limestone is limited to a simple recrystallization. The degree of recrystallization is dependent on organic content of the limestone and this depends largely on the stratigraphical horizon at which the whin sill is intruded. Where the whin sill is intruded into the pure limestones of the Lower Limestone Group there has been extensive recrystallization producing marmorization of the Melmerby Scar Limestone for about 70-90 ft. (21·3-27·4 m.) from the contact. The production of this extensive saccharoidal marble, or sugar limestone, as it is known to biologists, is almost unique and wide areas of sugar limestone soils have been produced on Cronkley and Widdybank fells in upper Teesdale. A small thickness of Melmerby Scar Limestone, underlying the whin sill, has also been marmorized, as seen at Caldron Snout and Falcon Clints. The marmorized limestone consists of dodecahedral to rounded grains of calcite varying in average grain size from 0·05 mm. at 60 ft. (18·3 m.) from the contact to 0·5 mm. at the contact. Over most of Durham the whin sill is intruded into the Middle Limestone Group and, although at least one less-pure blue-grey limestone is found within 50 ft. (15·2 m.) of the contacts, saccharoidal limestone is rarely developed. Normally there has been limited recrystallization with the elimination of carbon to grain boundaries. There is a basic difference between the limestones of the Middle and Lower Groups as recognized by Johnson and Dunham (1963). The Lower Limestone Group consists of light grey limestones while the Middle Group consists of blue-grey limestones which contain quantities of organic matter, occurring as a dark pigment. It seems, therefore, that the organic matter plays the dominant role in the suppression of marmorization. Randall (1959) has recorded a related feature in saccharoidal limestone, from Barrasford, Northumberland, where the grain size is related to the carbon content of the limestone. Although the whin sill

10. METAMORPHIC ROCKS

by

D. ROBINSON

METAMORPHIC EFFECTS OF THE WEARDALE GRANITE

The western half of Durham county is underlain by the major intrusive Weardale granite (text-fig. 2) which has been described in chapter 9. This granite was intruded at a temperature sufficient to alter the country rocks by contact metamorphism. A wide envelope of these metamorphic rocks must surround the granite, but they are only known from two places. Woolacott (1923) described metamorphosed Lower Palaeozoic slates beneath the Carboniferous sediments at the bottom of the Roddymoor boring at Crook. These slates were reported to be schistose, contorted, cleaved and folded with quartz veins and garnetiferous bands. The site of the boring is approximately one mile (1·6 km.) from the estimated margin of the granite. The slates outcrop in the Teesdale inlier where they have been shown, by the presence of rare graptolites, to belong to the upper part of the Skiddaw Slate Series (page 21). The inlier is four miles (6·4 km.) from the estimated margin of the Rookhope cupola and is underlain at depth by granite. Here, thin sections show the slate to be distinctly spotted with incipient hornsfelsing. Exposures of Skiddaw slate, beneath the Carboniferous, in the Cross Fell inlier, although phyllitic and recrystallized, show no signs of alteration attributable to the Weardale granite and these exposures must lie outside the metamorphic aureole of the granite. The smaller Skiddaw granite at the north-eastern corner of the Lake District (Eastwood *et al.*, 1968) is also intruded into Skiddaw slates; spotting and the development of garnet is found only in the outer zone of the metamorphic aureole. Comparison with this granite suggests that the metamorphic rocks seen around the Weardale granite constitute the outermost part of the aureole.

METAMORPHIC EFFECTS OF THE WHIN SILL

In the early part of the last century, when there was doubt over the origin of the whin sill, Sedgwick (1827) used the evidence of the metamorphic alteration of the county rock, both above and below the sill, as proving that the whin was in fact of igneous origin and intrusive in nature. Although the metamorphism had been mentioned by several authors, their descriptions only mention the induration of shales and sandstones with the development of porcellanite, and limestones rendered crystalline or granular in form. Sedgwick noted the presence of garnets in an impure limestone, but Hutchings (1895, 1898) made the first and only detailed examination of whin metamorphism; previous work was reviewed by Dunham (1948). The metamorphism is relatively restricted and the maximum effect is seen where the whin sill reaches its greatest thickness of 240 ft. (73·2 m.) in upper Teesdale. Here, limestones are altered for over 100 ft. (30·4 m.) from the contact and the metamorphic

Contr. Mineral. and Petrol. 32, 245—250 (1971)

The Inhibiting Effect of Organic Carbon on Contact Metamorphic Recrystallization of Limestones

Douglas Robinson
Department of Geology, University of Durham, South Road, Durham City, England

Received July 2, 1971

Abstract. In Upper Teesdale, Northern England, some limestones have been metamorphosed to a saccharoidal marble near to the contacts with the Whin Sill. This marble is virtually restricted to Upper Teesdale although the Whin Sill is found, intruded into the Carboniferous sequence, over most of Northern England.

Petrographical and geochemical studies have shown that the marmorisation of the limestones is mainly dependent upon their non-carbonate carbon content and also the distance from the Whin Sill contact. Analyses show that only small amounts of carbon (0.5–1.0%) are required to inhibit recrystallization in the limestones.

Introduction

The Whin Sill of Northern England is a quartz-dolerite intrusive complex, intermediate in composition between the tholeiitic and alkaline basalt series (Dunham, 1970). It intrudes Carboniferous strata ranging from the Lower Limestone Group (Viséan) to the Coal Measures (Westphalian) but is found mainly in the Middle Limestone Group (Upper Viséan) throughout Durham and Northumberland (Fig. 1). The stratigraphical terms used in this communication are based upon local usage, which are related to the general nomenclature below:

Table. *Stratigraphical Nomenclature in Co. Durham*

Upper Limestone Group	Namurian
Middle Limestone Group	Viséan
Lower Limestone Group	Viséan

K-Ar age determinations, on the Whin Sill, suggest a late Coal Measures age of 295 ± 6 m.y. (Fitch and Miller, 1967). The strata adjacent to the upper and lower contacts of the sill have been metamorphosed and this note is concerned with those contact metamorphic effects seen in the limestones within 31 m of the contact.

The Whin Sill is at its lowest stratigraphical position and attains its maximum thickness, of more than 73.1 m in the Cow Green area of Upper Teesdale (Fig. 1). Here it intrudes the Melmerby Scar Limestone (Lower Limestone Group) and away from this region the sill gradually rises in the succession becoming generally thinner in all directions (K. C. Dunham, 1948; A. C. Dunham, 1970). The maximum metamorphic effect is also seen in Upper Teesdale, with the development of wollastonite in appreciable quantities. Evidence of metamorphism based on

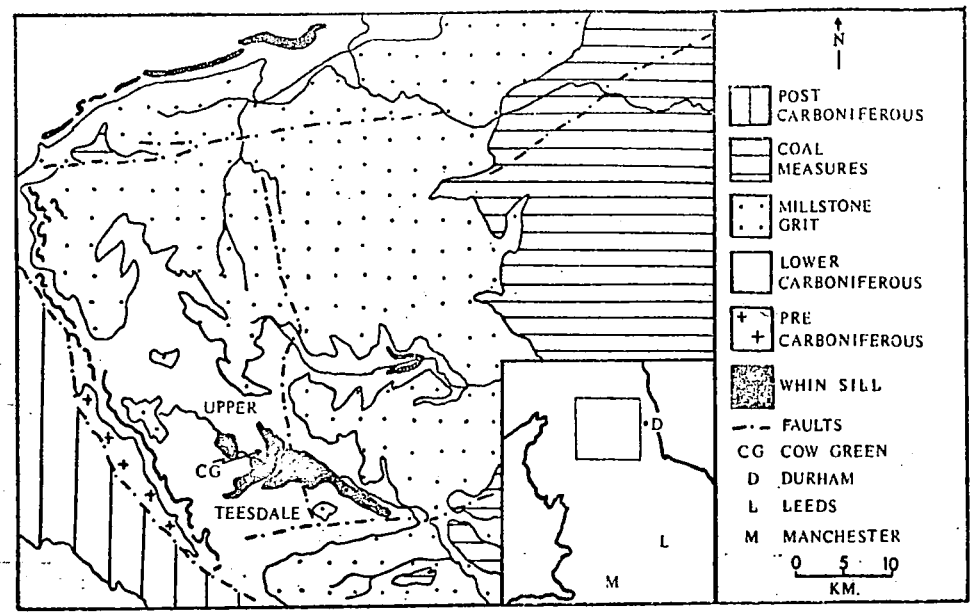

Fig. 1. Map showing location and geological setting of the Teesdale area, Northern England

spotting in the shales can be seen at over 36 m from the contact. A recent general account of the metamorphism has been published by the writer (Robinson, 1970). One of the main features of Upper Teesdale geology is the extensive occurrence of saccharoidal marble produced by the metamorphism of the Melmerby Scar Limestone. These marbles consist of rounded grains of pure white calcite, which decrease in size away from the contact. Grain-size measurements undertaken on samples from a borehole show a range of grain-size from 0.5 mm at the contact to 0.05 mm at a distance of 18.3 m. The marmorisation of the original limestone to a saccharoidal marble has resulted in the obliteration of all the sedimentary features, including the bedding. In order to explain the development of this rather unique marble it is necessary to consider first the sedimentary characteristics of the limestones.

Limestones Prior to Metamorphism

Two distinct types of limestone have been recognised in the Northern Pennine region by Johnson and Dunham (1963). Light-coloured limestones are dominant in the Lower Limestone Group, while those of the Middle and Upper Limestone Groups are chiefly dark in colour. Johnson and Dunham attributed the difference in colour to the presence of organic and terrigenous impurities in the dark limestones. Jones and Cooper (1970) have shown that the carbonaceous material of Carboniferous argillaceous sediments in Northern England has components similar to those of coal. This material consists of fusinite and spores, with a disseminated, amorphous, organic phase (kerogen) also present. This is the carbonaceous material believed to be present in varying quantities in most of the

limestones. Johnson (1962) has shown the type of limestone present in the Northern Pennines depends basically upon the depositional environment. The limestones of the Lower Limestone Group of Teesdale were laid down as an open-sea marine facies with dominant, massive, light-coloured limestones. When traced north into the Northumberland trough (a deltaic environment) the limestones bifurcate and become dark grey in colour. The overlying Middle and Upper Limestone Groups, with dominantly dark limestones, were also deposited in a deltaic environment. This scheme is generalized since lenses of dark limestone do occur in light limestones and *vice versa*.

Petrographic examination of the light-coloured limestones shows them to be bioclastic and of fine to medium grain-size. Evidence of recrystallization is often present in the groundmass, which is for the main part fine grained and buff coloured. The dark limestones are also bioclastic with a fine-grained groundmass of calcite. Where the groundmass in these dark limestones is very fine grained, the rock has a dark, earthy-brown colour. However, where the calcite becomes coarser a definite rim of dark brown, carbonaceous material can be seen around the calcite grain boundaries.

Saccharoidal Development in Contact Zones

The development, near to the Whin Sill contacts, of saccharoidal marble, is mainly dependent upon the stratigraphical horizon at which the sill is intruded (Robinson, 1970). In Upper Teesdale the Whin Sill intrudes the Lower Limestone Group, but over most of its outcrop and known subsurface position it is found in the Middle Limestone Group. The combination in Upper Teesdale of the thick (33 m), light-coloured, Melmerby Scar Limestone and one of the thickest sections of the Whin Sill accounts for the maximum development of over 25 m of saccharoidal marble in this area. Over most of the areal extent of the sill, only dark limestones are present in the succession and even through a dark limestone horizon is never more than 15.2 m from a contact, saccharoidal development is virtually absent.

The difference in metamorphism between the two types of limestone can be demonstrated where both varieties occur in the same contact zone. Dunham (1948, p. 56) gave details of the Ettersgill borehole (ET/16) in which the sill was found to be over 67.1 m in thickness. In this section the Single Post Limestone, a light limestone within the Middle Limestone Group, is completely marmorised at a distance of 5.5 m from the contact, whereas the dark Cockle Shell Limestone is unaltered only 11 m from the contact. A similar feature is shown in Fig. 2 which displays the succession recorded in borehole 40 in the Cow Green area. In this section the Upper Robinson and a lens of the Peghorn Limestone are dark limestones within the Lower Limestone Group. These two dark limestones are non-saccharoidal and virtually unrecrystallized whereas medium grained saccharoidal marble, developed from light coloured limestones, is present both above and below. The variation in crystallinity in the limestones is especially evident in the case of the dark lens in the Peghorn Limestone, where the junction between dark and saccharoidal limestone is sharp at both upper and lower contacts.

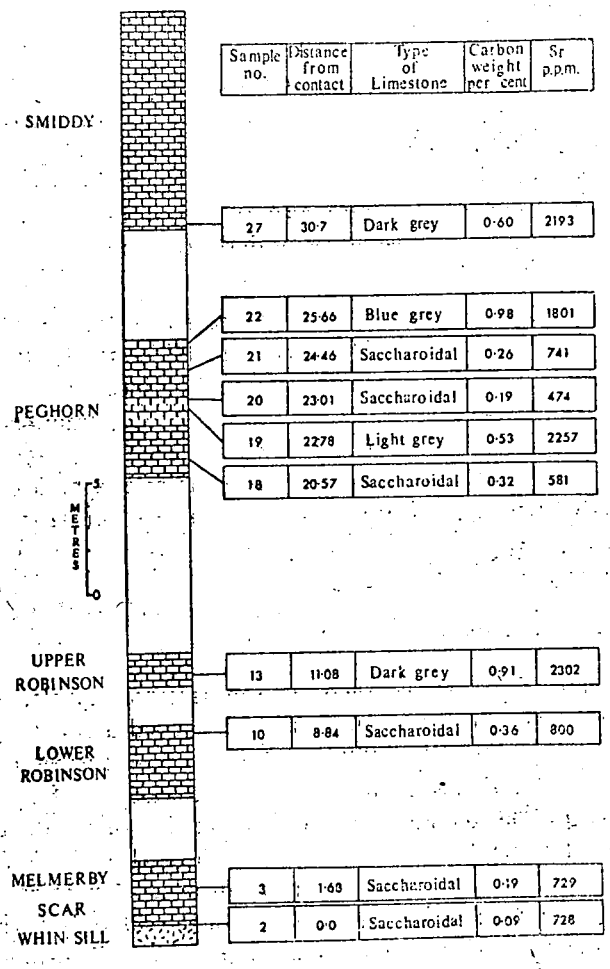

Fig. 2. Simplified log of borehole 40 in the Cow Green area, showing location and nature of samples with analytical data for carbon and strontium. C determined by the absorption train method and Sr by X-ray fluorescence analysis

Geochemistry of Limestones

The results of non-carbonate carbon and strontium determinations of limestone samples from the borehole are given in Fig. 2. The carbon data show a definite correlation between the amount of carbon present and the type of limestone analysed. The dark limestones have a relatively high content of carbon, almost 1.0% in two of the samples and always greater than 0.5%. The light limestones always have low carbon below 0.4% with an average in the range 0.2–25%. The difference in amount of carbon between the two types of limestone is not great but petrographic examination of dark limestones reveals that the carbonaceous material is very finely disseminated. The strontium values are of great interest as it is well known that strontium is readily released from the crystal lattice of calcite upon recrystallization, even during diagenesis (Kulp *et al.*, 1952). Strontium values from Fig. 2 show that in saccharoidal marble, values of less than 800 ppm are normal. The dark limestones, however, have significantly higher values of strontium with over 2000 ppm of strontium normal with a maximum

of 2291 ppm. Samples 18, 19 and 20 (Fig. 2) show the difference in strontium values, between the two types of limestone. Sample 19, a dark limestone, has over 2200 ppm of strontium while saccharoidal limestones above and below, samples 18 and 20, have strontium values below 600 ppm. The values of strontium in limestones not under the influence of the Whin Sill have also been determined by the author. Values for dark limestones similar to the Peghorn Limestone are in the range 2000–2500 ppm, while samples of light limestones give values in the region of 1200 ppm. The difference in strontium values between the two types of limestone is most likely due to some loss of strontium from the light limestones during diagenesis. Depletion of strontium in limestone may also occur in wall-rocks adjacent to mineralization in the Northern Pennines as shown by Ineson (1969). The samples from borehole 40 are not affected by this depletion as no sign of vein mineralization was present and the site was over 61 m from the nearest vein. This places the borehole well outside the vein dispersion aureoles, which as Ineson showed vary from cms to a maximum of 9 m. Examination of many limestone samples has shown that there is a complete gradation between the high carbon, unrecrystallized limestones and the totally recrystallized, saccharoidal marbles.

X-ray diffraction analysis of the dark limestones from the borehole shows that they are quite pure with no detectable quartz or clay minerals. The samples were also digested in dilute acetic acid but only small quantities of clay minerals could be detected in the residues along with carbon and some sulphides.

Discussion

Recently Suess (1970) has shown that organic carbon, dissolved in sea-water is readily adsorbed by calcite. He also showed that even a monomolecular layer of carbon can produce physical isolation of a calcite surface area and can completely inhibit carbonate equilibria with the surrounding sea-water. It is most probable that the carbon is chemi-adsorbed onto the calcium cation sites on the surface of the calcite grains. The amount of carbon required to form a monomolecular layer is small. Suess showed that for powdered calcite $<43\,\mu$ in size and with a surface area of 0.714 m per g, 0.1–1.5 mg carbon per m is sufficient for a monomolecular layer. Grain size in a limestone is, of course, very variable but the calcite matrix is <0.01 cm so that sufficient carbon is present, according to the analyses, to provide more than a molecular layer on grains.

Spry (1969) has shown that there are three main "driving" forces for the growth of crystals, chemical, lattice strain and grain boundary energy. Heat is the activating mechanism for either one or a combination of the above forces. Chemical energy is not relevant in this case as no new phase is developed, just a simple recrystallization of the original calcite. In a contact environment such as that under consideration, where there has been the very minimum of deformation, the main recrystallization force must therefore be dominantly grain boundary energy. According to Spry (1969) this is the smallest energy available for recrystallization, and a mantle of carbon around the calcite grains, as demonstrated here, is quite sufficient to inhibit grain boundary movement of material thus preventing any recrystallization.

Conclusions

The development of saccharoidal marble in Northern England is shown to be virtually restricted to Upper Teesdale, where it is formed by contact metamorphism of the light-coloured limestones of the Carboniferous Lower Limestone Group.

The light-coloured limestones, with low carbon content ($<0.4\%$), are readily recrystallized to coarse (0.5 mm) saccharoidal marble at the contact with the Whin Sill, with a decrease in grain-size away from the contact. During the metamorphic recrystallization, strontium has been depleted in the light limestones. The dark limestones, with relatively high carbon content (0.5–1.0%) are not recrystallized during the metamorphism. This is because grain boundary movement is prevented by a mantle of carbon around the calcite grains. No strontium is lost from the dark limestones values for unmetamorphosed examples being compatible with those for dark limestones near to the Whin Sill.

Acknowledgements. The Work currently in progress by the writer is supported by a Nature Conservancy Award (N.E.R.C. Research Assistantship). The Tees Valley and Cleveland Water Board kindly gave the author access to the Cow Green boreholes and permission to publish the borehole section in Fig. 2. The author is also grateful to Professor G. M. Brown, Dr. G. A. L. Johnson and G. H. Gale for their constructive criticism, thereby greatly improving the style of the manuscript.

References

Dunham A. C.: Whin Sills and dykes. In: Geology of Durham County. Trans. nat. Hist. Soc. Northumb. 41, 92–100 (1970).

Dunham, K. C.: Geology of the northern Pennine orefield. 1, Tyne to Stainmore. Mem. geol. Surv. G.B. (1948).

Fitch, F. J., Miller, J. A.: The age of the Whin Sill. Geol. J. 5, 233–250 (1967).

Ineson, P. R.: Trace-element aureoles in limestone wallrocks adjacent to lead-zinc-barite-fluorite mineralization in the northern Pennine and Derbyshire ore fields. Trans. Inst. Metall. (Sect. B: Appl. earth sci.) 78, B 29–40 (1969).

Johnson, G. A. L.: Lateral variation of Marine and Deltaic sediments in cyclothemic deposits with particular reference to the Viséan and Namurian of Northern England. IV. Congr. Avanc. Et. Stratigr. Carbonif., 1958, tome II, 323–330 (1962).

— Dunham, K. C.: The geology of Moor House. Nature Conservancy Monograph No. 2. London: H.M.S.O. 1963.

Jones, J. M., Cooper, B. S.: Coal. In: Geology of Durham County. Trans. nat. Hist. Soc. Northumb. 41, 43–65 (1970).

Kulp, J. L., Turekian, K., Boyd, D. W.: Strontium content of limestones and fossils. Bull. Geol. Soc. Am. 63, 701–716 (1952).

Robinson, D.: Metamorphic Rocks. In: Geology of Durham County. Trans. nat. Hist. Soc. Northumb. 41, 119–123 (1970).

Spry, A.: Metamorphic Textures. Oxford-New York-London-Paris: Pergamon Press 1969.

Suess, E.: Interaction of organic compounds with calcium carbonate. I. Association phenomena and geochemical implications. Geochim. Cosmochim. Acta 34, 157–168 (1970).

D. Robinson
Department of Geology
University of Durham
South Road
Durham City, England